Neuronal Differentiation: A Study into Differential Gene Expression

by

Rachel de las Heras B.Sc. (Hons)

School of Biomolecular and Biomedical Science
Faculty of Science
Griffith University
Queensland

A Thesis Submitted in Fulfilment of the Requirements for the Degree of Doctor of Philosophy

April 2003

ABSTRACT

Neuronal differentiation encompasses an elaborate developmental program which until recently was difficult to study *in vitro*. The advent of several cell lines able to differentiate in culture proved to be the turning point for gaining an understanding of molecular neuroscience. In particular the olfactory epithelium provides an attractive tool with which to investigate fundamental questions relating to neuronal differentiation, as it displays a unique capacity to regenerate and to retain a neurogenetic potential from its genesis and throughout adult life.

The coordinated regulation of gene expression is fundamental to the control of neuronal differentiation. In order to reveal active processes at the molecular level and to dissect key components of molecular pathways, differential gene expression studies provide a foundation for the elucidation of dynamic molecular mechanisms. This thesis identified genes involved in neuronal differentiation by utilising a clonal olfactory receptor neuronal cell line (OLF442). Gene expression levels were identified using differential display and oligonucleotide array technology before and after serum deprivation. Differential display revealed two kinases whose expression levels were elevated during the differentiation of OLF442, identified as focal adhesion kinase (FAK) related non-kinase (FRNK) and mammalian ste20 like (MST)2 kinase. Furthermore, analysis of the oligonucleotide array data confirmed the expression of genes involved in altering presentation of extracellular matrix molecules, in mediating cytoskeletal re-arrangements, and in ceasing the cell cycle, supporting the use of OLF442 as a model for studying differentiation.

The differentiation of OLF442 results from the synchronisation of multiple transduction cascades and cellular responses as evidenced by the microarray data. A protein that can synchronise such signalling is the non-receptor protein tyrosine kinase, FAK. Thus the finding of the endogenous FAK inhibitor FRNK by differential display was intriguing as there was no difference in the expression level of FAK induced by differentiation, contrasting that of FRNK. This induced FRNK expression was derived autonomously as it was not responsive to the caspase-3 inhibitor, DEVD-CHO. This is particularly pertinent since the primary role of FRNK is to act as an inhibitor of FAK by competing with its substrates and reducing the phosphorylation of both FAK and its associated proteins.

Differential display also revealed the upregulation of another kinase, which had 90% homology with rat MST2 kinase within the 3′ UTR. Both mouse MST2 kinase (sequence submitted to GenBank, accession number AY058922) and the closely related family member MST1 kinase were sequenced and cloned. Moreover, evidence to support an autonomously expressed carboxyl-terminal domain of MST2 kinase is presented in Chapter 3 and provides a unique way in which MST2 may regulate its own activity. To further understand the role of MST in neuronal differentiation, a series of stable OLF442 transfections (with mutant and wild-type MST constructs) were carried out. MST was localised with cytoplasmic structures that may represent actin stress fibres, indicating a potential cytoskeletal role during neuronal differentiation. This indicated that MST1 may play a role in the morphological processes involved in neuronal differentiation.

The identification of two kinases by differential display provided the motivation to understand the cellular context of OLF442 and to determine the phosphorylation status of the mitogen-activated protein kinase (MAPK) signalling cascades. Differentiation of OLF442 induced high-level phosphorylation of a putative B-Raf isoform, MEK2 and ERK1/2. Interestingly, there was a switch between preferential phosphorylation of MEK1 in undifferentiated OLF442 to preferential phosphorylation of MEK2 following differentiation. SAPK/JNK was also phosphorylated, as was the transcription factor c-Jun, which is a common substrate of both the ERK and SAPK/JNK signalling modules.

The mapping of the cellular context of differentiating OLF442 has identified a promising model of a novel MAPK module. This consists of FAK signalling through Rap1 to ERK providing sustained activation, which is buffered or terminated by the expression of the endogenous FAK inhibitor FRNK. Furthermore, MST kinase could potentially play a role in regulating the cytoskeletal re-arrangements that are necessary for neuronal differentiation. MST kinase may signal transiently via the SAPK pathway to provide concomitant activation of c-Jun that is required for neuronal differentiation.

An understanding of the gene expression pattern of the normal neuronal differentiation program allows a greater understanding of potential developmental aberrations. This could provide an opportunity for therapies to be conceived, while understanding the complexity of neuronal determination could also provide opportunities for stem cell transplantation.

TABLE OF CONTENTS

LIST OF FIGURES

LIST OF TABLES

ABBREVIATIONS

Akt	Murine thymoma viral (v-akt) oncogene homolog-1 (PKB)
AMP	Ampicillin
ApoD	Apolipoprotein D
ATP	adenosine triphosphate
bFGF	basic fibroblast-derived growth factor
BJAB	murine myeloma (B cell) cell line
BMP	bone morphogenic protein
BSA	bovine serum albumin
CAD	Cath. a-differentiated CNS catecholaminergic cell line
CAM	Cell adhesion molecule
cAMP	cyclic adenosine monophosphate
CBF-A	nuclear transcription factor Y, alpha
Cdc42	cell division cycle 42
$CdCl_2$	cadmium chloride
CDK	cyclin dependent kinase
cDNA	complimentary DNA
cIAP	cellular inhibitor of apoptosis protein
CKI	CDK inhibitory protein
Crk	avian sarcoma virus CT10 (v-crk) oncogene homolog
cRNA	complimentary RNA
D	DEVD-CHO
DAG	diacylglycerol
DAPI	4',6-Diamidine-2'-phenylindole dihydrochloride
Daxx	Fas binding protein
DD	differential display
DD-PCR	differential display PCR
DEVD-CHO	cell-permeable caspase-3 inhibitor
DMEM	Dubecco's Modified Eagle's Medium
DMSO	dimethyl sulfoxide
DNA	deoxyribonucleic acid
DNase	deoxyribonuclease
dNTP(s)	deoxynucleotide triphosphate(s)
DROP	directed random oligonucleotide primed
dsDNA	double-stranded DNA
DTT	dithiothreitol
ECM	extracellular matrix
EDTA	ethylene diaminetetra-acetic acid, disodium salt
EGF	epidermal growth factor
Enx-1	murine homolog of the Drosophila Enhancer of zeste
ER	endoplasmic reticulum
ERK	extracellular-signal-regulated protein kinase
EST	expressed sequence tag
EtBr	ethidium bromide
EtOH	ethanol
FA	focal adhesion
FACS	fluorescence activated cell sorting
FAK	focal adhesion kinase
FAT	focal adhesion targeting signal
FCS	foetal calf serum
FGF-2	fibroblast growth factor-2
FRNK	FAK related non-kinase
G_0	quiescent phase of the cell cycle
G_1	first gap phase of the cell cycle
G_2	second gap phase of the cell cycle
GAP-43	growth-associated phosphoprotein
GAPDH	glyceraldehyde-3-phosphate dehydrogenase
GBC	globose basal cell

GCK	germinal center kinase
GFAP	glial fibrillary acidic protein
GLUT	glutamine
Grb	growth factor receptor-bound protein
GTK	cytoplasmic tyrosine kinase of the Src family
GTP	guanosine triphosphate
GTPase	guanosine triphosphatase
H_2O_2	hydrogen peroxide
H19-7	SV40 Tts-immortalised rat hippocampal neuronal cell line
HBC	horizontal basal cell
HBSS	Hank's Balanced Salt Solution
HL-60	human promyelocytic cell line
HMG2	high mobility group 2 protein
HMG-CoA	3-hydroxy-3-methylglutaryl-CoA
HPK	hematopoietic progenitor kinase
hr	hour(s)
HRP	horse radish peroxidase
IL	interleukin
INP	immature neuron precursor
IPTG	isopropylthio-β-D-galactoside
kDa	kilo Dalton
KRS	kinase responsive to stress
L	litre
LB	Luria-Bertani medium
LD-PCR	long distance PCR
LPA	lysophosphatidic acid
M	mitotic phase of the cell cycle
MAP-4	microtubule associated protein-4
MAPK	mitogen-activated protein kinase
MAPKK	MAPK kinase
MAPKKK	MAPK kinase kinase
MASH 1	Mammalian aschaete-scute homologue 1
M-CSF	Macrophage colony-stimulating factor
MEK	MAPK/ERK kinase
min	minute(s)
MM	mismatch
MMLV-RT	Moloney Murine Leukaemia Virus reverse transcriptase
MOPS	3-(N-Morpholino) propanesulfonic acid
MQH_2O	MilliQ filter sterile water
mRNA	messenger RNA
MST	mammalian Ste20-like kinase
N1E-115	neuroblastoma cell line
NCAM	neural cell adhesion molecule
NES	nuclear export signal
NF-kappa-B	nuclear factor-kappa-B
NGF	nerve growth factor
NIC	rat olfactory epithelial neuroblast cell line
NLS	nuclear localisation signal
nm	nanometres
OE	olfactory epithelium
OLF442	clonal murine olfactory epithelial derived cell line
OMP	olfactory marker protein
Opn	osteopontin
ORN	olfactory receptor neuron
P19	mouse embryonal carcinoma cell line
$p21^{cip1}$	CDK-inhibitory protein
$p27^{kip1}$	CDK-inhibitory protein
PAGE	polyacrylamide gel electrophoresis
PAK	p21-activated protein kinase

PBS	phosphate buffered saline
PC12	rat adrenal pheochromocytoma clonal cell line
PC12D	PC12 cell subline
PCR	polymerase chain reaction
PD	PD98059
PD98059	specific MEK1/2 inhibitor
PDGF	platelet-derived growth factor
pfu	plaque forming units
PH	pleckstrin homology
PI3K	phosphatidyl-inositol-3-kinase
PKA	protein kinase A
PKB	protein kinase B
PM	perfect match
PP2A	serine/threonine phosphatase
PVDF	polyvinylidene fluoride
RAP-PCR	RNA arbitrary primed polymerase chain reaction
Rb	retinoblastoma
RNA	ribonucleic acid
RNase	ribonuclease
rpm	revolutions per minute
RT	reverse transcription
RTK	receptor tyrosine kinase
S	DNA synthesis phase of the cell cycle
SAGE	serial analysis of gene expression
SAM	surface adhesion molecule
SAPK	stress activated protein kinase
SC1	extracellular matrix associated protein 1
SDS	sodium dodecyl sulphate
sec	second(s)
SEK	SAPK kinase
SH	src homology
SH-SY5Y	neuroblastoma cell line
SN	supernatant
SNP	single nucleotide polymorphism
SnRNP	U1 small nuclear ribonucleoprotein
SOK	Ste20/oxidant stress response kinase
SPARC	secreted protein, acidic and rich in cysteine
Src	Rous sarcoma (Schmidt-Ruppin A-2) viral oncogene homolog
ssDNA	single-stranded DNA
SSC	standard sodium/citrate buffer
Ste20	sterile-20p
TBE	tris buffered EDTA
TBS	tris buffered saline
TE	tris-EDTA
TGF	transforming growth factor
TNF	tumour necrosis factor
TOGA	total gene expression analysis
TPA	12-0-tetradecnoyl-phorbol-13-acetate
TrkA	tyrosine receptor kinase A
TTF	thyroid transcription factor
UV	ultraviolet
V	volts
W	watt
X-gal	5-bromo-4-chloro-3-indoyl-β-D-galactoside
YVAD-CHO	specific caspase-1 like protease inhibitor
Z-VAD-FK	broad specificity caspase inhibitor

ACKNOWLEDGEMENTS

First and foremost I thank Associate Professor Gillian Bushell and Professor Alan Mackay-Sim, and Drs Wayne Murrell and Francois Feron, for the encouragement, direction, patience and friendship that you have collectively given me.

To the Garnett Passe and Rodney Williams Memorial Foundation, I express gratitude and appreciation for the receipt of a Postgraduate Research Scholarship, together with laboratory funding.

I also thank my colleagues and friends within the School of Biomolecular and Biomedical Science for the assistance, honesty, and many social occasions that we have shared. I also thank Dr Peter Wilce and members of the Alcohol Research Unit for the patience and friendships that I have encountered.

To my family, particularly my parents Julio and Maria, I extend my sincerest gratitude for your unceasing love, and support, and above all, for the admiration and respect that you have inspired in your relationships with and amongst my siblings Julio, Paul, Maria, and myself.

Finally I say thank you to Dave, for your love and affection. Rarely does a testing moment unsettle you, part of your character that has provided me with the resilience and buoyancy to finish in spite of the obstacles encountered along the way.

STATEMENT OF ORIGINALITY

The work described in this thesis was carried out in the School of Biomolecular and Biomedical Science, Faculty of Science, Griffith University, under the supervision of Associate Professor Gillian Bushell, Professor Alan Mackay-Sim and Dr Wayne Murrell. This work has not previously been submitted for a degree or diploma in any university. To the best of my knowledge and belief, the thesis contains no material previously published or written by another person except where due reference is made in the thesis itself.

Rachel de las Heras

1 GENERAL INTRODUCTION

1.1 Introduction

Neuronal differentiation encompasses an elaborate developmental program controlled by both endogenous and exogenous factors. The orchestrated expression of transcription factors, cell surface markers, structural proteins and signal transduction pathway components is required, and these are but a few of the necessary molecules that must interact and relay information within each precursor cell, and more globally within the neural tissue. Cells readily couple the extracellular matrix and associated regulatory factors with intracellular phosphorylation events, gene expression and protein production to induce growth, differentiation, survival and apoptotic responses (Boudreau and Jones, 1999; Vleminckx and Kemler, 1999; Blanchard, 2000). In the discourse to follow, particular emphasis is placed on neuronal differentiation of the mammalian olfactory system, a model upon which many research studies have been based, given the inherent obstacle of investigating conditions of the nervous system, highlighted by the inability to directly sample tissue that in most cases has undergone development without the opportunity for repair processes to occur. The olfactory epithelium therefore provides an attractive tool with which to investigate fundamental questions relating to neuronal differentiation, an understanding of which could provide preventative or management therapies, while understanding the complexity of neuronal determination could also provide cell transplant opportunities.

1.2 Neuronal Differentiation

The organised execution of the differentiation program requires the expression of a molecular hierarchy of genes in sequence (Crews and Hunter, 1994). Determining molecular regulation can be difficult with contradictory results and cellular multitasking (Jordan et al., 2000) problems to resolve. What dictates the transition between proliferation, apoptosis, growth arrest and differentiation? Paradoxically, a growth factor can induce survival and proliferation but can also arrest growth and cause apoptosis. For example, in the olfactory epithelium the current view is that fibroblast growth factor 2 (FGF2) stimulates proliferation of the globose basal cells (Newman et al., 2000), however in a human derived olfactory cell line, FGF2 stimulated proliferation and induced differentiation (Ensoli et al., 1998). The view that growth factors and other signals vary

the probability of some event happening, such that in a population of cells the event will happen but not necessarily be seen in every individual cell (Mackay-Sim, personal communication) can clarify discrepancies between in vivo and in vitro studies. However, the lack of universality between in vitro models and outcomes for a particular neurotrophic factor provides evidence that the paradigm illustrated does not address an important issue, that is, what is the effect of the context of the cell? For example, a quiescent cell may not respond with quiescence but only with proliferation, and likewise a proliferating cell may respond not with proliferation but with differentiation (Blagosklonny, 1999). The linear view that a growth factor binds to its receptor and elicits a direct single response does not take into account cellular context. More appropriate is the idea "that stimuli that regulate cell growth may initiate proliferative and anti-proliferative signals simultaneously" (Blagosklonny, 1999). Additionally, exposure to a growth factor may prime the cell to respond to stimuli otherwise ignored, but present within the extracellular environment. Cellular context questions the state of the cell at a given point in time. A detailed analysis of growth factors is beyond the scope of the present discussion but for a thorough review of neurotrophic factors in the primary olfactory pathway see Mackay-Sim and Chuah, (2000).

Beyond growth factors lies a greater quandary, that of intracellular signalling pathways. Signalling networks represent a common characteristic between all cell types, that is, the ability to coordinate their activities with environmental changes. Hence a cellular response to a growth factor is only as strong as the ability of the intracellular machinery to detect it. In turn, cell fate determination governed by transcriptional events in response to external communication relies on this signalling machinery. Like the growth factor dilemma, signal transduction is dependent on cellular context. The rat adrenal pheochromocytoma clonal cell line PC12 has provided useful insight into the regulation of the signal transduction cascade during neuronal differentiation and death. PC12 cells differentiate with neuron-like characteristics. Treatment of PC12 cells with nerve growth factor (NGF) results in neurite extension (Greene and Tischler, 1976). Upon binding of NGF, the cell surface receptor tyrosine kinase (Trk) A is activated. Active TrkA recruits via adapter proteins and exchange factors, the GTP-binding protein (G-protein) Ras. Ras in turn activates members of the mitogen-activated protein kinase (MAPK) cascade, including MAPK kinase kinase (MAPKKK)/Raf, a serine threonine kinase, that activates MAPK kinase (MAPKK)/MEK and finally MAPK/extracellular

signal-regulated kinase (ERK) which translocates and transactivates transcription factors, changing gene expression to promote growth, differentiation or mitosis (Seger and Krebs, 1995; Tibbles and Woodgett, 1999). Stimulation of the ERK pathway is believed to play a crucial role in NGF-induced neurite extension (Cowley et al., 1994). Studies have shown that constitutively active MEK, induced neurite outgrowth and that blockade of the ERK pathway using dominant-negative MEK or the MEK inhibitor PD98059 resulted in inhibition of NGF-induced neurite development (Dudley et al., 1995; Fukuda et al., 1995; Pang et al., 1995). Nonetheless contradictory findings have been reported, in which NGF-induced neurite outgrowth of PC12D cells, a subline of PC12 cells, was shown to be resistant to the addition of PD98059 (Sano and Kitajima, 1998). Furthermore, neuronal differentiation of PC12 cells in the absence of ERK activation was induced by treatment with bone morphogenic protein (BMP)-2 (Iwasaki et al., 1996). Consequently it is clear that signalling pathways other than the ERK cascade also contribute to neuronal differentiation of PC12 cells. This illustrates well the importance of cellular context, particularly as it becomes apparent that linear signal transduction pathways are not "free-standing entities but parts of larger networks" (Jordan et al., 2000), where junctions and nodes are significant components of the network as a whole, providing means by which signals can be integrated, split and routed to generate multiple outputs. Jordon et al. (2000) clearly describe the cellular networking of transduction cascades with relevant examples to illustrate the complexity of understanding cellular context (Figure 1-1) (Jordan et al., 2000).

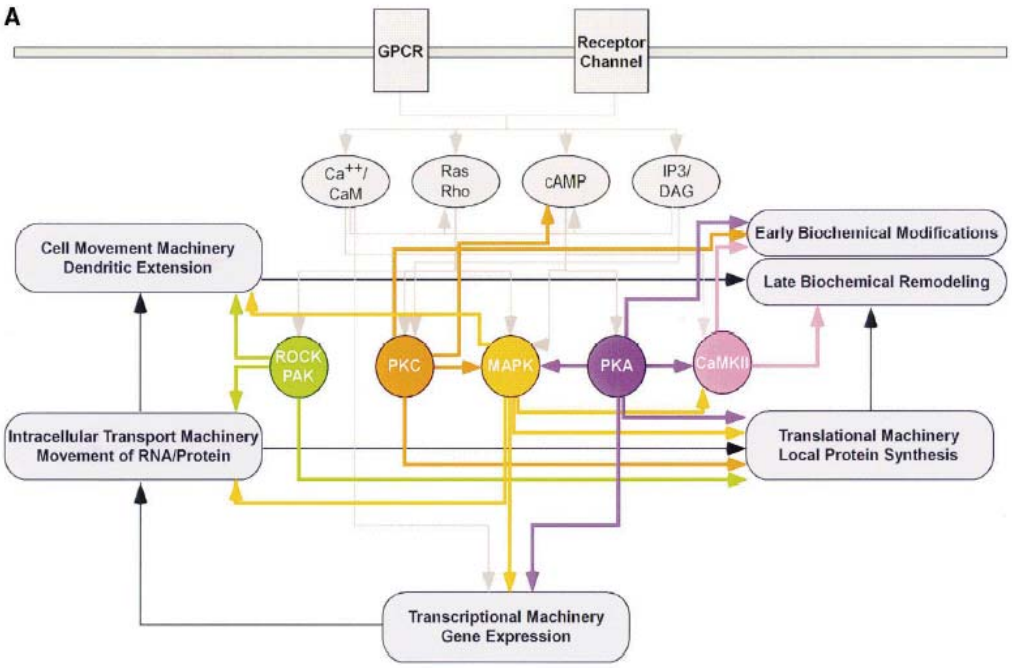

Figure 1-1 Postsynaptic signalling network.

Key elements of the postsynaptic signalling network in the CA1 pyramidal neuron highlighting the connections between the different kinases and cellular machinery. Each protein kinase in the network can regulate multiple cellular functions. Figure from Jordan et al. (2000).

1.2.1 Neuronal Differentiation And The Cell Cycle

As has been briefly illustrated above, cellular context questions the state of a cell. However it is well established that several distinct cellular processes, including neuronal precursor exit from the cell cycle, govern neuronal differentiation. The molecular processes regulating the cell cycle are fundamentally similar in all eukaryotic cells (Bybee and Thomas, 1991). The cell cycle consists of four distinct phases, G_1 phase (the first gap) before DNA synthesis occurs, S phase when DNA replication occurs, G_2 phase (the second gap) after DNA synthesis and the M (mitotic) phase when cell division occurs. When growth conditions are limiting, cells exit the cell cycle during G_1 and remain in a G_0 state as nongrowing, nondividing (quiescent) cells. Appropriate stimulation of quiescent cells induces them to return to G_1 and resume growth and division (Lodish, 1995). Heterodimeric protein kinase complexes control cell cycle progression. The regulatory subunit is comprised of a cyclin, so named because its concentration cycles in phase with the cell cycle. The constitutively expressed catalytic subunit known as a cyclin dependent

kinase (CDK) does not display any kinase activity unless associated with a cyclin. Each CDK catalytic subunit can associate with different cyclins, and the associated cyclin determines which proteins the cyclin-CDK complex phosphorylates. Different cyclin-CDK complexes control progression through the distinct stages of the cell cycle (Arellano and Moreno, 1997; Roovers and Assoian, 2000). Importantly the duration and timing of cyclin expression determines the phase of the cell cycle in which their associated CDK is active. Therefore "cyclin abundance is rate limiting for progression through the different stages of the cell cycle" (Lees, 1995).

Environmental cues from growth factors and the extracellular matrix provide the level of control that determines whether a cell will proliferate or lay quiescent. The binding of growth factors to various receptors and matrix proteins to integrins transduces signals via the cytoplasmic MAPK cascades to exert their effects on key cell cycle regulators (Roovers and Assoian, 2000). During normal growth conditions, the cell cycles continuously. Progression through the G_1 phase is regulated by cyclin D-CDK4/CDK6 and cyclin E-CDK2 complexes (Sherr, 1994), the stimulatory effects of which can be counteracted by CDK inhibitory proteins (CKIs) (Roovers and Assoian, 2000). Both CDK4/CDK6 and CDK2 also require activation via phosphorylation by cyclin-activating kinase (CAK). Research to date has demonstrated that extracellular signals through receptor kinases (eg. receptor tyrosine kinase) and integrins control G_1 progression by regulating the expression of cyclinD and/or down-regulating the CDK-inhibitory proteins, $p21^{cip1}$ and $p27^{kip1}$ (Roovers and Assoian, 2000).

The cyclin-E/CDK2 complex is responsible for the G1 to S phase transition. Following entry into the S phase, CDK2 associates with cyclin-A, a complex that is responsible for DNA synthesis and progression through the S phase. During the G_2 phase, complexes necessary for mitosis accumulate. Cyclin-B, first synthesised during the S phase, associates with CDC2 (CDK1), while cyclin-A, now associated with CDC2 (CDK1), also increases in concentration as the cycle proceeds through the G_2 phase, peaking in early mitosis (Figure 1-2), (Lees, 1995; Roovers and Assoian, 2000). The question of how the cell cycle machinery is tightly and co-ordinately regulated and controlled by various mechanisms has been reviewed thoroughly (Lees, 1995; Arellano and Moreno, 1997; Cook et al., 2000; Harbour and Dean, 2000).

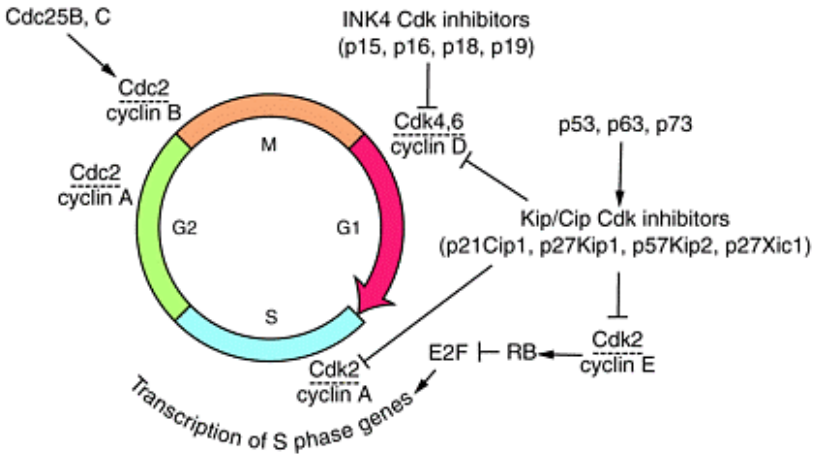

Figure 1-2 Cell cycle components.

Components of the cell cycle responsible for progression through the indicated phase. Figure from Ohnuma et al. (2001).

The mechanism that directs neuronal differentiation must be linked, directly or indirectly, to cell cycle regulation. When terminal differentiation occurs the cell must exit the cell cycle and enter quiescence or G_0. A variety of experimental conditions, including addition of growth factors, extracellular matrix molecules, or serum deprivation, have been used to differentiate neuronal precursor cells (Tomaselli et al., 1990; Kuo et al., 1997; Qi et al., 1997; Ensoli et al., 1998; Klesse et al., 1999; Newman et al., 2000). In each case a common theme is the subsequent activation of the ERK cascade. Activation of the Ras→Raf→MEK→ERK pathway has been tied to induction of cyclin D1 (Lavoie et al., 1996). Importantly, the intensity and duration of the ERK activation state are crucial for determining whether a cell proliferates or arrests during G_1 passage. Sewing et al. (1997) demonstrated that a strong Raf signal is required for G_1-specific cell cycle arrest by inducing the CDK-inhibitory protein, $p21^{cip1}$, which inhibits cyclin D and cyclin E dependent kinases (Sewing et al., 1997; Woods et al., 1997). It appears that the "critical determinant in the induction of cyclin D1 is the duration, rather than the intensity of the ERK signal (Figure 1-3)" (Roovers and Assoian, 2000).

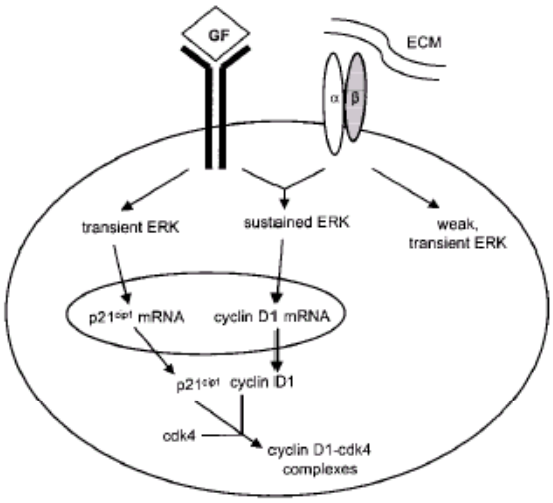

Figure 1-3 Sustained versus transient ERK activation on the cell cycle.

The cooperative effects of integrins and growth factor receptors results in a sustained ERK signal associated with the induction of cyclin D1. Initiation of integrin signalling results in a transient and relatively weak activation of ERK, while initiation of receptor tyrosine kinase signalling by strongly mitogenic concentrations of growth factors results in a strong, transient ERK signal sufficient to induce $p21^{cip1}$. Figure from Roovers and Assoian (2000).

In the nervous system as in other systems, the cell cycle is closely tied to cell determination, and consequently cell differentiation (Ohnuma et al., 2001). McConnell and Kaznowski (1991) demonstrated that the laminar fate of cortical neurons is determined during the S phase or G_2 phase of the final cell cycle, indicating the influence that the cell cycle has on the determination process. Ohnuma et al. (2001) summarise recent experiments demonstrating the various molecules that can actively participate in determining neuronal cell fate choice and regulating cellular differentiation, including CDKs and CDK inhibitors. Regulators of the cell cycle can also influence the differentiation of neural cells, as demonstrated by the simultaneous down-regulation of CDC2 and CDK2 activity necessary for neuronal differentiation of PC12 cells (Dobashi et al., 2000). Recently however, it was found that neuronal differentiation of P19 mouse embryonal carcinoma cells with retinoic acid required the up-regulation of $p27^{kip1}$ (CDK-inhibitory protein), indicating that $p27^{kip1}$ expression is indispensable for neuronal differentiation (Sasaki et al., 2000). Whilst, dominant negative mutants of CDK4 and CDK6 effectively induced mitotic arrest in primary neural precursor cells, independent of the previously proposed binding and sequestration of $p21^{cip1}$ and $p27^{kip1}$ via the tumour suppressor retinoblastoma (Rb) pathway (Ferguson et al., 2000). These examples highlight the intricate nature of determining which cell cycle components are crucial for neuronal differentiation and determination. Evidently different cell lines rely on different key cell cycle regulatory components. The challenge is to determine the signalling pathways that lead to activation of these components, which may provide some insight

into the discrepancies between *in vitro* neuronal differentiation model systems. Understanding the signalling cascades involved in progression through the cell cycle, relative to associated changes in cell shape and cytoskeletal tension imparted by the extracellular matrix, provides an understanding of the importance of the structural and mechanical complexity of the cell environment (Huang and Ingber, 1999). In the discussion to follow, the ability of the extracellular matrix to regulate the cell cycle via signal transduction pathway modulation will be discussed.

1.2.2 Neuronal Differentiation And The Extracellular Milieu

Cellular recognition of the extracellular environment is fundamentally important for development, maintenance of normal adult tissue architecture and function (McCarthy, 1993). Execution of neuronal differentiation requires that the immediate extracellular environment is conducive to cell cycle arrest and differentiation. Far from being a passive structure the extracellular matrix (ECM) plays a pivotal role in the presentation of locally acting molecules such as growth factors, ephrins and cadherins from neighbouring cells, laminin, fibronectin, collagen, and proteoglycans (Streuli, 1999; Bovolenta and Fernaud-Espinosa, 2000). The ECM can influence cell behaviour, actively sequestering or mobilising mitogenic molecules (eg. growth/survival factors and cytokines) by matrix remodelling through the action of serine proteases and matrix metalloproteinases (Streuli, 1999). By cleaving specific ECM proteins, proteases can create architectural changes in the matrix structure allowing the concealment or exposure of growth factors to cell surface signalling receptors (Figure 1-4) (Nagase and Woessner, 1999). Moreover, cell-cell and cell-ECM interactions are required to guide processes such as cell migration and neurite extension, via mediation with cell surface glycoproteins and ECM constituents (Suter et al., 1995). Cell adhesion molecules and surface adhesion molecules form the core components of this interactive process (Edelman and Crossin, 1991). Unlike other proteins, adhesion molecules can provide an explanation of how a “one-dimensional genome can control the formation of three-dimensional structures” (Jones and Murray, 1991).

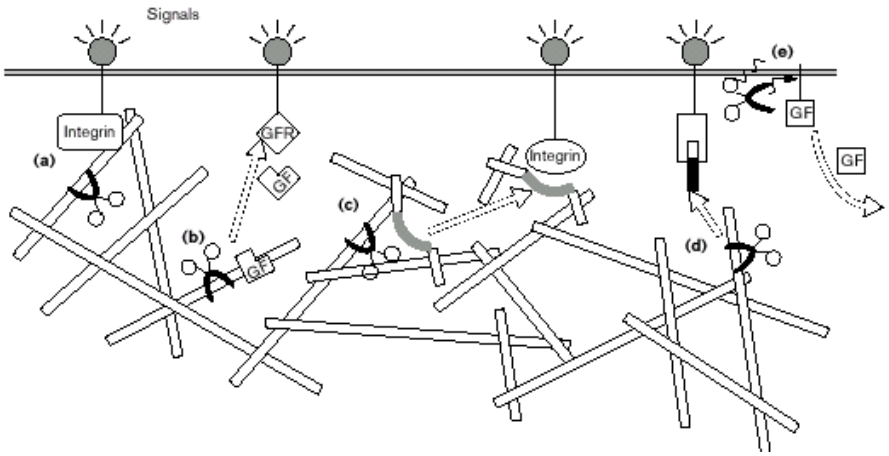

Figure 1-4 ECM remodelling can affect cellular differentiation in several ways.

(a) Remodelled ECM directly changes cell-ECM interactions. (b) ECM remodelling releases bound growth factors (GF). (c) Exposure of cryptic sites (grey bands) within the ECM alters integrin signalling. (d) ECM remodelling releases active ECM fragments (black bar). (e) Surface-bound ECM remodelling enzymes shed growth factor ectodomains. GFR, growth factor receptor. Figure from Streuli et al., (1999).

Cell adhesion molecules belong to the immunoglobulin superfamily, and are involved in calcium dependent homophilic binding to identical molecules and heterophilic binding to structurally unrelated molecules on neighbouring cells (Suter et al., 1995). Cell surface expressed adhesion molecules have the capacity to potentiate this interaction via their ability to link cells together, thus cell adhesion molecules can guide correct development and can maintain tissue structure in the mature form (Jones and Murray, 1991). Over 30 different cell adhesion molecules have been classified, a subset of which undergo alternative splicing and post-translational modifications (eg. amount of associated sialic acid) (Jones and Murray, 1991). Although cell adhesion molecules are highly dynamic and are also environment dependent to some extent, their action relies more heavily on the genetic program of the cell at different developmental stages. In contrast, surface adhesion molecules mediate cell-surface adhesive contacts. Surface adhesion molecules are more responsive to the extracellular environment, thus environmental stresses may be transduced to the cell interior and consequently magnified in terms of the effects that result on development. Transmembrane proteins link the ECM with the intracellular environment mediating this responsive and dynamic process.

Integrins are transmembrane proteins that provide an important information route and a mechanism for cells to regulate cell migration, cell adhesion, wound healing, and the inflammatory response (Sjaastad et al., 1994). Binding of the integrins to the ECM, triggers intracellular signalling pathways that also regulate molecular mechanisms such as proliferation, genetic induction and ultimately cellular differentiation. The integrins are a family of heterodimeric, trans-membrane glycoproteins that are comprised of α and β subunits in a noncovalent association (Coppolino et al., 1995). The domains of the α and β subunits together form a ligand binding site on the cell exterior, allowing cell association with the ECM and some serum and complement proteins (Hemler, 1993). As different integrins bind distinct subsets of ligands, cells can express a diverse repertoire of integrins on their surface providing a source of diversity for cell-matrix interactions and an array of cellular responses. The cytoplasmic domains of both the α and β integrin subunits can partake in interactions with intracellular proteins, which unlike extracellular ligand binding can occur independently of subunit association in vitro (Hemler, 1993). The broad programs of cellular responses to the ECM come about by the existence of approximately 20 distinct α-β heterodimers. These different integrins translate adhesive signals into a diversity of post-ligand-binding events by virtue of the β cytoplasmic domain of the integrin (Hemler, 1993). For example the β_1 subunit has been shown to interact with components of the cytoskeleton allowing a mechanical link to the ECM (Chen et al., 2000). Cytoplasmic interactions involving the α subunits have been less well characterised.

The dynamics of cellular adhesion are diverse, and include several aspects of regulation of the mechanism of adhesion itself. Integrin receptors mediate an assorted array of cellular responses. Receptor occupancy and aggregation provide a means by which a single integrin can produce a repertoire of functions, by virtue of the association of the integrin with other integrins (Miyamoto et al., 1995). A series of experiments performed by Miyamoto et al. (1995), demonstrated that integrin receptors induce distinct cellular responses to binding of a ligand, to receptor aggregation, or to a combination of receptor binding and aggregation. For example integrin occupancy by monovalent ligand redistributed integrins but failed to induce tyrosine phosphorylation signalling and cytoskeletal reorganisation. In contrast, integrin aggregation by non-inhibitory monoclonal antibodies induced intracellular accumulation of focal adhesion proteins and

their phosphorylation, but failed to accumulate other cytoskeletal proteins. However a combination of integrin aggregation and occupancy resulted in accumulation of cytoskeletal proteins (Miyamoto et al., 1995). Other regulatory aspects of cellular adhesion rely on the activation state of the ligand and functionality of certain integrins that are expressed inactive, but that can be rapidly converted to an active state without the requirement for new protein synthesis (Hemler, 1993). In contrast, other cell types express functionally active integrins, which lose their function during cell differentiation, although surface expression continues (Hemler, 1993). Consequently the dynamics of adhesion is dependent on the activation state of the integrin, the external environment, and the intracellular context of the cell and on the association of integrins with intracellular proteins.

One of the key players in regulating cell cycle progression is focal adhesion kinase (FAK, or $pp125^{FAK}$), which communicates with extracellular matrix signals via the integrins. FAK was functionally linked to the integrins because of the observation that clustering of integrins, either with anti-integrin antibodies or by plating cells on fibronectin, resulted in tyrosine phosphorylation of a 120-130 kDa protein(s) (Guan et al., 1991; Kornberg et al., 1991). Hence FAK is a downstream transducer of an integrin mediated-signal, one of the first proteins to relay extracellular information to the intracellular signalling complex. Upon phosphorylation of FAK by active integrins, FAK is able to form protein complexes with the SH2 domains of other signalling molecules including, sarcoma (Schmidt-Ruppin A-2) viral oncogene (Src), growth factor receptor bound (Grb)7, and phosphatidyl-inositol-3-kinase (PI3K) (Reiske et al., 2000). Differential complex formation by FAK results in different biological outcomes. For instance the FAK/Src complex plays a critical role in cell cycle regulation by signalling through ERK, as opposed to the FAK/PI3K and FAK/Grb7 complexes (Reiske et al., 2000). FAK also participates centrally in cell migration and neurite extension processes driven by the ECM. FAK is further discussed in Chapter four.

1.2.3 Neuronal Differentiation And Neurite Extension And Migration

An important component involved in cell migration and neurite extension is the actin cytoskeleton. Bi-directional signalling between the cytoskeleton and the ECM through the integrins provides a means by which information can be transferred back and forth as cells adjust their morphology and position to maximise survival and growth (Schoenwaelder and Burridge, 1999). The information encoded in ECM molecules must culminate in cytoskeletal rearrangement and the addition of new membrane to the extending neurite (Perron and Bixby, 1999). This process is achieved by various signal transduction pathways activated by a variety of axon growth inducers such as growth factors, N-cadherin and laminin which exert their actions on the actin cytoskeleton (Perron and Bixby, 1999; Dimitropoulou and Bixby, 2000). For example, the neuroblastoma cell N1E-115 deprived of serum and grown on a laminin matrix, exhibits integrin-dependent neurite outgrowth by signalling via Ras through PI3K to the Rho family GTPases (Rho, Cdc42, and Rac) (Sarner MCB 2000). While ERK activation is a convergence point for signalling pathways generated by a variety of axon growth inducers (Perron and Bixby, 1999; Dimitropoulou and Bixby, 2000), FAK participates centrally in neurite extension and migration. In PC12 cells Anneren et al. (2000) demonstrate increased neurite outgrowth by a signalling pathway through FAK, while a subline, PC12-E2, induced to extend neurites with neural cell adhesion molecule, was dependent on activation of FAK and the MAPK signalling cascade (Kolkova et al., 2000).

Importantly, neurite outgrowth involves transmembrane links between the ECM and the actin cytoskeleton, formed by the integrins and clustered into specialised adhesive structures termed focal adhesions (FAs) and focal complexes (Schoenwaelder and Burridge, 1999). Numerous signalling components reside within focal complexes. However, much of the actin organisation and integrin distribution is driven by the Rho family GTPases by signalling through several serine/threonine kinases that promote myosin filament assembly and actin-activated myosin ATPase activity (Schoenwaelder and Burridge, 1999). By controlling the actin cytoskeleton and the formation of focal contacts, the cell is able to anchor to a substrate or allow migration and extension of long processes. An important aspect of movement is the assembly and disassembly of the focal adhesions that occur at the tips of filopodia or lamellipodia. The rapid turnover of focal

complexes at these sites is primarily driven by FAK, as cells deficient in FAK display reduced motility (Ilic et al., 1995). Although adhesive interactions influence cytoskeletal organisation the cytoskeleton also affects the organisation and function of adhesive molecules at the cell surface by clustering integrins into focal adhesions and focal complexes (Schoenwaelder and Burridge, 1999). The reciprocal nature of this interaction allows the cytoskeleton not only to cause morphology change and neurite outgrowth, but to act as a sensor and respond to change by signalling through FAK to alter focal complexes and subsequently to signal through the Ras/ERK signalling cascade (Irigoyen and Nagamine, 1999).

1.2.4 Neuronal Differentiation And Apoptosis

A normal phenomenon of neuronal differentiation is apoptosis, otherwise known as programmed cell death. Apoptosis is considered an active process because in contrast to passive cell death induced by toxins (necrosis), apoptosis requires the synthesis of new proteins (Altman, 1992). The importance of apoptosis is evident when one considers that between 30% and 40% of all cells generated in the nervous system die by the time maturation is reached (Cowan et al., 1984). For example, in the olfactory epithelium some cells die shortly after division (Carr and Farbman, 1992; Holcomb et al., 1995), whilst the majority of developing neurons die approximately 2 weeks later, after which any surviving neurons are sustained for several months (Moulton, 1974; Hinds et al., 1984; Mackay-Sim and Kittel, 1991). Widespread-programmed cell death may appear to be an unfavourable and wasteful exercise, however multiple chances of generating functional connections is fundamental. Without this process, correct neuronal density, connectivity and function may not be achieved.

Apoptosis is regulated by a series of orchestrated biochemical cascades, dubbed the death program, as they commit a cell to death (Altman, 1992). In *C.elegans*, it appears that the expression of various genes within the ces (cell death specification) and ced (cell death abnormal) families are responsible for:

1) determination, specifying which cells will die,

2) triggering an internal factor presumed to initiate the lethal cascade,

3) killing, initiation of the biochemical events that destroy the cell,

4) protection, the blockade of apoptotic pathways if the responsible gene is activated,
5) engulfment, the mediation of phagocytosis, and,
6) degradation, the expression of nuclease-1 that results in the breakdown of nucleic acids (Margolis et al., 1994).

The characteristic morphology of apoptotic cells includes cytoplasmic shrinkage, membrane blebbing, nuclear condensation and DNA fragmentation (Widmann et al., 1998), processes that accompany the activation of caspases, a family of aspartic acid-directed proteases (Alnemri et al., 1996). Caspases are synthesized as zymogens that undergo a minimum of two cleavages to generate a mature enzyme with enhanced catalytic activity (Earnshaw et al., 1999). Caspase mediated proteolysis of their natural substrates, including protein kinases (eg. FAK), signal transduction pathway kinases (eg. MEKK1), and proteins involved in proliferation and the cell cycle, results in irreversible commitment to cell death (Earnshaw et al., 1999). Typically initiator zymogens undergo scaffold-mediated activation, a mechanism that involves assembly of a molecular platform in response to death stimuli triggered by cell surface receptors (TNF receptor, death receptor (DC) 3/4 and 5, and CD95/Fas/Apo-1) which provide the scaffold upon binding of their ligands (Earnshaw et al., 1999). Scaffold-mediated activation can also occur in response to environmental insults without prior ligation of death receptors. Recruitment of initiator caspases to the scaffold provides an environment in which the local zymogen concentration is increased and conformation changes can occur, allowing zymogens to efficiently catalyse each other and/or autocatalyse themselves producing highly active mature caspases (Ramage et al., 1995; Earnshaw et al., 1999). Once activated caspases cleave numerous cellular targets, disrupting cellular function. Caspase activation can be regulated at several levels, most notably by the anti-apoptotic Bcl-2 family members and by the cellular inhibitor of apoptosis proteins (cIAPs) (Earnshaw et al., 1999). Although caspase activation is a typical response of apoptotic cell death, recent data has illustrated an unlikely role for activation of caspases, that is as key proteases in the process of erythroid differentiation (Zermati et al., 2001) and in the terminal differentiation of epidermal keratinocytes (Weil et al., 1999). Both erythroid and keratinocyte terminal differentiation require nuclear condensation, loss of organelles and enucleation, processes that share similarities to the morphological changes observed during apoptosis (Zermati et al., 2001). This illustrates the point that although the classical view of caspase activation

is in their involvement in cell death, increased understanding of caspase function reveals that they may be involved in activation of molecules required for processes such as transcription factor activation and signal transduction component activation, without eliciting cell death (Zeuner et al., 1999).

1.3 Neuronal Differentiation And The Olfactory Epithelium

Understanding the complex molecular events that direct neuronal differentiation forms the basis of a plethora of research, both at the fundamental pure science and clinical levels. An inherent obstacle in neuroscience stems from the inability to directly sample tissue that has undergone development. An understanding of the normal neuronal differentiation program would undoubtedly allow a greater understanding of potential developmental deviations. This could provide an opportunity for therapies to be conceived, while understanding the complexity of neuronal determination could also provide opportunities for stem cell transplantation. As illustrated below, the developmental program affected during the birth and restructure of the olfactory neuroepithelium provides an opportunity to examine such processes.

1.3.1 The Significance Of The Olfactory Epithelium

An understanding of the fundamental molecular mechanisms involved in olfactory neurogenesis has arisen in part due to the popularity of using the olfactory epithelium in neuronal differentiation studies. Several important attributes unique to the olfactory epithelium are responsible for this. One such feature is the peripheral location of the olfactory epithelium, which provides non-invasive access to sample fresh tissue from laboratory animals, humans involved in case studies (Feron et al., 1999) and at autopsy (Murrell et al., 1996). More importantly, the olfactory epithelium displays a unique capacity to regenerate (Figure 1-5) and to retain a neurogenetic potential from its genesis and throughout adult life (Graziadei, 1978; Gordon et al., 1995; Roskams et al., 1998). The intrinsic regenerative capacity of the olfactory epithelium is demonstrated by the ability of the basal cells within the olfactory neuroepithelium to sustain the replacement of neurons, even when experimentally induced destruction of the mature olfactory receptor neurons has occurred, leading to complete restoration of the morphology and functionality

of the olfactory epithelium (Graziadei, 1978). For this reason the olfactory epithelium is a model system for neuronal differentiation, providing insights into the mechanisms responsible for neurite extension, axon guidance and neuronal patterning.

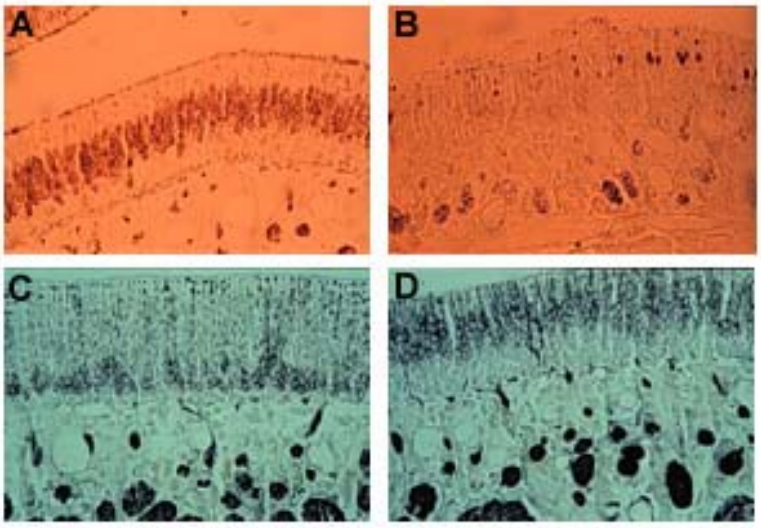

Figure 1-5 Olfactory epithelium dynamics identified immunologically during regeneration.

Olfactory sensory neurons are identified with an antibody to olfactory marker protein (A). The neuronal cell bodies located in the central region of the olfactory epithelium extend dendrites forming a knob at the lumenal surface. (B) The olfactory epithelium is devoid of sensory neurons positive for olfactory marker protein following bulbectomy. (C) Growth associated protein-43 (GAP-43) staining in normal olfactory epithelium detects immature neurons located beneath the olfactory sensory neurons. (D) GAP-43 positive immature neurons respond to migratory cues within the bulbectomised epithelium and migrate away from the lower portion of the epithelium. The immature neurons differentiate as they migrate up through the epithelium becoming mature sensory neurons. All images are courtesy of Dr. François Féron.

The regenerative capacity of the olfactory epithelium has also been shown to be indistinguishable from that which occurs initially at the olfactory placode (Roskams et al., 1998). The mechanisms responsible for olfactory receptor neuronal differentiation from basal cells at the embryonic stage are analogous to those active mechanisms that cause differentiation in the adult olfactory epithelium. This concept has been demonstrated by expression studies of neuron-specific β-tubulin type III, in which the developmental expression pattern is recapitulated when neurons undergo a synchronised neurogenic response, as occurs following chemical lesion in the adult neuroepithelium (Roskams et al., 1998). In addition, cells expressing Mash 1 (Mammalian aschaete-scute homologue 1), a transcription factor expressed in neural precursors, behave analogously in adult and embryonic olfactory epithelium (Guillemot et al., 1993), suggesting that the part of the

olfactory receptor lineage pathway responsible for Mash1 expression is conserved from embryo to adult (Gordon et al., 1995). The evidence for retention of a conserved neurogenic program supports the use of the regenerating olfactory epithelium to study and model normal neuronal development, particularly for areas of the nervous system in which regeneration does not occur. Hence the olfactory epithelium is expected to reveal general neurogenetic principles and mechanisms common to other neural regions.

1.3.2 Development Of The Olfactory Epithelium

The concept of primary olfactory neuronal differentiation occurring exclusively from the olfactory placodes was reported by His (1889), Cajal (1890) and Disse (1901,1902) [quoted in (Graziadei, 1978)]. The olfactory epithelium is initially seen as a horseshoe structure that envelops the olfactory pits, which form from the rapid expansion of mesenchyme around the olfactory placodes. It is presumed that as development continues, the heightening mesenchyme generates a depression (olfactory pit) which consists of the presumptive olfactory tissue (Getchell, 1991). The placodal patches that form are part of the anterolateral edge of the neural plate and these areas become detached from the surrounding mesenchyme as a result of differential growth preceding closure of the neural tube (Verwoerd et al., 1979) [quoted in (Getchell, 1991)]. Recently it was shown that the key initiating signal, retinoic acid, released from the lateral cranial mesoderm activates a retinoic acid inducible transgene in neuroepithelial cells in the olfactory placode and the ventrolateral forebrain (LaMantia et al., 1993). This signal appears to be sufficient to drive localised neuronal differentiation and axon innervation into the ventrolateral forebrain forming the mammalian olfactory pathway (LaMantia et al., 1993). This finding was confirmed by another study, in which the absence of an olfactory epithelium and olfactory bulb in homozygous Pax6 mutant mice results from the inability of these mice to produce retinoic acid from the frontonasal mesenchyme (Anchan et al., 1997).

The olfactory pit is lined with a pseudostratified columnar epithelium which consists of three rudimentary cell types: 1) olfactory receptor neurons; 2) basal cells; and 3) supporting cells (Farbman, 1977). The nuclei of the basal cells lying nearest to the basement membrane of the epithelium pass through a restricted lineage pathway resulting

in the production of olfactory receptor neurons. The nuclei of the olfactory neurons which rest in the central region of the epithelium send their axons to contact the telencephalic region that will subsequently differentiate and give rise to the olfactory bulb, and establish synaptic contact with the mitral, tufted and periglomerular cells. The olfactory receptor neurons also extend a dendritic process to the epithelial luminal surface that terminates in a ciliated knob and provides direct contact with the environment (Getchell, 1991). These dendritic processes are protected by the sustentacular (supporting) cells, which lie closest to the lumenal surface (Crews and Hunter, 1994).

As noted earlier, the ability of the olfactory epithelium to produce a new set of mature olfactory receptor neurons on demand is a result of an asymmetrically dividing stem cell located within the basal cell layer (Mackay-Sim and Kittel, 1991). The asymmetric division produces another stem cell that stays close to the basement membrane and a neuronal precursor that undergoes several rounds of division to produce a series of immature neurons. The immature neurons then differentiate and migrate away from the basement membrane to assume a central position within the epithelium when differentiation is complete (Figure 1-6) (Mackay-Sim and Kittel, 1991; Mackay-Sim and Chuah, 2000). Mackay-Sim and Kittel (1991) determined the life span of olfactory receptor neurons by injection of a retrograde tracer into the olfactory bulb. Labelled mature olfactory receptor neurons located at the olfactory epithelium were found at periods of at least 90 days post olfactory bulb injection. Previously the life span of olfactory receptor neurons was estimated to be 30 days by [^{3}H] thymidine tracking (Moulton, 1974; Graziadei, 1978) and up to 1 year when adult mice were reared in a laminar flow hood (Hinds et al., 1984). These estimates were challenged however (Mackay-Sim and Kittel, 1991), because [^{3}H] thymidine only labels dividing cells and thus would estimate the lifespan of neuronal precursors and not necessarily the neurons themselves. Additionally, the assumption that labelled cells had “entered the population via division of basal cells and left it as mature neurons” also gave a false indication of life span (Mackay-Sim and Chuah, 2000). At any given point in time there exists a broad population of olfactory receptor neurons of different ages and hence different stages of neuronal differentiation. This does not indicate that subpopulations of receptor neurons exist (Allen and Akeson, 1985), simply that there are cells of differing ages (Getchell, 1991; Crews and Hunter, 1994).

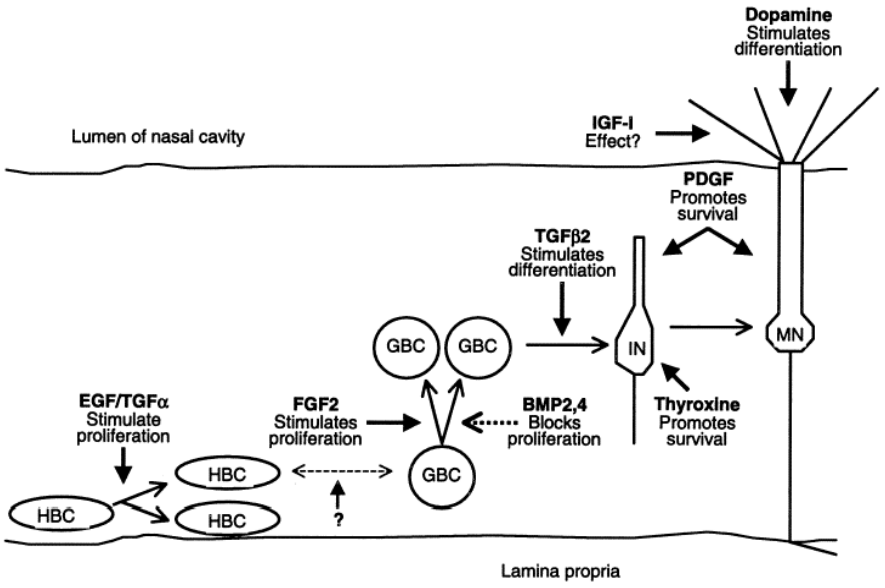

Figure 1-6 A schematic diagram of the cell lineage relations between basal cells and mature olfactory receptor neurons.

The relationship between horizontal basal cells (HBC) and globose basal cells (GBC) has yet to be defined. Neurotrophic factors important for various processes of neuronal development are shown. IN, immature neuron; MN, mature neuron. Figure from Mackay-Sim and Chuah (2000).

A particular problem of determining how olfactory receptor neurons arise from undifferentiated, multipotential, self-renewing stem cells is the identity of the true stem cell within the olfactory epithelium. The precursors of olfactory receptor cells are the basal cells, however two distinct basal cell types exist, based on histological appearance, location within the epithelium and protein expression profile. The horizontal basal cells are ovoid and lie nearest to the basal lamina whilst the globose basal cells are more nearly spherical and are located more superficially (Crews and Hunter, 1994). All globose basal cells can be identified with the antibody GBC1-3 (Goldstein and Schwob, 1996), whilst Guillemot and colleagues (Guillemot et al., 1993) showed that some globose basal cells express Mash1, a transcription factor expressed early in the lineage pathway. However, this study did not show whether Mash1 positive cells are GBC1-3 positive. Double label studies of GBC1-3 and Mash1 are necessary to support the idea that Mash1 positive cells are indeed globose basal cells as suggested by Guillemot et al. (1993). Meanwhile the horizontal basal cells lie beneath the globose basal cells, express keratin and are identified by a surface glycoprotein that interacts with lectin BS-I (Holbrook et al., 1995). The relationship between the globose and horizontal basal cells remains elusive, with no

concrete evidence to suggest or dismiss a link between them. Similarly the unknown identity of the true stem cell within the olfactory epithelium impedes work on understanding the molecular events leading to cell fate determination and consequently the early steps of the differentiation program.

1.3.3 Immortalised Cell Lines

Aside from stem cell identity problems, the difficulty with observing the molecular pathway that a given cell population has executed *in vivo* is the complexity of dissecting the signalling cues that a cell has perceived from its environment. *In vitro* work attempts to simplify the context within which a cell finds itself, and cellular context can be further reduced with the use of a clonal cell line. Clonal cell lines have been used extensively in research (Schubert et al., 1974; Pleasure et al., 1992; Howard et al., 1993; Eves et al., 1994; Barber et al., 2000) as they provide a homogeneous population of cells that can be grown indefinitely in vitro (Lendahl and McKay, 1990). Numerous techniques have been used to establish clonal cell lines, with retroviral vector-mediated transduction of myc oncogenes into mitotically active progenitor cells proving popular (Ryder et al., 1990). This method allows the production of immortalised cell lines that have unlimited mitotic activity without the inducing properties associated with tumourigenicity (Ryder et al., 1990). Importantly, an immortalised clonal cell line will retain features from the originating tissue and thus allow the study of a single cell. Extensive collections of immortalised cell lines have been used to investigate events crucial for neuronal differentiation.

Since the inception of the clonal cell line PC12 (Greene and Tischler, 1976) endless studies have been carried out on diverse aspects of neuronal differentiation. For example, over-expression of the murine thymoma viral (v-akt) oncogene homolog-1 (Akt, also known as protein kinase B) in NGF treated PC12 cells results in differentiation arrest (Bang et al., 2001), while c-Jun over-expression in PC12 cells leads to enhanced neuronal morphology and apoptosis protection, without reaching complete differentiation as detected with patch clamping (Dragunow et al., 2000). Likewise H19-7 cells, an SV40 Tts-immortalised rat hippocampal neuronal cell line (Eves et al., 1996), have been used to determine the role of apoptosis induced by differentiation or serum deprivation. H19-7

cells have also been used to study signal transduction pathways induced by basic fibroblast-derived growth factor in neuronal cell differentiation (Kuo et al., 1997) and to investigate the role of cyclins during neuronal differentiation (Xiong et al., 1997). Finally, neural cell adhesion molecule positive and neurofilament positive cell lines from human embryonic spinal cord have been generated with the ability to differentiate into mature functional neurons (Li et al., 2000). These examples illustrate the diversity of reported clonal cell lines, and the insight they can provide into multifaceted and complex in vivo processes.

1.3.4 OLF442

The benefit of working with clonal cell lines is several fold. In the first instance, one is able to isolate a cell or population of identical cells and maintain a high degree of environmental control, accounting not only for immediate control from neighbouring cells which may be of different type, but also for intrinsic differences between test animals/groups. Secondly, one can be assured that any observed response is a direct result of a given stimulus or test condition. This is particularly useful in situations where the test hypothesis is not established, for example, the identification of factors involved in the proliferation and differentiation of developing olfactory precursors with differential display.

This study utilises an olfactory neuronal derived cell line previously prepared by immortalisation of precursor cells isolated from the adult mouse olfactory epithelium (MacDonald et al., 1996). Several immortalised clonal cell lines were generated by the retroviral insertion of the n-myc oncogene during cell division of the neuronal precursors (Bartlett et al., 1988; MacDonald et al., 1996). Of the clonal cell lines produced, one specific clonal cell line was particularly interesting. Designated as OLF442, this cell line has the capacity to exhibit a neuronal morphology and a genetic fingerprint consistent with the process of neuronal maturation [eg. expression of neurofilament protein, growth-associated phosphoprotein (GAP-43) and β-tubulin] when induced to differentiate upon serum depletion (Figure 1-7) (MacDonald et al., 1996; Zehntner, 1998b).

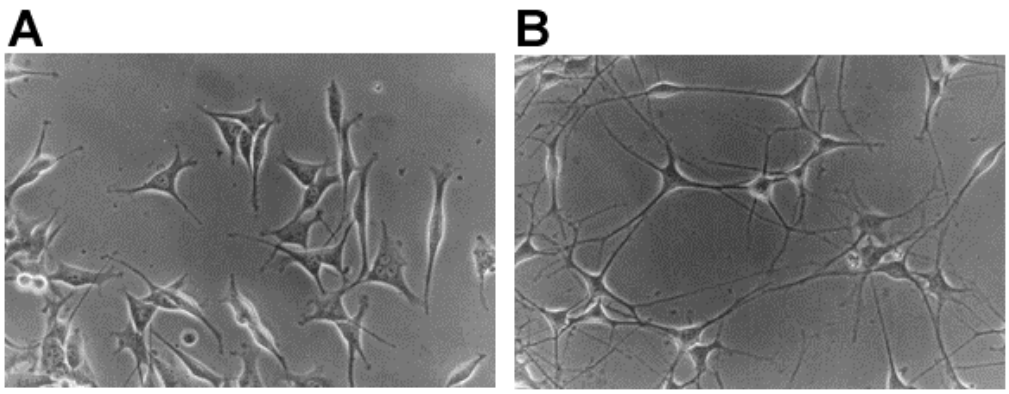

Figure 1-7 OLF442 differentiation.

Non-differentiated OLF442 grown in complete serum (A). Culture of OLF442 for 48 hr in serum deplete medium extends long processes (B).

Serum depletion has been used extensively to differentiate cells in culture. A neuronal catecholaminergic cell line, CAD (Cath.a-differentiated), is analogous to OLF442 as removal of serum from the culture medium results in the cessation of proliferation, extension of long processes and expression of neuron-specific proteins, such as class III β-tubulin and GAP-43, but not glial fibrillary acidic protein (Suri et al., 1993; Qi et al., 1997). Additionally, NIC, a cell line derived from the rat olfactory epithelium also up-regulates its expression of β-tubulin and NCAM when placed in serum deplete medium. However, NIC does not appear to express olfactory marker protein (OMP), an indicator of olfactory neuron maturation, suggesting that differentiation into the mature olfactory receptor neuron is incomplete (Goldstein et al., 1997). Like NIC, differentiated OLF442 may represent a cell state approaching maturity but without attaining it. OLF442 OMP expression has been reported (MacDonald et al., 1996), however it has also been questioned by several studies in which OMP was not detected (Zehntner, 1998b; Behrens et al., 2000). Zehntner et al. (1998b) demonstrated, by flow cytometric analysis, that OLF442 cultures maintained in serum-deplete medium for 12 hr display a cell cycle distribution consistent with a quiescent state, whereby 87% of cells were arrested in the first gap phase of the cell cycle (G_1) in a nongrowing, nondividing state that leads to cell cycle exit into G_0. Given that cell cycle cessation per se does not appear to be a sufficient initiator of differentiation and neurite extension, as observed in GOTO cells (Tsuneishi et al., 1993), OLF442 maintained in serum deplete medium for longer periods of time resulted in greater neurite extension (Zehntner, 1998b). Importantly, in OLF442 cells

neurites continue to extend longer processes with time, as was also demonstrated by CAD cells, which continue neurite extension for up to four days in culture (Qi et al., 1997).

It is well established that cell cycle arrest of proliferating neuronal precursor cells by nutrient withdrawal can result in either apoptosis or alternatively differentiation (Howard et al., 1993; Eves et al., 1996). A balance between apoptosis and differentiation represents a major point of regulation during neuronal differentiation in vivo (Holcomb et al., 1995; Blagosklonny, 1999). In serum-depleted OLF442 cultures apoptosis has not been detected, as serum deplete cultures lack the presence of apoptotic cell debris, and DAPI staining does not show irregular nuclei characteristic of apoptosis. Moreover the morphological differentiation induced by serum withdrawal over a 48 hr period can be reversed in OLF442 by serum repletion, indicating that they have not been committed to execute the apoptotic pathway. Thus OLF442 can provide insight into how undifferentiated, immature neuronal precursors give rise to mature olfactory receptor neurons.

1.4 The Aim Of This Thesis

The aim of this study was to characterise the gene expression profile of an olfactory neuronal derived cell line OLF442 by differential display. The clonal cell line OLF442, prepared by immortalisation of precursor cells isolated from the adult mouse olfactory epithelium (MacDonald et al., 1996) exhibits a neuronal morphology when induced to differentiate upon serum deprivation (MacDonald et al., 1996; Zehntner, 1998b). By using differential display and comparing an undifferentiated neuronal precursor population to a differentiated population extending neurites, it is possible to infer information about active processes at the molecular level and to dissect key components of molecular pathways. The differential display procedure was also expected to allow the identification of novel genes required for the process of differentiation.

Chapter Two illustrates the differential display method used and discusses the results obtained in light of data subsequently attained by cDNA Microchip Array analysis. Ensuing experiments and discussions centre on this information and provide a picture of some of the molecular processes active during neuronal maturation.

2 IDENTIFICATION AND CHARACTERISATION OF GENES REGULATED BY NEURONAL DIFFERENTIATION

2.1 Introduction To Differential Gene Expression

The coordinated regulation of gene expression is fundamental to the control of normal physiological phenomena within a cell, specifying cellular characteristics and responses to intracellular and extracellular cues. In order to reveal active processes at the molecular level and to dissect key components of molecular pathways, differential gene expression studies provide a foundation for the elucidation of dynamic molecular mechanisms. Furthermore, the study of differential gene expression is particularly useful when an experimental hypothesis has not been established, as may occur in an uncharacterised biological model. This situation may arise when identification of factors involved in a complex process such as cellular proliferation, differentiation, or tumourigenesis is pursued.

Various approaches to investigate differential gene expression have been utilised including differential hybridisation (Sambrook et al., 1989), subtractive hybridisation (Lee et al., 1991; Byers et al., 2000), and differential display (Liang and Pardee, 1992), predecessors to the more advanced technologies of SAGE (serial analysis of gene expression), TOGA (total gene expression analysis), and GeneCalling, collectively referred to as 'open'architecture systems, that do not need any pre-existing biological or sequence information (Green et al., 2001). This contrasts the so-called 'closed' systems such as quantitative PCR and oligonucleotide or cDNA microarray technologies (Schena et al., 1995) that require knowledge about a given genome (Green et al., 2001).

2.1.1 Differential And Subtractive Hybridisation

The earliest method described for the comparison of expressed genes between control and experimental samples was differential hybridisation (St John and Davis, 1979; Sambrook et al., 1989). This technique compares cDNA probes from control and test samples by screening test cDNA against duplicate control cDNA libraries (Sambrook et al., 1989) and was first used by St John and Davis in 1979 when they characterised galactose-inducible DNA sequences from *Saccharomyces cerevisiae* by differential plaque filter hybridisation (St John and Davis, 1979). However, unlike

subsequent hybridisation procedures, classical differential hybridisation is technically challenging, with high background and cDNA library duplication problems encountered. The innovation of superior hybridisation techniques resulted from these technical problems and the inability of differential hybridisation to detect rare transcripts (Sambrook et al., 1989).

Subtractive hybridisation, unlike differential hybridisation is a positive selection system, as control mRNA is directly hybridised with test cDNA resulting in double stranded RNA:DNA hybrids representative of transcripts common to both populations. The distinctive feature of subtractive hybridisation that placed it at the forefront of differential gene expression was its ability to create a pool of cDNAs enriched for the sequences unique to an experimental condition (Lee et al., 1991), where the single stranded cDNA represents transcripts unique to the experimental population (Sambrook et al., 1989). When combined with poly(A) reverse transcription (RT) polymerase chain reaction (PCR) [poly(A) RT-PCR], usually used to generate the starting cDNA for the technique, the advantages become greater (Brady and Iscove, 1993; Byers et al., 2000), including the ability to detect rare mRNAs, which represent as little as around 0.01% of the total number of mRNA species present. However, it is generally accepted that the technique will reliably isolate genes enriched at least 5-10 fold in the experimental pool compared to the control (Byers et al., 2000). Additionally, the identification of genes present in the subtracted pool is not dependent on their prior characterisation; therefore this method is ideal for identifying novel genes (Matz and Lukyanov, 1998; Byers et al., 2000). Although subtractive hybridisation has several advantages over differential hybridisation, there are several major shortcomings associated with the technique. These include the possibility of subtracting family members containing high levels of sequence homology (Sambrook et al., 1989), the comparison of only two populations simultaneously (Matz and Lukyanov, 1998), the bias one-way nature of the selection process in which only up-regulation or down-regulation can be assessed, and the technical difficulty of performing subtractive hybridisation. Nonetheless, both the differential hybridisation and subtractive hybridisation methodologies have been extended and improved with the advent of PCR (as mentioned above for increasing the sensitivity of subtractive hybridisation) however some of the fundamental drawbacks still persist.

Since its inception, subtractive hybridisation has yielded many related techniques including representational difference analysis (RDA). Here the complexity of the cDNA populations to be compared is reduced by digestion with frequently cutting restriction enzymes, ligation to adaptors, and amplification by PCR, followed by subtraction (Hubank and Schatz, 1994; Byers et al., 2000). Another technique, directed random oligonucleotide primed (DROP) subtractive hybridisation (Telenius et al., 1992) results in detection of mRNAs in the region of moderate-to-low abundance (0.06%) and can detect differences in both directions (Byers et al., 2000). Furthermore, subtractive hybridisation has also been combined with the more popular differential hybridisation technique resulting in enhanced reproducibility, increased sensitivity, and reduced false positive results (Byers et al., 2000). However, increased methodological complexity can result in very technical and laborious experiments that can outweigh their apparent advantages. As a result differential display was introduced as the method of choice a decade ago, as outlined in the ensuing discussion.

2.1.2 Differential Display

Differential display (DD) (Liang and Pardee, 1992) and RNA arbitrary primed polymerase chain reaction (RAP-PCR) (McClelland et al., 1993) were simultaneously introduced in 1992 as a means to identify and compare genes expressed as mRNA in various cell populations under specified conditions (Liang and Pardee, 1995). Most eukaryotic mRNAs contain a polyadenylate [poly(A)] tail (Jackson and Standart, 1990), a feature on which differential display relies for anchorage of the poly-T primer used in reverse transcription. The resultant cDNA is then PCR amplified with an arbitrary primer and poly-T primer, this contrasts with RAP-PCR which uses arbitrary primers for both the RT reaction and for the subsequent amplification by PCR (Liang and Pardee, 1995). In both cases the amplified subpopulation of cDNA is resolved on a DNA sequencing gel and the test samples are visualised against adjacently processed control samples, thus allowing the differential display of cDNA bands (Figure 2-1).

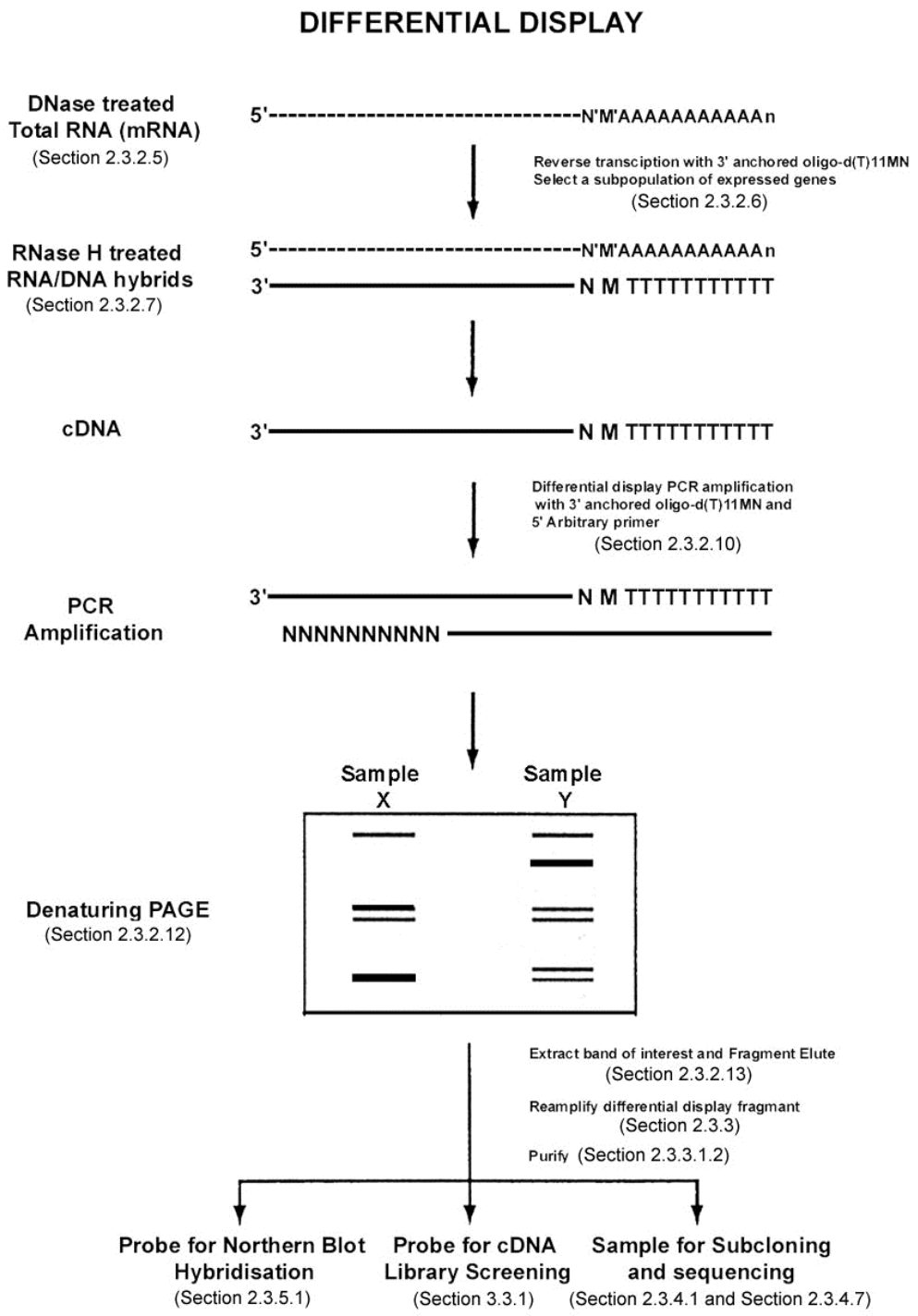

Figure 2-1 Schematic diagram of the differential display protocol.

Details of the methods used here are given in the Sections indicated.

Classical differential display employs the use of a degenerate two-base-anchored oligo-dT primer [$d(T)_{11}$NN where N= G, A, T, C] to reverse transcribe a subset of the total mRNA population extracted from cell lines or tissues under various conditions (Liang and Pardee, 1992). More recently a one-base anchored oligo-dT primer set [$d(T)_{11}$MN where M=G, A, or C] with a degenerate base at the penultimate nucleotide was used in differential display to further increase the size of the reverse transcribed subset so that it represents one quarter of the total mRNA present in a sample (Liang et al., 1994).

Amplification of the cDNA by PCR using the 3′ anchored oligo dT primer and a 5′ arbitrary decamer which anneals randomly along the length of the cDNA results in the amplification of a subset of the total cDNA population, which is resolved by denaturing polyacrylamide gel electrophoresis (PAGE). In order to increase the cDNA amplified, it may be necessary to perform multiple amplifications with different primer combinations, although redundancy in cDNA amplification is likely as an alternative decamer may anneal upstream of a cDNA already represented in an amplified subpopulation of another primer set (Matz and Lukyanov, 1998). Given that twenty different arbitrary decamers (priming as 6- to 7- mers) combined with twelve different combinations of oligo $d(T)_{11}$ MN primers are estimated to be required to display the approximately fifteen thousand individual mRNA species expressed in an average eukaryotic cell (Liang and Pardee, 1992), which likely represents an underestimate if system redundancy is taken into account, many amplifications and gels would need to be run to display the whole set, a disadvantage of differential display.

Differentially expressed genes are represented by bands that are present on the gel in one sample but not in another, or at different intensities indicating varying levels of abundance between samples (Matz and Lukyanov, 1998). Thus specific advantages of differential display include the simultaneous detection of both up-regulated and down-regulated genes and the comparison of more than two RNA populations, in fact limitations to the number of comparisons that can be done are only imposed by the size of the gel. Although PAGE analysis and autoradiography provide several of the advantages that make differential display popular, an inherent

problem of differential display stems from the low resolution of polyacrylamide gels (Byers et al., 2000). Hence, apparently single bands may contain multiple cDNA species. Additionally it may be hard to select a highly expressed, highly distributed sequence, for example where the differences in transcript concentrations between the samples exceeds 100 fold, as differences in fragment abundance of 50:1 or 1000:1 are likely to have the same appearance on a polyacrylamide gel due to autoradiographic saturation (Matz and Lukyanov, 1998). These technical problems cause a large portion of the observed false positives obtained with differential display, which can account for up to 50% or more of the observed transcripts (Wan et al., 1996). However the single greatest contributor to false positives is arbitrarily primed PCR using short oligos (Matz and Lukyanov, 1998), which can be solved with the use of longer arbitrary primers (Zhao et al., 1995). Nonetheless differential display has advantages over other methods which include: the use of small amounts of total RNA, the identification of mRNA species independent of prevalence (Wan et al., 1996), and the detection of rare and abundant transcripts of both known and novel genes (Matz and Lukyanov, 1998). As with subtractive hybridisation, differential display is biased towards the 3′ end of mRNA that does not contain the coding regions of genes. Therefore, cDNA bands of interest must be further amplified and characterised by library screening to identify coding regions or to obtain full-length cDNA clones (Matz and Lukyanov, 1998). Confirmation of cDNA expression levels by Northern blotting or RNase protection must also be carried out to ensure the isolated clone does not represent a false positive.

Differential display, until recently the method of choice by many investigators as shown by its prominence in PubMed literary searches, has proven technically challenging and frustrating. However, it has been successfully used to isolate novel genes and to imply function for many genes otherwise not thought to play a role in a particular process. Biological processes such as differentiation (Nishinaka et al., 2000), apoptosis (Barzilai et al., 2000) and cell growth (Johnsen et al., 2000) have been investigated with differential display. Moreover, differential display has been used in conjunction with a variety of total RNA sources including primary cell cultures (Seidel et al., 1998), transformed cell cultures (Zehntner et al., 1998a), tumour cell lines (Kito et al., 1997), and tissue samples such as the study of neuron

regeneration in the dorsal root ganglion (Livesey and Hunt, 1998). The contribution that differential display has made to molecular biology is noteworthy, however with the advent of robotics, the looming completion of genome sequences for model organisms and the vastness of the expressed sequence tag (EST) databases, differential display will surely become an archaic methodology in the not too distant future. Microarray technology is here.

2.1.3 Microarray Technology

Advances in molecular and computational biology have resulted in the generation of powerful, high-throughput methods for the analysis of differential gene expression (Carulli et al., 1998). Microarray technologies first appeared in the literature in 1995 with the development of a ‘‘chip’’ based approach for the monitoring of plant gene expression, utilising microarrays of cDNA clones as gene-specific hybridisation targets to quantitatively measure expression of corresponding plant genes (Schena et al., 1995). Later applied to evaluating the differential expression of 1046 human cDNAs of unknown sequence (Schena et al., 1996), the reality of further miniaturisation and therefore, more comprehensive gene expression analysis and gene discovery led to two major types of microarrays. Both cDNA microarrays and oligonucleotide microarrays share one distinguishing feature, the ability to allow “parallel quantification of the expression levels of an almost unlimited number of genes from a given genome” (Deyholos and Galbraith, 2001). Coupled with the exponential growth of genomic sequence information and ESTs, each of which contains the partial sequence of an expressed gene, a minefield of opportunity has been uncovered.

Capable of monitoring gene expression in cell lines and tissues by providing elaborate mRNA fingerprints (Carulli et al., 1998) microarray technology has become an important part of biological research (Alon et al., 1999). The use of microarrays for expression profiling is based on two key points. First, an alteration in abundance of mRNA precedes changes in expression of many genes, excluding post-transcriptional gene expression events (alternative splicing, RNA editing, expressed single nucleotide polymorphisms – cSNPs, etc) (Deyholos and Galbraith, 2001; Green

et al., 2001). Second, a stable DNA duplex can only form between DNA strands possessing complimentary sequences (Deyholos and Galbraith, 2001). These two fundamental principles are employed by microarrays through immobilisation of millions of single-strand copies of gene fragments on a solid support surface as individual array features. The array surface, which is then hybridised with labelled cDNA or cRNA, is washed and assessed for bound target to probe and subsequently analysed using various algorithms to determine gene expression levels in a given tissue, cell line or disease state (Carulli et al., 1998; Schadt et al., 2000).

DNA microarrays are comprised of large fragments of genes (400–2,000 bp) typically produced through PCR amplification of cDNA or EST libraries using vector-specific primers, obviating the need for sequence information (Deyholos and Galbraith, 2001). However, as portions of the vector sequence and poly(A) tail can be included in each probe amplified, the hybridisation specificity of the microarray may decrease, therefore gene specific primers are often used for each probe amplification. Gene specific primers can also be used for probe amplification of genomic DNA negating the need for cDNA/EST libraries; see Deyholos and Galbraith, 2001 for a thorough review of DNA microarray technology (Deyholos and Galbraith, 2001). In contrast, oligonucleotide-based microarrays consist of short (20-25 bp) synthetic DNA molecules such as the present day Affymetrix GeneChip® probe arrays (see Section 2.3.6 for manufacture of oligonucleotide arrays). Currently the Affymetrix GeneChip® probe arrays have the capacity to represent in excess of 10,000 gene sequences comprising fully characterised full-length genes and expressed sequence tag (EST) clusters on a single array (Affymetrix, ; Alon et al., 1999). Although oligonucleotide arrays are expensive, they provide the capacity to analyse the expression pattern of literally thousands of different genes in a matter of days. Therefore they allow the identification of gene associations in a particular cell type, tissue or biological process providing a broad perspective of the state of the cell (Alon et al., 1999; Byers et al., 2000). The utility of microarrays have been challenged as many have claimed that arrays can only screen for predetermined, and therefore known, genes, limiting their use for detection of novel, or unsuspected genes (Carulli et al., 1998; Byers et al., 2000). However, with the presence of exponentially expanding EST databases that will inevitably represent entire genomes, the technique does allow great flexibility in mining for novel genes.

2.2 Aim

The objective of this study was to identify novel neuroregulatory genes that direct differentiation of an olfactory neuronal derived cell line, OLF442, as it undergoes differentiation *in vitro*. The differentiation exhibited by OLF442 was investigated using both differential display and cDNA microarray technology. It was anticipated that the combination of these two techniques would provide an adequate representation of the active processes that a cell employs during initiation and progression through the differentiation program.

2.3 Methods

Primer sequences and recipes to all reagents and buffers mentioned throughout the methods are provided in Appendix I.

2.3.1 Cell Culture

2.3.1.1 Routine Maintenance And Passage Of OLF442

The immortalised mouse olfactory epithelium clonal cell line OLF442 was maintained in low glucose Dulbecco's Modified Eagle Medium (DMEM) (Gibco BRL®, Melbourne, VIC, Australia), supplemented with 10% (v/v) heat-inactivated foetal calf serum (FCS; Gibco BRL®) and 100 µM glutamine (GLUT; Gibco BRL®). Cells were grown in 25 cm^2 TPP (Life Technologies Pty. Ltd. Melbourne, Australia) tissue culture flasks and incubated in a 5% CO_2 humidified atmosphere at 37ºC. Upon reaching confluency (>80% flask cover) cells were passaged by aspirating the medium from culture vessels and washing adherent cells with Hank's Balanced Salt Solution (HBSS; Gibco BRL®). The HBSS was aspirated and cells were dislodged by addition of Trypsin-EDTA (Gibco BRL®): 0.5 mL for 25 cm^2 flasks, 1 mL for 75 / 175cm^2 flasks, and incubated at 37°C for 2-3 min, at which time 10% FCS/DMEM/GLUT was added to the flasks and the cells triturated. Cell suspensions were centrifuged for 5 min at 1500 rpm in a bench top centrifuge (Sigma, Castle Hill, NSW, Australia). Cell pellets were resuspended in 10% FCS/DMEM/GLUT and cell number was determined using a 0.5% (w/v) Trypan blue (Trace® Scientific Ltd. Noble Park, VIC, Australia) viability exclusion stain and counted in a haemocytometer (Weber Scientific International, Lancing, England). Cells were replated at a density of 30 cells per mm^2 of tissue culture flask surface area at 3-4 day intervals.

2.3.1.2 Serum Depletion

For differentiation studies of OLF442, cultures were grown in a medium depleted of exogenous growth factors by replacing medium containing 10% FCS with serum depleted medium comprising DMEM supplemented with 1% bovine serum albumin

(BSA; Sigma) and 100 μM GLUT. Prior to serum depletion, cells were seeded at the appropriate density: 30 cells/mm^2 for 10% FCS treated cells and 90 cells/mm^2 for 1% BSA treated cells for 48 hr cultures; 60 cells/mm^2 for 10% FCS treated cells and 90 cells/mm^2 for 1% BSA treated cells for 24 hr cultures; and 90 cells/mm^2 for 1% BSA treated cells and 10% FCS treated cells for 1, 4 and 8 hr cultures. All cultures were initially grown in control medium (10% FCS/DMEM/GLUT) for 18-24 hrs prior to treatment. Following the initial 18-24 hr settling phase, control medium was aspirated and cultures were washed with HBSS three times. The appropriate medium was then added to the culture vessels and the cells were incubated for the required periods of time.

2.3.1.3 Storage

Cells were routinely prepared for storage in liquid nitrogen. Confluent cultures were harvested by trypsinisation (refer to 2.3.1.1), then triturated in 10% FCS/DMEM/ GLUT and centrifuged at 1500 rpm in a bench top centrifuge for 5 min. The cell pellet was resuspended in 1 mL freezing medium composed of 90% FCS, 10% dimethyl sulfoxide (DMSO; Sigma) and 500 μL aliquoted into a single cryotube (Nunc, Roskilde, Denmark). Generally, one confluent 25 cm^2 flask was frozen into two 1 mL cryotubes. Cryotubes were placed at -70ºC overnight in a cotton wool package, following which they were transferred to liquid nitrogen for long term storage. Retrieval of frozen stocks from liquid nitrogen was carried out when maintained cultures exceeded 15 passages. Cells were immediately thawed by placing cyrotubes in a 37ºC water bath, followed by dilution in 1 mL 10% FCS/DMEM/GLUT and centrifugation at 1500 rpm for 5 mins. The resultant cell pellets were resuspended and split between two 25cm^2 flasks containing 10% FCS/DMEM/GLUT.

2.3.2 Differential Display

2.3.2.1 Total RNA Extraction

Preparation of total RNA was performed as described previously (Chomczynski, 1987). Briefly, at the completion of the 48 hr OLF442 cell growth period in 10% FCS or 1% BSA supplemented medium, culture flasks were washed three times with sterile ice-cold HBSS and lysed directly in the tissue culture flask with the addition of 2 mL denaturing solution D per 175cm^2 flask. Solution D was prepared as a stock solution in Milli Q filter sterile water (MQ H_2O) and stored at room temperature, the stock solution was supplemented with 0.1 M 2-mercaptoethanol (Sigma) prior to use. The denatured cell lysates were transferred to 10 mL polypropylene tubes (Sarstedt, Technology Park, SA, Australia) and placed on ice. Sequentially, 2 M sodium acetate, pH 4 added to a final concentration of 0.2 M, 2 mL phenol, pH4.5 (water saturated), and 0.2 mL of chloroform-iso-amyl alcohol mixture (49:1; Sigma) were added to the lysates, with thorough mixing after the addition of each reagent. Samples were incubated on ice for 15 min, following which lysates were transferred to microcentrifuge tubes (QSP, Quality Scientific Plastics, USA) and centrifuged at 15,000 rpm for 20 min at 4ºC in a microcentrifuge (Sigma). After centrifugation, the aqueous phase containing the RNA was transferred to a clean microcentrifuge tube and precipitated with 1 volume of isopropanol (Ajax Chemicals, Auburn, NSW, Australia) at -20ºC for 1 hr. The suspensions were centrifuged at 15,000 rpm for 20 min at 4ºC. Pellets were resuspended in 0.3 mL of solution D and once again precipitated with 1 volume isopropanol at -20ºC for 1 hr. Following sedimentation at 15,000 rpm for 10 min at 4ºC the RNA pellets were washed with 75% (v/v) ethanol (EtOH; Ajax Chemicals) centrifuged and air-dried for 10 min at room temperature. Finally the RNA pellets were resuspended in 50 µL MQ H_2O or TE, incubated at 65ºC for 10 min, and stored at -20ºC for future use.

2.3.2.2 RNA Quantitation: Concentration and Purity

The relative purity and concentration of the isolated RNA was determined by spectrophotometry: an optical density of 1 at an absorbance wavelength of 260 nm

corresponds to 40 µg/mL of RNA (Sambrook et al., 1989). Relative RNA purity was determined by assessment of the ratio of absorbance at 260 and 280 nm (the A260/280 ratio). Although there is significant variability in the A260/280 ratio depending on sample pH, it is generally accepted that a ratio of 1.5 to 2.0 for slightly alkaline samples (pH 7.5-8.5) denotes pure RNA (Wilfinger et al., 1997).

2.3.2.3 RNA Integrity: RNA Formaldehyde Gel Electrophoresis

Electrophoresis of RNA through agarose gels containing formaldehyde is necessary to ensure that RNA does not form secondary structures by remaining single stranded. Electrophoresis remains the method of choice to quickly determine RNA quality and integrity (Lehrach et al., 1977) and to confirm concentration/purity of RNA determined by spectrophotometry. RNA gel electrophoresis was carried out as described by GeneScreen™ and GeneScreen Plus® Transfer and Detection Protocols (GeneScreen). In short, 5 µg total RNA was added to 20 µL RNA sample loading buffer, heat denatured at 95ºC for 2-5 min, and cooled on ice prior to loading onto a 1.5% agarose gel containing 0.66 M deionised formaldehyde (Sigma) and 1X 3-(N-morpholino) propanesulfonic acid (MOPS) buffer. The RNA gel was electrophoresed in 1X MOPS buffer at 80 V at room temperature until the bromophenol blue dye front had migrated three quarters of the length of the gel. Following electrophoresis the gel was soaked in 1X MOPS buffer containing 0.5 µg/mL ethidium bromide (EtBr) for several hours and viewed under UV light using UVP's Gel documentation and Analysis System – GDS 7600 (UVP, Upland, California, USA).

2.3.2.4 Isolation of mRNA

mRNA was prepared from total RNA with the oligotex mRNA extraction kit (QIAGEN, Hilden, Germany) as per the manufaturers instructions (QIAGEN, 1999). Briefly, approximately 200 µg total RNA was diluted in MQ H_2O to a final volume of 250 µL, to which 250 µL of binding Buffer OBB and 15 µL Oligotex Suspension was added and thoroughly mixed. Samples were heated to 70ºC for 3 min to disrupt RNA secondary structure then placed at room temperature for 10 min to allow oligo dT_{30} of the Oligotex particles to hybridise with the poly-A tail of the mRNA. The Oligotex: mRNA complexes were pelleted by centrifugation for 2 min at 14,000 rpm, and

resuspended in 400 µL of wash Buffer OW2 and pipetted onto a small spin column and centrifuged for 1 min at 14,000 rpm. The column was again washed with 400 µL Buffer OW2. Finally 20 µL of 70ºC elution Buffer OEB was used to resuspend the Oligotex: mRNA complexes in the spin column and centrifuged for 1 min at 14,000 rpm. The eluate was used for a second elution to ensure maximal yield and mRNA concentration.

2.3.2.5 Chromosomal DNA Removal: DNase Treatment

mRNA was treated with 10 Units of RNase free DNase I (Boehringer Manheim, Manheim, Germany) to remove chromosomal DNA contamination in the presence of 10 Units rRNasin (Promega, Madison, Wisconsin, USA), 10 mM Tris-HCl (pH 8.3), 50 mM KCl, 1.5 mM $MgCl_2$ and 5 mM dithiothreitol (DTT) at 37ºC for 30 min (Kienzle et al., 1996). The digested samples were extracted with Phenol/Chloroform (3:1) and the aqueous phase was precipitated with 3 M sodium acetate and 100% EtOH at -70ºC for 30 min. The treated samples were centrifuged at 14,000 rpm for 10 min; pellets were washed with 70% EtOH, air-dried and resuspended in 20 µL MQ H_2O.

2.3.2.6 Reverse Transcription

mRNA was reverse transcribed with one of four different degenerate 3' anchored oligo-dT primer sets (T_{12}MN: T_{12}MG, T_{12}MC, T_{12}MA and T_{12}MT, where M is G, A or C) as follows, 0.1 µg DNase I treated mRNA in the presence of 1X Superscript II buffer, 20 µM deoxynucleotide triphosphates (dNTPs), 10 mM DTT and 20 pmol 3′ anchored primer, was incubated at 65ºC for 5 min to denature the mRNA secondary structure and subsequently incubated 10 min at 37ºC to allow primer annealing. Recombinant Moloney Murine Leukaemia Virus derived reverse transcriptase without RNase H activity (MMLV-RT RNase H^-, Superscript II, Gibco-BRL)(200 units) was added, and incubated at 37ºC for 50 min, following which the reverse transcriptase was heat inactivated for 5 min at 95ºC.

2.3.2.7 RNase H Treatment

The cDNA was digested with 1.5 Units of RNase H (Promega) added directly into the post heat inactivated reverse transcriptase reaction and incubated at 37ºC for 30 min. The RNase H was inactivated by incubation for 5 min at 95ºC. Samples were stored at -20ºC for future use.

2.3.2.8 cDNA Integrity

cDNA quality and integrity was confirmed by the presence of a well known housekeeping gene glyceraldehyde-3-phosphate dehydrogenase (GAPDH), with polymerase chain reaction (PCR) amplification using, 1 µM GAPDH forward primer and 1 µM GAPDH reverse primer (Lycke and Larsen) in the presence of 1X PCR buffer (Perkin Elmer, Roche, Branchburg, New Jersey, USA), 250 µM dNTPs, 1.5 mM $MgCl_2$ and 0.625 Units AmpliTaq® Polymerase (Perkin Elmer) in a final reaction volume of 25 µL. An equal volume of autoclaved mineral oil (Sigma) was layered on top of the reaction mixture and the samples were placed in an OmniGene thermal cycler (HB TR3-CM, Hybaid, Teddington, Middlesex, U.K), and subjected to a 94ºC x 5 min incubation, followed by 35 cycles at 94ºC x 1 min, 55ºC x 30 sec, 72ºC x 30 sec, with a final extension at 72ºC x 5 min.

2.3.2.9 PCR Product Analysis

Agarose gel electrophoresis was used routinely for separation and purification of DNAs greater than 200 bp. Electrophoresis was carried out as described (Sambrook et al., 1989), in brief, 0.2 volumes of 6X DNA gel loading buffer was added to each sample and loaded onto a gel of 0.8%-1.5% agarose (Sigma) in 0.5X TBE buffer containing 0.5 µg/mL EtBr, submerged in 0.5X TBE. DNA was separated electrophoretically at 100 V at room temperature for approximately 1 hr or until the bromophenol blue dye front had migrated three quarters through the gel. Following electrophoresis the gel was viewed under UV light using UVP's Gel documentation and Analysis System.

2.3.2.10 Differential Display (DD) PCR

Approximately 0.5 µg cDNA was amplified in a PCR containing a degenerate anchored oligo (2.5 µM) DD-C [T_{11}-CC/T_{11}-AC/ T_{11}-GC], an arbitrary oligo (2.5 µM) W2, 2 µM dNTPs, 1.0 uL 10 µCi/µL [α^{32}P] dATP (>1000Ci/mmol, Amersham Int., Amersham, UK), 1.5 mM $MgCl_2$, 1X PCR buffer and 1 unit AmpliTaq® polymerase (Perkin Elmer) in a final reaction volume of 20 µL, in thin walled PCR tubes. An equal volume of autoclaved mineral oil (Sigma) was layered on top of the reaction mixture and the samples were placed in an OmniGene thermal cycler to proceed through the following PCR program: thirty five cycles of denaturation at 94ºC x 30 sec, annealing at 42ºC x 2 min and extension at 72ºC x 30 sec, preceded by a 5 min incubation at 95ºC and followed by a 5 min extension at 72ºC. Three µL of each DD-PCR were mixed with 4 µL formamide loading buffer and incubated for 10 min at 85ºC and kept on ice until loaded onto a 6% denaturing polyacrylamide sequencing gel, along with a control sequencing reaction.

2.3.2.11 Sequencing Reaction

A sequencing reaction was performed with control single stranded M13mp18 DNA using the United States Biochemical (USB) Sequenase® version 2.0 DNA sequencing kit (USB, Cleveland, Ohio, USA), and M13 (-40 universal) primer as outlined in the manufacturer's protocol (Sequenase, 1993). The control sequence reaction was run alongside the DD-PCR products, as a size marker and to control for radioactive label intensity during autoradiographic exposure. Single stranded DNA (1.0 µg) was annealed to 0.5 pmol M13 primer with 1X Sequenase® reaction buffer in a 10 µL reaction volume and incubated at 65ºC for 2 min followed by slow cooling to room temperature over 30 min. A labelling reaction was carried out by addition of 5 mM DTT, 0.5 µL [α^{32}P] dATP (Amersham), 2 µL of 1X labelling mix and 2 µL of dilute Sequenase® version 2.0 DNA polymerase to the annealing mixture. The labelling reaction was incubated at room temperature for 5 min, then 3.5 µL was transferred into 2 µL of four separate termination mixes (G, A,T, and C) and further incubated at 37ºC for 5 min. Each reaction was terminated by addition of 4 µL of stop solution (dye) incubated for 5 min at 80ºC, and kept on ice until loaded onto a 6% denaturing polyacrylamide-sequencing gel.

2.3.2.12 Sequencing Gel

The complete DD-PCR and sequencing reactions were prepared as described above ready for separation on a denaturing polyacrylamide gel. The 6% denaturing sequencing gel mix was prepared fresh prior to use and poured by the sliding plate method, using 0.4 mm-1.2 mm wedge spacers and a shark tooth comb (Zehntner, 1998b). The gel was run in 1X TBE at 60 W for approximately 3 hr or until the Xylene Cyanol dye front had migrated to within 10 cm from the bottom of the gel. Following electrophoresis the top plate was removed and the gel was separated from the bottom plate by placing 3MM filter paper (Whatman International, Maidstone, England) over the entire surface of the gel. The filter paper and attached gel were gently peeled back away from the bottom plate and covered in plastic wrap. Fluorescent tracker tape (Amersham) markers were placed on the gel to produce orientation marks to allow alignment following film exposure. The gel was subjected to autoradiography with a Cronex intensifying screen (Dupont, Australia) at -70°C for 48 hrs using RX-80 Fuji medical X-ray film (Fuji Photo Film Co., Ltd., Japan).

2.3.2.13 Fragment Elution

Differentially expressed bands of interest were identified and excised from the sequencing gel by alignment with the autoradiograph. Differential display fragments were eluted from the gel by incubation in 100 µL of MQ H_2O at room temperature for 10 min followed by 15 min at 100ºC. Gel slice and filter paper debris was pelleted at 14,000 rpm for 2 min. The supernatant was decanted into a clean tube and 0.3 M sodium acetate, 50 µg glycogen (Sigma), and 400 µL of 100% EtOH was added and incubated for 30 min at -70ºC, followed by a 10 min centrifugation step (14,000 rpm) at 4ºC. Pellets were rinsed with 500 µL 85% EtOH, sedimented, air-dried, and resuspend in 10 µL MQ H_2O.

2.3.3 Secondary PCR

The extracted DD fragment was used for re-amplification by placing 1 µL of the eluted DNA in a 40 µL reaction volume using the same degenerate anchored oligo

(dT) primer set and PCR conditions as were used in the DD-PCR, except that isotope was ommited and 20 μM dNTPs were used. Negative controls included eluent from blank gel pieces and a PCR without template (MQ H_2O). The remaining recovered DNA was stored at -20ºC for future re-amplification if necessary.

2.3.3.1 Secondary PCR Product Analysis

2.3.3.1.1 DNA Agarose Gel Electrophoresis

20 μL of the secondary PCR was analysed by agarose gel electrophoresis as described in Section 2.3.2.9 PCR Product Analysis.

2.3.3.1.2 QIAGEN Gel Extraction

Relevant bands were excised from the agarose gel under UV illumination and purified using the QIAquick Gel Extraction Kit (Qiagen, Clifton Hill, VIC, Australia) as per the manufacturer's instructions. Briefly, excised gel fragments were solubilised in 3 volumes of Buffer QG and incubated at 50ºC for 10 min until the gel slice had completely dissolved. If the PCR fragment was <500 bp and >4 kb, 1 gel volume of isopropanol was added to the sample. Samples were added to a QIAquick spin column and centrifuged at top speed (14,000 rpm) for 1 min, after which 0.5 mL of Buffer QG was added to the spin column and again centrifuged for 1 min. Wash Buffer PE (0.75 mL) was added to the spin column and allowed to stand for 2-5 min. The spin column was centrifuged at 14,000 rpm to elute the wash buffer and again centrifuged to remove any residual EtOH prior to elution of the PCR fragment from the column with 30 μL of Buffer EB.

2.3.3.1.3 DNA non-denaturing Polyacrylamide Gel Electrophoresis (PAGE)

Non-denaturing polyacrylamide gel electrophoresis (PAGE) was used for the separation and purification of dsDNA, compared to denaturing PAGE used for the separation and purification of ssDNA, as, unlike agarose gels, PAGE can adequately resolve DNAs between 5-200 bp in size (Sambrook et al., 1989). Briefly, glass plates

and spacers were thoroughly cleaned and dried. Non-denaturaing PAGE gels (8%) were prepared in a Miniprotean apparatus (Bio-Rad, Richmond, CA, USA) using a 29:1 acrylamide:bis-acrylamide stock solution, with 1X TBE buffer. Following acrylamide polymerisation (approximately 60 min at room temperature), the combs were removed and the wells flushed with buffer. The re-amplified DD-PCR samples (20 µL) were mixed with 0.2 volume 6X gel loading buffer and loaded into wells. Gels were run in 1X TBE at 80 V (1-8 V/cm) or until the marker dye had migrated the desired distance. The apparatus was dismantled and the gel was stained, by immersing in 0.5 µg/mL EtBr in 1X TBE. Gels were stained for 30-45 mins at room temperature and visualised on a UV transilluminator. Where DD-PCR products could not be visualised by agarose gel electrophoresis they were run on non-denaturing PAGE and fragments isolated as described in Section 2.3.2.13 Fragment Elution.

2.3.4 PCR Product Cloning

Differential display fragments, amplified and gel extracted, were quantitated by spectrophotometry; an optical density of 1 at an absorbance wavelength of 260 nm corresponds to 50 µg/mL of dsDNA (Sambrook et al., 1989).

2.3.4.1 pGEM-T Vector Cloning

Isolated fragments were cloned into pGEM®-T (3 Kb) or pGEM®-T Easy (3 Kb) Vector Systems (Promega, Madison, WI, USA), as instructed by the manufacturer's protocol [Promega, 1998 #313]. Although AmpliTaq® was used, providing PCR products with 3' A ends, the standard tailing procedure was carried out to ensure that the fragments being cloned had a high proportion of 3' A tails, in order to increase ligation efficiency. Briefly, 2 µL of purified PCR fragment was added to 1 µL of 1X PCR buffer, 1 µL of 25 mM $MgCl_2$, 0.2 mM dATP and 5 Units AmpliTaq® Polymerase (Perkin Elmer) in a final reaction volume of 10 µL, and incubated at 70ºC for 30 min. The fragment concentration to be used was calculated by size and vector: insert molar ratios. Optimal ligations were done at a 1:6 (vector: insert) ratio. Once the fragment (insert) concentration had been determined, a 10 µL ligation reaction was set up with 1 µL pGEM®-T (50 ng) or pGEM®-T Easy (50 ng) Vector, 5 µL 2X

rapid ligation T4 DNA ligase buffer and 1 μL of T4 DNA ligase (3 Weiss units/1 μL). Following an overnight incubation at 4ºC, the ligations were transformed into JM109, DH5α, or DH10β competent cells.

2.3.4.2 JM109 Transformations

JM109 high efficiency competent cells (Promega) were transformed as described (Promega, 1998); in short, 2 μL of each ligation reaction were placed in an ice cold centrifuge tube containing 50 μL of recently thawed JM109 competent cells and incubated on ice for 20 min. The cells were heat shocked for 45 sec at exactly 42ºC and then incubated on ice for a further 2 min. SOC medium (950 μL) was added to the cells and incubated for 60-90 min with shaking (approximately 150 rpm) at 37ºC. Transformed cells (20 μL and 200 μL aliquots) were plated onto Luria-Bertani (LB) plates with ampicillin (AMP)/ isopropylthio-β-D-galactoside (IPTG)/ 5-bromo-4-chloro-3-indoyl-β-D-galactoside (X-gal) to select for the appropriate plasmid, and incubated at 37ºC in the inverted position overnight.

2.3.4.3 Preparation of DH5α and DH10β Electro-competent Cells

Prewarmed (37ºC) LB medium (1 L) was inoculated with 1/50 volume of fresh overnight culture and incubated at 37ºC with rigorous shaking at 150-180 rpm, to an optical density of A_{600}= 0.5-0.8 (cell growth in early to mid log phase). The culture was chilled in a slurry of ice water for 15-30 min and centrifuged in a cold rotor at 4ºC for 15 min at 5,000 rpm. The cell pellet was resuspended in 800 mL of sterile ice-cold MQ H_2O and centrifuged at 4ºC for 15 min at 5,000 rpm. The cell pellet was again resuspended in 500 mL of sterile ice-cold MQ H_2O and centrifuged at 4ºC for 15 min at 5,000 rpm. This procedure was repeated twice more, each time resuspending the cell pellet in a smaller volume of liquid: ie. 20 mL 10% sterile ice-cold glycerol and 2 mL 10% sterile ice-cold glycerol. The resulting cell suspension was aliquoted in 40 μL lots into 1.5 mL centrifuge tubes, snap frozen in liquid nitrogen, and stored at -80ºC.

2.3.4.4 DH5α and DH10β Electro-competent Cell Transformations

Cuvettes, ligation reactions and aliquots of electro-competent DH5α or DH10β cells were placed on ice to thaw while the Gene Pulser (BioRad, Regents Park, NSW, Australia) was set to 2.5 kV for 0.2 cm cuvettes. The ligation reactions (1-2 μL) were added to the thawed cells and gently mixed, transferred immediately to a pre-chilled cuvette and pulsed at 2.5 kV. Following electro-transformation cells were instantly resuspended in 1 mL SOC medium and incubated at 37ºC for 45-60 min with vigorous shaking at 225 rpm. Aliquots of transformed cells (20 μL and 200 μL) were then plated onto LB plates with AMP/IPTG/X-gal to select for the appropriate plasmid, and incubated in the inverted position overnight at 37ºC.

2.3.4.5 Plasmid Isolation

Small scale plasmid mini preparations from cultures grown in liquid medium (LB with AMP) that had been inoculated with a single colony picked from an agar plate were carried out as described below [STET preparation method adapted from Sambrook et al., (1989)]. However, although the purity of the plasmid preparations was sometimes excellent, the variability in purity of plasmids prepared this way meant that further purification was often required. This was generally done when a plasmid was required for direct sequencing, further cloning, PCR analysis, or probe preparation.

2.3.4.5.1 Plasmid Isolation - STET Preparation

A single bacterial colony was transferred with a toothpick onto a master plate and into a 10 mL tube containing 2 mL LB supplemented with AMP(100 μg/mL) and incubated overnight at 37ºC. An aliquot of 1.5 mL from the culture was transferred into a microfuge tube and spun at 15,000 rpm for 60 sec at 4ºC. The supernatant (SN) was removed and the cell pellet was resuspended in 400 μL STET solution, with 30 μL lysozyme (10 mg/mL; Boehringer Mannheim), and vortexed until resuspended. Samples were boiled for 60 sec and centrifuged at 15,000 rpm for 15 min at 4ºC. The resulting mucous pellet of cell debris was removed from the SN with a toothpick and discarded. To the SN, 400 μL isopropanol (-20ºC) was added and samples were

thoroughly mixed and centrifuged at 15,000 rpm for 10 min at 4ºC to precipitate plasmid DNA. The resulting plasmid pellet was washed with 200 µL 70% EtOH and sedimented at 15,000 rpm at 4ºC for 10 mins. Finally the SN was removed and the pellets were air-dried on the bench for about 10 min. Pellets were resuspended in 100 µL TE (or MQ H_2O) and incubated at 65ºC for 15 min.

2.3.4.5.2 Plasmid Isolation - Qiagen Mini Preparations

STET preparations were further purified using the QIAprep Spin Miniprep Kit (Qiagen) as instructed by the manufacturer's handbook. Briefly, STET preparations were dissolved in 5 volumes Buffer PB, mixed and loaded onto a QIAprep column and centrifuged for 60 sec. The column was washed with 0.75 mL Buffer PE and again centrifuged for 60 sec. The flow-through was discarded and the column spun again for an additional 60 sec. The QIAprep column was transferred to a fresh 1.5 mL microfuge tube and the DNA was eluted from the column with 50 µL Buffer EB and centrifuged at 14,000 rpm for 60 sec.

2.3.4.6 Plasmid DNA Digestion

Generally 5-10 µL of plasmid DNA was routinely digested in a final reaction volume of 20 µL. Restriction enzyme buffer (1X) and 1-2 Units of Restriction enzyme formed the core components of the reaction. Additives such as BSA were added when specified as per manufacturer's instructions, and the digest made up to the final volume with MQ H_2O. Reactions were incubated at the specified temperature for optimal cutting for 2-16 hrs. Following digestion, reactions were loaded and run on an agarose gel (refer to Section 2.3.2.9) with 0.2 volumes of 6X DNA gel loading buffer.

2.3.4.7 Sequence Analysis

All sequencing was done using the ABI PRISM® BigDye™ Terminator Cycle Sequencing Ready Reaction Kit as indicated by the manufacturer's instructions and samples were electrophoresed on an ABI Prism 377A DNA Sequencer.

2.3.5 Expression Analysis Of Differential Display Fragments

Confirmation of differential expression of cloned fragments was done by Northern blotting onto GeneSreen Plus® membranes (Du Pont, Boston, MA, USA) following the manufacturer's protocol. Probes were labelled by random hexamer priming and hybridised as detailed below. Briefly, total RNA was isolated as described in Section 2.3.2.1, and samples were assessed for purity and integrity as indicated in Section 2.3.2.2. Total RNA (20 μg) was electrophoresed through an agarose gel containing formaldehyde (refer to Section 2.3.2.3).

2.3.5.1 Northern Blotting

Following electrophoresis the formaldehyde agarose RNA gel was soaked in 5 volumes of MQ H_2O for 5 mins and the soak was repeated four times to remove excess formaldehyde from the gel. The GeneSreen Plus membrane (Du Pont) was cut to size and hydrated in MQ H_2O for 30 sec, then soaked in the transfer solution (10X SSPE) for 15 min. A capillary blot was set up as described in the GeneScreen Plus® Transfer and Detection Protocols (GeneScreen). In short, three pieces of Whatman 3MM chromatography paper large enough to accommodate the agarose gel and to extend into the buffer tray were soaked in 10X SSPE and suspended on a glass plate above the buffer tray creating a wick. The agarose gel, membrane, another 3 pieces of dry Whatman 3MM paper and a four-inch stack of paper towel were placed sequentially on top of the wick. Another glass plate was placed on the assembly and weighted down with a water filled conical flask. The transfer in the presence of 10X SSPE proceeded for 16-24 hr, following which the assembly was dismantled and the membrane was rinsed in 2X SSPE for 5 min to remove residual agarose gel that may lead to high autoradiographic background. The RNA was fixed to the membrane by UV crosslinking (254 nm X 1 min 40 sec or 1200 $\mu W/cm^2$, which is optimal for a wet membrane) and the membrane was then oven baked at 80ºC for 1-2 hr to reverse the formaldehyde reaction. Membranes were either stored desiccated at 4ºC or prehybridised immediately.

2.3.5.2 Labelling Probes

Probes were radiolabelled with [α^{32}P] dATP (>1000Ci/mmol), using a Random Primed DNA Labelling Kit (Boehringer Mannheim). The procedure was carried out as instructed by the manufacturer. Briefly, 25 ng of double stranded DNA was diluted in MQ H_2O to a final volume of 9 µL and heat denatured for 10 min at 100°C, followed by incubation on ice for 10 min. dTTP, dGTP and dCTP mix (1 µL of each) was added along with 2µL of reaction mixture, 5µL of [α^{32}P] dATP and 1 µL of Klenow enzyme. The labelling reaction was incubated at 37°C for 30 min and terminated with the addition of 2 µL 0.2M EDTA (pH 8.0). The reaction was diluted with 80 µL TE buffer and passed through a Sephadex G-25 or G-50 (Sigma) spin column (Sambrook et al., 1989) as described below.

2.3.5.3 Probe Purification

To separate labelled DNA from unincorporated nucleotides, the Random Primed DNA probes were passed through a TE equilibrated Sephadex G-25 or G-50 (Sigma) spin column. Briefly, Sephadex was hydrated in TE buffer and autoclaved. A disposable 1 mL sterile syringe was plugged with cotton wool and placed into a polypropylene centrifuge tube, filled with hydrated Sephadex and centrifuged at 4000 rpm for 5 min. The syringe was repeatedly refilled with Sephadex and centrifuged until the packed bed volume was 0.8 mL. The TE diluted probes were loaded onto the column and centrifuged at 4000 rpm for 5 min. The eluant containing radiolabelled probe fragments was collected and transferred to a fresh 1.5 mL centrifuge tube and heat denatured at 100°C for 10 min, then placed on ice for 10 min.

2.3.5.4 Northern Blot Hybridisation

Oven baked RNA membranes were prewet with 2X SSPE prior to prehybridisation. Membranes were incubated in hybridisation bottles in a hybridisation rotisserie (Amersham) at 42°C for 3-4 hr in prehybridisation solution [5X SSPE, 50% w/v deionised formamide, 5X Denhardts solution, 1% sodium dodecyl sulphate (SDS), 10% dextran sulphate (Sigma) and 100 g/mL denatured, sheared herring sperm DNA (Sigma)]. Following prehybridisation, heat denatured α^{32}P-labelled DNA was added

to the solution and allowed to hybridise at 42°C overnight. The membranes were washed twice in 2X SSPE for 15 min at room temperature in hybridisation bottles with slow rotation in a hybridisation rotisserie, and twice in 2X SSPE, 1% SDS for 15 min at 65°C. Probed membranes were placed in a plastic bag and subjected to autoradiography using RX-80 Fuji medical X-ray film with an X-ray cassette and intensifying screen (Kodak) overnight at -70°C. Membranes were stripped by boiling in 0.1X SSC, 1% SDS for 30 min. Stripped membranes were hybridised as indicated above without prehybridising.

2.3.6 Oligonucleotide Array Data

OLF442 was supplied to Dr Lubert Stryer and Research scientist Dr Yanxiang Cao (Affymetrix and Department of Neurobiology, Stanford University, USA) who grew the cells as described and carried out Affymetrix GeneChip® analysis as per standard Affymetrix procedures. This collaboration was facilitated and directed by Associate Professor Alan Mackay-Sim.

The Affymetrix GeneChip® probe arrays are high-density arrays of oligonucleotide probes that are synthesized using a combination of photolithography and oligonucleotide chemistry (Lockhart et al., 1996). Briefly, genes are represented on a probe array by typically 20 sequences of generally 25 nucleotides in length, uniquely identifying chosen genes or ESTs which have relatively uniform hybridisation characteristics (Affymetrix, ; Schadt et al., 2000). Each oligonucleotide, or probe, is synthesized in a small region termed a feature (the length and width of which is either 50 μm for the low-density arrays or 24 μm for the high-density arrays), which can contain between 10^6 to 10^7 copies of a given probe (Schadt et al., 2000). The oligonucleotide probes are synthesized on a glass wafer using a series of photolithographic masks to define chip exposure sites, followed by solid-phase chemical synthesis, resulting in the construction of high-density oligonucleotide arrays, with each probe in a predefined position in the array (Affymetrix).

Importantly, each oligonucleotide probe, designed to correspond to the perfect match (PM) oligonucleotide from a gene sequence (or EST), has a partner mismatch

(MM) oligonucleotide, in which the centre base position of the oligo has been mutated (Schadt et al., 2000). The MM probes provide an estimate of the degree of random hybridisation and cross hybridisation, when PM and MM probe intensities are compared (Schadt et al., 2000). mRNA from the sample to be analysed is fluorescently labelled according to the protocol defined by Lockhart et al. (1996), prior to hybridisation with corresponding probes on the array (Byers et al., 2000). Following hybridisation the array is subjected to a series of automated stringency washes then is scanned with a confocal laser scanner. The laser, which excites each feature, detects the photon emissions from the fluorescently labelled RNA that has hybridised to the probes in the feature, and creates an image ready for analysis (Schadt et al., 2000). The resulting PM/MM feature intensities are assessed statistically to determine whether a gene is present and the level of its expression using GeneChip software supplied by Affymetrix (Schadt et al., 2000). The Genechip software performs the fundamental operations to analyse the imaged array, including (1) image segmentation, (2) correction of background noise, (3) scaling/normalising arrays for array-to-array comparisons, and (4) statistical calculations to indicate whether a gene transcript is present and differentially expressed (Schadt et al., 2000).

2.4 Results

2.4.1 OLF442 Differentiation

Prior to serum depletion, the optimal OLF442 seeding density for growth of cultures over a 48 hr period in complete medium was determined. It had been observed that the rapid proliferation of cells grown in complete medium over a 48 hr period resulted in cultures containing colonies/spheres of cells with a heterogeneous morphology, when seeded at the same density as cultures depleted of serum (Figure 2-2, Panel C). Cultures containing spheres were composed of flat rounded cells that clumped together forming a colony attached to neighbouring colonies by multipolar cells with long processes. However, when seeding density was lowered such that clump formation was avoided in cultures grown in complete medium over a 48 hr period, the equivalent seeding density resulted in cell loss of the serum deplete cultures due to insufficient cell numbers and therefore (presumably) lack of trophic support. Considering that cell density could be an uncontrolled factor in the culture of proliferating cells versus quiescent cells, an optimised seeding density of 30 cells/mm^2 for serum complete (10% FCS treated cells) and 90 cells/mm^2 for serum deplete (1% BSA treated cells) 48 hr cultures was used throughout this study (Figure 2-2, Panel A and B).

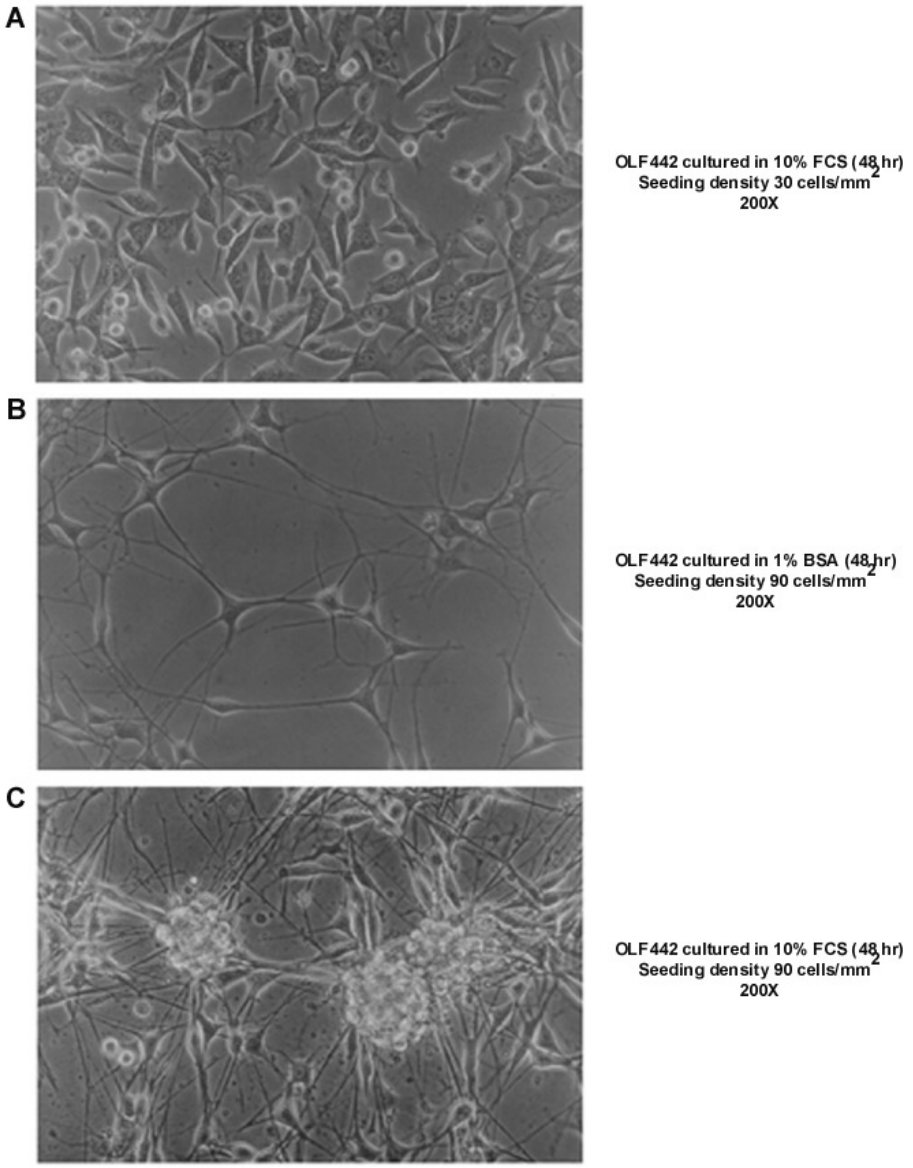

Figure 2-2 OLF442 48 hr cultures.

Seeding density was optimised such that growth in serum free medium and complete medium resulted in healthy cultures. Panels A and B show healthy cultures in complete medium and serum free medium respectively. Panel C illustrates the consequence of over seeding, resulting in a heterogeneous population of non-differentiated cells and cells extending long processes reminiscent of differentiated OLF442, with the formation of extensive cell aggregates.

2.4.2 Total RNA To cDNA

Prior to differential display PCR, the total RNA isolated from serum complete (10% FCS) and serum deplete (1% BSA) cultures was assessed for purity and estimated concentration (Figure 2-3).

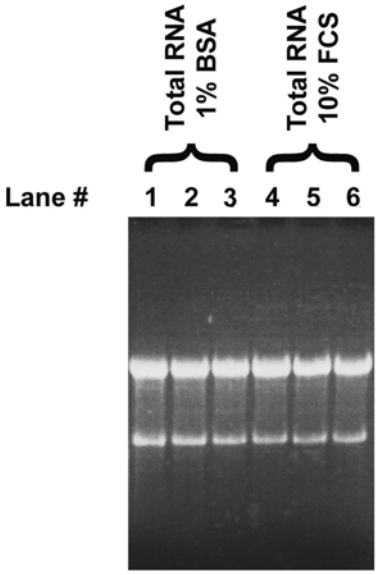

Figure 2-3 RNA formaldehyde gel.

Total RNA (5 μg) from cultures grown for 48 hr in serum deplete medium (1% BSA) lanes 1-3, and complete medium (10% FCS) lanes 4-6 are shown.

cDNA integrity was analysed by PCR amplification of the "house keeping" gene glyceraldehyde-3-phosphate dehydrogenase (GAPDH). The forward GAPDH primer and reverse GAPDH primer (Lycke and Larsen) had been designed to amplify a region of GAPDH spanning exon 7 of the human GAPDH gene (bp 4348-4614) resulting in amplification of a 266 bp amplicon. Both the forward and reverse primers have 100% homology with mouse GAPDH mRNA although the mouse 266 bp amplicon shares 91% homology with the human amplicon. PCR amplification of GAPDH in cDNA samples to be used for differential display confirmed cDNA integrity whilst lack of amplification of minus reverse transcriptase (-RT) samples confirmed the absence of genomic DNA contamination (Figure 2-4).

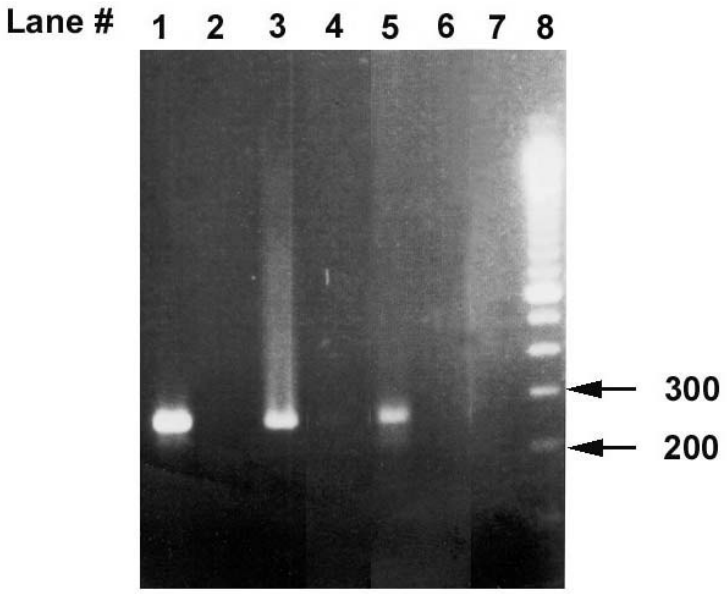

Figure 2-4 cDNA integrity.

cDNA integrity was analysed by resolving PCR amplified GAPDH on a 1% agarose gel. Lane 1 shows amplification of GAPDH from cDNA isolated from 10% FCS treated OLF442, and lane 2 is a negative control without reverse transcriptase added (no DNA contamination). Lane 3 shows GAPDH amplification from cDNA isolated from 10% FCS treated OLF442 cells that had formed cell clumps/aggregates in culture due to high seeding density, while lane 4 is the negative control without reverse transcriptase. Lane 5 shows amplification of GAPDH from cDNA isolated from 1% BSA treated OLF442 and lane 6 is a negative control without reverse transcriptase. Lane 7 is the negative PCR control and lane 8 shows a 100 bp ladder.

2.4.3 Differential Display

Differential display was performed as described (Section 2.3.2) with a degenerate anchored oligo DD-C and an arbitrary oligo W2. Reactions were done in duplicate, including MQ H_2O controls and the internal experimental minus (-) RT controls. Differential display experiment number 5 (DD5) was the most successful display done and produced all the bands that were subsequently gel-extracted, re-amplified and cloned. In excess of 30 bands were identified with a differentially displayed pattern, that is, present/absent or of higher/lower intensity in differentiated OLF442 (1%BSA) compared with non-differentiated OLF442 (10%FCS). Of these, 12 differentially expressed bands were identified and recovered from the gel by alignment with the autoradiograph (Figure 2-5).

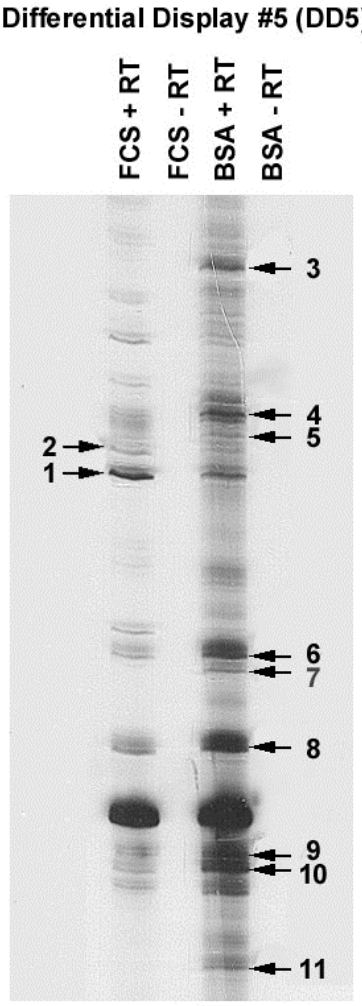

Figure 2-5 Differential display number 5 (DD5).

The differentially expressed cDNA amplification fragments isolated are indicated. 10% FCS treated OLF442 (FCS + RT) and 1% BSA treated OLF442 (BSA + RT) cDNA amplification PCR products display a different banding pattern, indicating differential gene expression during OLF442 differentiation over a 48 hr period. 10% FCS treated OLF442 without reverse transcriptase added (FCS - RT) and 1% BSA treated OLF442 without reverse transcriptase added (BSA - RT) controls demonstrate that the cDNA was free of genomic DNA contamination.

The differentially expressed cDNA amplification fragments isolated are indicated in Table 2-1. The relative signal intensity of up-regulated or down-regulated is also indicated and refers to that which occurs in the serum complete (10% FCS) treated OLF442, compared to the serum deplete OLF442 (1% BSA) condition that becomes differentiated following a 48 hr incubation. Induced refers to a band absent in the 10% FCS treated OLF442 DD-PCR and present in the 1% BSA treated OLF442.

Table 2-1 Outline of differential display products isolated [a]

Fragment Name	Size (bp) (Approximate)	Expression Level
DD5-1	300	Downregulated
DD5-2	320	Downregulated
DD5-3	420	Induced
DD5-4	350	Upregulated
DD5-5	330	Upregulated
DD5-6	280	Upregulated
DD5-7	260	Induced
DD5-8	250	Upregulated
DD5-9	230	Upregulated
DD5-10	220	Upregulated
DD5-11	200	Induced
DD5-16	350	Down-regulated

[a] The table shows a list of the isolated bands and their approximate size as determined from a manual sequencing reaction. Relative expression level was assessed for serum depleted (1% BSA) OLF442 samples as compared to serum complete (10% FCS) samples.

Interestingly, upon re-amplification of the differential display fragments, one of the excised bands produced two amplification products (data not shown). Differential display product DD5-3 contained two cDNA species within the one band (DD5-3A was approximately 460 bp and DD5-3B was approximately 420 bp).

2.4.4 Differential Display Fragment Cloning

All re-amplified amplicons were cloned into the pGEM®-T/pGEM®-T Easy cloning systems as they take advantage of the ability of Taq polymerase to add a terminal 3'deoxyadenosine during the PCR. These vectors contain a single 3'-T overhang at the cloning site, allowing sticky end ligation that is more successful than blunt end ligating. Individual colonies were screened until a positive insert clone was identified. Curiously, differential display products DD5-5 and DD5-7 produced two bands of different size and sequence upon cloning (Figure 2-6). This is most likely due to the re-amplification of multiple differential display products from single band excisions as mentioned above. However the resolution of the re-amplified PCR products on a 1.5% agarose gel was insufficient to detect 5-20 bp differences and multiple products were not observed until cloned fragments were digested and electrophoresed on a 2% agarose gel (Figure 2-6 and Figure 2-7).

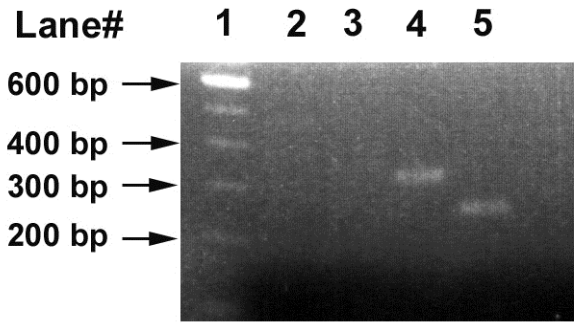

Figure 2-6 Secondary PCR amplification of DD5-5 and DD5-7.

Differential display products DD5-5 (lane 4) and DD5-7 (lane 5). Only one band was visible following 1.5% agarose gel electrophoresis of re-amplified differential display products.

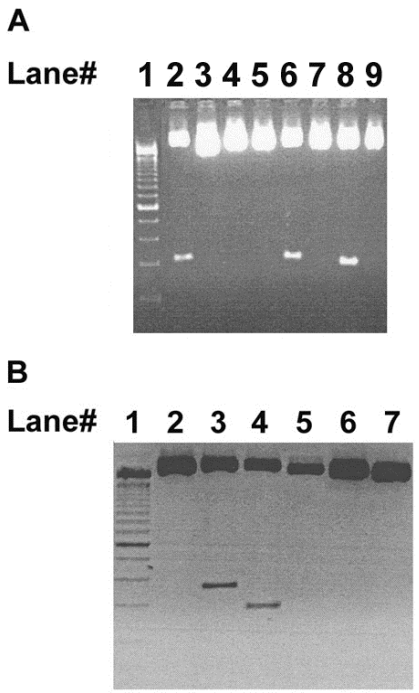

Figure 2-7 DD5-7 and DD5-5 cloned fragments.

(A) DD5-7 minipreparations digested with Nco I and Not I run on a 2% agarose gel. Two different sized inserts are apparent, lane# 6, DD5-7(5) contains as insert of 265 bp, while lane# 8, DD5-7(7) contains an insert of 260 bp. (B) DD5-5 minipreparations digested with Nco I and Not I run on a 2% agarose gel. Two different products were cloned from one re-amplified differential display fragment. Lane# 3, DD5-5(2) contains an insert of 317 bp and lane# 4, DD5-5(3) contains an insert of 296 bp (refer to Table 2-2).

Clones containing an insert were further purified and sequenced. Sequences were analysed using chromatogram analysis software, Chromas 1.5 (McCarthy, 1998). The sequences were analysed using the nucleotide-nucleotide blast (blastn) (Madden et al., 1996; Altschul et al., 1997) program to identify homology with known sequences in the non-redundant database (Table 2-2). At the time of writing, the mouse genomic sequences were not accessible to us and therefore differential display fragments with no known homology have not yet been compared to this resource.

Table 2-2 Differential display product sequence homology [a]

Fragment	Size (bp)	Sequence Homology
DD5-1(1)	325	No homology - unknown sequence
DD5-2	320	No clone
DD5-3A	480	No clone
DD5-3B(5)	400	No homology - unknown sequence
DD5-4	350	No clone
DD5-5(2)	317	97% Homology with mouse Focal adhesion kinase (FAK)
DD5-5(3)	296	97% Homology with mouse Ribosomal protein L3 (Rp13)
DD5-6(5)	300	No homology - unknown sequence
DD5-7(5)	265	92% Homology with mouse Fas-Binding protein Daxx
DD5-7(7)	260	90% Homology with Rat mRNA for MST2 Kinase
DD5-8(4)	250	No homology - unknown sequence
DD5-9(6)	199	No homology - unknown sequence
DD5-10	210	No clone
DD5-11	200	No clone
DD5-16(1)	350	No homology - unknown sequence

[a] The table illustrates the observed fragment size of each differential display product, upon cloning and sequencing. Only four fragments exhibited homology with known mRNAs, whilst six fragments represent novel sequences. The 'No clone' indicates fragments that were not successfully cloned.

2.4.5 Expression Analysis Of Differential Display Fragments

The cloned differential display products were used to probe total RNA isolated from OLF442 serum complete and deplete conditions by Northern Blot analysis. Confirmation of the observed differential display expression levels was necessary to eliminate possible false positive differential display results. Random primed DNA radiolabelled probes effectively incorporated [α^{32}P] dATP and provided sufficient sensitivity for detecting their target mRNAs. Differential display products DD5-5(2), DD5(3), DD5-7(7) and DD5-9(6) all produced signal intensities that supported the expression levels seen in the differential display. However, DD5-5(2) probe detected two transcripts, a larger transcript corresponding to full-length FAK mRNA and a

smaller transcript corresponding to focal adhesion kinase related non kinase (FRNK) (Figure 2-8, A). DD5-5(3) and DD5-9(6) both appeared up-regulated in the serum deplete (1% BSA) conditions versus the serum complete (10% FCS) conditions as indicated (Figure 2-8, C and D). On the other hand, DD5-7(7) probing of total RNA by Northern blotting exhibited an up-regulation of MST2 in serum depleted cultures, not an induction as illustrated (Figure 2-8, B) indicating that this message not only participates in the process of OLF442 differentiation but may also play a role in mitotic OLF442. Equalised RNA loading was confirmed in all Northern blots by probing with the "house keeping" gene GAPDH. As shown (Figure 2-8) the mRNA expression level of GAPDH was equal in both the control and test samples. Confirmation of the expression levels for the remaining differential display products was unsuccessful as Northerns were not sufficiently sensitive to detect a signal.

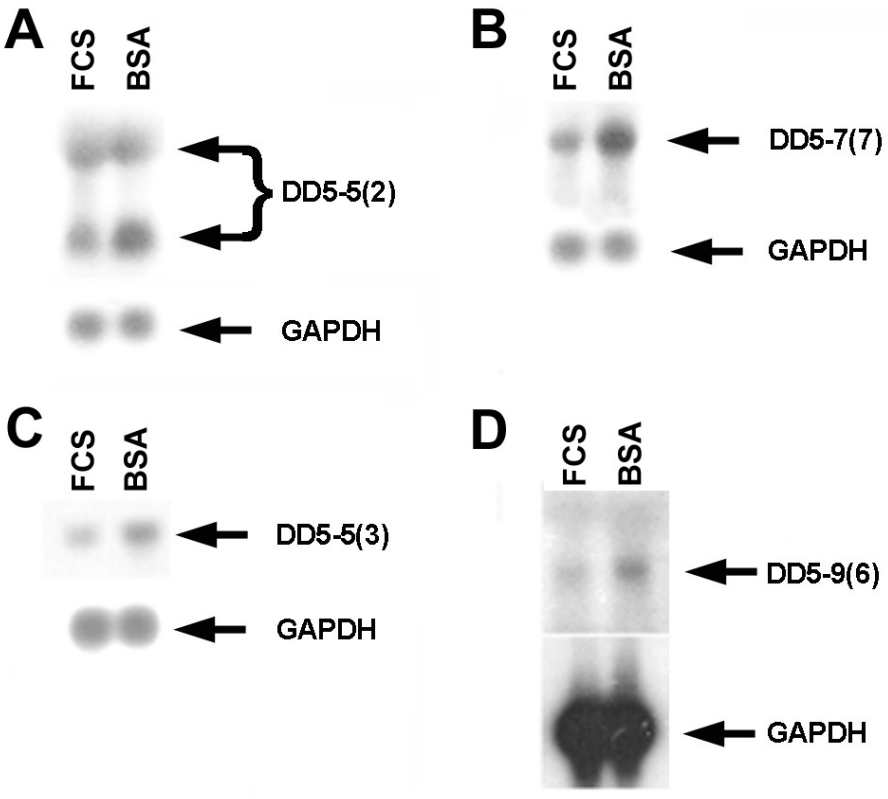

Figure 2-8 Northern analysis of differential display products.

Probes used are indicated, along with GAPDH used to confirm equal RNA loading.

2.4.6 cDNA Array Data

The cDNA array data was received from Affymetrix in the form of a Microsoft® Excel spreadsheet containing the top 138 expressed genes with a three fold or greater difference in differentiated OLF442 (1% BSA) versus non-differentiated OLF442 (10% FCS). In addition, the top 100 expressed genes that were downregulated by three fold or greater in differentiated OLF442 (1% BSA) versus non-differentiated OLF442 (10% FCS) were also included. This data was clustered and characterised into predominant functional groups (Table 2-3), refer to Appendix II for clustered gene lists.

Table 2-3 cDNA array data [a]

Functional Group	Upregulated Genes	Downregulated Genes
Signalling molecules	9	4
Cell cycle control	3	15
Cell death control	1	1
Growth factors and/or receptors/secretory proteins/neurotransmitters and chemokines	19	2
Nuclear proteins (transcription factors, DNA/RNA processing enzymes and binding proteins)	13	26
Protein processing, protein/vesicle transport, chaperones and protein folding molecules	10	15
Metabolic associated molecules and enzymes, transporters, ion channels	18	18
Cytoskeletal components, and accessory proteins involved in migration	8	3
Extracellular matrix proteins and molecules involved in adhesion and cell-cell interactions	13	1
Other	18	
Expressed Sequence Tags (ESTs)	20	23

[a] The cDNA array data was categorised into functional groups. The number of genes assigned to each functional set provides a broad indication of the overall status of OLF442 during neuronal differentiation. The complete data set is given in Appendix II.

2.5 Discussion

2.5.1 Differential Display

The aim of this work was to identify novel neuroregulatory genes that may be involved in processes that accompany the morphological differentiation of OLF442 upon serum depletion. The differential display produced twelve differentially expressed bands of which fifteen bands were generated upon secondary amplification and cloning. As mentioned previously, the low resolution of polyacrylamide gels is probably the key factor in explaining why one isolated band can produce numerous re-amplification products. Additionally, the ability of the researcher to precisely line up the autoradiograph with the sequencing gel requires precision so that extraction of the correct band is in fact carried out. Of the re-amplified and cloned fragments, six had no homology to any sequence in the non-redundant database (including ESTs); considering that the mouse genomic database (Celera) was not accessible, these sequences are potentially very interesting. Of the differentially displayed fragments with sequence homology to known genes, DD5-5(2) shared 97% homology with mouse focal adhesion kinase (FAK) and DD5-7(7) shared 90% homology with rat mammalian ste20 like (MST) 2 kinase. These two kinases provided the impetus for the work described in following chapters, primarily because they could provide additional information about possible signal transduction pathways that may be active during OLF442 differentiation. Furthermore, their expression levels were confirmed with Northern blot analysis (Figure 2-8). Importantly, Northern anlysis of DD5-5(2) detected two bands, one which corresponds to full-length FAK whose expression was not significantly different between the cultures, and one which corresponds to focal adhesion kinase related non kinase (FRNK), the expression of which was elevated in differentiated OLF442. The implications of increased FRNK expression are further studied and discussed in Chapter four.

Northern blot analysis only confirmed the expression level of four differentially displayed fragments. Presumably the expression level of the remaining fragments was below that detectable by Northern blotting. These probably could have been detected by RNase protection, which displays a 2-5 fold increase in sensitivity

over Northern analysis (Sambrook et al., 1989). Interestingly, two of the fragments identified as upregulated with differential display were also shown to be upregulated by oligonucleotide array analysis and are therefore implicated in the differentiation process of OLF442. The detection of the same genes with increased expression using the two distinct techniques gives credence to each result and illustrates the ability of these two methodologies to produce true data sets that can be further confirmed and studied.

2.5.2 Comparison Of The Differential Display And Oligonucleotide Array Data

The oligonucleotide array data received was the result from a single trial pilot study and therefore although interesting is only suggestive. However several aspects of the data are promising. A simple ratio comparison of the average difference values between the top 200 expressed genes in differentiated OLF442 versus non-differentiated OLF442 shows a 3 fold increase in SPARC (secreted protein, acidic and rich in cysteine). SPARC gene expression elevation was shown in a differential display study of OLF442 to participate in the embryonic development of the olfactory epithelium (Zehntner, 1998b), in agreement with the array data. Additionally, the array data shows a 1.8 fold increase in Ribosomal protein L3, this study also demonstrated an elevation of Ribosomal protein L3 by differential display and confirmed by Northern blotting (Figure 2-8C). Furthermore, differential display product DD5-7(5), which has 92% homology with mouse Fas-binding protein Daxx (Table 2-2), was found to be upregulated 6.6 fold in differentiated OLF442 by the array data (Appendix 2). Finally, the ratio comparison of the array data indicates a 0.8 fold change in GAPDH expression in differentiated OLF442 compared to non-differentiated OLF442. Such a low GAPDH fold change is not significant and therefore provides an adequate loading control for experiments such as Northern blotting.

2.5.3 Oligonucleotide Array Data: Implications

Although the possibilities appear boundless, cDNA arrays present several problems. Firstly, high throughput assays generate exhaustive amounts of data that require sophisticated computational and statistical techniques for their analysis. The vastness of the data combined with various algorithms to determine background/gradient correction values and scaling/normalization values results in a plethora of functional data values. For example, Affymetrix currently determines background variation by partioning the array into 16 equal squares each containing many features. The assumption that feature-to-feature background variation is not significant is in most cases reasonable, nonetheless it is not a rule. As demonstrated by Schadt et al. (2000), within each partitioned segment the lower 2% of the feature intensities for that block are averaged, and this average is subtracted from each feature in the block. However analysis of one section of an array covered by four separate partitioned segments displays variability in the reported intensity values illustrating the break-down in this rule (Schadt et al., 2000).

Additionally, Affymetrix assumes intensity differences between two or more arrays as linearly related (using least squares regression), however by simply changing such calculations to take into account a zero y-intercept, normalisation values can be dramatically affected (Alon et al., 1999; Schadt et al., 2000). Such data analysis variations ultimately can impact on whether a gene is reported as differentially expressed or even present. Probe hybridisation efficiency is also an unknown quantity, as hybridisations defined by Affymetrix are carried out at 45°C in a rotisserie oven set at 60 rpm for 16 h. Probe melting temperatures significantly greater can influence PM/MM differences as it would be expected that PM and MM probes would bind the RNA more tightly resulting in smaller PM/MM differences and biasing differential expression results (Schadt et al., 2000). Although an awareness of these issues is important, the current Affymetrix analysis software parameters are optimised to provide algorithms suitable for most applications. However, extracting the most accurate results and information from array data sets has further to evolve, and can only occur by understanding limitations and sources of variation (Schadt et al., 2000).

2.5.4 Oligonucleotide Array Data Analysis

The cDNA array data is fascinating, particularly as it confirms much of what one would expect during the implementation of the neuronal differentiation program. It also provides clues and significant insight into the mechanisms active during OLF442 differentiation. As illustrated in Chapter one, the extracellular medium is a supportive and instructional entity that both nurtures the cell and directs neuronal differentiation. Array data goes a long way toward providing an overall picture of active cellular processes, and in the situation investigated here indicates an elevation in the expression of numerous proteins involved in extracellular matrix remodelling and deposition.

2.5.4.1 The Extracellular medium

The collagens are a family of fibrous proteins that constitute the framework upon which the extracellular matrix is assembled. Collagen alpha 1 type VI and alpha 2 type VI have been shown to be the primary component of the extracellular matrix deposited along neural crest migratory pathways and are implicated in the regulation of cell movement by functioning as a migratory substrate (Perris et al., 1993), whilst alpha 1 type XVIII collagen, a homotrimeric basement membrane molecule of unknown function, is found in low amounts in all basement membranes and accumulates at high levels in the nervous system. Deletions in the carboxyl terminal domain of alpha 1 type XVIII collagen results in multiple cell migration and axon guidance defects indicating the importance of this molecule in neurite extension (Ackley et al., 2001). The up-regulation of associated molecules such as the membrane glycoprotein, nidogen (entactin), which forms a complex with laminins and is a major component of basement membranes (Dziadek, 1995), and laminin alpha 4 chain, a member of the heterotrimeric extracellular matrix glycoproteins involved in processes such as cell migration, proliferation and differentiation (Kortesmaa et al., 2000), confirm the dynamic restructure which the extracellular matrix undergoes during neuronal differentiation of OLF442. Other up-regulated glycoprotein molecules including EGP314 precusor (Wurfel et al., 1999), extracellular matrix associated protein (SC1) (Fujii et al., 2000), and osteopontin

(Opn), a secreted, glycosylated phosphoprotein (O'Regan and Berman, 2000), facilitate cellular adhesion. SC1 is particularly interesting as it is specifically and transiently expressed during the axonal growth of motorneurons, although on its own appears to be insufficient for the guidance mechanism of axonal outgrowth (Fujii et al., 2000). Additionally the elevated expression of ryudocan core protein, a ubiquitous type I integral membrane heparan sulfate proteoglycan present in focal adhesions (Woods and Couchman, 1994), has been implicated in promoting neurite growth (Kojima, 2000). Interestingly, ryudocan core protein contains potential binding sites for the transcription factors C/EBP and NF-kappa-B (Tsuzuki et al., 1997), both of which were found to be upregulated approximately 10 and 16 fold respectively during OLF442 differentiation, by the cDNA array results. Furthermore the up-regulation of the metalloproteinase bone morphogenetic protein 1 (BMP-1) that cleaves procollagen (Garrigue-Antar et al., 2001) and activates latent growth factors such as the TGF-beta superfamily has been linked to cell differentiation and pattern formation during development (Sarras, 1996). These results confirm the widespread architectural changes made during the differentiation program of OLF442, however these alone are insufficient to support the orchestrated co-ordination of diverse biological processes required for olfactory receptor neuronal precursor maturation and neurite extension.

2.5.4.2 The Cytoplasmic Environment

In order to achieve concomitant process extension on a conducive extracellular matrix support, cytoskeletal changes are fundamental. The actin cytoskeleton is an essential scaffold for integrating membrane and intracellular functions. The cDNA array data indicated that the level of A-X-actin in differentiating OLF442 cells is increased 4-6 fold when compared to non-differentiating cultures. Along with elevated actin levels, accessory actin binding and regulatory proteins such as gelsolin, an actin filament severing and capping protein implicated in actin remodeling (Sun et al., 1999), and eplin, which localises to filamentous actin and suppresses cell proliferation when overexpressed (Maul and Chang, 1999), are upregulated, indicating active cytoskeletal processesing in the presence of cellular differentiation. Likewise, the microtubule cytoskeleton composed of tubulin heterodimers assembled

into polymers are essential for, among other functions, mitotic spindle formation, axonal transport and organelle positioning (Dutcher, 2001) and are remodelled in response to differentiation. This is illustrated by the increased expression of a core component of microtubules β-tubulin type I, the microtubule stabilising factor microtubule-associated protein 4 (MAP4) required to promote tubulin polymerisation (Andersen, 2000), and the decrease of the destablising factor stathmin (Andersen, 2000) indicating that the microtubule cytoskeleton, although undergoing possible polymerisation (albeit slowly), is probably relatively stable.

The upregulation of cytosolic dynein, a molecular motor that produces directed movement along microtubules towards the proximal or minus-end (Asai and Koonce, 2001) would imply that differentiation of OLF442 requires movement of cargo toward the centrosome. Given that dynein plays an important role in the maintenance of the Golgi apparatus integrity and intracellular location, and that together with the centrosomes it co-localises to the site of newly emerging axons in cerebellar granule neurons (Zmuda and Rivas, 1998), it is apt to consider exactly what the Golgi does. The Golgi apparatus is involved in the "post-translational modification of newly synthesised membrane lipids and secretory proteins, which are received from the endoplasmic reticulum (ER) and en route to the plasma membrane or the endocytic pathway" (Roghi and Allan, 1999). Speculation about the cargo of dynein is premature, however the cDNA array data indicates that during OLF442 differentiation cholesterol biosynthesis is upregulated. The upregulation of 3-hydroxy-3-methylglutaryl-CoA (HMG-CoA) and HMG-CoA reductase results in the synthesis of mevalonate (Mathews and Van Holde, 1990). The upregulation of squalene synthase would indicate that OLF442 potentiates the conversion of mevalonate to squalene with the expected upregulation of cholesterol synthesis. The upregulation of Apolipoprotein D (ApoD) and bilirubin, both of which can bind cholesterol (Rassart et al., 2000), may indicate a role for dynein based transport of cholesterol (among numerous other molecules) from the endoplasmic reticulum to the Golgi for further processing prior to transport to the outgrowing cellular membrane. This may also be the method by which OLF442 is able to process and package numerous upregulated secretory proteins and chemokines (Table 2-3).

2.5.4.3 The Cell Cycle

Thus far the array data has provided the opportunity to make inferences about active processes in the cytoplasmic quarters of the cell and in the extracellular matrix. Here the array data confirms a previous study which showed that the olfactory-derived immortalised cell line OLF442 rapidly proliferates in control medium with a doubling time of 20 ± 1 hr, slowing down to a doubling time of 34 ± 1 hr upon serum deprivation (Zehntner, 1998b). As a result within 24 hr of serum depletion 87% of OLF442 cells quiesce in the G_1-G_0 transition of the cell cycle compared to 50% occupying G_1-G_0 in serum complete cycling cells, as shown by FACS analysis (Zehntner, 1998b). Accordingly, OLF442 begins to differentiate and extend long processes which continue to grow as the serum deplete culture time is increased. This observation is consistent with the idea that the removal of growth factors from the culture medium results in the downregulation of transcription from genes encoding CDK2, CDK4 and cyclins D and E. Therefore the levels of all these proteins fall rapidly, particularly as cyclin D mRNA and protein is unstable (Lodish, 1995). For that reason, cells in G_0 lack the cell cycle regulatory proteins required to promote passage through the cell cycle restriction point and which compose the S phase promoting factors (Lodish, 1995). The array data shows that cyclins A and B1 are downregulated 4.6 fold and 6.2 fold respectively, both of which are required for progression through S phase and the mitotic phase. Also CDK4 and CDK6 inhibitor protein (p16ink4a), that inhibits the CDK4/6-cylin D complex preventing progression through the G_1 phase, is upregulated 3.5 fold. These proteins and other cell cycle regulatory proteins also detected by the array all confirm the cessation of the cell cycle and are in agreement with the study that shows OLF442 serum deplete cell cultures are quiescent (Zehntner, 1998b).

2.5.4.4 The Nucleus

It is also interesting to note that while processes involved in broad morphological changes were upregulated during the differentiation of OLF442, the nucleus is far from inactive. The oligonucleotide array data reveals a situation where the expression level of numerous transcription factors is elevated even though DNA

replication is downregulated, as would be expected in quiescent differentiating cells. This is evidenced by the downregulation of primase, the enzyme responsible for initiation of all new DNA strands (Arezi and Kuchta, 2000) from which DNA polymerase can proceed with replication. Primase is also required for the unwinding of the parental DNA strands ahead of the replication fork and for RNA priming of Okazaki fragments on the lagging strand during DNA replication (Mathews and Van Holde, 1990). Importantly, RNA primer removal of Okazaki fragments during DNA replication is necessary and carried out by Flap endonuclease-1 (FEN-1), a structure-specific and multifunctional nuclease that plays important roles in DNA base excision repair and maintenance of genome stability (Qiu et al., 2000). The decreased expression of the DNA polymerase alpha catalytic subunit p180, primase small subunit, Flap endonuclease-1, and of molecules involved in nucleotide metabolism such as ribonucleotide reductase subunit M1/M2 and nucleoside diphosphate kinase A/B, thymidylate synthase and thymidylate kinase, illustrate the general reduction in DNA synthesis. This conclusion can be further supported by the downregulation of various histones, responsible for structuring DNA into chromatin and nucleosomes to compact DNA into the nucleus (Mathews and Van Holde, 1990). Likewise, the downregulation of the nonhistone chromosomal high mobility group 2 (HMG2) protein, that binds DNA in a sequence-nonspecific manner causing structural alterations in DNA such as bending, kinking and unwinding. HMG2 can also participate as a transcriptional activator and a DNA binding regulatory component of DNA-dependent protein kinase which may participate in cell proliferation (Nakamura et al., 2001), and its downregulation is testimony that OLF442 differentiation leads to a generalised suppression of DNA replication and associated processes.

The histone H2A.X from which polyadenylated and 3' processed mRNAs are transcribed as a short form (replication type histone) or a long form (basal type histone) is also downregulated, which compares favourably with a study confirming that H2A.X decreased in amount when cell cultures were incubated with inhibitors of DNA synthesis (Mannironi et al., 1989). Moreover, RNA processing proteins such as pre-mRNA splicing factor (SRP20), involved in alternative splicing of transcripts in a cell cycle dependent manner (Jumaa et al., 1997), and cleavage stimulation factor required for polyadenylation and 3' end cleavage of mammalian pre-mRNAs (Takagaki et al., 1992), are downregulated. Another downregulated RNA processing

protein, U1 small nuclear ribonucleoprotein (SnRNP) specific protein C, important for complex formation with the pre-mRNA 5' splice site (Tang et al., 1997) and for assembly of the spliceosome which performs nuclear pre-mRNA splicing (Labourier and Rio, 2001), again confirms the extensive downregulation of OLF442 DNA processing requirements. The expression level of translational proteins including elongation factor 1-delta, large ribosomal subunit protein, ribosomal protein L36, and 60S ribosomal L6 protein are also decreased, and may indicate that the translational ability of differentiated OLF442 cultures is compromised. Curiously several transcriptional activators were also downregulated, including the putative transcriptional regulator mEnx-1, the murine homolog of the Drosophila Enhancer of zeste gene and a member of the Polycomb group of genes which are transcriptional regulators of homeobox gene expression (Hobert et al., 1996). A recent study investigating the role of Enx-1 in various haematopoietic cells showed that Enx-1 is involved in proliferation, accordingly the promyelocytic cell line HL-60 when differentiated to mature granulocytes with all-trans retinoic acid exhibited a downregulation of Enx-1. Moreover, Enx-1 antisense oligodeoxynucleotide suppressed DNA synthesis in HL-60 cells (Fukuyama et al., 2000). Other downregulated transcription factors include cellular binding protein (CNBP), originally reported to be a single-stranded DNA-binding protein specifically interacting with sterol responsive elements of the low-density lipoprotein (De Dominicis et al., 2000), which also binds as a trans-acting factor upstream of the Macrophage colony-stimulating factor (M-CSF; CSF-1) promoter (Konicek et al., 1998) and Carg-binding factor A (CBF-A) (Bushweller, 2000; Mikheev et al., 2000).

2.6 Conclusion

Differential display has revealed the upregulation of several fragments, the most interesting of which are kinases, including FRNK and MST2 kinase, and whose expression levels were confirmed by Northern analysis. Given that no mouse MST2 homologue has been described, and that no functional role for full-length MST2 has been proposed in neuronal cells, the full-length isolation of murine MST2 will be outlined in the following Chapter.

The comparison of the differential display results and the oligonucleotide array data indicate that both techniques are reliable and informative. The choice of one technique over the other relies primarily on laboratory resources and the nature of the model system to be analysed. Furthermore, post-data acquisition management of arrays is crucial, as more questions will be raised than can be answered by simple binary comparisons (Green et al., 2001). As illustrated here, array data provides insight and opportunity to ask specific questions and to make inferences about active processes, however it must be coupled with thoughtfully planned experiments to ensure that assumptions are not drawn from speculation but instead from tangible evidence.

3 MAMMALIAN STE20 LIKE (MST) KINASE: ISOLATION AND CHARACTERISATION

3.1 Extracellular To Nuclear Communication

The intracellular signal transduction cascades that communicate external environmental stimuli to the cell interior undoubtedly convey the initiating signals that lead to the morphological differentiation of OLF442 by serum depletion. The prevailing belief of the mechanism utilised by the mitogen-activated protein kinase (MAPK) superfamily is the amplification of signals originating at the cellular membrane by the use of multiple messengers whose activity is regulated by reversible phosphorylation and/or in some instances by irreversible proteolysis. As discussed below, mammalian Ste20-like (MST) kinase can be regulated by phosphorylation and proteolysis, however the MAPK pathways in which it functions remains to be elucidated.

3.1.1 Mitogen-Activated Protein Kinase (MAPK)

Signalling networks represent a common characteristic between all cell types, which is the ability to coordinate cellular activities with environmental changes. Perception of the extracellular milieu by the internal signalling machinery provides cues for cell fate determination and represents the principle communication system utilised by cells to traffic information from the external membrane to the cell nucleus. The delivery of extracellular signals to their intracellular targets is mediated by a network of interacting proteins directing a large number of cellular processes, including proliferation, differentiation, oncogenic transformation, immune responses and apoptosis (Pawson and Scott, 1997; Tibbles and Woodgett, 1999). In both mammals and lower eukaryotes the archetypal MAPK cascade is arranged in a conserved three-kinase tier (Figure 3-1), consisting of a MAPK that is phosphorylated and activated by a MAPK kinase (MAPKK/MEK/MKK). MAPKKs are characteristically dual specificity kinases which catalyse the phosphorylation of MAPKs on both tyrosine and threonine residues. The MAPKKs are themselves phosphorylated and activated by serine/ threonine kinases that function as MAPKK kinases (MAPKKKs/MEKKs/MKKKs) (Garrington and Johnson, 1999). The MAPKKKs have distinct defined regulatory motifs that are not found in MAPKKs or MAPKs. These motifs include pleckstrin homology (PH) domains, proline-rich sequences for binding SH (Src-homology) 3 domains, binding sites for G-proteins,

leucine zipper dimerisation sequences, and phosphorylation sites for tyrosine and serine/threonine kinases. Thus MAPKKKs can be differentially regulated by a variety of upstream inputs for their selective regulation of MAPKKs (Garrington and Johnson, 1999). This organisation allows transmission of signals by sequential phosphorylation and activation of the components specific to a respective cascade, resulting in activation of different MAPKs. Consequently, activated MAPKs phosphorylate appropriate substrates, including other protein kinases and transcription factors, to evoke a cellular response to extracellular stimulation (Pawson and Scott, 1997; Ip and Davis, 1998). In the budding yeast *Saccharomyces cerevisiae*, and the fission yeast *Schizosaccharomyces pombe*, these cascades are activated principally by cellular stresses. The evolutionary conservation of these cascades in mammals, to primitive stress responses such as osmolar shock demonstrates their effectiveness and efficiency (Pombo et al., 1996). Additionally, these cascades have evolved further in mammals to provide responses to elaborate stimuli such as cytokines and growth factors.

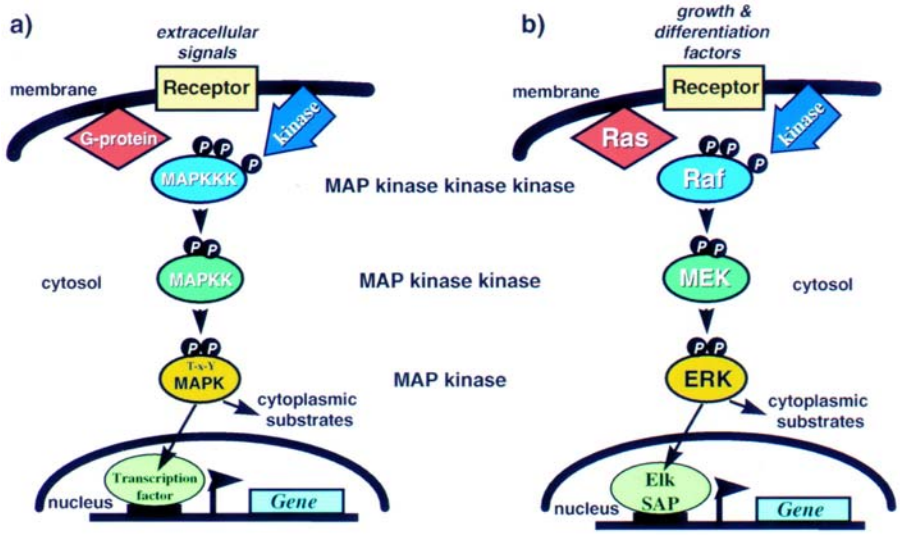

Figure 3-1 Schematic representation of the generic MAPK cascade.

Panel A, depicts the three-kinase tier arrangement. Panel B illustrates the core components of the ERK cascade specifically. Figure from Kolch (2000).

In the budding yeast, *S. cerevisiae*, at least six MAPK pathways have been identified, regulating diverse biological processes [reviewed in (Herskowitz, 1995; Elion, 2000)]. By far the best-characterised and understood receptor-G protein coupled MAPK cascade, is the pheromone response pathway. It is comprised of a p21-activated protein kinase (PAK) family member Ste20, a MAPKKK Ste11, a MAPKK Ste7, and two MAPKs Fus3 and Kss1 (Figure 3-2) (Elion, 2000). The pheromone response pathway stimulates several cellular responses including cell cycle arrest in G_1 phase, transcriptional changes and polarised morphogenesis (Leeuw et al., 1998). The upstream regulator of signals transduced by this cascade, Ste20, was the first identified member of the serine/threonine protein kinases of the Ste20/Pak family, a component that exerts its effects upstream of the MAPKKK position (Figure 3-2) (Leberer et al., 1992; Ramer and Davis, 1993). Although Ste20 is central to the pheromone response pathway its activity is not restricted solely to this cascade. In fact Ste20 is rather promiscuous and is utilised by three other signalling pathways in *S. cerevisiae*, including the osmotic stress pathway (O'Rourke and Herskowitz, 1998), nutrient deprivation response pathway and the vegetative growth pathway (Lee and Elion, 1999; Elion, 2000). Given that functional redundancy between family members is minimal, the promiscuous nature of Ste20 implies that the members of this family may be universal regulators of multiple biological processes. Combined with a growing family tree, Ste20 is becoming one of the most interesting kinases currently under investigation, as many of its mammalian counterparts have no defined function.

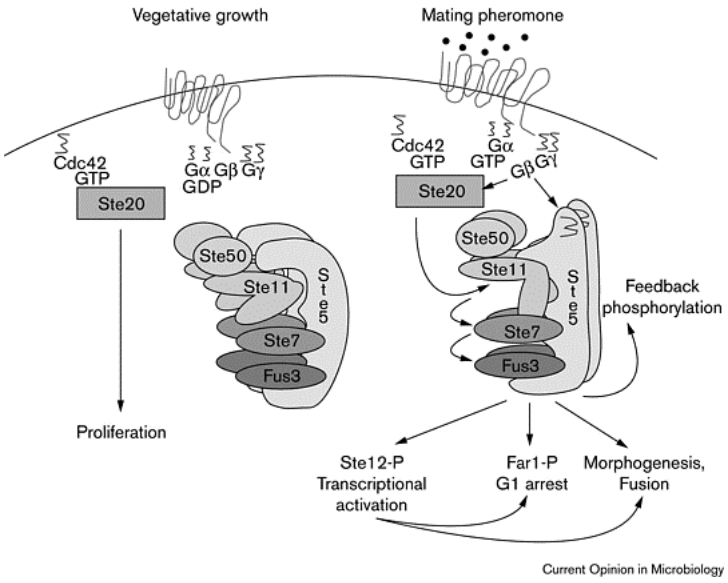

Figure 3-2 Schematic model of the role of Ste20 in the activation of the pheromone response pathway.

Activation of the pathway requires that pheromone binding activate the G protein complex leading to an exchange of GDP to GTP on Gα, followed by dissociation of the Gα,β, and γ subunits to allow binding of Gβ to downstream targets. Figure from Elion, (2000).

3.1.2 Ste20/PAK Serine/Threonine Protein Kinase Family

Yeast Ste20 (Ramer and Davis, 1993), and mammalian homologue PAK (Manser et al., 1994), are the founding members of the Ste20/PAK family as both share significant homology throughout their catalytic domains (Sells and Chernoff, 1997). Mammalian and yeast homologues of the Ste20/PAK family of kinases are divided into two classes based on their organisation. Class I (Ste20, Cla4 and PAK) contain a carboxyl-terminal catalytic domain, an amino-terminal regulatory domain and are activated by the small guanosine triphosphatases Cdc42 and/or Rac1 (Sells and Chernoff, 1997). Members of class II, which include Sps-1, germinal center kinase (GCK), hematopoietic progenitor kinase (HPK), kinase responsive to stress (KRS) 1/2, mammalian Ste20-like (MST) kinase 1/2/3, and Ste20/oxidant stress response kinase (SOK1), lack GTPase binding domains, but are conserved throughout their amino-terminal catalytic domain (Figure 3-3) (Creasy et al., 1996; Sells and Chernoff, 1997).

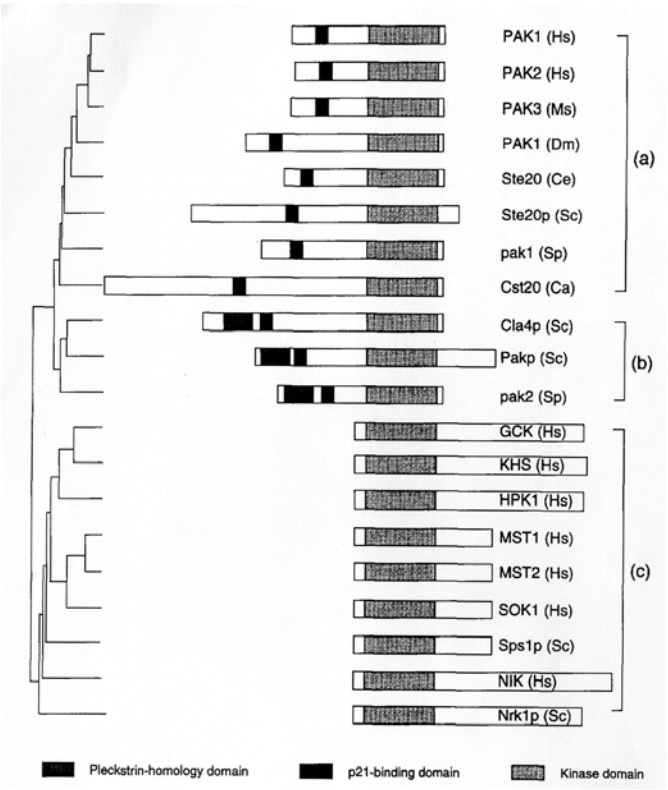

Figure 3-3 The p21-activated protein kinase (PAK) family.

The PAK family can be divided into three categories: true PAKs (a), pleckstrin-homology (PH)-PAKs (b) and GCKs (c). Figure from Sells and Chernoff (1997).

The Ste20/PAK family of protein kinases has emerged as a necessary component of the morphological signalling process (Daniels and Bokoch, 1999). The principle function of Ste20 appears to be its ability to regulate cell polarity during growth and in response to numerous extracellular signals (Pruyne and Bretscher, 2000a). Controlled changes to the actin cytoskeleton are fundamental for numerous cellular processes including motility, cell division, cell adhesion, and cell death (Daniels and Bokoch, 1999). In *S. cerevisiae* the Rho-family G-protein Cdc42 is central to changes in the actin cytoskeleton during vegetative growth (Pruyne and Bretscher, 2000a), high osmolarity and nutrient deprivation (Elion, 2000). GTP-bound Cdc42 localises Ste20 to the site of new growth at the cell cortex and activates a MAPK cascade resulting in cytoskeletal reorganisation (Pruyne and Bretscher, 2000b). However in response to pheromone, mating projections develop when Ste20 localises to and associates with an active heterotrimeric G-protein directly (Leeuw et

al., 1998), thereby activating a MAPK cascade and producing distinct cytoskeletal structures (Daniels and Bokoch, 1999). The downstream response to each signal is the rearrangement of the actin cytoskeleton and consequently control of various other processes such as the cell cycle. In mammalian fibroblasts PAK1 regulates cell motility (Sells et al., 1999b) while in Drosophila the Ste20-related kinase misshapen regulates axonal targeting and dorsal closure (Su et al., 1998; Su et al., 2000). It appears obvious that global cytoskeletal changes required for polarity and motility are central to the growth and survival of *S. cerevisiae* in a manner that may be analogous to processes involved in mammalian cells. Evidence is limited however, and dissecting elaborate signalling processes in higher order cells is challenging. Members of the mammalian Ste20/PAK family with undefined function indicate that they may participate in subtle processes whose transduction cascades have yet to be elucidated.

3.1.3 Mammalian Ste20-Like (MST) Kinase

Wang and Erikson (Wang and Erikson, 1992) observed a 63-kDa protein kinase activity identified late in the transformation of chicken embryo fibroblasts by $pp60^{v\text{-}src}$, whose activity correlated with the presentation of the transformed cell phenotype. Later identified as mammalian Ste20-like (MST)2, this protein kinase activity was observed in mammalian cells treated with okadaic acid (OA) or following staurosporine (STR) treatment (Taylor et al., 1996). Subsequent isolation of the cDNAs by Taylor et al. (1996) identified two serine/threonine protein kinases shown to be members of a subfamily of kinases related to yeast Ste20p. The specificity of activation of these enzymes, designated as KRS-1 (63 kDa) and KRS-2 (61 kDa), for kinase responsive to stress, suggested that they might function early in a mammalian cell stress response pathway (Taylor et al., 1996). Sequencing of the p63 and p61 cDNAs indicated that the clones encoded two distinct but closely related protein kinases with predicted molecular weights of 56.3 kDa and 55.6 kDa (Taylor et al., 1996). However the sequences of these cDNAs had been reported previously (Creasy and Chernoff, 1995a, 1995b) and are designated MST1/KRS-2 and MST2/KRS-1. In fact, MST1 kinase was first cloned and characterised in 1995 by cDNA amplification of a human lymphocyte cDNA library with degenerate oligonucleotide primers that

corresponded to conserved amino acids present in the catalytic domains of serine/threonine kinases (Creasy and Chernoff, 1995b). A polyclonal antiserum directed against the carboxyl-terminus of MST1 (aa 276-487) identified a 57 kDa polypeptide. The amino-terminal half of MST1 contains the 11 subdomains characteristic of a serine/threonine protein kinase while the carboxyl-terminal half is relatively acidic (pI 4.4) and lacks any notable sequence motifs (Creasy and Chernoff, 1995b). Interestingly, a short acidic region (10–15 aa in length) in their noncatalytic domains is a trait shared with other Ste20 family members (Taylor et al., 1996). A second human homologue of the Ste20-kinase family, known as MST2, shares significant homology with MST1 (78% identity, 88% similarity) and encodes a protein of 56kDa (Creasy and Chernoff, 1995a). While MST1 and MST2 are two different proteins encoded by distinct genes (Taylor et al., 1996) much of the published work has found that they share the same (or very similar) functional properties, therefore much of what is reported for one protein may also correspond to its counterpart (refer to Appendix III and IV for relevant MST1/2 alignments).

MST1/2 are allocated within the serine/threonine protein kinase Ste20/PAK family as both share significant homology with Ste20p and p21-activated kinase (PAK) (62-65% similar) throughout their catalytic domains (Creasy and Chernoff, 1995a, 1995b). Preliminary data suggested that MST1/2 do not interact with recombinant glutathione S-transferase-tagged Cdc42, Rac1 or Rho as they lack the necessary interacting domains (Taylor et al., 1996). Additionally, MST1/2 lack a potential SH3-binding domain present in some but not all Ste20p family members (Taylor et al., 1996) and do not contain an obvious pleckstrin homology domain through which they might interact with heterotrimeric G proteins (Musacchio et al., 1993).

Further, Schinkman and Blenis (1997) cloned and characterised a novel human member of the Ste20/PAK family termed MST3, which awaits identification of a physiological function. Based on its domain structure MST3 belongs to the Sps1 subfamily of Ste20-like kinases with an amino-terminal kinase domain and a carboxyl-terminal regulatory domain. MST3 more closely resembles SOK1, with amino acid similarities of 88 and 68.8% in the kinase domain and overall protein sequence respectively, however MST3 is not regulated by oxidative stress as is SOK1

(Pombo et al., 1996; Schinkmann and Blenis, 1997). Also the recently identified MST4 which is most closely related to MST3 (Qian et al., 2001) and has been found to participate in the activation of the MEK/ERK pathway and in mediating cell growth and transformation (Lin et al., 2001).

3.1.4 MST Catalytic Activity

The catalytic activity of MST1 is characteristic of a serine/threonine kinase capable of phosphorylating an exogenous substrate as well as itself (Creasy and Chernoff, 1995b). Creasy and Chernoff (1995b) found that MST1 activity increased 3-4 fold upon treatment with PP2A (a serine/threonine phosphatase), suggesting that MST1 is negatively regulated by phosphorylation. At present no obvious biological role has been assigned to MST1, as treatment with several agents such as calf serum, lysophosphatidic acid (LPA), 12-0-tetradecnoyl-phorbol-13-acetate (TPA), heat shock, and high salt failed to alter MST1 activity (Creasy and Chernoff, 1995b). As MST1 does not appear to function in any known MAPK signal transduction cascade (because its activity is not increased in response to growth factors, heat shock or high osmolarity), it was concluded that MST1 would probably be involved in an unknown pathway. Likewise, MST3 activity, which does not change upon growth arrest, serum deprivation or growth promoting agents such as serum, LPA, epidermal growth factor (EGF), and platelet-derived growth factor (PDGF), is probably involved in an unknown pathway (Schinkmann and Blenis, 1997). Additionally, stress stimuli such as anisomycin, sorbitol, staurosporine, and UV exposure also failed to increase MST3 kinase activity (Schinkmann and Blenis, 1997). However, the delayed activation of MST2/KRS-1 by Src, and lack of regulation by growth promoting stimuli, suggest that MST2 might function in the late morphological alterations that result upon $pp60^{v\text{-}src}$ transformation. In addition to a pivotal role that this kinase may play in the cellular response to extreme stress (Taylor et al., 1996), it appears that cell cycle progression does not affect MST1 activity and it is believed that inhibition of activity is not specific to quiescence, instead, MST1 appears to be maintained in a partially inactive state through serine/threonine phosphorylation (Creasy and Chernoff, 1995b).

Although the biological function of MST1/2 has yet to be definitively elucidated, it is apt to consider that the founding member of the Ste20/PAK family, namely

Ste20, partakes in roles reminiscent of differentiating eukaryotic cells. Since genetic screens of proteins required for mating in the budding yeast *S. cerevisiae* were conducted (Leberer et al., 1992), it has been shown that Ste20 acts upstream of the MEK kinase position and stimulates a MAPK cascade essential for cell-cycle arrest and transcription of mating specific genes (Figure 3-2) (Leberer et al., 1997). Activation of this cascade through binding of pheromones to G-protein-coupled receptors results in growth arrest in G_1 phase of the cell cycle, differential gene expression and formation of mating-specific projections otherwise termed polarised morphogenesis (Leeuw et al., 1998). Importantly however, MST1 does not appear to be functionally analogous with Ste20p as it is unable to complement a ste20 null allele in *S.cerevisiae* using a quantitative mating assay (Creasy and Chernoff, 1995b). This evidence does not necessarily refute a possibility that in mammalian cells MST1/2 may play a similar role. Data obtained to date suggests that members of the MST subfamily are likely to lie immediately downstream of a Ras-related or heterotrimeric G protein (Taylor et al., 1996). Stimuli identified to date that "induce MST activity have common phenotypical ramifications; all reduce cell attachment and result in eventual death, with the exception of transformation by $pp60^{v\text{-}src}$ " (Taylor et al., 1996). However, the identification by an in-gel kinase assay of a 56 kDa serine/threonine kinase that is able to phosphorylate thyroid transcription factor-1 (TTF-1) exclusively on serine residues in thyroid cells suggests a functional role besides apoptosis (Aurisicchio et al., 1998). The rat homologue of the human MST2 kinase was found to be constitutively active in thyroid cells and was responsible for the phosphorylation of TTF-1, otherwise known as Nkx2.1, a member of the NK-2 family of vertebrate homeobox genes which play an essential role in tissue differentiation and organogenesis (Bingle, 1997; Small et al., 2000). Additionally, a role for MST1 has been proposed in megakaryocyte differentiation by signalling from the megakaryocyte growth and development factor (Mpl ligand) to promote induction of lineage-specific cellular programming (Sun and Ravid, 1999).

3.1.5 MST Kinase Homodimerisation

The homodimerisation of MST1 is a process likely to be necessary for the interaction of MST1 with its effector molecule, or for phosphorylation of its substrate (Creasy et al., 1996). MST3 can also dimerise therefore resembling MST1 in this respect (Schinkmann and Blenis, 1997). The self association capability exhibited by MST1 is dependent on the extreme carboxyl-terminal 57 amino acids which are essential for this process, however loss of dimerisation does not appear to affect its kinase activity (Creasy et al., 1996). In addition, an inhibitory domain mapped by a series of carboxyl-terminal and internal deletions indicate the presence of an element within a central 63 amino acid (aa 331-394) region of MST1 that inhibits kinase activity, as removal of this domain increases kinase activity approximately 9 fold (Creasy et al., 1996). This is supported by the expression of a smaller 40-kDa carboxyl-terminal truncated form of MST1 that arises from proteolysis. This proteolytic cleavage product has a greater kinase activity than full-lengthMST1, indicating that the carboxyl terminus has an inhibitory role (Creasy and Chernoff, 1995b). Interestingly, both functional domains lie in regions conserved between MST1 and MST2, and the molecule without the dimerisation and inhibitory domains is not as active as one, which only lacks the inhibitory domain (Creasy et al., 1996). It is also important to note that MST1 is associated with a high molecular weight complex in cells, therefore it may oligomerise with other proteins (Creasy et al., 1996). Several examples of serine/threonine protein kinases that dimerise exist, including homodimerisation of the amino-terminal domain of Akt, a cytoplasmic serine/threonine protein kinase coded for by the c-akt proto-oncogene (Datta et al., 1995), and chemically induced oligomerisation of Raf-1 (Morrison and Cutler, 1997). Dimerisation of ERK2 (a tyrosine/threonine MAPK) does not appear to increase its kinase activity but has been shown to play important roles in ERK2 substrate interactions and subcellular targeting (Cobb and Goldsmith, 2000).

3.2 Aim

In the previous Chapter the detection of MST2 kinase in a differentiated mouse olfactory neuronal derived cell line OLF442 by differential display was described. Given that no mouse MST2 homologue had been identified the cloning of full-length mouse MST2 kinase was undertaken.

3.3 Methods

Recipes for all reagents and buffers mentioned throughout the methods are provided in Appendix I. Also listed in Appendix I are bacterial genotypes and primer sequences.

3.3.1 Mouse Olfactory Epithelium cDNA Library Screening

A mouse olfactory epithelium cDNA library (primary titre of $6x10^5$ plaque forming units (pfu), amplified titre of 10^{10} pfu/mL) was screened with several probes as described below.

3.3.1.1 Titering the Amplified Library

A single, isolated colony from the working stock plate of XL1-Blue (Stratagene, Integrated Sciences, Melbourne, Australia) was used to inoculate 10 mL of LB/10 mM $MgSO_4$ (Sigma)/10%(v/v) maltose broth without antibiotics (Clontech). The culture was incubated overnight at 37°C with shaking at 140 rpm until the OD_{600} of the culture reached 1.0. Cells were centrifuged in a sterile conical tube for 10 min at 2000 rpm and the supernatant was removed. The cell pellet was resuspended in 10 mM $MgSO_4$ until an OD_{600} of 0.5 was reached. Dilutions of the phage lysate (library) were prepared serially in SM buffer. To the diluted phage, 200 µL of OD_{600} = 0.5 XL1-Blue host cells were added and incubated at 37°C for 15 min. Melted NZY top agar (3 mL) at 45 °C was added to each phage/XL1-Blue preparation mixed by inversion and poured onto separate NZY plates, ensuring that the top agar was evenly distributed on the plates. The plates were left at room temperature to allow the top agar to harden, then incubated overnight at 37°C. The plaques were counted in order to determine the titre (pfu/mL) as follows:

$$\text{Pfu/mL} = \frac{\text{number of plaques x dilution factor x } 10^3 \text{ µL/mL}}{\text{X µL of diluted phage plated}}$$

3.3.1.2 cDNA Library Plaque lifts

Phage was plated at a concentration of $1x10^9$ pfu as described above. Plates were chilled to 4°C for 1 hr prior to performing plaque lifts. Plaque lifts were onto NEN Colony/Plaque Screen Hybridisation Transfer Membranes (Perkin Elmer Life Sciences, Melbourne, VIC, Australia) according to the manufacturer's recommendations. Briefly, the first filter disc (dry membrane) was placed in contact with the agar plate for 2 min, ensuring that the membrane was evenly placed on the plate without trapping air bubbles. The duplicate plaque lift was allowed to transfer for approximately 4 mins. Disc positions were marked with three asymmetrical needle stick holes in the filter and plate using sterile Indian Ink (Sigma). Following plaque lifts, the transfer membranes were denatured by submerging in denaturing solution (1.5 M NaCl, 0.5 M NaOH) for 2 min, followed by incubation in neutralising solution (1.5 M NaCl, 0.5 M Tris-HCl, pH 8.0), for 5 min and finally rinsed in 2X SSC, 0.2 M Tris-HCl, pH 7.5, for no more than 30 sec. Excess buffer was blotted from the membranes (plaque side up) on Whatman 3MM paper and transferred to a sheet of dry Whatman 3MM paper (plaque side up). DNA was fixed to membranes by oven baking filters at 80°C for 2 hrs.

3.3.1.3 Plaque Lift Hybridisation and Screening

Prior to prehybridisation the oven-dried membranes were pre-wet in 2X SSC for 1 min and placed in hybridisation bottles interleaved with separating mesh. Membranes were prehybridised for 3 hrs at 62.5°C in prehybridisation solution (1% SDS, 1% Dextran Sulphate, 5X Denhardts solution and 0.58gm NaCl/10ml). Probes were radiolabelled with [α^{32}P] dATP (> 1000Ci/mmol), using a Random Primed DNA Labelling kit (refer to Section 2.3.5.2) and were subsequently column purified as indicated in Section 2.3.5.3. Probe eluant was diluted to 900 µL with MQH_2O and 100 µL of sheared herring sperm or salmon sperm DNA (5 mg/mL) was added. The probe mixture was denatured at 100°C for 10 min then chilled on ice for 15 min. The probe solution was added to the prehybridisation mixture and allowed to hybridise overnight at 62.5°C. Membranes were washed twice with 2X SSC at room temperature for 10 min, twice with 2X SSC, 0.1% SDS at 60°C for 20 min, and once with 0.1X SSC, at room temperature for 10 min. Wet membranes were placed on

plastic wrap and exposed to RX-80 Fuji medical X-ray film with an X-ray cassette and intensifying screen (Kodak) overnight at -70°C. Membranes could be stripped and reprobed by incubating the membrane discs in 100 mL of 0.4 M NaOH at 42°C for 30 min, followed by incubation in100 mL of 0.1 X SSC, 0.1% SDS, 0.2 M Tris-HCl (pH 7.5) at 42°C for 30 min with gentle agitation.

3.3.1.4 Picking Plaques

Aligning the film with the master plate according to the India ink orientation marks allowed the selection of positive plaques that were identified on duplicate filters. The chosen plaque was stabbed out of the agar plate by using a glass Pasteur pipette. These plaque/agar plugs were placed into a 1.5 mL centrifuge tube containing 300 µL of SM buffer and 1.5 µL of chloroform. The plug suspension was briefly vortexed and incubated at room temperature overnight to allow phage particle diffusion out of the agar. The isolated phage solution was used for further rounds of plating and hybridisation. Secondary, tertiary and up to quaternary screens were routinely done to ensure the correct plaque had been isolated. Plugs taken using a glass Pasteur pipette placed in 300 µL of SM buffer overnight produced yields of approximately 10^6-10^7 pfu/ml.

3.3.1.5 Excision: Converting λTriplEx2 to pTriplEx2

Conversion of a λTriplEx2 (phage) clone to a pTriplEx2 plasmid involves in vivo excision and circularisation of a complete plasmid from the recombinant phage. The plasmid is released as a result of cre-recombinase-mediated site-specific recombination at the loxP sites that occurs when the recombinant phage is transduced into an appropriate host with cre-recombinase expression such as *E.Coli* BM25.8 and grown at 31°C. The conversion was carried out as per the Clontech instruction manual. Briefly, a single isolated colony from the working stock plate of BM25.8 host cells was used to inoculate 1 mL of LB/$MgSO_4$ broth. The BM25.8 suspension was incubated overnight at 31°C with shaking at approximately 150 rpm until the OD_{600} reached 1.1-1.4 then 100 µL of 1 M $MgCl_2$ was added to the culture. The eluted phage (150 µL) from a positive plaque was combined with 200 µL of BM25.8

culture and incubated at 31°C for 30 min without shaking, following which 400 µL of LB broth was added. The phage/BM25.8 suspension was incubated for an additional 1 hr with shaking (225 rpm) at 31°C. The infected cell suspension (1-10 µL) was then spread onto an LB/AMP plate and grown overnight at 31°C to obtain isolated colonies. Plasmid DNA was prepared as described (Section 2.3.4.5) and analysed by DNA digestion (Section 2.3.4.6) and sequence analysis (Section 2.3.4.7).

3.3.2 Full-length MST Kinase Isolation From cDNA

3.3.2.1 Serum Depletion and mRNA Extraction

OLF442 cells were differentiated as described (Section 2.3.1.2). Total RNA was extracted as outlined in Section 2.3.2.1 and the relative purity was determined by absorbance at 260 and 280 nm (A_{260}/A_{280} ratio). mRNA was prepared from approximately 200 µg total RNA with the oligotex mRNA extraction kit (Section 2.3.2.4) and was quantitated by spectrophotometry.

3.3.2.2 SMART cDNA Synthesis

mRNA was reverse transcribed using the SMART™ PCR Library Construction Kit (Clontech, Palo Alto, California, USA) as per the manufacturer's instruction. Briefly 0.075 µg mRNA was combined with 1 µL of (10 µM) SMART III Oligonucleotide and 1 µL of (10 µM) CDS III/3' PCR primer and made up to 5 µL with MQH_2O. Reactions were incubated at 72°C for 2 min then cooled on ice for 2 min, and the following reagents were added in order: 2 µL of 5X First-strand buffer, 1 µL DTT (20 mM), 1 µL dNTP mix (dATP, dCTP, dGTP, dTTP, 10 mM each). Finally, 1 µL (200 Units) of recombinant Moloney Murine Leukaemia Virus derived reverse transcriptase without RNase H activity (MMLV-RT RNase H^-; Superscript II, Gibco-BRL) was added and the reaction was overlayed with 20 µL mineral oil and incubated at 42°C for 2 hr.

3.3.2.3 cDNA Amplification by Long Distance (LD) PCR

cDNA was amplified by LD-PCR using the Advantage cDNA PCR Kit (Clontech) as follows: 2 µL first strand cDNA was added to 1X cDNA PCR reaction buffer, 2 µL 50X dNTP mix (dATP, dCTP, dGTP, dTTP, 10 mM each), 2 µL 5'-PCR primer (10 µM), and 2 µL (10 µM), CDS III/3' PCR primer and 2 µL 50X Advantage cDNA Polymerase Mix. The reaction was made up to 100 µL with MQH_2O, overlaid with 50 µL mineral oil and subjected to the following PCR program: 95°C x 1 min 20 sec, 95°C x 20 sec, 68°C x 6 min for 24 cycles.

3.3.2.4 cDNA Quality and Integrity

cDNA quality was analysed by resolving a 5 µL aliquot of the LD-PCR amplified cDNA on a 1.1% agarose gel (Section 2.3.2.9). The integrity of the cDNA was confirmed by analysing for the presence of GAPDH by PCR amplification (Section 2.3.2.8). Briefly 2 µL of LD-PCR amplified cDNA was subjected to PCR using GAPDHF and GAPDHR primers and the following PCR program: 95°C x 5 min, followed by 4 cycles at 95°C x 1 min, 57°C x 1 min, 72°C x 1 min 30 sec, followed by 20 cycles at 95°C x 1 min, 65°C x 1 min, 72°C x 1 min 30 sec with a final extension at 72°C x 10 min. PCR amplification products were resolved on an agarose gel as above.

3.3.3 Full-length Amplification Using Rat MST2 Kinase Primers

A forward primer (rMST2F) and reverse primer (rMST2R) were designed to flank the rat MST2 coding sequence using the web based primer prediction and analysis program Primer3 (Rozen and Skaletsky, 1998). The Expand Long Template PCR System (Roche, Castle Hill, NSW, Australia) was used to amplify full-length mouse MST2 kinase. Master mix 1 was prepared by adding 1 µM of rMST2F and rMST2R, to 500 µM dNTPs in a final volume of 20 µL with MQH_2O. Master mix 2 was prepared by combining 1X Expand buffer, 0.75 mM $MgCl_2$ and 2.5 Units of Expand enzyme mix to a volume of 25 µL with MQH_2O. Master mix 1 was combined with master mix 2, and 5 µL of amplified cDNA was added. The 50 µL reaction was

overlayed with 50 µL mineral oil and subjected to the following PCR program: 94°C x 2 min, followed by 10 cycles at 94°C x 10 sec, 57°C x 30 sec, 68°C x 2 min, proceeded by 25 cycles at 94°C x 10 sec, 65°C x 30 sec, 68°C x 2 min with a 20 sec increment per cycle, followed by a final extension at 68°C x 7 min. PCR products were visualised by agarose gel electrophoresis (Section 2.3.2.9).

3.3.3.1 PCR Product Cloning

MST2 PCR amplified products were gel extracted using the QIAquick Gel Extraction Kit (Section 2.3.3.1.2) and quantitated by spectrophotometry. Gel extracted PCR products were cloned into pGEM®-T (3 Kb) or pGEM®-T Easy (3 Kb) Vector Systems as instructed by the manufacturer's protocol (Promega, 1998). PCR products were A tailed and ligated using a vector: insert ratio of 1:2 (Section 2.3.4.1). Ligations were incubated at 4°C overnight prior to transformation (see below).

3.3.3.2 XL10-Gold Transformations

Epicurian Coli® Solopack™ Gold Supercompetent Cells (XL10-Gold) have an extremely high transformation efficiency (1 x 10^9 cfu/µg), (Stratagene). Transformations were carried out as indicated by the manufacturer's instructions (Stratagene, 1998). In short, XL10-Gold cells were thawed on ice and 1 µL of β-mercaptoethanol mix was added to each aliquot of cells, followed by incubation on ice for 10 min with gently swirling every 2 min. Approximately 0.01-50 ng of DNA (2 µL of ligation reaction mix) was added to the cells, gently mixed and incubated on ice for 30 min. Cells were heat pulsed at 54°C for exactly 60 sec, placed on ice for 2 min then resuspended in 150 µL of NZY broth and incubated for 1 hr at 37°C with shaking (225 rpm). Aliquots (20µL and 180 µL) of transformed cells were plated onto LB/AMP plates with IPTG/X-gal to select for the appropriate plasmid and incubated in the inverted position overnight at 37°C. Positive colonies were picked and plasmid preparations were carried out as described (Section 2.3.4.5) and analysed by DNA digestion (Section 2.3.4.6) and sequence analysis (Section 2.3.4.7).

3.3.4 Mouse MST2 Kinase Putative Sequence And Primer Design

The known Rattus norvegicus MST2 kinase nucleotide sequence was analysed for homology against the mouse expressed sequence tag (EST) database (NCBI) using the standard nucleotide-nucleotide (blastn) program (Madden et al., 1996; Altschul et al., 1997), to generate a putative mouse MST2 kinase sequence. When ESTs containing homology were found, these were compared against the mouse EST database in order to find ESTs with overlapping regions of homology. This process was repeatedly cycled until a putative full-length mouse MST2 kinase cDNA sequence containing an ORF was established. The putative coding sequence was then aligned with the known rat and human MST2 kinase orthologues and found to contain a high level of conservation. Primers flanking the potential coding sequence were designed using Primer3 (Rozen and Skaletsky, 1998) ready for cDNA amplification (refer to Table 3-1).

3.3.4.1 Full-length Amplification Using Putative Mouse MST2 Kinase Primers

SMART capped cDNA prepared as described (Section 3.3.2.2), was used with the putative mouse MST2 kinase forward primer (mMST2F) and mouse MST2 kinase reverse primer (mMST2R) to amplify the coding sequence of mouse MST2 kinase using the Expand Long Template PCR System. Master mix 1 was prepared by adding 1 µM of forward and reverse primer, 500 µM dNTPs to a final volume of 20 µL with MQH_2O. Master mix 2 was prepared by combining 1X Expand buffer and 2.5 Units of Expand enzyme mix to a volume of 25 µL with MQH_2O. Master mix 1 was combined with master mix 2 and 5 µL of amplified cDNA was added. The 50 µL reaction was overlayed with 50 µL mineral oil and subjected to the following PCR program: 94°C x 2 min, followed by 10 cycles at 94°C x 10 sec, 65°C x 30 sec, 68°C x 2 min, then 20 cycles at 94°C x 10 sec, 65°C x 30 sec, 68°C x 2 min with a 20 sec increment per cycle, followed by a final extension at 68°C x 7 min. PCR products were visualised by agarose gel electrophoresis (Section 2.3.2.9).

3.3.4.2 Mouse MST2 Kinase PCR Product Cloning

MST2 PCR amplified products were gel extracted using the QIAquick Gel Extraction Kit (Section 2.3.3.1.2) and quantitated by spectrophotometry. Gel extracted PCR products were cloned into the pGEM®-T Easy (3 Kb) Vector System (Section 2.3.4.1). PCR products were A tailed and ligated using a vector: insert ratio of 1: 3. Ligations were incubated at 4°C overnight prior to transformation, into XL10-Gold cells (Section 3.3.3.2).

3.4 Results

3.4.1 cDNA Library Screening With Differential Display Product DD5-7(7)

The differential display fragment DD5-7(7) was used to probe a mouse olfactory epithelium library constructed in the laboratory using a SMART™ PCR Library Construction Kit (Clontech, Palo Alto, California, USA). Tertiary screening was carried out as described above and positive λTriplEx2 (phage) were converted to pTriplEx2 plasmid. Several clones were identified and isolated: a 500 bp fragment with 94% identity to mouse cysteine rich intestinal protein (Crip), a 1.1 kb fragment of 85% identity with rat MST2 kinase, a 1.2 kb fragment with 92% identity to rat MST2 kinase, and a 1.6 kb clone sharing 86% identity with mouse zinc finger protein Zfp-37. The 1.1 and 1.2 kb fragments both represented the putative mouse MST2 kinase, however both fragments fell short of the expected 2.6 kb full-lengthclone and alignment against the human and rat orthologues indicated that both fragments represented the entire 3' UTR, encoding none of the coding sequence.

3.4.2 Amplification Of Smart cDNA With Rat MST2 Kinase Primers

PCR primers flanking the rat MST2 kinase coding sequence were designed in an attempt to amplify the full-length mouse orthologue. SMART cDNA was synthesised from mRNA derived from differentiated and non-differentiated OLF442 (Figure 3-4). SMART cDNA integrity was verified with the amplification of GAPDH as shown in (Figure 3-5). The amplification of a 266 bp fragment coincides with the expected GAPDH amplicon size. The absence of GAPDH in the minus reverse trancriptase (-RT) samples confirms the absence of genomic DNA contamination.

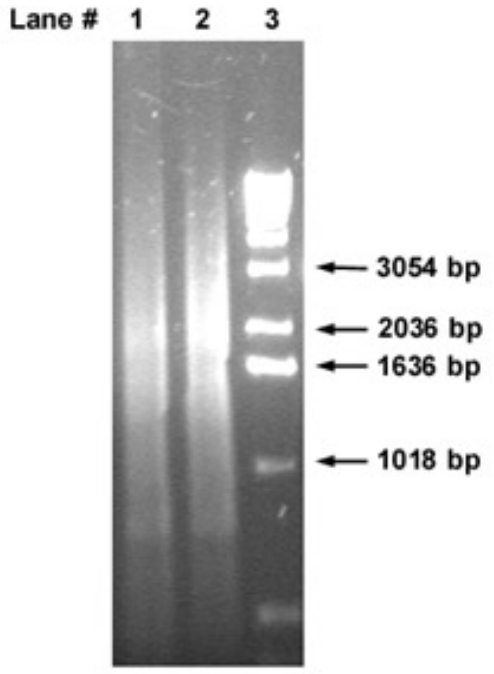

Figure 3-4 SMART cDNA.

Lane # 1, SMART cDNA synthesised from non-differentiated OLF442 grown in 10% FCS/DMEM. Lane # 2, SMART cDNA synthesised from differentiated OLF442 cultured in 1% BSA/DMEM. Lane# 3, 1 kb DNA ladder.

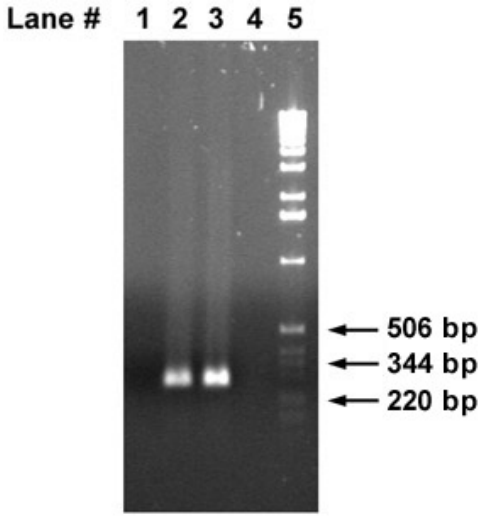

Figure 3-5 SMART cDNA integrity.

Lane 1, negative control of SMART cDNA synthesised from 10% FCS treated OLF442, without reverse transcriptase added (no DNA contamination). Lane 2, amplification of GAPDH from SMART cDNA synthesised from 10% FCS treated OLF442. Lane 3, GAPDH amplification from SMART cDNA isolated from 1% BSA treated OLF442. Lane 4 is a negative control without reverse transcriptase. Lane 5: 1 kb ladder.

PCR amplification of the SMART cDNA with the rat forward and reverse MST2 kinase PCR primers produced several bands of distinct size in the two different samples, ie. the OLF442 serum deplete (differentiated) versus OLF442 serum complete (non-differentiated) cultures. Of the amplified products two represented possible mouse MST2 kinase amplicons, as the expected size was approximately 1.5 kb of coding sequence (Figure 3-6). Upon cloning and sequencing of the 1.8 kb and 2.0 kb amplified cDNAs neither had homology with MST2 kinase, instead both products amplified from OLF442 serum deplete conditions had high homology with rat Agrin.

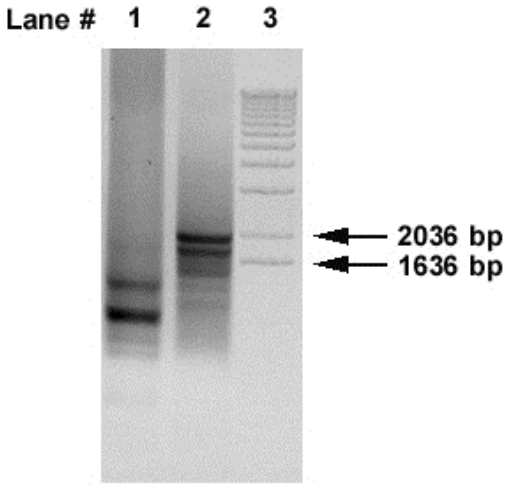

Figure 3-6 MST2 kinase PCR amplification of SMART cDNA using the rat MST2 forward and reverse primers.

Lane 1, SMART cDNA derived from complete medium (10% FCS treated) OLF442, Lane 2, SMART cDNA derived from deplete medium (1% BSA treated) OLF442, Lane 3: 1 kb DNA ladder.

3.4.3 Mouse MST2 Kinase Putative Sequence Construction And Primer Design

The known Rattus norvegicus MST2 kinase nucleotide sequence was analysed for homology against the mouse expressed sequence tag (EST) database (NCBI) using the nucleotide-nucleotide blast (blastn) program to identify homology with ESTs. Firstly, the differential display product DD5-7(7) was checked against the EST database to find a corresponding EST from which the sequence could be anchored and built upon with overlapping ESTs at the 5' DD5-7(7) terminus. DD5-7(7) had high

homology with EST AI391371 at the 5' end and with EST AV004508 at the 3' end. Unfortunately this contig did not possess any overlapping sequence with any other ESTs that could be used for further assembly (Figure 3-7). Therefore the rat MST2 kinase sequence was compared to the mouse EST database and two ESTs with significant overlapping portions were identified that shared 335 bp of homologous sequence with rat MST2 kinase. This contig, representative of the 5' terminal portion of the putative mouse MST2 kinase sequence, was compared to the mouse EST database and a corresponding EST with an overlapping region was identified. This process was repeated and ESTs were sequentially pasted together to build a putative or consensus mouse MST2 kinase sequence (Figure 3-7). When the putative full-length mouse MST2 kinase cDNA sequence containing an ORF with significant homology to rat and human MST2 kinase proteins when translated was established (Appendix III and IV), primers mMST2F and mMST2R flanking the potential coding sequence were designed (Table 3-1).

Table 3-1 PCR primers designed from the putative mouse MST2 kinase sequence [a]

PRIMER NAME	PRIMER SEQUENCE (5'-3')	LENGTH	Tm (°C)	POSITION
mMST2F	ATGGAGACCGTGCAGCTGAGGAAC	24 bp	73.4	33-56
mMST2R	ACTTCTGACAACACCAGCCCAGCC	24 bp	73.2	1489-1512
1mMST2F	GACCCCGTTTTGGATGGCTCCTGA	24 bp	76.1	590-613
1mMST2R	CAGCGGGAAGTGGACCAGGACGAC	24 bp	77.2	957-980
3UTRMST2F	ATGCCATTGAAGCCAAGAAGAG	22 bp	66.3	1456-1477
3UTRMST2R	TGTGTAATTGACCTGGGACCAG	22 bp	65.8	2227-2248

[a] mMST2F/R primer set flank the entire coding sequence, 1mMST2F/R primer set are internal primers binding within the coding sequence and 3UTRMST2F/R primer set flank the 3' UTR. Position denotes the base call on the putative mouse MST2 kinase sequence.

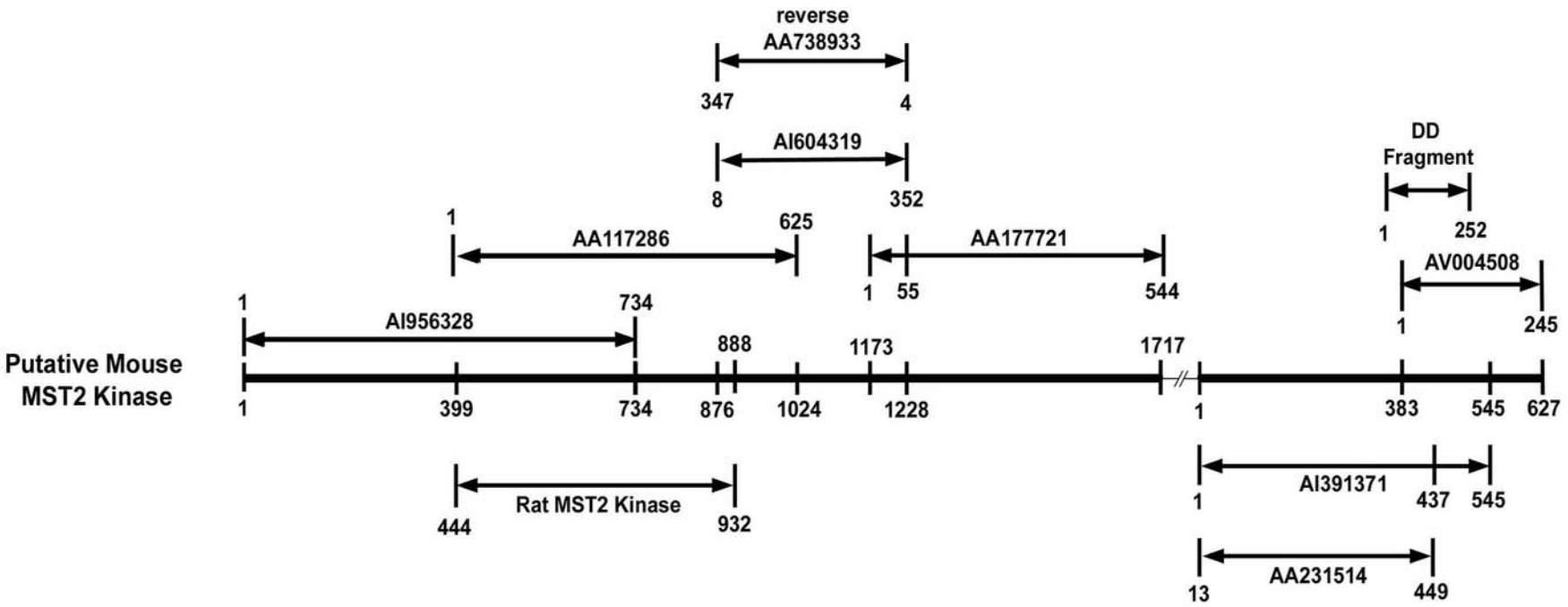

Figure 3-7 Schematic diagram of the putative mouse MST2 kinase sequence.

The ESTs show some degree of overlapping/identical sequence, which allowed the contig to be assembled. The double break in the sequence reflects the portion of the putative sequence where no overlap could be found.

3.4.4 Full-length Mouse MST2 Kinase Amplification Using Putative Mouse MST2 Kinase Primers

Once the putative mouse MST2 kinase sequence was established, the primers flanking the putative coding sequence were used to amplify the mouse homologue. SMART cDNA synthesised previously from mRNA derived from differentiated and non-differentiated OLF442 (Figure 3-4) was used in conjunction with the mMST2F and mMST2R primer set (Table 3-1). PCR amplification of SMART cDNA derived from serum depleted OLF442 (differentiated) produced several bands of distinct size including faint bands at approximately, 1.8 kb and 2.8 kb. Importantly, an abundant 1.5 kb amplified product of the expected size was obtained, corresponding to the open reading frame of MST2 (Figure 3-8).

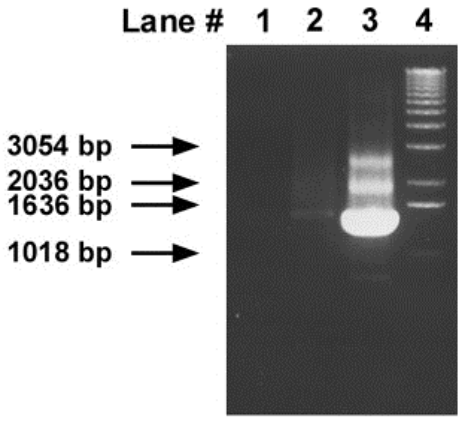

Figure 3-8 MST2 kinase PCR amplification of SMART cDNA using the putative mouse MST2 forward and reverse primers.

Lane 1, negative PCR control (water), Lane 2, SMART cDNA derived from complete medium (10% FCS treated) OLF442, Lane 3, SMART cDNA derived from deplete medium (1% BSA treated) OLF442, Lane 4, 1 kb DNA ladder.

Ligation of the 1.5 kb amplicon into pGEM®-T Easy at a vector: insert ratio of 1:3, followed by transformation of XL10-Gold cells, produced approximately 90% positive clones (Figure 3-9). When sequenced and compared to the GenBank database it became apparent that the putative MST2 kinase clone actually encoded the coding sequence of MST1 kinase. Sequence alignment at the nucleotide level with

that of the putative mouse MST2 kinase sequence, and with the available human and rat MST1/2 kinase sequences, showed that the isolated clone had greater similarity to MST1 kinase at the nucleotide level (Appendix III).

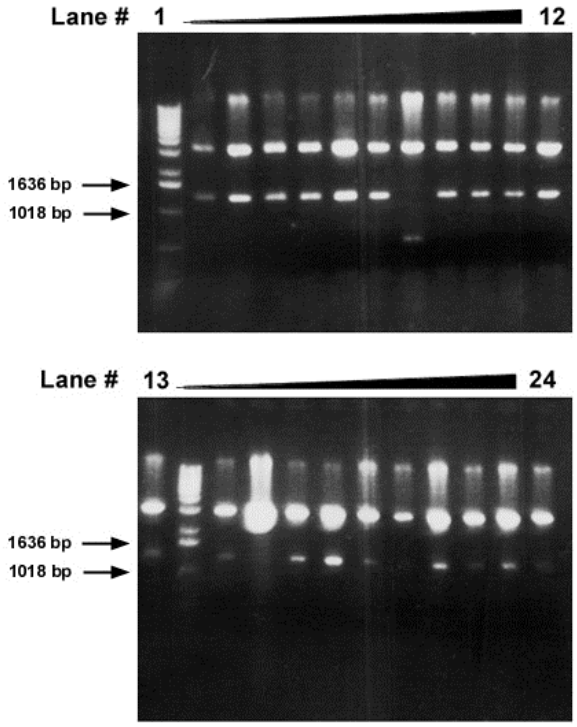

Figure 3-9 Miniprep digests of PCR-amplified mouse MST kinase cloned into pGEM-T.
Miniprep samples from 24 colonies were digested with EcoR1 and separated on a 1.2% agarose gel.

3.4.5 cDNA Library Screening With Mouse MST1 Kinase Coding Sequence

Subsequent to the full-length isolation of the MST1 kinase-coding region, the mouse olfactory epithelium cDNA library was again screened. Using the isolated MST1 kinase as the probe (1.5 kb), several positive clones were isolated. Conversion of λTriplEx2 phage to pTriplEx2 plasmid followed by digestion resulted in the isolation of a 1.6 kb fragment and another fragment approximately 2.6 kb in size. Sequence comparison of the 1.6 kb clone with GenBank using blastn showed that the 1.6 kb fragment shared 87% identity with mouse lipocortin I mRNA. Fortunately, sequence alignment of the larger 2.6 kb clone with the putative mouse MST2 kinase

sequence assembled from ESTs (Section 3.4.3) was similar, furthermore comparison of the clone with GenBank using blastn also confirmed that it had greater homology with human and rat MST2 kinase than with MST1 kinase (Appendix III).

3.4.6 Evidence For The Expression Of An Autonomously Expressed Carboxyl-Terminal Domain Of MST2 Kinase

Upon investigation of the mouse MST2 kinase nucleotide sequence a second Kozak signal sequence was identified approximately 70 bp upstream from the caspase-3 cleavage site (Appendix III). This raised the possibility of the expression of an mRNA species 1.6 kb in size. Interestingly, an mRNA species of this approximate size was identified by Northern blot analysis probed with a carboxyl-terminal mouse MST2 kinase probe (Figure 3-1) as indicated (Section 2.3.5). It was hypothesised that this mRNA species may be an autonomously expressed carboxyl-terminal domain of MST2 kinase. This hypothesis was further strengthened using a database approach.

Brief use of the Celera Discovery System allowed the analysis of the mouse genome. MST2 kinase was found to be located on chromosome 15, whilst human MST2 kinase is located on the equivalent chromosome, which is chromosome 8. Like mouse, the human MST2 kinase is composed of 11 exons (Figure 3-11A). Interestingly, several human EST sequences were identified that contained 100% homology with human MST2 kinase in only a portion of the EST. These were found to be located with close proximity to the second Kozak sequence and in frame start codon, present approximately twenty four amino acids upstream from the caspase cleavage site (also present in the mouse orthologue), further supporting the idea that the carboxyl terminal domain of MST2 kinase may be autonomously expressed. Comparison of the EST (AA464628) using blastn to the human genome localised the putative 5' leader sequence within an intron of MST2 positioned 5' of exon 8 encoding sequence for the non-catalytic domain. The alternative splicing of this putative exon (termed 7a) into the mRNA would result in the expression of the carboxyl terminal half of MST2 kinase (Figure 3-11B).

In contrast another EST (AI189947) represents exon 8, however it extends a further 285 bp downstream from the expected splicing position. An alternative

splicing event at this new position could result in the expression of an mRNA species expressing only the amino terminal half of MST2 kinase that corresponds to the entire kinase domain terminating just two amino acids upstream from the caspase cleavage site (Figure 3-11C). The resulting expression of an approximately 1 kb size mRNA species correlates well with that observed previously by Northern blot analysis using a probe corresponding to the kinase domain (nt 233-463) of human MST2 (Creasy and Chernoff, 1995a).

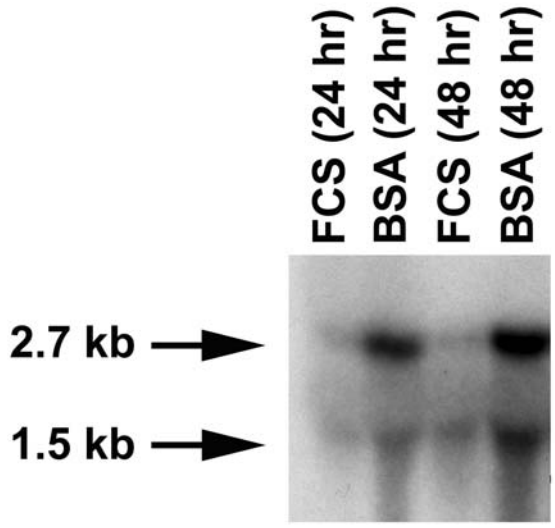

Figure 3-10 Northern analysis of differentiated OLF442 cultures with mouse MST2 kinase.

Two bands at approximately 2.7kb and 1.5kb in size, representing full-length and the carboxyl-terminal half of MST2 kinase were identified using an MST2 kinase probe directed to the carboxyl-terminal end. Differentiated (BSA) and non-differentiated (FCS) cultures were grown over a 24hr and a 48 hr period.

Figure 3-11 Schematic illustration of the genomic organisation of human MST2 kinase.

(A) Genomic organisation of human MST2 kinase that is composed of 11 exons, and the resulting mRNA sequence. (B) Alternative splicing of exon 7a (replacing exon 7) could result in the expression of the C-terminal half of MST2 kinase, encoding the regulatory domain. (C) Alternative splicing of exon 8, 285bp further downstream, could generate a truncation expressing the N-terminal half of MST2 kinase encoding the kinase domain.

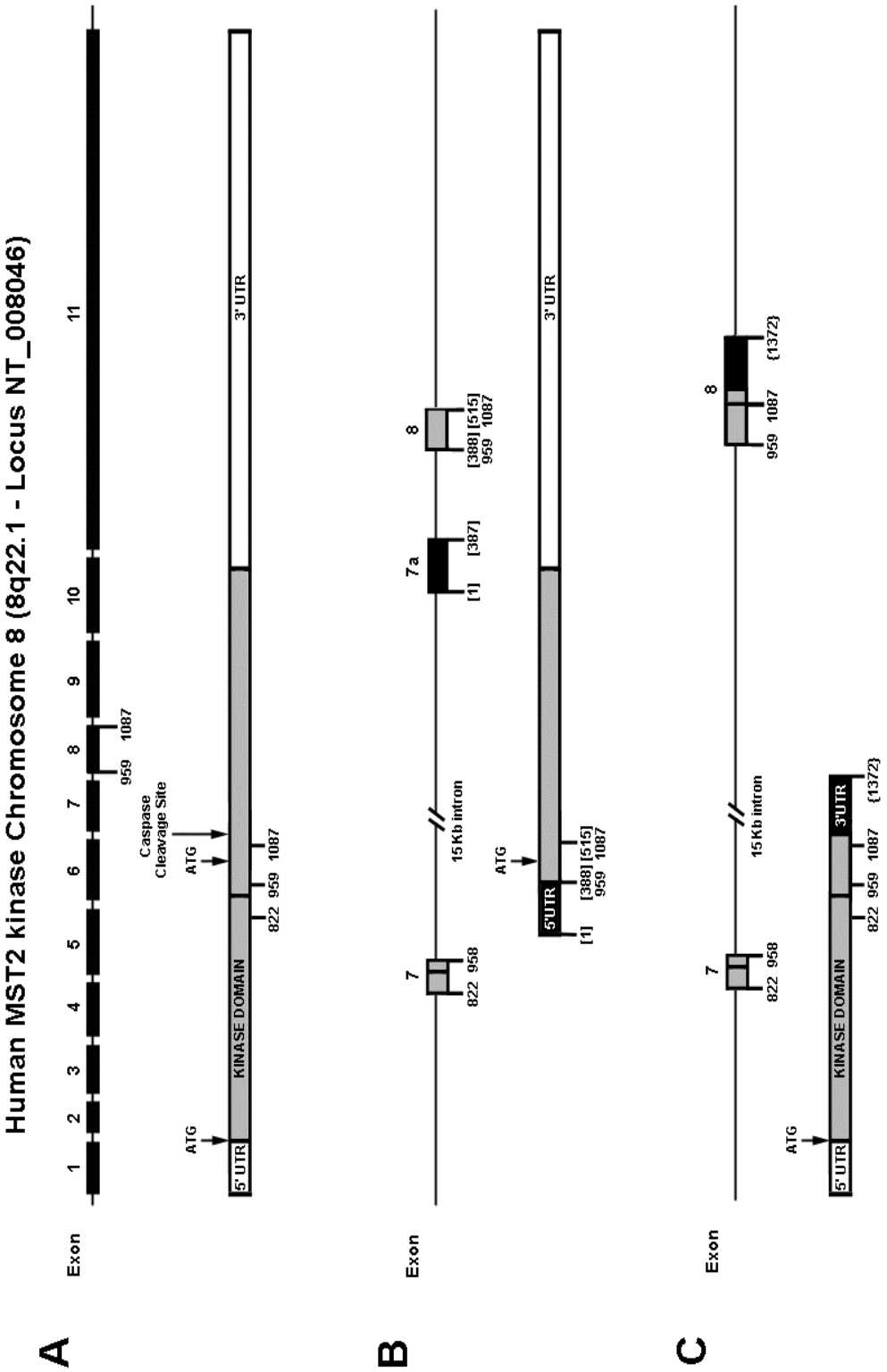

3.5 Discussion

3.5.1 Full-length Isolation Of Mouse MST2 Kinase

The differential display fragment DD5-7(7) shared 90% identity with Rattus norvegicus mRNA for MST2 kinase between base pairs 2351-2423 and 2477-2534 of the 3' UTR. As there was no mouse sequence for MST2 kinase available, a full-length clone was sought. The differential display fragment was used to probe a mouse olfactory epithelium cDNA library. Four different sized clones were isolated and identified, of which only two encoded the putative mouse MST2 kinase sequence. The 1.1 and 1.2 kb fragments fell short of the expected 2.6 kb full-lengthclone and alignment against the human and rat orthologues indicated that both fragments represented the entire 3' UTR.

The inability to isolate the full-length clones from the cDNA library led to a PCR based approach in which primers flanking the rat MST2 kinase coding sequence were designed in an attempt to amplify the mouse orthologue. SMART cDNA (full-length enriched) was synthesised from mRNA derived from differentiated and non-differentiated OLF442 and PCR amplified with the rat forward and reverse MST2 kinase PCR primers. Two amplification products of 1.8 kb and 2.0 kb in size were isolated. Upon sequencing, neither amplified cDNA had homology with MST2 kinase, instead both products amplified from OLF442 serum deplete conditions had high homology with rat Agrin (accession number NM_175754).

Failing the amplification of mouse MST2 kinase using the rat primers, the known Rattus norvegicus MST2 kinase nucleotide sequence was analysed for homology against the mouse expressed sequence tag (EST) database (NCBI) to identify homology with ESTs. A putative mouse MST2 kinase contig was assembled (Figure 3-7) that contained an ORF with significant homology to rat and human MST2 kinase proteins when translated. Primers mMST2F and mMST2R flanking the potential coding sequence were designed and used to amplify mouse MST2 kinase. PCR amplification of SMART cDNA derived from serum depleted OLF442 (differentiated) in conjunction with the putative mouse MST2 primer set, produced an

abundant 1.5 kb amplified product of the expected size (Figure 3-8). Sequencing of this amplicon revealed that the putative MST2 kinase clone encoded the coding sequence of mouse MST1 kinase (accession number AF271360). Consequently, the mouse olfactory epithelium cDNA library was again screened using MST1 kinase as the probe. Two different sized positive clones were isolated following the screen. A 1.6 kb clone shared 87% identity with mouse lipocortin I mRNA (accession number X07486) and a second 2.6 kb clone was indeed mouse MST2 kinase (including flanking vector sequence). This clone encoded the same sequence as the smaller clone isolated previously from the library screened with the differential display product and included an extra 1110 bp of 5' sequence.

Taken together these clones represented 2210 bp of the mouse MST2 Kinase mRNA, however the 5' UTR and a portion of the 5' coding sequence were missing. Attempts to 5' RACE the mouse MST2 kinase sequence from the OLF442 cell line failed, therefore the remaining unknown sequence was obtained using a database approach. Briefly, the incomplete mouse MST2 kinase nucleotide sequence was analysed for homology against the mouse EST database (NCBI) using the basic BLAST algorithm, facilitating the identification of an EST (H3025B05-5) that overlaped with the 5' segment of the library clone and which comprised the remaining 427 bp of unknown sequence. The complete sequence submitted to GENBANK (accession number AY058922) consists of 2639 nucleotides with an open reading frame encoding a protein of 497 aa. This cDNA contains a strong Kozak sequence (GCCATGG) at the putative start site and a polyadenylation signal (AATAAA) 53 bp upstream from the poly A tail. Designated mouse MST2 kinase, it shares high homology with its human and rat counterparts showing 90% identity and 93% identity respectively at the nucleotide level. Importantly it comprises a more complete sequence to an earlier mouse MST2 kinase sequence posted on the database by Lee, K. et al. (accession number AF271361) that lacks any sequence information about the 5'UTR and 3' UTRs.

3.5.2 MST Kinase Expression Profile

Northern analysis of MST2 kinase in OLF442 produced a transcript size of

approximately 2.7 kb, however a smaller band was also present. Upon investigation of the mouse MST2 kinase nucleotide sequence a second Kozak signal sequence was identified approximately 70 bp upstream from the caspase-3 cleavage site. The approximate size of an mRNA species beginning at this position would be at least 1.6 kb without any 5' UTR sequence. The observation of a second mRNA species of approximately 1.6 kb by Northern blot analysis raised the possibility that the carboxyl-terminal domain of MST2 kinase may be autonomously expressed in an analogous manner to FRNK (Focal adhesion kinase Related Non-Kinase) (Nolan et al., 1999). FRNK is the autonomously expressed non-catalytic carboxyl-terminal portion of FAK (Focal Adhesion Kinase) whose expression is directed by an alternative promoter, located within an intron of FAK residing 5' from the exon encoding the carboxyl-terminal domain and 3' to the exon encoding sequences for the catalytic domain (Nolan et al., 1999). FRNK has been demonstrated to act as a negative regulator of FAK activity by displacing FAK as they compete for common binding proteins (Richardson and Parsons, 1996). Further evidence for the expression of the carboxyl-terminal domain of MST2 kinase came from the identification of an EST whose 5' sequence had no homology to human MST2 kinase but whose terminal 128 bp shared 100% homology with human MST2 kinase. This EST (AA464628) was located on chromosome 8 in the intron between exon 7, encoding the amino terminal kinase domain and exon 8 (of the human genome), encoding the second Kozak and start sequence of the non-kinase domain of the human MST2 kinase (Figure 3-11B).

Additionally, a second EST (AI189947) was also identified and was identical to exon 8 but contained an extra 285 bp of sequence. Alternative splicing, 285 bp further downstream would result in the expression of an mRNA species expressing only the amino terminal kinase domain of MST2 kinase (Figure 3-11C). The resulting expression of an approximately 1 kb size mRNA species correlates well with that observed previously by Northern blot analysis using a probe corresponding to the kinase domain (nt 233-463) of human MST2 (Creasy and Chernoff, 1995a).

MST1/2 and 3 are ubiquitously expressed (Creasy and Chernoff, 1995a, 1995b; Schinkmann and Blenis, 1997). Northern analysis of a human MST1 probe specific to the kinase domain (nucleotides 178-481) detected two transcripts (7kb and 3.4kb)

with high expression levels in all tissues, except the heart and brain, which only expressed the larger 7kb transcript. A probe to the 3' UTR (nucleotides 1529-1930) was found to only detect the 7kb transcript (Creasy and Chernoff, 1995b), indicating that the 3.4 kb transcript probably represented a gene encoding MST2. This was demonstrated by Northern analysis of MST2 using a probe directed to the protein kinase domain (nucleotides 233-463). This probe detected 3 transcripts, of 5.5kb, 3.4kb and less than 1kb whose expression levels were greatest in kidney, skeletal muscle and placental tissue (Creasy and Chernoff, 1995a). Again brain tissue only expressed the larger 5.5kb transcript. A probe directed to the 3' UTR (nucleotides 2130-2820) of MST2 hybridised to only the 3.4kb transcript (Creasy and Chernoff, 1995a) therefore indicating that the larger 5.5kb transcript was not a splice variant. In addition it was noted that the 7kb MST1 transcript did not cross hybridise with either MST2 probe even though MST1 and MST2 are 70% identical at the nucleotide level (Creasy and Chernoff, 1995b). Therefore it was postulated that the 5.5kb transcript probably represented another MST2 encoding gene. By comparison, Northern analysis using a probe specific to the entire coding region of rat MST2 (nucleotides 81-1574) detected a transcript of 3.4 kb in all cell lines tested and these expression levels correlated well with the presence of the kinase activity identified by in-gel kinase assay (Aurisicchio et al., 1998). Here Northern analysis using a probe directed to the kinase domain of mouse MST2 detected a transcript of approximately 3 kb as did a probe directed to the 3' UTR which detected an additional transcript of approximately 1.6 kb.

3.6 Conclusion

Full-length mouse MST2 kinase cDNA was isolated from differentiating mouse olfactory receptor neurons (ORNs) using a combination of techniques including RT-PCR and cDNA library screening. MST1/2 are serine/threonine protein kinases that are activated by a subset of stress conditions and apoptotic agents but not activated by commonly used mitogenic stimuli. Given that apoptosis does not appear to be an active process during the differentiation of OLF442 it will be prudent to assess the phosphorylation status of the signal transduction cascades and of MST2 kinase itself. Importantly, it will be of interest to determine whether MST2 kinase is cleaved and whether or not cleavage is affected by caspase inhibition. These questions may offer further insight into the evidence that has been put forward in this chapter arguing for the expression of an autonomously expressed carboxyl-terminal domain of MST2 kinase.

4 SIGNAL TRANSDUCTION STATUS OF OLF442

4.1 Signal Transduction By The MAPK Superfamily

As noted, signalling cascades participate in most cellular processes conveying vital information from various sources to targets within the cell cytoplasm and nucleus. The MAPK signalling cascades can be divided into two phases, one being membranous and the other cytoplasmic (Pearson et al., 2001). The first phase originates at the inner plasma membrane. For the ERK pathway this occurs at the receptors for mitogens or growth factors, which recruit and activate a small GTP binding protein (Ras) via the adapter molecule (Grb2) and the guanine nucleotide exchange factor (mSOS). Phase two is initiated when the sequential stimulation of several cytoplasmic protein kinases occurs. In the ERK cascade Ras activates Raf, a serine threonine kinase, which activates MEK1 and MEK2. MEK, in turn phosphorylates and activates ERK1 and ERK2, which translocate and transactivate transcription factors, changing gene expression to promote growth, differentiation or mitosis (Garrington and Johnson, 1999; Tibbles and Woodgett, 1999; Kolch, 2000). Likewise, the stress activated protein kinase (SAPK) and p38 kinase pathways are also hierarchically arranged in order to elicit a cellular response to toxins, physical stresses and inflammatory cytokines (Tibbles and Woodgett, 1999; Kyriakis and Avruch, 2001).

MAPK signalling cascades are a cellular information superhighway. They have several salient features, including highly specific and reversible substrate phosphorylation by protein kinases and phosphatases, and localisation of protein kinases into modules through direct protein-protein interactions of scaffolding and anchoring proteins (Garrington and Johnson, 1999). In contrast, a pseudo-redundancy that is built into the system by protein kinase isoforms that serve related but distinct functions, non-reversible proteolysis and pathway crosstalk, give MAPK signalling cascades a highly elaborate level of control (Seger and Krebs, 1995). Further complexities include changes to the magnitude, duration and frequency of activation, which influences cellular outcome (Roovers and Assoian, 2000). Therefore the control mechanisms that terminate and/or modulate transduced signals are important in deciding the fate of a response. Signal transduction by this strategy gives the cell various options for amplifying and or modifying the output signal (Tibbles and

Woodgett, 1999; Kolch, 2000). Moreover, interactions between cascades are evident and occur in various ways to integrate and control outputs.

Currently, in eukaryotic cells, nearly twenty MAPKs have been identified (Pearson et al., 2001), and these can be grouped into five discrete and evolutionarily conserved subfamilies based on sequence homology and function (Weber, 1999). These include the ERK1/2 cascade, that preferentially regulates cell growth and differentiation (Pearson et al., 2001), the c-Jun N-terminal kinase (JNK/SAPK – stress activated protein kinase), p38 MAPK and ERK5 cascades, which primarily function in response to environmental stress and inflammatory cytokines (Kyriakis and Avruch, 2001), and the poorly characterised ERK7 and newly identified ERK8 cascades (Abe et al., 2001; Abe et al., 2002). Seven MEKs have been functionally identified in mammalian cells representing the fewest number of members in the MAPK cascade. MEKs also have high specificity for their MAPK substrates allowing minimal variation of the MEK-MAPK part of the MAPK module. In contrast, fourteen MEKKs have been functionally identified that are quite diverse in structure (Garrington and Johnson, 1999). The disparity between the numbers of MEKKs, MEKs and MAPKs suggest that there is infidelity of MAPK pathway members confirming the notion that MAPKs have overlapping substrate specificities that are co-ordinated by scaffold and docking proteins (Pearson et al., 2001). Notably, it has been demonstrated that docking proteins themselves can directly affect catalytic activity. Bardwell et al. (2003) demonstrated that upstream MEKs, inactivating phosphatases and downstream phosphorylation substrates can all compete with each other for binding to the same docking site on ERK2. These protein-protein interactions play a critical role in the catalytic activity of the kinases and phosphatases involved (Bardwell et al., 2003). It is not surprising that competitive docking, in addition to reversible phosphorylation, directly influences the catalytic activity of MAPKs. Hence MAPK phosphorylation levels alone cannot be relied upon to provide a snapshot of signalling potential without appreciating the auxiliary effect of cellular context, for example scaffolding and substrate availability.

4.1.1 MAPK Signalling In Neurons

MAPK signalling particularly through the ERKs is responsible for the regulation of many neuronal events including synaptic plasticity, long-term potentiation, neuronal differentiation and survival (Grewal et al., 1999). As discussed in Chapter 1, several studies have characterised the regulation of MAPK family members during neuronal differentiation. Used extensively as a model system, PC12 cells have provided many insights into the signalling mechanisms active during neuronal differentiation. The general consensus is that NGF activation of the cell surface receptor TrkA recruits and activates Ras via the adapter protein (Grb2) and exchange factor (mSOS), Ras activates Raf, which activates MEK1/2 and ERK1/2. Yet several studies have also shown that ERK activation is not necessary for PC12 neurite extension and differentiation. These include the neuronal differentiation of PC12 with bone morphogenic protein BMP-2 in the absence of ERK activation (Iwasaki et al., 1996) and the neurite outgrowth of PC12D in the presence of PD98059, a specific MEK1/2 inhibitor (Sano and Kitajima, 1998). It is clear that signalling pathways other than the ERK cascade also contribute to neuronal differentiation of PC12 cells.

The lesser-characterised stress induced MAPK cascade that culminates in p38 MAPK activation can also induce neuronal differentiation of PC12 cells (Iwasaki et al., 1999). The p38 MAPK pathway alone is sufficient for PC12 neuronal differentiation, as expression of constitutively active forms of the p38 MAPK pathway upstream activators MEK3/6 induced neurite outgrowth, and their inhibition with SB203580 abolished it (Iwasaki et al., 1999). Interestingly, the stress induced JNK/SAPK pathway is simultaneously activated alongside the classic mitogenic ERK cascade by the proto-oncoprotein Cot that directly activates MEK-1 and SEK-1, inducing neurite outgrowth of PC12 cells (Hagemann et al., 1999). The dual stimulation of ERK and the JNK/SAPK do not exhibit any antagonistic effects (Hagemann et al., 1999), although Leppa et al. (1998) show that the common substrate c-Jun is differentially regulated by the ERK and JNK/SAPK pathways following NGF induced PC12 differentiation. Again these examples highlight the infidelity of MAPK pathway members, whose overlapping substrate specificities are defined via scaffolding and docking proteins. Evidence for a spatio-temporal effect

on signalling cascades comes from studies of growth factor induced activation of G-proteins Ras and Rap1 whose cytoplasmic location varies between cell types (Mochizuki et al., 2001). Variations in Ras and Rap1 distribution within the cytoplasmic domain may explain how the signals for differentiation and survival are distinguished by neuronal cells (Mochizuki et al., 2001).

Neuronal differentiation via the MAPK cascades has been intensively studied, yet differences between cell models and effectors of differentiation shed light on the signalling strategy employed by cells to respond to all environmental cues with a given set of proteins. OLF442 differentiation induced by serum deprivation resulted in the upregulation of two protein kinases (refer Chapter 2). MST2 kinase a member of the Ste20/PAK protein family responsible for regulating cell polarity during growth (Pruyne and Bretscher, 2000a) and in response to nutrient deprivation (Elion, 2000) highlighted the possible involvement of a MAPK cascade signalling to the cytoskeleton in response to differentiation. In addition, the identification of focal adhesion kinase (FAK/pp125^{FAK}) and focal adhesion kinase related non-kinase (FRNK), both integral to the response to the ECM via the integrins and signalling to the MAPK cascade, indicated another mechanism of OLF442 differentiation initiated by serum deprivation.

4.1.2 Focal Adhesion Kinase

FAK was originally identified in pp60v-src-transformed chicken embryo cells as a substrate that is localised within focal adhesions and becomes highly tyrosine phosphorylated (Schaller et al., 1992). Subsequently isolated from mouse (Hanks et al., 1992) and human, (Andre and Becker-Andre, 1993) the primary role of FAK is to convey signals from the integrins which contain short cytoplasmic domains lacking enzymatic activity. FAK is a non-receptor tyrosine kinase whose catalytic domain is flanked by a large amino-terminal integrin-binding domain and a carboxyl-terminal domain containing an SH3 motif and focal adhesion targeting (FAT) sequence (Zachary, 1997). The localisation of FAK to focal adhesions along with other proteins including paxillin, talin and the src family of protein tyrosine kinases (pp60$^{c\text{-}src}$ and pp59$^{c\text{-}fyn}$) with whom FAK can directly bind, suggests that FAK is at the

junction of signalling by integrins, oncogenes and neuropeptides (Ilic et al., 1997). Ubiquitously expressed throughout development (Furuta et al., 1995; Hens and DeSimone, 1995) and in most cell lines (Hanks et al., 1992) and adult tissues, the highest level of FAK expression occurs in the brain (Andre and Becker-Andre, 1993). Although localised primarily in focal adhesions it is not restricted to these sites in neural tissue where it is distributed throughout the cytoplasm (Grant et al., 1995). Throughout brain development multiple transcripts with different patterns of expression are observed (Burgaya and Girault, 1996; Serpente et al., 1996). These isoforms are dynamic in their expression, phosphorylation and interaction with substrates (Serpente et al., 1996). The preferential expression of alternative splice isoforms in rat brain with elevated autophosphorylation activity suggests neural specific properties.

Differentiation requires the systematic integration of signals from the ECM, the cell cycle, and the cytoskeleton to control neurite extension and neuronal maturation. Besides serving as a platform for the assembly of signalling cascades, studies have demonstrated a role for FAK in such diverse cellular roles as neuronal signalling and synaptic plasticity, as illustrated by *fyn* mutant mice deficient in long-term potentiation (Grant et al., 1995), to apoptosis, embryonic development and migration (Zachary, 1997). FAK responds to fluid shear stress (Li et al., 1997), can be regulated by changes in cell density (Xu and Zhao, 2001), and, importantly for this study, has been shown to be involved in PC12 neurite outgrowth (Anneren et al., 2000), and implicated in the neuronal differentiation of SH-SY5Y neuroblastoma cells (Bruce-Staskal and Bouton, 2001).

FAK located within focal adhesions can be activated by the ECM via the integrins, or by serum factors (lysophosphatidic acid) and bioactive peptides (endothelin, bombesin) via their specific cell surface receptors (Ilic et al., 1997). The small G-protein family, of which Rho is a member, mediates the effects of these factors on organisation of the cytoskeleton (Nobes and Hall, 1995). However, integrin activation of FAK can occur directly via the β1 cytoplasmic domain of integrins or by association of auxiliary proteins (eg. talin, paxillin and tensin) located within the focal adhesion that bind integrins and FAK (Guan, 1997). Importantly FAK has six tyrosine phosphorylation sites, the selective phosphorylation of which

allows FAK a diverse signalling repertoire in response to integrin activation. Autophosphorylation at Tyr397 leads to the generation of a binding site for the SH2 domain of Src-family non-receptor protein tyrosine kinases. The subsequent interaction of Src with FAK results in the phosphorylation of several other tyrosine residues maximising FAK kinase activity, but more importantly results in the phosphorylation of Tyr925 creating a Grb2-binding site (Ilic et al., 1997). Grb2 binds to mSOS, a guanine exchange factor for Ras, connecting FAK signalling to the MAPK cascade (Guan, 1997). FAK can also activate the second messenger PI3K (Guan, 1997). The activation of several distinct signalling cascades can explain the diverse range of cellular responses elicited by FAK. Moreover, as discussed below, an independently expressed carboxyl-terminal domain of FAK may modulate its function and consequently that of its downstream effectors.

4.1.3 FAK-Related Non-Kinase (FRNK)

In some cells the carboxyl-terminal domain of FAK is expressed autonomously as a 41 kDa protein termed FRNK, for FAK-related non-kinase or pp41/43^{FRNK} (Schaller et al., 1993). FRNK overexpression can inhibit tyrosine phosphorylation of FAK, and that of tensin and paxillin, resulting in the delay of cell spreading on fibronectin surfaces (Richardson and Parsons, 1996). Richardson and Parsons (1996) found that the inhibitory effects of FRNK could be reversed by co-expression with FAK, suggesting that both compete for common binding protein(s) whose association with FAK is necessary for signalling. As such, *fak* was the first non-receptor tyrosine kinase found to generate an endogenous regulator *frnk,* whose expression is directed by an alternative promoter residing within an intron of *fak* positioned 3' of the exon encoding sequences for the catalytic domain of FAK (Nolan et al., 1999). Expression of an endogenous regulator is a strategy that can further regulate FAK tyrosine kinase activity and localisation (Richardson and Parsons, 1996) from signals that do not necessarily emanate from the focal adhesion itself. Alternatively an FRNK-like polypeptide can also be generated by caspase-3 and caspase–6 cleavage of FAK (Gervais et al., 1998). Although FAK has been shown to suppress apoptosis by activating the PI3K-Akt survival pathway, resulting in activation of NF-kappaB and induction of inhibitor-of-apoptosis proteins (IAPs: cIAP-1, cIAP-2, XIAP) (Sonoda et

al., 2000), the apoptotic cascade can overcome this ability by generating FRNK and blocking FAK function. Together FAK and FRNK may regulate the initiating signal directing OLF442 to commit to differentiation via the MAPK cascades.

4.2 Aim

The identification of increased mRNA expression levels for FRNK, and MST2 kinase indicate that signal transduction cascades are active during OLF442 differentiation. The specific aims of this chapter are as follows:

1) To determine which of the MAPK cascades are functionally active during OLF442 differentiation using Western blotting and phosphorylation specific antibodies.
2) To establish the effect of inhibiting the mitogenic ERK1/2 cascade implicated in neuronal differentiation of various cell lines, by using the MEK1/2 specific inhibitor PD98059 in OLF442 cultures.
3) To confirm the elevated expression of FRNK and MST2 kinase protein during OLF442 differentiation.
4) To determine the level of FAK expression in OLF442 before and after differentiation by serum depletion.
5) To verify that FRNK expression is autonomous and not a result of caspase-3 cleavage of FAK by treating cultures with DEVD-CHO, a specific caspase-3 inhibitor.

4.3 Methods

4.3.1 Cell Culture

OLF442 cells cultured under serum deplete (1% BSA/DMEM/GLUT) and serum complete (10% FCS/DMEM/GLUT) conditions (Section 2.3.1.2), were harvested by trypsinisation from 25/75 cm^2 tissue culture flasks as indicated in Section 2.3.1.1. Cultures treated with the cell-permeable caspase-3 inhibitor, DEVD-CHO (dissolved in DMSO - Calbiochem, Merck, Kilsyth, VIC, Australia) were seeded at the appropriate density: 30 cells/mm^2 for 10% FCS treated cells and 90 cells/mm^2 for 1% BSA treated cells for 48 hr cultures. All cultures were initially grown in control medium (10% FCS/DMEM/GLUT) for 18-24 hrs prior to treatment. Following the initial 18-24 hr settling phase, control medium was aspirated and cultures were washed with HBSS three times. The appropriate medium supplemented with 10 nM DEVD-CHO was then added to the culture vessels and the cells were incubated as follows: one batch for 48 hrs and one batch for 24 hrs at which time the media was replaced with media minus the inhibitor and further incubated for 24 hr. Cultures treated with the MEK1/2 inhibitor PD98059 (dissolved in DMSO - Cell Signalling Technology; Genesearch, Arundel, QLD, Australia) were treated the same as the caspase-3 inhibitor cultures except that the appropriate incubation media was supplemented with 5 μM PD98059. Vehicle controls were ommited as the final DMSO concentration in tissue culture was 0.01%.

4.3.2 Protein Analysis

4.3.2.1 Protein Extraction

Cell pellets collected by trypsinisation were resuspended in 5 mL ice cold HBSS and centrifuged at 1500g for 5 min. Pellets were washed three times and resuspended in protein extraction buffer (Appendix I) at approximately $1X10^4$ cells/μL. Cell suspensions underwent three cycles of freeze thawing in liquid nitrogen followed by sonication for 5 min to shear DNA. Cell suspensions were sedimented at 14,000g for

10 min. The supernatant containing the cytoplasmic protein fraction was removed and transferred to a clean microcentrifuge tube for protein quantitation.

4.3.2.2 Coomassie Blue Protein Estimation

Estimation of protein concentration in cell extracts was done using a Bradford assay, a colorimetric Coomassie Brilliant Blue G-250 binding protocol (Bradford, 1976). A standard curve (with a concentration range of 10 μg to 0.313 μg) was prepared by serial dilution with bovine serum albumin (BSA) diluted in protein extraction buffer, and plated out (20 μL/well) on a microtitre plate in triplicate. Sample protein extracts were diluted (1/20) with protein extraction buffer and also plated out in triplicate. Bradford reagent (BioRad) diluted 1/5 with MQH_2O was added to samples (200 μL/well) and incubated at room temperature for 5 min to allow maximal colour reaction. Absorbance was read on a Titertek Multiscan ELISA plate reader (MTX Labs, Virginia, USA) at a wavelength of 595 nm. Protein concentrations were calculated from the standard curve and adjusted with protein extraction buffer to a given concentration and quantitated again. Prior to SDS-PAGE, 1/5 of the sample volume to be loaded on the gel of 20% (w/v) SDS, 10% (v/v) bromophenol blue was added to each sample and the capped centrifuge tubes were boiled for 5 min and cooled prior to gel loading.

4.3.2.3 SDS-Polyacrylamide Gel Electrophoresis

Protein separation was achieved with SDS-PAGE (Laemmli, 1970) using a BioRad Protean II minigel apparatus (BioRad, Hercules, CA, USA). OLF442 protein preparations were loaded at 10 μg/lane, as was Benchmark protein ladder (Invitrogen, Mount Waverley, VIC, Australia). Protein was run through a 4% polyacrylamide stacking gel, and then separated in a 10% polyacrylamide separating gel with 1X SDS-PAGE running buffer, at 150 V for approximately 90 min. When the bromophenol blue dye front reached the bottom of the gel, the apparatus was disassembled and the gels were prepared for Western blotting, by removing the stacking gel.

4.3.2.4 Western Blotting

Transfer of proteins from SDS-PAGE gels onto polyvinylidene fluoride (PVDF) Immobilon-P Transfer Membrane (Millipore, North Ryde, NSW, Australia) was done with a vertical tank transfer assembly (Bio-Rad) and 1X transfer buffer. Transfer proceeded overnight at 4°C at 150 mAmps. Gels were subsequently stained in Coomassie solution to observe transfer efficiency. The PVDF membranes were placed into blocking solution [2% (v/v) fish gelatin (Sigma)/1X tris buffered saline (TBS)/0.1% (v/v) Tween-20 (Sigma)] and incubated with rocking at room temperature for 1 hr or alternatively overnight at 4°C. Following optimisation, primary antibodies were diluted appropriately (Table 4-1) in blocking solution and incubated overnight at 4°C. Membranes were then washed three times with TBS-T for 10 min at room temperature with rocking and placed in one of the following horseradish peroxidase (HRP) conjugated secondary antibodies; Rabbit Anti-Goat, Goat Anti-Rabbit, or Goat Anti-Mouse (Bio-Rad), each diluted (1:2000) in blocking solution, and incubated at room temperature for 1 hr. Membranes were washed three times with TBS-T for 10 min at room temperature with rocking and incubated with a 1/5 dilution of SuperSignal Ultra Chemiluminescent Substrate (Pierce; Progen Industries, Darra, QLD, Australia). Membranes were then exposed to Hyperfilm (Amersham Biosciences, Castle Hill, NSW, Australia).

Table 4-1 Primary antibodies used in Western blotting [a]

Antibody	Source	Dilution	MW	Supplier
Phosphorylated c-Raf (Ser338)	Rabbit	1:2000	74 kDa	Cell Signalling Technology
Phosphorylated-MEK1/2 (Ser217/221)	Rabbit	1:2000	43.5/44.5 kDa	Cell Signalling Technology
Phosphorylated-ERK1/2 (Thr202/Tyr204)	Rabbit	1:2000	44/42 kDa	Cell Signalling Technology
Phosphorylated-ERK1/2 (Tyr204)	Mouse	1:2000	44/42 kDa	Santa Cruz Biotechnology
TOTAL ERK1/2	Rabbit	1:2000	44/42 kDa	Cell Signalling Technology
Phosphorylated-p90RSK (Ser380)	Rabbit	Undetected [b]	90 kDa	Cell Signalling Technology
Phosphorylated-ELK-1 (Ser383)	Rabbit	Undetected [b]	62 kDa	Cell Signalling Technology
Phosphorylated-ELK-1 (Ser383)	Mouse	Undetected [b]	90 kDa	Santa Cruz Biotechnology
Phosphorylated SEK1/MKK4 (Thr223)	Rabbit	1:2000	46 kDa	Cell Signalling Technology
Phosphorylated SAPK/JNK (Thr183/Tyr185)	Rabbit	1:2000	46/54 kDa	Cell Signalling Technology
Phosphorylated SAPK/JNK (Thr183/Tyr185)	Mouse	Undetected [b]	46/54 kDa	Santa Cruz Biotechnology
Phosphorylated ATF-2 (Thr71)	Rabbit	1:2000	70 kDa	Cell Signalling Technology
Phosphorylated ATF-2 (Thr71)	Mouse	Undetected [b]	70 kDa	Santa Cruz Biotechnology
Phosphorylated c-Jun (Ser73)	Rabbit	1:2000	48 kDa	Cell Signalling Technology
Phosphorylated p38 (Tyr182)	Mouse	Undetected [b]	38 kDa	Santa Cruz Biotechnology
FAK/FRNK	Mouse	1:2000	125/43/41 kDa	Santa Cruz Biotechnology
MST2/KRS-1	Goat	Undetected [c]	63 kDa	Santa Cruz Biotechnology
MST2&1/KRS-1&2	Mouse	Undetected [c]	63/61 kDa	Zymed Laboratories

[a] The Table shows a list of all the primary antibodies used, the dilution, and the position of the phosphate to which the antibody was generated.
[b] No immunoreactive bands were observed.
[c] Identity of the correct band was not possible due to high background.

4.4 Results

4.4.1 MAPK Cascade Activation Status Of Differentiating Olfactory Receptor Neurons

The phosphorylation status of the mitogen (ERK) and stress responsive (SAPK/JNK and p38) protein kinase cascades was investigated following the *in-vitro* differentiation of OLF442 following 4, 8, 12, 24 and 48 hr culture periods. However, the most notable changes in phosphorylation status were observed at 48 hr, and data shown is representative of this time point (Figure 4-1, representative of experiments done in triplicate). The phosphorylation of c-Raf was not significantly different between the undifferentiated (FCS) and differentiated (BSA) cultures, however the antibody used also detected a signal of higher molecular weight of unknown identity that was more highly phosphorylated in the differentiated culture. Although the incoming signal from c-Raf was presumably of the same intensity, the resulting phosphorylation of MEK1/2 was not. Notably, there is a switch between the preferential phosphorylation of MEK 1 in undifferentiated OLF442 to MEK2 during differentiation over 48 hr. This results in a high level of phosphorylation of both ERK1/2 in the differentiated cultures. It is noteworthy that the activation level in undifferentiated cultures does not appear to match the intensity of phosphorylation from its upstream effector MEK1. The differential activation of ERK1/2 does not reflect a difference in the total content of ERK1/2 (phosphorylated and unphosphorylated) between the cultures, and does not result in differential activation of the transcription factor, ELK-1, downstream of ERK. Also of note was the detection of a higher molecular weight signal with both the phosphorylated MEK1/2, and phosphorylated ERK1/2 antibodies. These immunoreactive bands may represent isoforms of the MEK and ERK proteins.

Interestingly, activation of the stress responsive cascade p38 was not observed, however activation of the SAPK/JNK cascade was apparent. The upstream effector SEK1 was phosphorylated, albeit to a relatively low level during differentiation, which resulted in the activation of SAPK. In undifferentiated OLF442, SEK1 phosphorylation was not detected despite the detection of a low-level of SAPK

phosphorylation. Nonetheless, the phosphorylation of c-Jun (on Ser73) downstream of SAPK was detected equally in differentiated and undifferentiated OLF442.

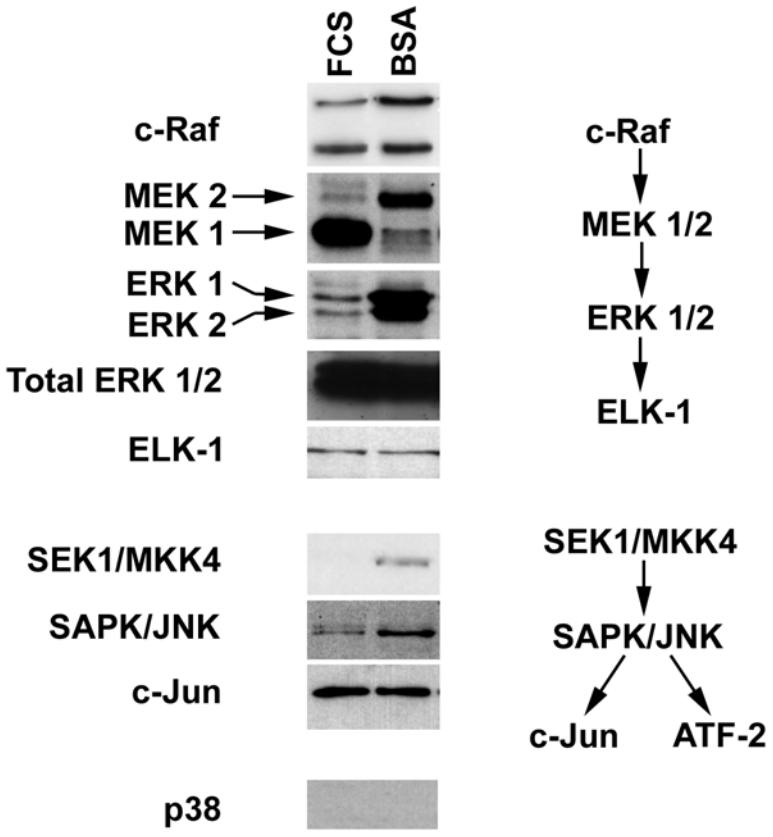

Figure 4-1 Composite image of Western Blots of MAPK pathway members phosphorylated during OLF442 differentiation.

FCS: OLF442 grown in complete medium for 48 hr, BSA: OLF442 grown in serum deplete conditions for 48 hr, resulting in differentiation. All antibodies used specifically detected only the phosphorylated form of the protein except for the detection of total ERK1/2 that detected both phosphorylated and unphosphorylated forms of the protein, n=3. The antibodies used are described in Table 4-1.

4.4.2 Olfactory Receptor Neuronal Differentiation In The Presence Of PD98059; A MEK Specific Inhibitor

Treatment of OLF442 cultures with the specific MEK1/2 inhibitor PD98059 (PD, 5 μM) for 48 hr did not display morphological differences. However, a decrease of MEK1 and MEK2 phosphorylation in undifferentiated and differentiated cultures respectively were observed (Figure 4-2, representative of experiments done in

triplicate). This selective inhibition however, did not decrease the level of ERK1/2 phosphorylation in differentiated cultures. The removal of PD98059 and addition of serum to the differentiated culture reversed both the effects of PD98059 and serum deprivation (Figure 4-2, BSA+PD+BSA), resulting in a phosphorylation status that closely mirrored that of undifferentiated OLF442 (Figure 4-2, FCS). The phosphorylation of c-Raf in treated cultures was also decreased, possibly indicating the action of a feedback mechanism as it was depleted in BSA+PD compared with FCS+PD (Figure 4-2). The activation level of c-Jun was also reduced in both cultures treated with PD98059, again to a greater level in BSA compared with FCS and its phosphorylation levels could be increased by removal of the MEK inhibitor and addition of serum. SEK1/MKK4, SAPK/JNK and p38 phosphorylation was not detected in PD98059 treated cultures.

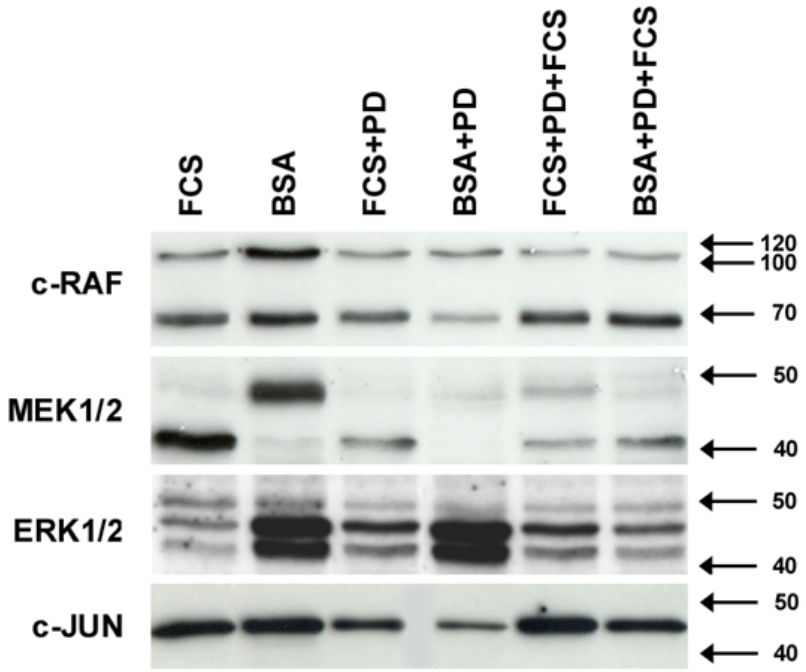

Figure 4-2 Composite image of Western Blots of MAPK pathway members phosphorylated during OLF442 differentiation in the presence of the MEK1/2 specific inhibitor PD98059.

FCS: OLF442 grown in complete medium for 48 hr, BSA: OLF442 grown in serum deplete conditions for 48 hr, resulting in differentiation. FCS+PD: culture supplemented with 5 µM PD98059 and incubated for 48 hr, BSA+PD: culture supplemented with 5 µM PD98059 and incubated for 48 hr. FCS+PD+FCS: culture supplemented with 5 µM PD98059 and incubated for 24 hr at which time the medium was replaced with complete medium without inhibitor and incubated for a further 24 hr. BSA+PD+FCS: serum deplete culture supplemented with 5 µM PD98059 and incubated for 24 hr at which time the medium was replaced with complete medium without inhibitor and incubated for another 24 hr, n=3. The antibodies used are described in Table 4-1.

4.4.3 Olfactory Receptor Neuronal Differentiation In The Presence Of DEVD-CHO A Specific Caspase-3 Inhibitor

OLF442 cultures treated with the caspase-3 inhibitor, DEVD-CHO (10 nM) did not display morphological differences. At the signal transduction level, differences in phosphorylation of MAPK components was negligible with only a slight decrease in the activation state of MEK2 in the differentiated cultures treated with DEVD-CHO (Figure 4-3, BSA+D, representative of experiments done in triplicate). Disparity in the levels of c-Jun activation between the cultures is more prominent here and may reflect some (unknown) variations in culture conditions, as only FCS treated (undifferentiated) OLF442 c-Jun phosphorylation is decreased with respect to previous blots (Figure 4-2). Furthermore, no cell culture synchronisation was done and may reflect this observed difference. In agreement with differentiated cultures treated with PD98059, differentiated cultures exposed to DEVD-CHO for 24 hr and whose medium was then replaced with 10%FCS/DMEM/GLUT, display the ability to restore the same phosphorylation levels as that of undifferentiated OLF442. In particular MEK2 phosphorylation is reverted to preferential phosphorylation of MEK1 and ERK1/2 phosphorylation is decreased to the basal levels observed in undifferentiated OLF442. The caspase-3 inhibitor did not present any significant effect on these cultures, and the ability of the differentiated cultures to parallel the signal transduction status of undifferentiated cells probably reflects the resistance of these cells to commit to apoptosis within 24 hr of serum depletion. This is consistent with the observation that differentiated OLF442 cultures subsequently exposed to serum containing media retracted processes (Section 1.3.4). However, an apparent loss of the high molecular weight Raf band was observed in FCS cultures treated with the caspase-3 inhibitor. Once more, SEK1/MKK4, SAPK/JNK and p38 phosphorylation was not detected in these cultures.

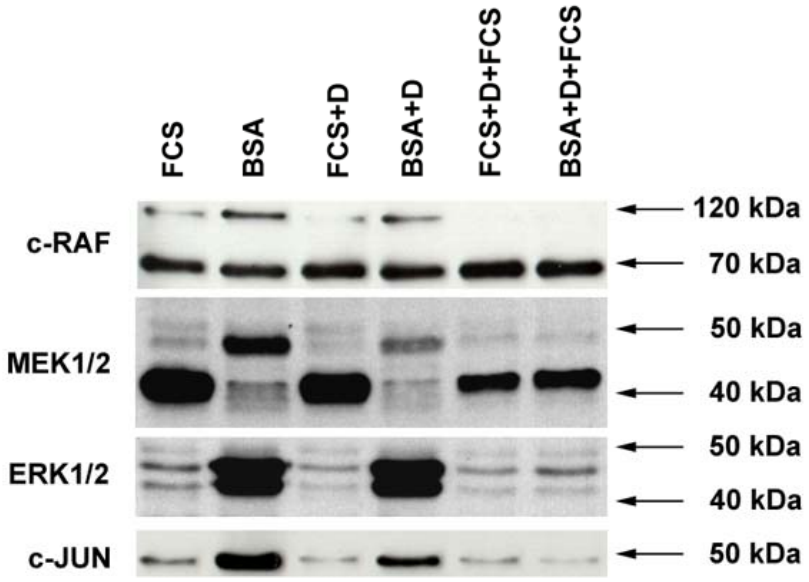

Figure 4-3 Composite image of Western Blots of MAPK pathway members phosphorylated during OLF442 differentiation in the presence of the specific caspase-3 inhibitor DEVD-CHO.

FCS: OLF442 grown in complete medium for 48 hr, BSA: OLF442 grown in serum deplete conditions for 48 hr, resulting in differentiation. FCS+D: culture supplemented with 10 nM DEVD-CHO and incubated for 48 hr, BSA+D: culture supplemented with 10 nM DEVD-CHO and incubated for 48 hr. FCS+D+FCS: culture supplemented with 10 nM DEVD-CHO and incubated for 24 hr at which time the medium was replaced with complete medium without inhibitor and incubated for a further 24 hr. BSA+D+FCS: serum deplete culture supplemented with 10 nM DEVD-CHO and incubated for 24 hr at which time the medium was replaced with complete medium without inhibitor and incubated for another 24 hr, n=3. The antibodies used are described in Table 4-1.

4.4.4 Olfactory Receptor Neuronal Differentiation And Focal Adhesion Kinase

The protein expression level of FAK did not appear significantly elevated in undifferentiated cultures (Figure 4-4, BSA, representative of experiments done in triplicate), in accord with the mRNA expression level of full-length FAK observed by Northern blotting between the two cultures (Figure 2-8, A; larger transcript). However the level of FRNK was increased relative to that in undifferentiated OLF442, also consistent with the higher expression level of FRNK mRNA observed by Northern blotting (Figure 2-8, A; smaller transcript). Treatment of OLF442 cultures with the caspase-3 inhibitor DEVD-CHO did not decrease the protein level of FRNK in agreement with the conclusion (Chapter two) that FRNK in differentiated OLF442 is derived from autonomous expression, not cleavage of FAK by caspase-3. In addition, the exposure of cultures to DEVD-CHO resulted in the detection of an

immunoreactive band at approximately 31 kDa that was highly expressed in differentiated cultures treated with either DEVD-CHO or PD98059 (Figure 4-4, BSA+D and BSA+PD), and only faintly visible in untreated differentiated OLF442 (Figure 4-4, BSA). Furthermore, treatment of differentiated cultures with PD98059 for 48 hr resulted in a marked decrease of full-length FAK protein expression that increased again when serum was added back to the cultures. Therefore it is possible that MEK2 activation is important for high level expression of FAK during differentiation, by a cascade that functions independently of ERK1/2 activation but that requires an input signal from MEK2, since PD98059 treatment of OLF442 differentiation cultures still results in high level phosphorylation of ERK1/2 (Figure 4-2).

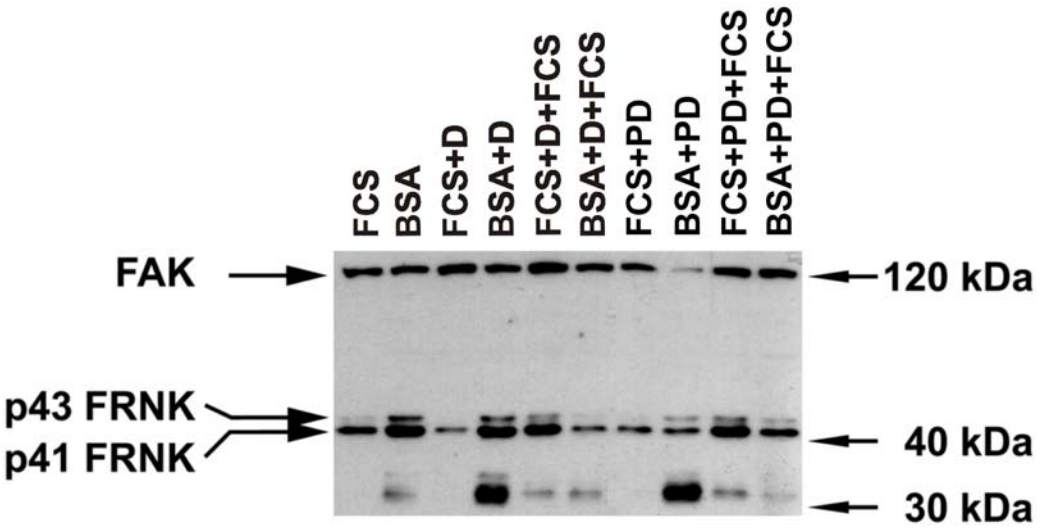

Figure 4-4 Western blot of FAK and FRNK during OLF442 differentiation and treatment with DEVD-CHO and PD98059.

FCS: OLF442 grown in complete medium for 48 hr, BSA: OLF442 grown in serum deplete conditions for 48 hr, resulting in differentiation. FCS+D: culture supplemented with 10 nM DEVD-CHO and incubated for 48 hr, BSA+D: culture supplemented with 10 nM DEVD-CHO and incubated for 48 hr. FCS+D+FCS: culture supplemented with 10 nM DEVD-CHO and incubated for 24 hr at which time the medium was replaced with complete medium without inhibitor and incubated for a further 24 hr. BSA+D+FCS: serum deplete culture supplemented with 10 nM DEVD-CHO and incubated for 24 hr at which time the medium was replaced with complete medium without inhibitor and incubated for another 24 hr. FCS+PD: culture supplemented with 5 μM PD98059 and incubated for 48 hr, BSA+PD: culture supplemented with 5 μM PD98059 and incubated for 48 hr. FCS+PD+FCS: culture supplemented with 5 μM PD98059 and incubated for 24 hr at which time the medium was replaced with complete medium without inhibitor and incubated for a further 24 hr. BSA+PD+FCS: serum deplete culture supplemented with 5 μM PD98059 and incubated for 24 hr at which time complete medium without inhibitor was added and incubated for another 24 hr, n=3. The antibodies used are described in Table 4-1.

4.5 Discussion

Investigation of the MAPK signal transduction cascades was prompted by the identification of two kinases (FRNK and MST2) whose expression was increased following OLF442 serum deprivation. Unfortunately the protein expression levels of MST1/2 were not adequately determined due to problems encountered using commmercial antibodies from two separate sources (refer Table 4-1). High-level background was a big problem with the presence of several bands close in size to the approximate molecular weight of MST2, making accurate identification virtually impossible. Nonetheless, differentiation of OLF442 resulted in the differential regulation of the mitogenic ERK1/2 and stress responsive SAPK/JNK signal transduction cascades, whilst activation of the stress responsive/inflammatory p38 cascade was not observed (Figure 4-1).

4.5.1 Differential Phosphorylation Of Members In The MAPK Cascade Coincides With OLF442 Differentiation

Numerous studies have cited the necessity of ERK phosphorylation for neuronal differentiation (Cowley et al., 1994; Seger and Krebs, 1995; Leppa et al., 1998; Tibbles and Woodgett, 1999). In accord with these studies, OLF442 differentiation caused a high level phosphorylation of ERK1/2 compared to undifferentiated OLF442 (Figure 4-1). Remarkably, the high level phosphorylation of ERK1/2 was resistant to MEK1/2 inhibition with the specific inhibitor PD98059 (Figure 4-2), and also did not reflect a difference in the total content of phosphorylated and unphosphorylated ERK between the cultures. Unexpectedly however, there was a switch between the preferential phosphorylation of MEK1 in undifferentiated OLF442 to MEK2 during differentiation over a 48 hr culture period. Although a switch in activation of the MEKs is seldom reported during neuronal differentiation, the MEK isoforms can be differentially regulated in distinct cell lines by common ERK regulators (Xu et al., 1997). The differential switch between activated MEK1 to MEK2 indicates that a unique signal is involved in OLF442 differentiation, particularly as integrin and growth factor activation of MEKs is generally non-discriminatory. Moreover, both of the phosphorylated MEK1/2 and

ERK1/2 antibodies used in this study detected higher molecular weight bands of unknown identity. Further, analysis of the putative ERK isoform identified was carried out using an ERK1b antibody obtained from Yung et al. (2000). Interestingly, ERK1b is a novel 46 kDa ERK1 isoform that is differentially regulated by MEK and may relay extracellular signals under conditions of persistent stimulation (Yung et al., 2000; Yung et al., 2001). However, this antibody did not successfully detect ERK1b in OLF442 cultures. Nonetheless, the presence of signalling cascade isoforms imparts additional complexity that may be essential for delineating signals that may utilise overlapping MAPK components as demonstrated by Raf.

The activation of c-Raf upstream of the MEKs in OLF442 was not significantly different between the undifferentiated (FCS) and differentiated (BSA) cultures, however the antibody used also detected a higher molecular weight band of unknown identity that was more pronounced in the differentiated culture (Figure 4-1). Three cytosolic phosphoprotein kinases make up the Raf family, consisting of A-Raf (68 kDa), B-Raf (95 kDa) and c-Raf (74 kDa) (Hagemann and Rapp, 1999). In addition ten isoforms of B-Raf with molecular weights ranging from 67 kDa to 99 kDa generated by alternative splicing have been reported (Barnier et al., 1995), while another study found several proteins with apparent molecular weights ranging from 65 kDa to 70 kDa and 95 kDa to 105 kDa in mouse brain extracts with a polyclonal antibody specific to the 12 C-terminal amino acids of B-Raf (Moodie et al., 1994). The Raf isoform identified in this study is approximately 110 kDa in size and was detected with an antibody generated by immunizing rabbits with a synthetic phosphopeptide corresponding to residues surrounding Ser338 of human c-Raf (Cell Signalling Technology). A protein alignment of mouse B-Raf and human c-Raf revealed that eight of the eleven amino acids surrounding Ser338 of human c-Raf were identical with those of mouse B-Raf. However, it has been reported that B-Raf is not phosphorylated at Ser338, and instead phosphorylation occurs at Ser445 (Hagemann and Rapp, 1999). Whether the level of homology around Ser338 is sufficient for antibody cross-reactivity is not known, particularly as the serine residue is not phosphorylated in B-Raf. Yet, the immunoreactive band may represent a Raf isoform that may be specifically expressed in OLF442. This is consistent with the restricted expression of one of the larger B-Raf isoforms (99 kDa) whose expression occurs solely in the brain and spinal cord (Barnier et al., 1995). B-Raf is the main

MEK activator in bovine brain (Yamamori et al., 1995) and differentiated PC12 cells (Traverse and Cohen, 1994), and this Raf isoform may be responsible for the preferential phosphorylation of MEK2 in OLF442. What drives the activation switch from MEK1 in undifferentiated OLF442 to MEK2 in differentiated OLF442 is a matter of speculation but could involve any one of the upstream effectors belonging to the small G-protein family.

Importantly for this study, TC21 is an upstream effector of B-Raf and a member of the small G-protein family that specifically binds B-Raf (Hagemann and Rapp, 1999), and results in PC12 differentiation when overexpressed (Graham et al., 1999). PC12 cells proliferate with EGF stimulation and differentiate when stimulated with NGF, both of which can activate Raf (Hagemann and Rapp, 1999). Wixler et al [(1999) in (Hagemann and Rapp, 1999)] found all three Raf isoforms (A,B and c) in PC12 cells, but only A- and B-Raf showed sustained activation in response to NGF stimulation. Conversely, a transient activation of all three Raf isoforms resulted in PC12 proliferation following exposure to EGF. However when expressed as oncogenic mutants having sustained activation these isoforms resulted in PC12 differentiation. Initial Raf activation requires the small G-protein Ras, but sustained activation of B-Raf is necessary for PC12 neuronal differentiation, and this sustained activation has been shown to be mediated by another small G-protein, Rap1 (Hagemann and Rapp, 1999). Various studies have described the following mechanism in PC12 cells: cAMP-dependent protein kinase (PKA) phosphorylates Rap1, which competes with Ras binding to c-Raf blocking its activation, and results in sustained activation of B-Raf leading to PC12 differentiation (Hagemann and Rapp, 1999). The control of ERK signalling via the small G-proteins Ras and Rap1 in response to multiple second messengers, such as cyclic adenosine monophosphate (cAMP), calcium, and diacylglycerol (DAG) is common in neurons, providing a broader signalling repertoire (Grewal et al., 1999).

The exposure of OLF442 cultures to the specific MEK1/2 inhibitor PD98059 (5 μM) for 48 hr resulted in a decrease of MEK1 and MEK2 phosphorylation in undifferentiated and differentiated cultures respectively (Figure 4-2). Curiously, the selective inhibition did not decrease the level of ERK1/2 phosphorylation in differentiated cultures as expected, suggesting that ERK1/2 activation may occur by

another pathway. PD98059 resulted in a decrease of Raf and c-Jun activity in the differentiated cultures. Furthermore, removal of PD98059 and addition of serum to the differentiated culture reversed the effects of differentiation, resulting in elevated activation of c-Raf and MEK1, and downregulation of the putative B-Raf isoform and ERK activity. The reversal of phosphorylation to the basal levels observed in undifferentiated OLF442 reflects the resistance of these cells to commit to apoptosis within 24 hr of serum depletion, consistent with the retraction of differentiated OLF442 processes when cultures are repleted with serum. This ability of the cultures to reverse their morphological and signalling state when differentiated was also observed in OLF442 cultures treated with the caspase-3 inhibitor, DEVD-CHO (10 nM) for 24 hr followed by serum repletion for a further 24 hr. Caspase-3 inhibition of OLF442 did not significantly affect the MAPK signal transduction levels as differences in phosphorylation of MAPK components were negligible, with only a slight decrease in the activation state of MEK2 in the differentiated cultures treated with DEVD-CHO (Figure 4-3). Phosphorylation of SEK1/MKK4, SAPK/JNK and p38 was not detected in the PD98059 cultures or the DEVD-CHO treated cultures. On the other hand, c-Jun activation levels did appear to change between undifferentiated (FCS) cultures, possibly reflecting slight variations in the culture conditions. Recently, overexpression of c-Jun was reported to delay apoptosis in serum-starved murine erythroleukemia cells (Poindessous-Jazat et al., 2002) and this may account for the high level of c-Jun activity observed in all differentiated cultures.

One common substrate that the ERK and SAPK/JNK signalling modules share is the c-Jun transcription factor. Exposure of PC12 cells to NGF, or expression of constitutively active MEK1, leads to activation of the ERK cascade and c-Jun phosphorylation (Leppa et al., 1998). Furthermore, constitutively activated c-Jun can induce differentiation independent of upstream signals, whilst c-Jun activation by the SAPK/JNK pathway via SEK1/MKK4 results in apoptosis (Leppa et al., 1998). It has since emerged that activation of c-Jun in naive PC12 cells (undifferentiated) is anti-apoptotic and does not require its transcription factor qualities, as mutations in these domains does not inhibit its survival inducing ability (Leppa et al., 2001). Instead the transcription factor qualities of c-Jun are essential for its ability to differentiate PC12 cells (Leppa et al., 2001). Activation of c-Jun in differentiated cells is apoptotic and requires SAPK/JNK activity (Leppa et al., 2001). The mechanism by which c-Jun is

able to induce survival in undifferentiated PC12 cells has yet to be described but possibly involves a fine balance between the activities of several other downstream MAPK effectors. The results presented here may also argue for the activation of a novel MAPK module that includes ERK1/2 activation by MEK2 (or a MEK2 splice variant), utilising B-Raf activation. In fact the identity of the MEK2 immunoreactive band identified in this study may be questioned particularly since the selective inhibition of MEK1/2 was unable to inhibit ERK1/2 activation during OLF442 differentiation. Therefore it is possible that the immunoreactive band identified is very closely related to MEK2 and could represent a splice variant.

4.5.2 Elevated FRNK Expression May Influence OLF442 Differentiation

Investigation of the protein expression level of FAK showed no significant difference between differentiated (FCS) and undifferentiated (BSA) cultures (Figure 4-4), consistent with the expression level of full-length FAK mRNA (Figure 2-8A; larger transcript). The protein expression level of FRNK was increased relative to that in undifferentiated OLF442, and again matched the higher expression level of FRNK mRNA observed by Northern blotting (Figure 2-8A; smaller transcript). Exposure of OLF442 cultures to the caspase-3 inhibitor DEVD-CHO did not result in a decrease of FRNK protein, confirming that FRNK in differentiated OLF442 is derived from autonomous expression, not cleavage of FAK by caspase-3. The appearance of a 31 kDa band recognised by the anti-FAK antibody, that was highly expressed in differentiated (BSA) cultures, was observed when OLF442 was treated with DEVD-CHO and with PD98059 (Figure 4-4). Notably, treatment of differentiated cultures with PD98059 for 48 hr resulted in a marked decrease of full-length FAK protein expression, whereas the expression was increased when serum was added to the cultures. Consequently MEK1/2 activation is important for high-level expression of FAK during differentiation. This may occur by a cascade that functions independently of ERK1/2 activation but which requires an input signal from MEK1/2, as PD98059 treatment of OLF442 differentiation cultures still show high-level phosphorylation of ERK1/2 (Figure 4-2). The significance of elevated FRNK expression becomes evident when one considers that the primary role of FRNK is to act as an inhibitor of FAK by transiently blocking the formation of focal adhesions

and reducing the phosphorylation of both FAK and other proteins bound in the focal adhesion complex. Activation and association of the adaptor protein Shc with Grb2 mediates integrin and growth factor signalling to ERK in response to matrix adhesion or growth factor stimulation (Wary et al., 1998). This process does not require FAK participation in cells that do not express B-Raf (Barberis et al., 2000), however, in B-Raf expressing cells, Shc mediates early integrin-dependent ERK activation, whilst FAK, $p130^{CAS}$ (Crk-associated substrate), Crk, and Rap1 signalling mediates the late phase of ERK activation (Schlaepfer et al., 1998; Barberis et al., 2000). Interestingly, FAK participates centrally in the transmission of signals emanating from GTK overexpression in PC12 cells (Anneren et al., 2000). Overexpression of GTK (a cytoplasmic tyrosine kinase of the Src family) in PC12 cells results in a larger fraction of cells exhibiting processes, a response not accompanied by increased ERK activity and not affected by PD98059 treatment (Anneren et al., 2000). Anneren et al. (2000) also noted that PC12 cells overexpressing GTK had a marked increase in the content of FAK, phosphorylation of the adaptor protein Shb (Src homolgy 2-domain protein of beta cells), and that inhibitors of the Rap1 pathway reduced the neurite outgrowth. Together these studies suggest that GTK participates in a signalling pathway, perhaps involving Shb, FAK, $p130^{CAS}$, CrkII, C3G (the specific guanine exchange factor for Rap1) and Rap1, that results in neurite outgrowth of PC12 cells. This may result in the activation of an as yet unidentified pathway (as observed in GTK overexpressing cells) that may function in parallel with the ERK cascade, the activation of which has been demonstrated in PC12 cells and may also operate in OLF442 undergoing differentiation.

The inhibitory effects of FRNK, which can be reversed by co-expression of FAK, would undoubtedly result in displacing FAK binding proteins. The disruption of protein binding may inhibit signalling to ERK, and could dramatically affect the response of PC12 cells or OLF442 to differentiation. The timing of FRNK expression may be crucial for determining the deactivation of the sustained ERK signal that appears important for neuronal differentiation, particularly as c-Jun activation is important in regulating apoptosis in serum-deprived and differentiated cells.

4.6 Conclusion

Western analysis of phosphorylated members of the MAPK cascades has revealed that a novel MAPK module may be active during OLF442 differentiation. It is likely that the elevated activation of ERK1/2 is necessary for neuronal differentiation as observed in OLF442, and may occur by preferential activation of MEK2 (or a MEK2 splice variant) that requires B-Raf activation. The case for the phosphorylation of a specific MEK2 isoform is strengthened by the inability of the MEK1/2 specific inhibitor (PD98059) to limit ERK1/2 activation during OLF442 differentiation. Furthermore, sustained activation of B-Raf - a necessity for PC12 neuronal differentiation – is mediated by another small G protein, Rap1. A cascade that links integrin signalling to ERK via FAK activates Rap1. In addition, components of the integrin-ERK signalling pathway are all required for neurite outgrowth of PC12 cells. Therefore a pathway of signal transduction has been mapped in differentiating OLF442 that is probably controlled by the endogenous expression of FRNK whose expression is not a result of cleavage by caspase-3. The expression of FRNK leading to disruption of FAK association with its binding partners may regulate signalling to ERK. Regulation of ERK phosphorylation is critical as sustained activation is required for differentiation, however its downstream effector c-Jun can also induce apoptosis in differentiated cells rather than aiding differentiation in naive cells.

5 EXOGENOUS MST KINASE EXPRESSION IN OLF442

5.1 Expression Of Cloned Genes In Mammalian Cells: A Basic Tool For Understanding Protein Function

An essential tool for understanding protein function is the expression of cloned genes in mammalian cells. Typically target genes are mutated to knockout/in a particular function, assumed from the presence of known motifs, and expressed in mammalian cells to observe phenotypic changes. However, "the level of protein expression from heterologous genes introduced into mammalian cells depends upon multiple factors including DNA copy number, efficiency of transportation, mRNA processing, mRNA transport, mRNA stability, and translational efficiency, and protein processing, transport, and stability" (Kaufman, 2000). Further, expression of exogenous proteins can be effected in a transient or permanent (stable) manner, and the expression level can be directly controlled in a time and concentration dependent way due to the vast array of vectors available for mammalian transfection and expression. The choice of experimental design is largely dependent on the protein under investigation and key factors (mentioned above) that affect the level of protein expression. Given the limited functional data available for MST kinase, the expression of native and mutant MST constructs in OLF442 should undoubtedly provide some insight into the role that this interesting protein has in neuronal differentiation. Known MST functions and cellular roles are outlined below, and are part of the necessary information required to design a meaningful experimental approach to mammalian transfection studies.

5.2 MST, A Physiological Caspase Substrate

Stimuli identified to date that induce MST1/2 activity, with the exception of transformation by $pp^{60v\text{-}src}$, have common phenotypical consequences; all reduce cell attachment and result in eventual cell death (Taylor et al., 1996). Stimuli that induce apoptosis include treatment with Fas/CD95, staurosporine (a serine/threonine kinase inhibitor), UV-irradiation and other genotoxic agents including etoposide, cytotrienin A, hydrogen peroxide (H_2O_2) and okadaic acid, resulting in the cleavage and activation of MST1/2 (Graves et al., 1998; Kakeya et al., 1998; Lee et al., 1998a; Kakeya et al., 1999). MST1/2 cleavage has also been observed in response to serum

withdrawal in NIH 3T3 cells and normal human smooth muscle cells, and NGF-withdrawal in PC-12 cells (Graves et al., 1998). Furthermore, overexpression of wild-type MST1, or a truncated mutant MST1Δ330, induces caspase activity and morphological changes characteristic of apoptosis including nuclear condensation (Graves et al., 1998). Although not required for Fas/CD95 induced apoptosis, the MST proteolytic activation observed is blocked by the caspase inhibitor Z-VAD-FK (a broad specificity inhibitor of caspases), indicating that proteolytic activation of MST1/2 plays a role in generating apoptosis-inducing signals downstream of caspases (Lee et al., 1998a; Lee et al., 2001). The active proteolytic (36 kDa) fragment generated during apoptosis is detected within 1 hr of anti-Fas treatment, when 80% of the cells are still viable, corroborating the idea that MST1 proteolysis not only results in an increase in its catalytic activity, but may also function in a positive feedback pathway that amplifies the apoptotic response via a JNK/SAPK and p38 MAPK pathway (Graves et al., 1998). Co-expression experiments of MST1 and MST1Δ330 with JNK/SAPK and p38 MAPK lead to a 7- and 5- fold increase in these MAPKs respectively, but not that of ERK (Graves et al., 1998). Additionally, MST1 activates MKK6 and MKK7 but has little effect on MKK4 and MKK3, and no effect on MKK1, consistent with its effects on JNK/SAPK and p38 MAPK (Graves et al., 1998). Recently however, Graves et al. (2001) suggest that MST1 acts as an apoptotic effector by activating the following MAPK module, MST1→ MEKK1→ MAPKK7 → JNK/SAPK, and exploiting the inherent amplification capacity of this protein kinase cascade to transduce the apoptotic signal. Although it is accepted that MST cleavage and kinase activation also results in the induction of p38 MAPK and consequently apoptosis, the mechanism by which this may occur remains unclear. Kakeya et al. (1998) failed to observe a block in MST cleavage and kinase activation resulting in apoptosis when human leukemia HL-60 cells were treated with cytotrienin A and the p38 MAPK specific inhibitor (SB203580). In contrast, transfection of wild-type MST1 into a highly transformed human renal epithelial cell line (293T) expressing two viral oncogenes (adenovirus E1a and SV40 large T antigen) and treated with SB203580 was able to inhibit apoptosis (Graves et al., 1998)). This is particularly interesting given that expression of MST1 from a strong promoter results in the production of a truncated MST1 species (Creasy and Chernoff, 1995b). As described below this 41 kDa product may result from proteolysis of MST1 at a second caspase cleavage site and may utilise the p38MAPK pathway.

MST1 has been shown to promote two independent events; first, caspase activation induced by MST1 promotes DNA fragmentation, and second, MST1 directs chromatin condensation and membrane blebbing exclusive of caspases (Ura et al., 2001a). Whether activation of the p38 MAPK pathway or JNK/SAPK pathway is a 'consequence rather than a cause of MST1-induced apoptosis' is an important question that needs to be addressed (Graves et al., 1998) in order to assess the role that MST cleavage plays. These results highlight the complexity of MST cleavage and its ability to induce apoptosis in different cell lines; whether or not this process is necessary to induce cell death has yet to be determined. Conflicting results also emphasise the importance of the cell setting with different cell contexts and phosphorylation potentials affecting the outcome and pathway of signal routing in overexpression experiments.

5.2.1 Multiple Size Caspase Cleavage Products And Phosphorylation

Creasy and Chernoff (1995b) observed a smaller hyper-active 40 kDa carboxyl-terminal truncated form of MST1 whose expression was only present when MST1 was expressed from a strong promoter during transient transfection of COS cells (Creasy and Chernoff, 1995b). A 40 kDa kinase activity was also observed following staurosporine stimulation of murine T-cell hybridomas (Taylor et al., 1996). Identification of caspase specific cleavage sites within MST producing a 36 kDa proteolytic fragment was determined from the amino acid sequence ^{323}DEMDS^{327} (MST1) and ^{319}DELDS^{323} (MST2), and mutant analysis [MST1(D326N) and MST2 (D322N)] in which aspartic acid, a conserved recognition amino acid of caspases, was replaced with asparagine at the putative caspase cleavage site, resulting in resistance to proteolytic cleavage (Graves et al., 1998; Lee et al., 1998a). The location of the caspase cleavage site at the junction of the catalytic and the regulatory domains of MST suggests that caspase-mediated cleavage releases the kinase domain from the regulatory domain resulting in MST kinase activation.

The synthetic compound, MT-21, induces apoptosis in HL-60 cells resulting in caspase-3 cleavage of a 36 kDa MST kinase active proteolytic product (Watabe et

al., 1999; Watabe et al., 2000a). Apoptosis induced by cytotrienin A also generates a 36 kDa proteolytic MST fragment that is resistant to a specific caspase-1 like protease inhibitor (YVAD-CHO) and a caspase-3 like protease inhibitor (DEVD-CHO). However, a broad spectrum caspase inhibitor (Z-Asp-CH_2-DCB) can successfully block both MST cleavage and apoptotic cell death in response to cytotrienin A, H_2O_2 and okadaic acid exposure (Kakeya et al., 1998, 1999; Watabe et al., 2000b). Recently, a second caspase cleavage site was identified in MST1, providing an explanation for the observed different sized cleavage products and caspase sensitivity. Graves et al. (2001) identified two MST1 cleavage products upon withdrawal of interleukin-2 (IL-2) from factor-dependent CTLL-2 cells. Firstly, a 41 kDa product was detected 3 hr after IL-2 withdrawal, followed by the appearance of the previously characterised 36 kDa product 6 hr after withdrawal, both of these products were catalytically active (Graves et al., 2001). Importantly the 41 kDa product was also observed following staurosporine treatment and may be the same activity observed by Creasy and Chernoff (1995b) and Taylor et al. (1996). A second caspase cleavage site was identified at ^{346}TMTDG^{350} in MST1, although not conserved in MST2 (implying differential targeting during apoptosis), the presence of which raised the possibility that each site is cleaved by different caspases (Graves et al., 2001). These authors found that caspases 3, 6, 7 and 9 cleaved MST1 at ^{323}DEMDS^{327} to yield the 36 kDa proteolytic fragment while only caspases 6 and 7 could cleave the second cleavage site ^{346}TMTDG^{350} to generate the 41 kDa fragment. Considering that kinase dead MST1(K59R) was not cleaved upon overexpression, and that apoptosis was not induced when transiently transfected into BJAB human B lymphoma cells, it is likely that MST1 must be catalytically active in order to mediate apoptotic events (Graves et al., 1998). Indeed, MST1 must be activated by a mechanism distinct from proteolysis in order to be fully stimulated by caspase cleavage. Such a mechanism requires that MST1 be phosphorylated prior to proteolysis and also implies that cleavage is required for the full activation of MST1 during apoptosis (Graves et al., 2001). A candidate autophosphorylation site is Ser 327, a serine residue that is adjacent to the ^{323}DEMDS^{327}cleavage site (Graves et al., 2001). Ser 327 has been shown to be a major in vitro MST1 autophosphorylation site whose activation state influences the sensitivity of MST1 to cleavage at ^{323}DEMDS^{327} by caspase-3 (Graves et al., 2001). However autophosphorylation at Ser 327 was caspase insensitive only when expressed in caspase-3-deficient cells (Glantschnig et al., 2002). Other residues have

also been identified within the activation loop of MST1 (Thr 183 and Thr 187) whose autophosphorylation within the MST1 dimer is essential for kinase activation (Glantschnig et al., 2002). These authors suggest that MST1 activation is induced by existing, active MST kinase, which phosphorylates Thr 183 and possibly Thr 187. Dimerisation promotes greater phosphorylation leading to induction of the JNK signalling pathway, caspase activation and apoptosis (Glantschnig et al., 2002). Interestingly PAK2, another member of the serine/threonine kinase Ste20/PAK family whose activity is regulated by Rac and Cdc42 has been reported to be involved in apoptosis, requiring activation by phosphorylation and caspase-dependent cleavage (Rudel and Bokoch, 1997; Graves et al., 2001; Lian et al., 2001). Therefore family members may have similar functional properties but may respond to varied stimuli.

5.2.2 MST1/2 Nuclear Localisation

MST1 has been implicated in chromatin condensation, a process that occurs exclusively in the nucleus (Ura et al., 2001a). Moreover, full-length MST1 is excluded from the nucleus and localised to the cytoplasm. Two functional nuclear export signals (NESs) in the carboxyl-terminal domain of MST1 have been identified; NES1 -^{361}LPSQLGTMVI^{370} and NES2 –^{441}VEDLQKRLLAL^{451} (Ura et al., 2001b). These authors demonstrated that truncation of the carboxyl-terminal domain, point mutation of the two putative NESs, and treatment with leptomycin B, an inhibitor of the NES receptor, results in nuclear localisation of MST1 (Ura et al., 2001b). Transfection studies using MST1(1-487) and a carboxyl-terminal MST1(331-487) fragment containing the putative NES sequences localised exclusively in the cytoplasm, whilst mutation of both NESs resulted in nuclear retention. Yet, an amino-terminal MST1(1-330) fragment lacking the NESs was found localised in the nucleus and cytoplasm (Ura et al., 2001b), indicating that a nuclear localisation sequence or nuclear anchor in the carboxyl-terminus is also present (Ura et al., 2001b). In fact MST1 contains a bipartite nuclear localisation signal-like motif in the carboxyl-terminus ^{469}KRQPILDAIEAKKRRQQ^{485} (Ura et al., 2001b). The location of the NESs is significant, particularly since cleavage activates MST1 kinase several fold. The full effects of MST1 kinase hyperactivity in the nucleus have yet to be

determined but are likely to result in activation of processes beyond chromatin condensation under different circumstances.

5.2.3 Non-Apoptotic Functions Of MST1/2

In addition to the activation of MST1, it is likely that the removal of the regulatory domain of MST1 contributes to other functions of the kinase, particularly as it mediates homo- and heterodimerisation and inhibits kinase activity. The presence of a putative nuclear exclusion sequence, as well as a bipartite nuclear localisation motif in the carboxyl-terminus further supports this notion (Graves et al., 2001; Ura et al., 2001b). Consequently, "substrate specificity, subcellular localisation and protein-protein interactions, are also likely to be influenced by the cleavage of MST1 by caspases" (Graves et al., 2001). Of particular interest and relevance to this study is the recent detection of a novel 33 kDa quiescence-activated kinase ($p33^{QIK}$) (Wang and Fecteau, 2000). Active during the quiescent phase of growth-arrested cells, $p33^{QIK}$ is readily deactivated upon cell cycle re-entry during the G_0/G_1 transition requiring new synthesis of regulatory proteins for deactivation (Wang and Fecteau, 2000). Moreover, $p33^{QIK}$ is recognised by anti-MST antibodies, and thus appears to represent a novel proteolytic product of MST1/2 distinct from the 36 kDa caspase cleaved derivative (Wang and Fecteau, 2000). Alternatively, $p33^{QIK}$ may represent an alternatively spliced product of the MST1/2 genes (as hypothesised in chapter three), or even a separate gene product altogether (Wang and Fecteau, 2000; Graves et al., 2001).

Also it is important to emphasize that, in addition to proteolytic activation during apoptosis, MST is likely to be regulated in a caspase-independent manner by stimuli that do not induce apoptosis (Graves et al., 1998). This has been demonstrated by the identification of a 56 kDa serine/threonine kinase rat homolog of human MST2 that is able to phosphorylate thyroid transcription factor-1 (TTF-1) exclusively on serine residues in thyroid cells (Aurisicchio et al., 1998). MST2 in this case may drive lineage specific determination as TTF-1 is a homeodomain-containing transcription factor, required for thyroid specific expression of the thyroglubulin and thyroperoxidase genes, as well as for lung-specific expression of other genes (Aurisicchio et al., 1998). Similarly, Sun and Ravid (1999) reported that MST1 is

involved in differentiation of megakaryocytes, the precursors to platelet cells in the blood. Megakaryocytes undergo endomitotic cell cycles, which are slightly different from the usual mitotic cell cycle in terms of the length of the different phases; these endomitotic cell cycles are involved in the maturation of megakaryocytes. The signalling pathway for differentiation involves the Mpl receptor, which is activated by thrombopoietin. Sun and Ravid (1999) noted that MST1 is activated following thrombopoietin binding to the Mpl receptor, resulting in the induction of megakaryocytic differentiation markers and proteins that cause polyploidy. The MST1 mediated polyploidy required activation of the p38 MAPK pathway, unlike the expression of differentiation markers that was p38 MAPK independent. Western analysis of MST1 expression in megakaryocytes under both inducing and noninducing conditions showed the absence of a caspase cleavage product (Sun & Ravid, 1999). Thus one important difference between the reported functions of MST is that whereas cleavage results in increased activation of MST1 within the apoptotic pathway, caspase cleavage is not required for megakaryocyte differentiation nor for TTF-1 induced gene expression, both of which lead to cellular lineage restriction.

5.3 Aim

Given that the MST2 kinase clone obtained from the library screen (Chapter three) lacked the first 150 bp of sequence including part of the open reading frame, that MST2 and MST1 kinase are highly conserved at the amino acid level (refer Appendix IV), and that published data for MST1 also largely applies to MST2, we used our full-length MST1 clone for protein expression studies. MST1 was used to generate a kinase dead MST1 mutant (MST1K59R), a caspase-3 insensitive mutant (MST1D326N), and an MST1 double mutant (MST1K59RD326N) that is kinase dead and insensitive to caspase cleavage. Mutant constructs were to be tagged with a FLAG epitope to allow differential recognition of endogenous MST1 and exogenous MST1. Recombinant proteins were to be used for stable transfection of OLF442 during differentiation in concert with an inducible mammalian expression vector, to determine the effect/s of the various mutants during normal OLF442 growth and during differentiation. These *in-vitro* experiments were designed to test the hypothesis that the MST subfamily is involved in important cellular functions besides mediating apoptosis.

5.4 Methods

5.4.1 Mutant Primer Design

PCR based mutagenesis requires the presence of suitable restriction enzyme sites that are in close proximity to the site of mutation for cloning of PCR products. Primer design was done using the Primer3 output at http://www.genome.wi.mit.edu/cgi-bin/primer/primer3. Candidate primers containing a suitable restriction enzyme site and satisfying primer melting temperature (Tm) and size restrictions were analysed against the non-redundant database using the nucleotide-nucleotide blast (blastn) program to confirm MST1 specificity and uniqueness. The mutagenic sites were then incorporated into the suitable primers as outlined. MST1 kinase contains a critical lysine residue (K59) required for ATP binding that is necessary for full kinase activity (Creasy et al., 1996). The kinase mutant (MST1K59R) contains an arginine substitution at this residue rendering the kinase inactive. A mutagenic primer designated MST1K59RF (31 mer) was designed to convert the AAG lysine codon to the highest occurring arginine codon (AGG) in murine coding sequences. The primer also incorporated Msc I, a unique restriction enzyme site that cleaves MST1 once and does not cleave pBluescript II KS(+) [pBSKS(+)] vector. A downstream primer 1mMST2R designed previously for sequencing MST was utilised in the mutatgenic PCR amplification. Likewise, the aspartic acid residue (D326) within the caspase-3 cleavage site of MST1 at ^{323}DEMD^{326}S was substituted with asparagine, resulting in resistence to proteolytic cleavage (Graves et al., 1998). A mutagenic primer designated MST1D326NR (27 mer) was designed to convert the aspartic acid codon (GAT) to the asparagine codon (AAT). The primer was designed to incorporate the Taq I restriction enzyme site that cleaves MST1 three times, as no other suitable restriction enzyme was found that did not cut pBSKS(+) vector. An upstream primer 1mMST2F designed previously for sequencing MST was utilised in the mutatgenic PCR amplification as described below.

5.4.2 Construction Of A Kinase Dead MST1 Mutant

MST1.pGEM-T Easy (refer Section 3.4.4) was PCR amplified using MST1K59RF, 1mMST2R, 200 μM dNTPs, 1.5 mM $MgCl_2$, 1X PCR buffer and 2 units AmpliTaq® polymerase (Perkin Elmer) in a final reaction volume of 50 μL, in thin walled PCR tubes. An equal volume of autoclaved mineral oil (Sigma) was layered on top of the reaction mixture and the samples were placed in an OmniGene thermal cycler to proceed through the following PCR program: thirty cycles of denaturation at 95ºC x 1 min, annealing at 70ºC x 1 min and extension at 72ºC x 1 min, preceded by a 5 min incubation at 95ºC and followed by a 5 min extension at 72ºC. The PCR products were digested with Msc I and Nde I (Section 2.3.4.6). Further, MST1.pGEM-T Easy was digested with Not I (Section 2.3.4.6) to excise the entire MST1 clone and pBSKS(+) was also digested with Not I and treated with 1 unit of calf intestinal alkaline phosphatase (CIAP, Gibco BRL®) at 37ºC for 5 min. All digested samples were resolved on a 1.5% agarose gel (Section 2.3.2.9), following which the Msc I/Nde I mutagenic MST1 amplified band, Not I digested MST1 fragment and CIAP treated Not I digested pBSKS(+) plasmid were gel extracted (Section 2.3.3.1.2), and quantitated by spectrophotometry; an optical density of 1 at an absorbance wavelength of 260 nm corresponds to 50 μg/mL of double stranded DNA (Sambrook et al., 1989). The Not I MST1 fragment was subcloned into Not I digested pBSKS(+) at a 1:6 (vector:insert) ratio as follows: a 10 μL ligation reaction was set up with Not I digested pBSKS(+) (250 ng), 1 μL 10X T4 DNA ligase buffer and 1 μL of T4 DNA ligase (3 Weiss units/1 μL, Boehringer Mannheim) and 750 ng of Not I digested MST1 insert. Ligations were incubated at room temperature for 1 hr. Two μL of the ligation was used to transform supercompetent XL10-Gold cells as described (Section 3.3.3.2). MST1.pBSKS(+) was then digested with Msc I/Nde I to produce two fragments, one of 4 kb in size and an MST1 internal fragment of 500 bp corresponding to the Msc I/Nde I mutagenic MST1 amplified band. The wildtype Msc I/Nde I fragment was replaced with the mutagenic Msc I/Nde I fragment by cloning as described above. The resulting MST1K59R construct in pBSKS(+) was sequenced (Section 2.3.4.7) to confirm the presence of the mutation and used to subclone into the mammalian expression plasmid (Section 5.4.5). A schematic outline of the MST1K59R mutant cloning strategy is illustrated below (Figure 5-1).

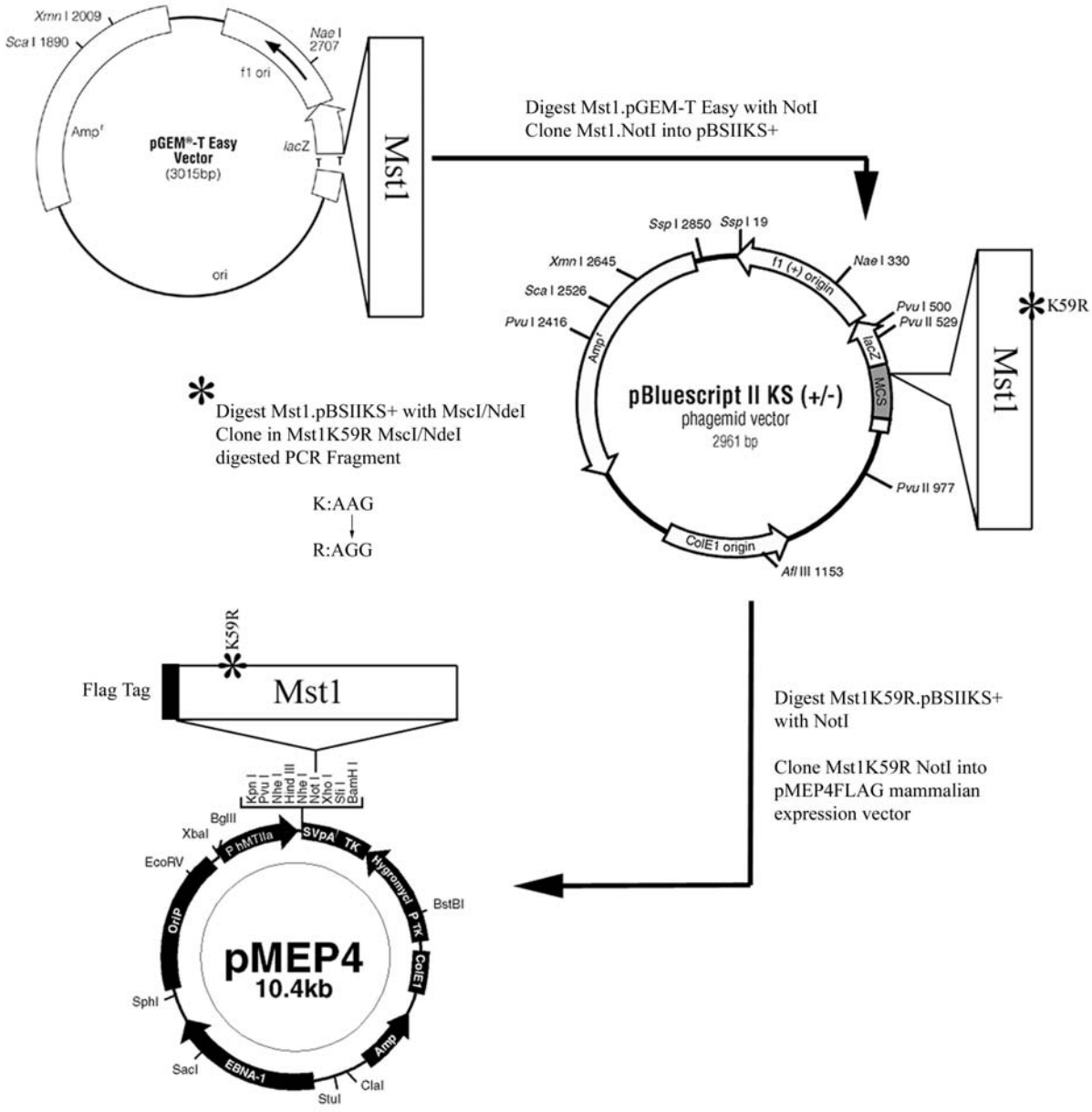

Figure 5-1 Schematic illustration of the MST1 kinase dead (MST1K59R) cloning strategy.

Cloning of the MST1K59R mutant in the pMEP4 mammalian expression vector containing a FLAG TAG, involved several sub-cloning steps to accommodate single site cleavage with the required restriction enzymes.

5.4.3 Production Of A Caspase-3 Insensitive MST1 Mutant

MST1.pGEM-T Easy (refer Section 3.4.4) was PCR amplified using 1mMST2F, MST1D326NR, 200 µM dNTPs, 1.5 mM $MgCl_2$, 1X PCR buffer and 2 units AmpliTaq® polymerase (Perkin Elmer) in a final reaction volume of 50 µL, in thin walled PCR tubes. An equal volume of autoclaved mineral oil (Sigma) was layered on top of the reaction mixture and the samples were placed in an OmniGene thermal cycler to proceed through the following PCR program: thirty cycles of denaturation at 95ºC x 1 min, annealing at 70ºC x 1 min and extension at 72ºC x 1 min, preceded by a 5 min incubation at 95ºC and followed by a 5 min extension at 72ºC. The PCR product was sequentially digested with Nde I, followed by Taq I (Section 2.3.4.6) and was resolved on a 1.5% agarose gel (Section 2.3.2.9) and gel extracted (Section 2.3.3.1.2). This MST1D326N Nde I/Taq I fragment was used to replace the homologous wildtype fragment lacking the D326N mutation. Taq I was the only restriction enzyme in close enough proximity to the caspase cleavage site to be mutated that cleaved MST1 less than three times and that did not cut the pBSKS(+) vector. It was therefore used for PCR fragment cloning of MST1D326N, however, Taq I cleaved MST1 in two locations. Thus a Taq I/Bcl I MST1 fragment was prepared. MST1.pBSKS(+) was digested with Not I and Taq I and separated on a 1.5% agarose gel generating three fragments of 1.1 kb, 359 bp and 100 bp in size in addition to the plasmid fragment. The Not I/Taq I MST1 359 bp fragment was further digested with Bcl I and run on a 12.5% DNA non-denaturing page (Section 2.3.3.1.3) resulting in a 113 bp and 246 bp fragments. The 113 bp Taq I/Bcl I MST1 fragment was gel excised (Section 2.3.2.13) and used in a three-way ligation as described below. Nde I and Bcl I digested MST1.pBSKS(+), along with the 324 bp MST1D326N Nde I/Taq I fragment, and the 113 bp Taq I/Bcl I MST1 fragment were ligated at a vector insert ratio of 1:6:9 respectively, with 3 units of T4 ligase. The ligation was incubated at 4ºC and phenol: chloroform extracted (Sambrook et al., 1989). The purified ligation reaction was resuspended in 2 µL of MQH_2O, the entire volume of which was used to transform supercompetent XL10-Gold cells as described (Section 3.3.3.2). The resulting MST1D326N construct in pBSKS(+) was sequenced (Section 2.3.4.7) to confirm the presence of the mutation and used to subclone into the mammalian expression plasmid (Section 5.4.5). A schematic outline of the

MST1D326N mutant cloning strategy is illustrated in Figure 5-2.

5.4.4 Production Of An MST1 Kinase Dead – Caspase-3 Insensitive Double Mutant

The MST1K59RD326N double mutant was made in much the same way as the caspase insensitive mutant described above. However the three way ligation was done with Nde I/Bcl I digested MST1K59R.pBSKS(+) instead of with the Nde I/Bcl I digested MST1.pBSKS(+), along with the 324 bp MST1D326N Nde I/Taq I fragment, and the 113 bp Taq I/Bcl I MST1 fragment which were ligated at a vector: insert ratio of 1:6:9 respectively, with 3 units of T4 ligase. The purified ligation reaction was resuspended in 2 μL of MQH_2O, and the entire volume was used to transform supercompetent XL10-Gold cells as described (Section 3.3.3.2). The resulting MST1K59RD326N construct in pBSKS(+) was sequenced (Section 2.3.4.7) and used to subclone into the mammalian expression plasmid pMEP4 FLAG (Section 5.4.5). A schematic outline of the MST1K59RD326N mutant cloning strategy is illustrated below (Figure 5-2).

5.4.5 Construction Of Mammalian Expression Plasmids

MST1.pBSKS(+), MST1K59R.pBSKS(+), MST1K59RD326N.pBSKS(+), and MST1D326N.pBSKS(+) were all digested with Not I (Section 2.3.4.6), resulting in the excision of MST1 which was ligated into pMEP4FLAG (generously donated by Wayne Schroder) previously digested with Not I and CIAP, using T4 DNA ligase and a vector: insert ratio of 1:3. Ligations were incubated overnight at 4ºC following which 2 μL of the reaction was used to transform supercompetent XL10-Gold cells as described (Section 3.3.3.2). The resulting constructs cloned in pMEP4FLAG were sequenced (Section 2.3.4.7) to confirm that they were in frame and juxtaposed to an amino terminal FLAG epitope (MDYKDDDDK). The MST1.pMEP4FLAG constructs (Figure 5-1 and Figure 5-2) were used in mammalian expression studies as outlined below.

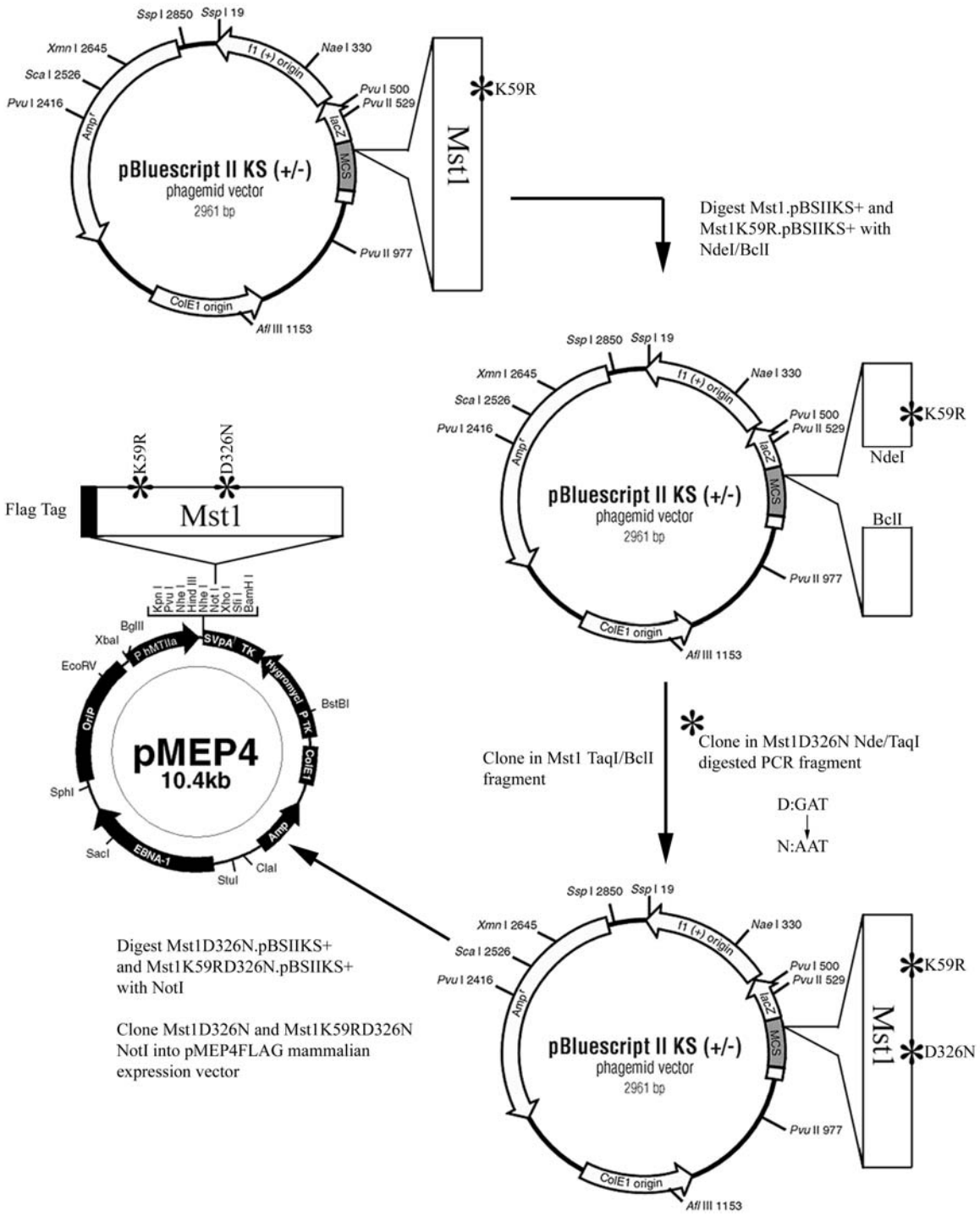

Figure 5-2 Schematic illustration of the MST1 caspase insensitive (MST1D326N) and double mutant (MST1K59RD326N) cloning strategy.

Cloning of the MST1D326N and MST1K59RD326N mutants into the pMEP4FLAG mammalian expression vector involved a three-way ligation and several sub cloning steps.

5.4.6 OLF442 Stable Cell Line Generation

OLF442 cells were cultured in 25cm^2 flasks to 80% confluency with 10% FCS/DMEM/GLUT complete medium (Section 2.3.1.1), and fed 2 hr prior to transfection with half the volume of fresh medium. Two µg of each plasmid (MST1.pMEP4FLAG, MST1K59R.pMEP4FLAG, MST1D326N.pMEP4FLAG, and MST1K59RD326N.pMEP4FLAG) was diluted in 100 µL of 1%BSA/DMEM/ GLUT, as was 12.5 µL of Lipofectamine (Gibco BRL®). Both the plasmid and Lipofectamine solutions were combined and mixed for each construct and incubated at room temperature for 45 min. Cells were rinsed with HBSS twice, followed by a final rinse with 1%BSA/DMEM/GLUT, at which time 800 µL of serum free media (1%BSA/ DMEM/GLUT) was added to the DNA/Lipofectamine complex and then added to separate cell culture flasks. Cells were incubated at 37º C with the DNA/Lipofectamine complex and were gently rocked every hour over a period of 4 hr. Each cell culture flask was supplemented with 10% FCS/DMEM/GLUT complete medium and incubated for 24 hr. Cultures were passaged into three 25cm^2 flasks for selection of transfected cells with hygromycin B (Gibco BRL®). A kill curve was established with varying concentrations (0-900 µg/mL) of hygromycin B in complete medium. Cultures were examined daily until complete cell death was observed; OLF442 cultures were not resistant to hygromycin B concentrations above 600 µg/mL. Thus transfected cultures were treated with 600 µg/mL hygromycin B for a period of 14 days, resulting in the generation of 1-3 resistant colonies within a flask. Hygromycin concentration was decreased to 150 µg/mL to allow expansion of the colony. Cultures were maintained and passaged as described (Section 2.3.1.1) with the inclusion of hygromycin B in the media.

5.4.7 Induction Of Exogenous Protein Expression

Stable cell lines were maintained for up to 3 months during which time exogenous protein expression was induced with cadmium chloride ($CdCl_2$, Sigma) diluted in the appropriate media. A recommended concentration of 5µM $CdCl_2$ was used for induction of expression over a number of time scales (1, 4, 8, and 24 hr) prior to fixation of cells for DAPI staining or immunocytochemistry (see below).

5.4.8 OLF442 DAPI Staining

The fluorescent dye 4',6-Diamidine-2'-phenylindole dihydrochloride (DAPI, Roche Diagnostics Australia PTY LTD, Castle Hill, NSW, Australia) selectively binds DNA and forms fluorescent complexes, allowing the detection of apoptosis and mycoplasma contamination. Stable OLF442 cultures were plated onto 60 mm^2 tissue culture dishes (Nunc) at the appropriate density: 30 cells/mm^2 for 10% FCS treated cells and 90 cells/mm^2 for 1% BSA treated cells for 48 hr cultures; 60 cells/mm^2 for 10% FCS treated cells and 90 cells/mm^2 for 1% BSA treated cells for 24 hr cultures; and 90 cells/mm^2 for 1% BSA treated cells and 10% FCS treated cells for 1, 4 and 8 hr cultures. Prior to serum depletion cells were induced with 5μM $CdCl_2$ (diluted in 10%FCS/DMEM/GLUT or 1%BSA/DMEM/GLUT) for 8 hr, at which time the appropriate media lacking $CdCl_2$ was added and incubated for 48 hr. Cells were fixed with 1% (v/v) paraformaldehyde (Sigma) in PBS for 20 min at room temperature and permeabilised with 0.1% (v/v) Triton X-100 (Sigma) in PBS for 5 min. Endogenous fluorescence was quenched with 1.5 mg/ml glycine (Sigma) in PBS for 10 min and cells were washed twice with PBS, then stained with 0.1 μg/μL DAPI in methanol for 10 min at room temperature in the dark. Cells were washed twice with methanol for 10 min and mounted with Vectashield (Australian Lab Services, Homebush, NSW, Australia) to prevent loss of fluorescence.

5.4.9 OLF442 Immunocytochemistry

Cells plated and induced as outlined above were processed for immunofluorescence microscopy 48 hr post-serum depletion. Briefly, cells were washed three times with ice-cold PBS, fixed in 4% (v/v) paraformaldehyde in PBS at room temperature for 30 min, permeabilised with 0.2% (v/v) Triton X-100 in PBS for 10 min, and incubated in blocking solution (1% [w/v] BSA, 0.3% [v/v] Triton X-100 in PBS) for 1 hr at room temperature. FLAG-MST1 and mutant recombinant proteins were visualised with anti-FLAG M2 mouse monoclonal antibody (1:250 - Sigma). Primary antibodies were diluted in blocking solution and incubated overnight at 4°C with permeabilised cells. Cells were then washed three times for 10 min at room temperature with blocking solution, followed by incubation with the appropriate secondary antibody,

Alexa 488 goat anti-mouse (1: 500 - Molecular Probes, Eugene, Oregon, USA). Finally, cells were rinsed three times with PBS for 10 min each and mounted with coverslips and Vectashield fluorescent mounting media. Fluorescent images were recorded using a BioRad Radiance 2000 confocal microscope using LaserSharp 2000 imaging software.

5.5 Results

5.5.1 Expression Of Recombinant MST1 Constructs

The MST1 structure is schematically shown in Figure 5-3, along with the kinase dead mutant (MST1K59RFLAG), the caspase-3 insensitive mutant (MST1D326NFLAG), and the double mutant (MST1K59RD326NFLAG). All mammalian expression plasmids encoding the various mutant constructs contained the correct mutant conversions and were all in frame with the upstream FLAG tag.

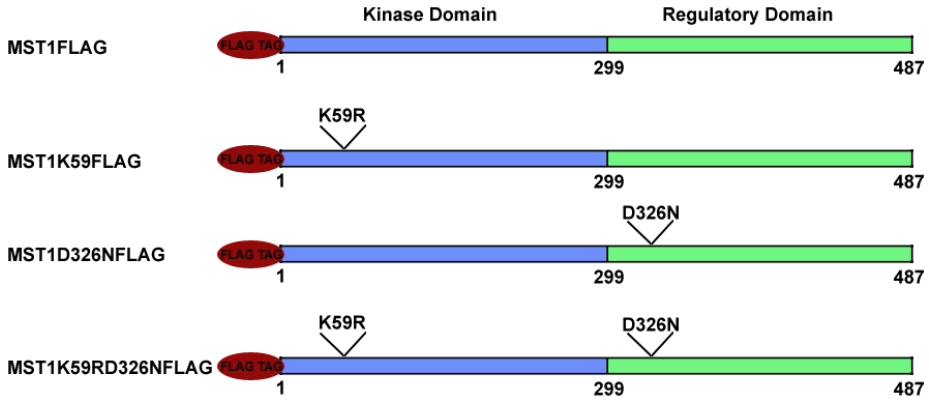

Figure 5-3 Schematic representation of MST1 constructs used for mammalian expression studies.

5.5.2 Exogenous MST1 Expression Does Not Induce Apoptosis

Stable cell lines of OLF442 were generated with an inducible mammalian expression plasmid encoding various mutant MST1 constructs. The very low transfection efficiency of OLF442 was the reason for generating stable cell lines as opposed to performing transient transfections. Behrens et al. (2000) noted a transfection efficiency of less than 5% with either calcium phosphate coprecipitation or lipofectamine mediated transient transfection of OLF442. The low transfection efficiency experienced with this cell line prompted the scale up in the transfection procedure. For that reason transfection of OLF442 was routinely done in 80% confluent 25cm^2 flasks, from which only 1-3 colonies were observed to survive

antibiotic selection with hygromycin B. The amplification of antibiotic resistant colonies generally occurred over a two-week period in reduced hygromycin B concentrations. Stable cell lines were then treated with $CdCl_2$ to induce recombinant protein expression and subsequently serum deprived to induce differentiation. Induction was done prior to serum deprivation, as concomitant treatment often resulted in cell death. Untreated control OLF442 cultures containing vector alone (pMEP4FLAG) exhibited signs of toxicity when exposed to $CdCl_2$ concentrations above 5 µM and for treatment periods greater than 8 hr. Stable OLF442 cultures were stained with the fluorescent dye DAPI, to view the nuclei of induced versus uninduced cells differentiated by serum deprivation. Fluorescent well-formed nuclei were readily observed and indicated that cells attached to the culture vessel surface did not show signs of apoptosis (Figure 5-4).

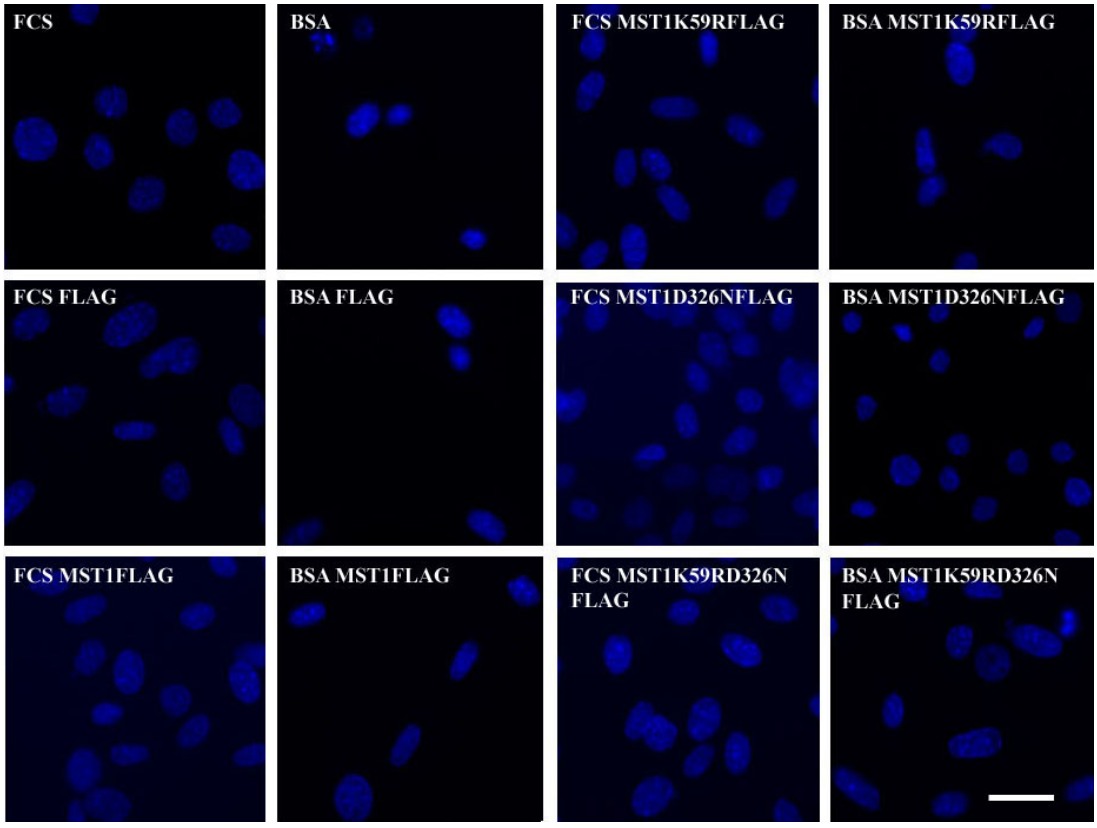

Figure 5-4 DAPI stained nuclei of stable OLF442 cell lines expressing exogenous recombinant MST1 constructs.

Well-formed fluorescent nuclei were readily observed in cells that remained attached to the surface of the culture vessel indicating the absence of apoptosis in these cells. Scale bar = 20 µm

5.5.3 Localisation Of Exogenous MST1 During OLF442 Differentiation

Overexpression of recombinant FLAG tagged MST1 constructs in stable OLF442 cell lines induced with $CdCl_2$ and detected with anti-FLAG M2 mouse monoclonal antibody revealed several interesting features. Preliminary immuno-cytochemical results show that expression of the FLAG tag alone does not affect the morphology of either undifferentiated (FCS) or differentiated (BSA) OLF442 cultures. Flag tag is diffusely localised throughout the cells and no significant morphological changes are observed in these cultures (Figure 5-5, FCS FLAG and BSA FLAG) as compared to untransfected uninduced OLF442 cells (Figure 1-7). However, recombinant MST1FLAG clearly associates with cytoplasmic structures, as the localisation of MST1FLAG appears organised and could reflect association with the cytoskeleton in serum complete (FCS) cultures, which also appear to contain much longer processes (Figure 5-5, FCS MST1FLAG) than wildtype OLF442 cells. In contrast, MST1FLAG assumes a peripheral localisation in differentiated OLF442 cells grown in serum deplete (BSA) medium. These cultures exhibit a morphology that is characteristic of wildtype differentiated OLF442, containing mostly bipolar cells with very long processes (Figure 5-5, BSA MST1FLAG).

Undifferentiated (FCS) OLF442 cells expressing the kinase dead mutant (MST1K59RFLAG) did not acquire long processes, instead these cells had a morphology reminiscent of untransfected uninduced cultures, even though the localisation of MST1 with some cytoplasmic structures was maintained (Figure 5-5, FCS MST1K59RFLAG), indicating that the kinase activity of MST1 is important for process formation. On the other hand, kinase dead MST1K59RFLAG mutant overexpression did not affect differentiated (BSA) OLF442 cultures. These cultures contained bipolar cells with long processes and the exogenous protein remained localised to the cell periphery (Figure 5-5, BSA MST1K59RFLAG). Overexpression of the caspase-3 insensitive mutant (MST1D326NFLAG) in undifferentiated (FCS) cultures resulted in a morphology that paralleled that seen with the induction of MST1FLAG, that is, the generation of long processes. However, localisation of the recombinant protein to the ordered cytoplsmic structures was less obvious, instead protein was mostly present at the cell periphery (Figure 5-5, FCS

MST1D326NFLAG). In the differentiated (BSA) cultures the MST1D326NFLAG caspase-3 insensitive mutant did not result in any significant differences in cell morphology (Figure 5-5, BSA MST1D326NFLAG) as compared with the induction of MST1FLAG. Although the staining appeared more cytoplasmic and localisation to the cell periphery was less obvious. Furthermore, the cytoplasmic structures that MST1FLAG appears to associate with in OLF442 where not characterised in this study, however double staining with members of the cytoskeleton could confirm whether or not these structures are actin stress fibres.

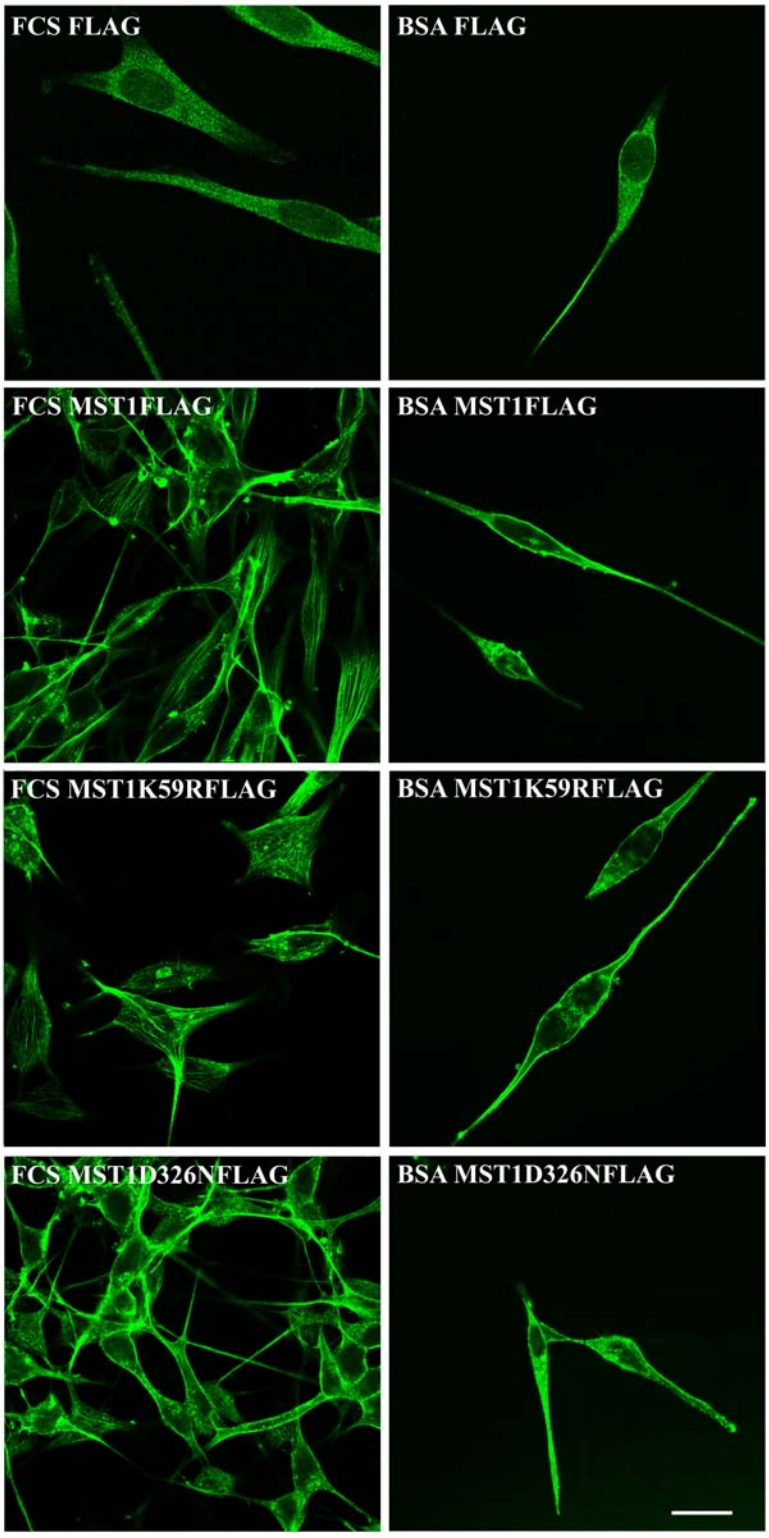

Figure 5-5 Stable OLF442 cell lines induced with cadmium chloride express exogenous recombinant FLAG tagged MST1 constructs.

FLAG tagged MST1 and mutant constructs were highly expressed in OLF442 cultures induced with cadmium chloride, as observed by immunocytochemistry with anti-FLAG M2 mouse monoclonal antibody, n=2. Scale bar = 20 μm

5.6 Discussion

A role for MST kinase in neuronal differentiation has not previously been demonstrated, however non-apoptotic MST activities have been described elsewhere. These include the phosphorylation of the transcription factor Nkx 2.1 by MST2 (Aurisicchio et al., 1998), and the induction of lineage-specific cellular programming of megakaryocytes to produce platelets by MST1 (Sun and Ravid, 1999). Further, apoptosis does not appear to be an active process following MST1 overexpression of differentiating OLF442 neuronal cultures as demonstrated by DAPI staining. Thus it is likely that this kinase participates in the morphological signalling process that accompanies neuronal differentiation.

Preliminary experiments show that overexpression of recombinant MST1FLAG in OLF442 cultures maintained in serum complete medium (FCS) induced the formation of long processes, not characteristic of wildtype OLF442. The recombinant protein was observed with the monoclonal anti-FLAG antibody to localise with ordered cytoplasmic structures. In contrast, the kinase dead mutant (MST1K59RFLAG) did not acquire long processes and the morphology of these cells was similar to that of untransfected uninduced cultures. The persistence of MST1K59RFLAG localisation with cytoplasmic structures may indicate that the kinase activity of MST1 is centrally involved in process formation. However, the overexpression of the caspase-3 insensitive mutant (MST1D326NFLAG) resulted in a morphology that paralleled that seen with the induction of MST1FLAG, including the generation of long processes in undifferentiated (FCS) cultures. The localisation of the recombinant protein to ordered structures within the cytoplasm was less obvious in these cultures; the protein was mostly present at the cell periphery with some puncta visible in the cytoplasm. Possibly the caspase-3 cleavage site is important in regulating the localisation of MST1. Cleavage by caspase-3 would yield the tagged amino-terminal kinase domain [MST1(1-326)FLAG] that may preferentially associate with cytoskeletal structures, whilst full-length MST1FLAG may associate with structures at the cell periphery. The absence of the two nuclear export signals from the tagged amino-terminal kinase domain may result in localisation to the nucleus as shown by an amino-terminal MST1(1-330) truncation mutant (Ura et al., 2001b). Yet, most of the fluorescence in this study was cytoplasmic with no evidence for

nuclear localisation of MST1. Regulation of MST localisation has been reported elsewhere (Lee et al., 1998a), and appears to rely on the removal of the carboxyl-terminal domain as noted here. In addition, comparison of MST1FLAG overexpression in OLF442 cultures maintained in serum complete medium (FCS) and serum deplete medium (BSA) suggests that MST1 may put in motion the necessary cascade of events that drives differentiation, particularly as the morphology of these cells begins to resemble that of differentiated OLF442.

The differentiated serum deprived OLF442 cultures proved to be less informative with regards to identifying key cellular processes affected by exogenous MST1 and mutant MST1 overexpression. This may in part be due to the masking effects of serum deprivation, particularly since this treatment likely activates parallel processes required for OLF442 differentiation. Nevertheless, overexpression of the various MST1 constructs in OLF442 cultures subsequently induced to differentiate by serum deprivation did not produce any significant changes in either cell morphology or protein localisation. Expressed MST1 recombinant proteins were localised to the outer cell membrane of differentiated OLF442 cells, which contained very long bipolar processes. Furthermore, the survival of these cells further strengthens the non-apoptotic role of MST1 in neuronal cells.

The regulation of MST kinase is likely to be intricate given that both MST1 and MST2 can be cleaved by caspase-3 at the DELDS cleavage site producing a 36 kDa protein that has greater kinase activity than the full-length transcript (Graves et al., 2001). In addition, the suggestion that MST1 is active in quiescent cells but inactivated in proliferating cells is consistent with the fact that EGF treatment of NIH3T3 cells inhibits MST activity (Creasy and Chernoff, 1995b). A cytostatic role has also been suggested for the Ste20 homologous proteins PAK-2, and HPK1, which are also caspase targets (Walter et al., 1998; Liou et al., 2000). MST may possibly transduce a different signal depending on its mechanism of activation. "According to this model MST1 activated phosphorylation/dephosphorylation in response to non-apoptotic stimuli would regulate a specific cellular process. However, in response to apoptotic stimuli involving both cleavage and phosphorylation, MST1 would contribute to the induction or progression of apoptosis" (Graves et al., 2001).

Limitations of the experimental protocol employed in this study primarily arise from the use of $CdCl_2$ to induce MST expression in OLF442 cultures. Cadmium is a toxic metal that can damage numerous cellular processes and result in both necrotic and apoptotic cell death (Lopez et al., 2003). A study of rat cortical neurons showed uptake of $CdCl_2$ in a dose and serum dependent manner, with concentrations from 1 μM or 10 μM (depending on the absence or the presence of serum) up to 100 μM resulting in a decrease of cellular metabolic activity (Lopez et al., 2003). Furthermore, cadmium-induced apoptosis is accompanied by caspase-3 activation in serum-free medium. Whilst apoptosis was not observed in this study variations in cell growth were observed between culture conditions making results difficult to interpret. Ideally an inducible expression vector utilising a non-toxic molecule to mediate protein expression would alleviate some of the irregularities observed between cultures and experiments in this study. Additionally, a study by Graves et al. (1998) revealed that the protein expression levels of myc-tagged wildtype MST1 and the truncated MST1(1-330) mutant declined rapidly with time from 6 hr after transfection and was barely detectable by 48hr post transfection. In contrast expression levels of the kinase dead MST1 mutant were relatively stable and no evidence of cleavage was observed (Graves et al., 1998). In this study immunocytochemistry was done 48 hr post induction of expression and although immunofluorescence was detected it may have been wise to observe cells at earlier time points. For this reason only preliminary data is shown and caution is used when interpreting observations from this work.

5.7 Conclusion

Stable transfection of OLF442 cultures with MST1 constructs were induced successfully to express exogenous recombinant proteins with $CdCl_2$. Although some differences between cultures were observed, this may have been due to the effects of $CdCl_2$ particularly since untransfected cultures exposed to $CdCl_2$ also showed similar variations (eg. reduced cell growth). However, undifferentiated serum complete (FCS) cultures did provide some insight into the effects of MST1 recombinant protein overexpression. Key findings include; 1) localisation to cytoplasmic structures is dependent upon an active caspase-3 cleavage site and, 2) kinase activity at lysine residue 59 is required for long process formation of OLF442 cells grown in serum complete medium. Although these findings are preliminary, MST1 appears to play a role in the morphological processes involved in differentiation and does not seem to induce apoptosis in OLF442 cultures.

6 GENERAL DISCUSSION

6.1 Neuronal Differentiation: A Study Into Differential Gene Expression Of Olfactory Receptor Neurons

The seminal work of Ramón y Cajal at the turn of the century provided a platform upon which modern neuroscientists could further the understanding of neurons and establish a cellular framework of neuronal differentiation. Although the neuronal doctrine which states that, each nerve fiber is the outgrowth of a single nerve cell and not the product of the fusion of many cells remains largely unchanged, one important objection came from Altman and Das (1965). Together they challenged the belief that neurons were irreplaceable and coined the term neurogenesis, following their observations of rodents treated with [^{3}H] thymidine to label dividing cells (Altman and Das, 1965). Since then numerous molecular processes have been detailed and are described by the term neuronal differentiation, which is controlled by endogenous and exogenous factors encompassing a complex array of signals emanating from the extracellular matrix and intracellular relay centres that regulate maturation, survival and apoptosis.

This thesis proposed to identify genes involved in neuronal differentiation by utilising a clonal olfactory receptor neuronal cell line (OLF442). Gene expression levels were identified using differential display and oligonucleotide array technology before and after serum deprivation. In the discourse to follow, particular emphasis is placed on intracellular signal transduction cascades, which communicate information from the external environment to the cell interior and which are ultimately responsible for transducing the external initiating signals to direct the morphological differentiation observed in neuronal cells.

Differential display revealed two kinases whose expression levels were elevated during the differentiation of OLF442, identified as FAK related non-kinase (FRNK) and mammalian ste20 like (MST)2 kinase. Analysis of the oligonucleotide array data confirmed the elevated expression of two of the fragments identified by differential display, ribosomal protein L3 and Fas binding protein Daxx. In Chapter 2 the microarray data is discussed in detail. Briefly, genes involved in altering presentation of extracellular matrix molecules, in mediating cytoskeletal re-arrangements, in

ceasing the cell cycle and in promoting an adequate nuclear response were all identified. Taken together this information corroborated the selection of OLF442 as a model for studying differentiation and provided the motivation to understand the cellular context of OLF442 and to determine the phosphorylation status of the mitogen-activated protein kinase (MAPK) signalling cascades.

6.2 MAPK Signalling

The MAPK superfamily utilises a conserved three-kinase cascade to amplify and deliver signals that originate at the cellular membrane by the use of multiple messengers whose activity is regulated by reversible phosphorylation and in some instances by irreversible proteolysis. The most intensely studied transduction cascades are composed of five evolutionarily conserved subfamilies (Weber, 1999), the ERK1/2 cascade, which preferentially regulates cell growth and differentiation (Pearson et al., 2001), the c-Jun N-terminal kinase (JNK/SAPK – stress activated protein kinase), and p38 MAPK cascades, that primarily function in response to environmental stress and inflammatory cytokines (Kyriakis and Avruch, 2001). Of these subfamilies only two appeared to be involved during the differentiation of OLF442, the mitogenic ERK1/2 and stress responsive SAPK/JNK signal transduction cascades (Figure 4-1).

Neuronal differentiation studies have previously reported the necessity of ERK phosphorylation for neuronal differentiation (Cowley et al., 1994; Seger and Krebs, 1995; Leppa et al., 1998; Tibbles and Woodgett, 1999). In agreement with these studies, differentiation of OLF442 induced high level phosphorylation of ERK1/2 compared to undifferentiated OLF442 (Figure 4-1), without changing the total content of phosphorylated and unphosphorylated ERK. Furthermore, the high level phosphorylation of ERK1/2 was resistant to inhibition of MEK1/2 with the specific inhibitor PD98059 indicating that MEK1/2 is not involved in phosphorylation of ERK1/2. Interestingly, there was a switch between preferential phosphorylation of MEK1 in undifferentiated OLF442 to preferential phosphorylation of MEK2 following differentiation. This switch between activated MEK1 and activated MEK2 reflects previous observations that MEK isoforms can be differentially regulated in

different cell lines by common ERK regulators (Xu et al., 1997), and indicates that a unique signal is involved in OLF442 differentiation. The present study also detected some high molecular weight proteins of unknown identity with the phosphorylated MEK1/2 and ERK1/2 antibodies. Furthermore, the identity of the MEK2 immunoreactive band identified in this study may be questioned, particularly as inhibition of MEK1/2 was unable to inhibit ERK1/2 activation during OLF442 differentiation. Hence, it is possible that the immunoreactive band identified is very closely related to MEK2 and could represent a splice variant. Isoforms of all components of the MAPK signalling module have been described and likely provide cells an increased repertoire of signalling molecules with which to respond to specific cues in different cell types (Yung et al., 2000; Yung et al., 2001). Detection of putative MAPK component isoforms was a recurring event in OLF442 as further detailed below.

The expression of c-Raf, an upstream regulator of MEK was also analysed and not found to be significantly phosphorylated by differentiation. However, as occured with the phospho-MEK and ERK antibodies, an unknown protein of a higher molecular weight, perhaps a c-Raf isoform, was induced by differentiation (Figure 4-1). Approximately 110 kDa in size, the Raf isoform identified in this study is consistent with the restricted expression of one of the larger B-Raf isoforms (99 kDa) whose expression occurs solely in the brain and spinal cord (Barnier et al., 1995). Whether the 110 kDa isoform is specific to olfactory neurons or OLF442 remains to be tested. Importantly, B-Raf represents the main MEK activator in bovine brain (Yamamori et al., 1995) and differentiated PC12 cells (Traverse and Cohen, 1994), and could be responsible for the preferential phosphorylation of MEK2 in OLF442. Hagemann and Rapp (1999) found that initially Raf activation required the small G protein Ras, but that sustained activation of B-Raf, necessary for PC12 neuronal differentiation, was dependent on another small G protein, Rap1. The following mechanism of activation is required for PC12 differentiation: cAMP phosphorylation of Rap1 displaces Ras binding to c-Raf, blocking its activation, and resulting in the sustained activation of B-Raf (Hagemann and Rapp, 1999). Thus, a switch from c-Raf to B-Raf signalling may also be responsible for the switch in MEK and ERK phosphorylation resulting in c-Jun activation as observed in OLF442 differentiation, complementing the transition from proliferation to differentiation which remains to be

tested (Figure 6-1).

The transcription factor c-Jun, which is downstream of MAPK and a common substrate of both the ERK and SAPK/JNK signalling modules has been implicated in neuronal differentiation and survival. For example, when PC12 cells are exposed to NGF, the ERK cascade is activated and c-Jun is phosphorylated (Leppa et al., 1998). In contrast, constitutively active c-Jun can induce differentiation independent of upstream signals, whereas c-Jun activation via the SAPK/JNK pathway results in apoptosis in differentiated neurons (Leppa et al., 1998). The ability of c-Jun to induce survival in undifferentiated PC12 cells has yet to be described but my observations in OLF442 are instructive. A novel MAPK module may be phosphorylated leading to activation of ERK1/2 by MEK2 (or a MEK2 splice variant), utilising B-Raf activation as observed in OLF442.

Neuronal differentiation results from a synchronisation of multiple transduction cascades and cellular responses as evidenced by the microarray data. A protein that can synchronise signalling to several pathways and which participates in the morphogenetic processes that occur during development is the non-receptor protein tyrosine kinase, FAK. Therefore the finding of the endogenous FAK inhibitor FRNK by differential display was intriguing particularly as there was no difference in the protein or mRNA expression level of FAK induced by differentiation. In contrast to FAK, both the protein and mRNA expression level of FRNK was induced by differentiation. This induced FRNK expression was derived autonomously because it was not responsive to the caspase-3 inhibitor, DEVD-CHO. This is particularly pertinent since the primary role of FRNK is to act as an inhibitor of FAK by competing with its substrates and reducing the phosphorylation of both FAK and other proteins bound in the focal adhesion complex. Activation and association of the adaptor protein Shc with Grb2 mediates integrin and growth factor signalling to ERK in response to matrix adhesion or growth factor stimulation (Wary et al., 1998). This process requires FAK participation in cells expressing B-Raf (Barberis et al., 2000), as Shc mediates early integrin-dependent ERK activation, whilst FAK, $p130^{CAS}$ (Crk-associated substrate), Crk, and Rap1 signalling mediates the late phase of ERK activation (Schlaepfer et al., 1998; Barberis et al., 2000). In PC12 cells FAK participates in the transmission of signals emanating from GTK overexpression

resulting in increased process formation (Anneren et al., 2000), which is inhibited by inhibitors of the Rap1 pathway (Anneren et al., 2000). Moreover, treatment of differentiated OLF442 cultures with PD98059 resulted in a marked decrease in the protein expression level of both FAK and FRNK. Consequently MEK1/2 activation is important for high-level expression of FAK and FRNK during differentiation. Whether the inhibition of MEK1/2 limited neurite extension in OLF442 is unknown, as this was not quantitated, however it is apparent that, in contrast to PC12 cells, FAK and FRNK expression is dependent on MEK1/2 signalling. This may occur by a cascade that functions independently of ERK1/2 activation but which requires an input signal from MEK1/2, as PD98059 treatment of OLF442 differentiation cultures still resulted in high-level phosphorylation of ERK1/2. The elevated expression of FRNK may displace FAK and its binding partners disrupting signalling to downstream effectors, regulating or terminating the MAPK signals that initiated neuronal differentiation and neurite extension (Figure 6-1). Investigation of the timing of FRNK expression during differentiation would help determine the necessity of deactivation of the sustained ERK signal that appears important for neuronal differentiation, particularly as c-Jun activation is important in regulating apoptosis in serum deprived and differentiated cells.

6.3 MST Kinase

The differential display also revealed the upregulation of another kinase following neuronal differentiation that had 90% homology with rat MST2 kinase within the 3′ UTR. Because there was no mouse MST2 sequence in the database I decided to obtain the full-length sequence of MST2 kinase mRNA (submitted to Genbank, accession number AY058922) and that of the closely related family member, MST1 kinase which was also cloned and sequenced. Moreover, evidence to support an autonomously expressed carboxyl-terminal domain of MST2 kinase is presented in Chapter 3 and provides a unique way in which MST2 may regulate its own activity. The cloning and sequence analysis of MST1/2 allowed further analysis of the role of MST in neuronal differentiation. To date MST has predominantly been implicated in apoptosis, with limited reports citing a role in the activation of TTF-1 (Aurisicchio et al., 1998), megakaryocyte differentiation (Sun and Ravid, 1999) and

induction of quiescence (Wang and Fecteau, 2000).

MST1/2 are serine/threonine protein kinases, which are not activated by commonly used mitogenic stimuli, but are activated by a subset of stress conditions and apoptotic agents. They can be regulated by phosphorylation and proteolysis, but the MAPK pathways in which MST1/2 functions remains to be elucidated. The Ste20/PAK family of protein kinases to which MST belongs are necessary for morphological signalling (Daniels and Bokoch, 1999). The principle function of Ste20 is to regulate cell polarity during growth and in response to numerous extracellular signals by re-arranging the actin cytoskeleton which is crucial for various cellular processes including cell cycle transition. To further understand the role of MST in neuronal differentiation, a series of stable OLF442 transfections (with mutant and wild-type MST contructs) were carried out. MST appeared to localise with an ordered cytoplasmic structure reminiscent of actin stress fibres, indicating a potential cytoskeletal role during neuronal differentiation. The inability of the caspase cleavage site mutant to localise to these structures indicates that cleavage at this site is important for this localisation. Furthermore, lysine residue 59 is important for MST kinase activity and for the formation of long processes in cultures grown in serum complete medium. These findings are preliminary, but indicate that MST1 may play a role in the morphological processes involved in neuronal differentiation, and although there was no evidence for inducing apoptosis in OLF442 cultures, MST may be at the crossroads of integrating differentiation and apoptosis. Particularly, since stress pathways have been shown to mediate effects in diverse biological processes including apoptosis, development and adaptation to environmental changes. Thus MST may be involved in signalling through the SAPK module whose concomitant activation alongside that of ERK results in neuronal differentiation, but whose activation in the differentiated mature neuron results in apoptosis (Leppa et al., 1998).

In conclusion, the cellular context of differentiating OLF442 cultures has been mapped and a novel MAPK module has been proposed. This consists of FAK signalling through Rap1 to ERK providing sustained activation, which is buffered or terminated by the expression of the endogenous FAK inhibitor FRNK. Furthermore, MST kinase may play a role in regulating the cytoskeletal re-arrangements that are

necessary for neuronal differentiation and neurite extension to occur. MST kinase may signal transiently via the SAPK pathway to provide concomitant activation of c-Jun which is required for neuronal differentiation, in contrast to signalling via SAPK in post-differentiated neurons which results in apoptosis (Figure 6-1).

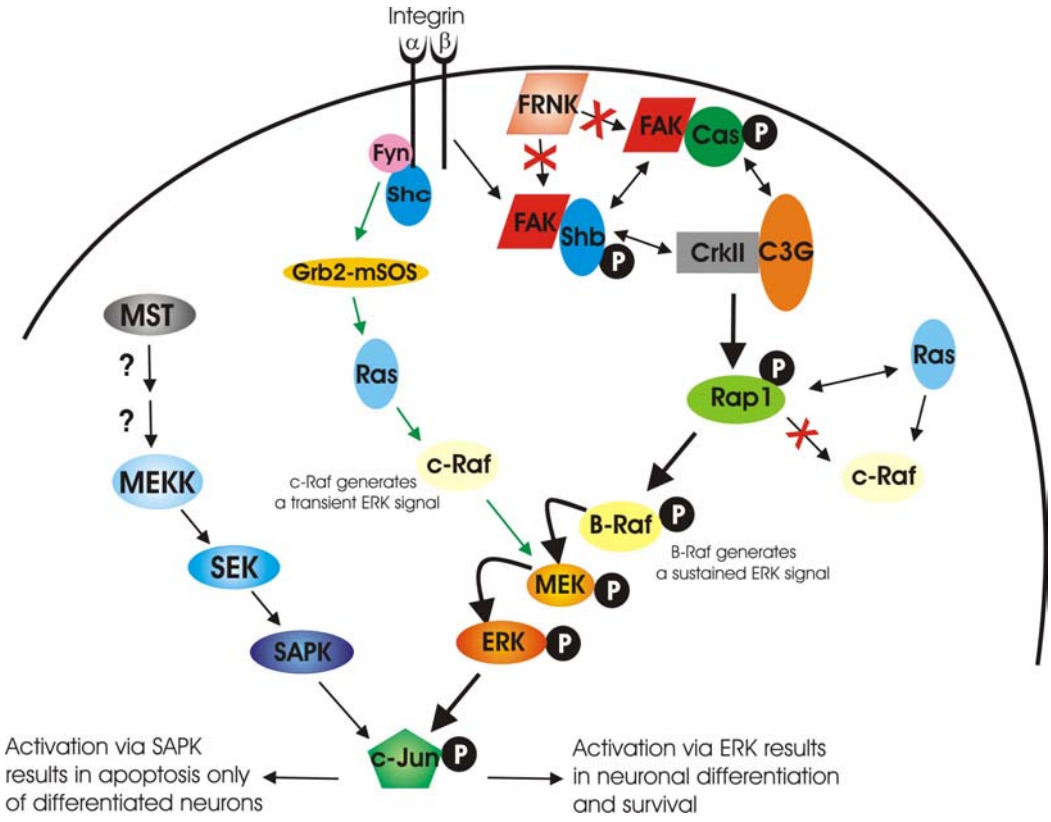

Figure 6-1 A model of the MAPK components that may be required for neuronal differentiation.

A summary of the MAPK signal transduction pathways that may be active during neuronal differentiation. Featured cascades include ERK and SAPK.

REFERENCES

Abe MK, Kahle KT, Saelzler MP, Orth K, Dixon JE, Rosner MR (2001) ERK7 is an autoactivated member of the MAPK family. J Biol Chem 276:21272-21279.

Abe MK, Saelzler MP, Espinosa R, 3rd, Kahle KT, Hershenson MB, Le Beau MM, Rosner MR (2002) ERK8, a new member of the mitogen-activated protein kinase family. J Biol Chem 277:16733-16743.

Ackley BD, Crew JR, Elamaa H, Pihlajaniemi T, Kuo CJ, Kramer JM (2001) The NC1/endostatin domain of Caenorhabditis elegans type XVIII collagen affects cell migration and axon guidance. J Cell Biol 152:1219-1232.

Affymetrix In: http://www.affymetrix.com.

Allen WK, Akeson R (1985) Identification of an olfactory receptor neuron subclass: cellular and molecular analysis during development. Dev Biol 109:393-401.

Alnemri ES, Livingston DJ, Nicholson DW, Salvesen G, Thornberry NA, Wong WW, Yuan J (1996) Human ICE/CED-3 protease nomenclature. Cell 87:171.

Alon U, Barkai N, Notterman DA, Gish K, Ybarra S, Mack D, Levine AJ (1999) Broad patterns of gene expression revealed by clustering analysis of tumor and normal colon tissues probed by oligonucleotide arrays. Proc Natl Acad Sci U S A 96:6745-6750.

Altman J (1992) Programmed cell death: the paths to suicide. Trends Neurosci 15:278-280.

Altman J, Das GD (1965) Autoradiographic and histological evidence of postnatal hippocampal neurogenesis in rats. J Comp Neurol 124:319-335.

Altschul SF, Madden TL, Schaffer AA, Zhang J, Zhang Z, Miller W, Lipman DJ (1997) Gapped BLAST and PSI-BLAST: a new generation of protein database search programs. Nucleic Acids Res 25:3389-3402.

Anchan RM, Drake DP, Haines CF, Gerwe EA, LaMantia AS (1997) Disruption of local retinoid-mediated gene expression accompanies abnormal development in the mammalian olfactory pathway. J Comp Neurol 379:171-184.

Andersen SS (2000) Spindle assembly and the art of regulating microtubule dynamics by MAPs and Stathmin/Op18. Trends Cell Biol 10:261-267.

Andre E, Becker-Andre M (1993) Expression of an N-terminally truncated form of human focal adhesion kinase in brain. Biochem Biophys Res Commun 190:140-147.

Anneren C, Reedquist KA, Bos JL, Welsh M (2000) GTK, a Src-related tyrosine kinase, induces nerve growth factor-independent neurite outgrowth in PC12 cells through activation of the Rap1 pathway. Relationship to Shb tyrosine phosphorylation and elevated levels of focal adhesion kinase. J Biol Chem 275:29153-29161.

Arellano M, Moreno S (1997) Regulation of CDK/cyclin complexes during the cell cycle. Int J Biochem Cell Biol 29:559-573.

Arezi B, Kuchta RD (2000) Eukaryotic DNA primase. Trends Biochem Sci 25:572-576.

Asai DJ, Koonce MP (2001) The dynein heavy chain: structure, mechanics and evolution. Trends Cell Biol 11:196-202.

Aurisicchio L, Di Lauro R, Zannini M (1998) Identification of the thyroid transcription factor-1 as a target for rat MST2 kinase. J Biol Chem 273:1477-1482.

Bang OS, Park EK, Yang SI, Lee SR, Franke TF, Kang SS (2001) Overexpression of Akt inhibits

NGF-induced growth arrest and neuronal differentiation of PC12 cells. J Cell Sci 114:81-88.

Barber RD, Jaworsky DE, Yau KW, Ronnett GV (2000) Isolation and in vitro differentiation of conditionally immortalized murine olfactory receptor neurons. J Neurosci 20:3695-3704.

Barberis L, Wary KK, Fiucci G, Liu F, Hirsch E, Brancaccio M, Altruda F, Tarone G, Giancotti FG (2000) Distinct roles of the adaptor protein Shc and focal adhesion kinase in integrin signaling to ERK. J Biol Chem 275:36532-36540.

Bardwell AJ, Abdollahi M, Bardwell L (2003) Docking sites on MEKs, MAP kinase phosphatases, and the Elk-1 transcription factor compete for binding to ERK2 and are crucial for enzymatic activity. Biochem J 370:1077-85.

Barnier JV, Papin C, Eychene A, Lecoq O, Calothy G (1995) The mouse B-raf gene encodes multiple protein isoforms with tissue-specific expression. J Biol Chem 270:23381-23389.

Bartlett PF, Reid HH, Bailey KA, Bernard O (1988) Immortalization of mouse neural precursor cells by the c-myc oncogene [published erratum appears in Proc Natl Acad Sci U S A 1989 Feb;86(3):1103]. Proc Natl Acad Sci U S A 85:3255-3259.

Barzilai A, Zilkha-Falb R, Daily D, Stern N, Offen D, Ziv I, Melamed E, Shirvan A (2000) The molecular mechanism of dopamine-induced apoptosis: identification and characterization of genes that mediate dopamine toxicity. J Neural Transm Suppl:59-76.

Behrens M, Venkatraman G, Gronostajski RM, Reed RR, Margolis FL (2000) NFI in the development of the olfactory neuroepithelium and the regulation of olfactory marker protein gene expression. Eur J Neurosci 12:1372-1384.

Bingle CD (1997) Thyroid transcription factor-1. Int J Biochem Cell Biol 29:1471-1473.

Blagosklonny MV (1999) A node between proliferation, apoptosis, and growth arrest. Bioessays 21:704-709.

Blanchard JM (2000) Small GTPases, adhesion, cell cycle control and proliferation. Pathol Biol (Paris) 48:318-327.

Boudreau NJ, Jones PL (1999) Extracellular matrix and integrin signalling: the shape of things to come. Biochem J 339:481-488.

Bovolenta P, Fernaud-Espinosa I (2000) Nervous system proteoglycans as modulators of neurite outgrowth. Prog Neurobiol 61:113-132.

Bradford MM (1976) A rapid and sensitive method for the quantitation of microgram quantities of protein utilizing the principle of protein-dye binding. Anal Biochem 72:248-254.

Brady G, Iscove NN (1993) Construction of cDNA libraries from single cells. Methods Enzymol 225:611-623.

Bruce-Staskal PJ, Bouton AH (2001) PKC-dependent activation of FAK and src induces tyrosine phosphorylation of Cas and formation of Cas-Crk complexes. Exp Cell Res 264:296-306.

Burgaya F, Girault JA (1996) Cloning of focal adhesion kinase, pp125FAK, from rat brain reveals multiple transcripts with different patterns of expression. Brain Res Mol Brain Res 37:63-73.

Bushweller JH (2000) CBF--a biophysical perspective. Semin Cell Dev Biol 11:377-382.

Bybee A, Thomas NS (1991) Cell cycle regulation. Blood Rev 5:177-192.

Byers RJ, Hoyland JA, Dixon J, Freemont AJ (2000) Subtractive hybridization - genetic takeaways and

the search for meaning. Int J Exp Pathol 81:391-404.

Carr VM, Farbman AI (1992) Ablation of the olfactory bulb up-regulates the rate of neurogenesis and induces precocious cell death in olfactory epithelium. Exp Neurol 115:55-59.

Carulli JP, Artinger M, Swain PM, Root CD, Chee L, Tulig C, Guerin J, Osborne M, Stein G, Lian J, Lomedico PT (1998) High throughput analysis of differential gene expression. J Cell Biochem Suppl 30-31:286-296.

Chen LM, Bailey D, Fernandez-Valle C (2000) Association of beta 1 integrin with focal adhesion kinase and paxillin in differentiating Schwann cells. J Neurosci 20:3776-3784.

Chomczynski P, . and Sacchi, N. (1987) Single-Step Method of RNA Isolation by Acid Guanidinium Thiocyanate-Phenol-Chloroform Extraction. Anal Biochem 162:156-159.

Clontech SMART™ PCR cDNA Library Construction Kit User Manual (PT3000-1). In, p 41. California: Clontech.

Cobb MH, Goldsmith EJ (2000) Dimerization in MAP-kinase signaling. Trends Biochem Sci 25:7-9.

Cook SJ, Balmanno K, Garner A, Millar T, Taverner C, Todd D (2000) Regulation of cell cycle re-entry by growth, survival and stress signalling pathways. Biochem Soc Trans 28:233-240.

Coppolino M, Leung-Hagesteijn C, Dedhar S, Wilkins J (1995) Inducible interaction of integrin alpha 2 beta 1 with calreticulin. Dependence on the activation state of the integrin. J Biol Chem 270:23132-23138.

Cowan WM, Fawcett JW, O'Leary DD, Stanfield BB (1984) Regressive events in neurogenesis. Science 225:1258-1265.

Cowley S, Paterson H, Kemp P, Marshall CJ (1994) Activation of MAP kinase kinase is necessary and sufficient for PC12 differentiation and for transformation of NIH 3T3 cells. Cell 77:841-852.

Creasy CL, Chernoff J (1995a) Cloning and characterization of a member of the MST subfamily of Ste20-like kinases. Gene 167:303-306.

Creasy CL, Chernoff J (1995b) Cloning and characterization of a human protein kinase with homology to Ste20. J Biol Chem 270:21695-21700.

Creasy CL, Ambrose DM, Chernoff J (1996) The Ste20-like protein kinase, Mst1, dimerizes and contains an inhibitory domain. J Biol Chem 271:21049-21053.

Crews L, Hunter D (1994) Neurogenesis in the olfactory epithelium. Perspect Dev Neurobiol 2:151-161.

Daniels RH, Bokoch GM (1999) p21-activated protein kinase: a crucial component of morphological signaling? Trends Biochem Sci 24:350-355.

Datta K, Franke TF, Chan TO, Makris A, Yang SI, Kaplan DR, Morrison DK, Golemis EA, Tsichlis PN (1995) AH/PH domain-mediated interaction between Akt molecules and its potential role in Akt regulation. Mol Cell Biol 15:2304-2310.

De Dominicis A, Lotti F, Pierandrei-Amaldi P, Cardinali B (2000) cDNA cloning and developmental expression of cellular nucleic acid-binding protein (CNBP) gene in Xenopus laevis. Gene 241:35-43.

Deyholos MK, Galbraith DW (2001) High-density microarrays for gene expression analysis. Cytometry 43:229-238.

Dimitropoulou A, Bixby JL (2000) Regulation of retinal neurite growth by alterations in MAPK/ERK kinase (MEK) activity. Brain Res 858:205-214.

Dobashi Y, Shoji M, Kitagawa M, Noguchi T, Kameya T (2000) Simultaneous suppression of cdc2 and cdk2 activities induces neuronal differentiation of PC12 cells. J Biol Chem 275:12572-12580.

Dragunow M, Xu R, Walton M, Woodgate A, Lawlor P, MacGibbon GA, Young D, Gibbons H, Lipski J, Muravlev A, Pearson A, During M (2000) c-Jun promotes neurite outgrowth and survival in PC12 cells [In Process Citation]. Brain Res Mol Brain Res 83:20-33.

Dudley DT, Pang L, Decker SJ, Bridges AJ, Saltiel AR (1995) A synthetic inhibitor of the mitogen-activated protein kinase cascade. Proc Natl Acad Sci U S A 92:7686-7689.

Dutcher SK (2001) The tubulin fraternity: alpha to eta. Curr Opin Cell Biol 13:49-54.

Dziadek M (1995) Role of laminin-nidogen complexes in basement membrane formation during embryonic development. Experientia 51:901-913.

Earnshaw WC, Martins LM, Kaufmann SH (1999) Mammalian caspases: structure, activation, substrates, and functions during apoptosis. Annu Rev Biochem 68:383-424.

Edelman GM, Crossin KL (1991) Cell adhesion molecules: implications for a molecular histology. Annu Rev Biochem 60:155-190.

Elion EA (2000) Pheromone response, mating and cell biology. Curr Opin Microbiol 3:573-581.

Ensoli F, Fiorelli V, Vannelli B, Barni T, De Cristofaro M, Ensoli B, Thiele CJ (1998) Basic fibroblast growth factor supports human olfactory neurogenesis by autocrine/paracrine mechanisms. Neuroscience 86:881-893.

Eves EM, Kwon J, Downen M, Tucker MS, Wainer BH, Rosner MR (1994) Conditional immortalization of neuronal cells from postmitotic cultures and adult CNS. Brain Res 656:396-404.

Eves EM, Boise LH, Thompson CB, Wagner AJ, Hay N, Rosner MR (1996) Apoptosis induced by differentiation or serum deprivation in an immortalized central nervous system neuronal cell line. J Neurochem 67:1908-1920.

Farbman AI (1977) Differentiation of olfactory receptor cells in organ culture. Anat Rec 189:187-199.

Ferguson KL, Callaghan SM, O'Hare MJ, Park DS, Slack RS (2000) The Rb-CDK4/6 signaling pathway is critical in neural precursor cell cycle regulation. J Biol Chem 275:33593-33600.

Feron F, Mackay-Sim A, Andrieu JL, Matthaei KI, Holley A, Sicard G (1999) Stress induces neurogenesis in non-neuronal cell cultures of adult olfactory epithelium. Neuroscience 88:571-583.

Fujii T, Funahashi J, Matsuura R, Izaki T, Nakamura H, Mikawa T, Tanaka H (2000) Axonal growth of the spinal cord interneurons expressing a homophilic adhesion molecule SC1 ectopically. Neurosci Res 38:175-181.

Fukuda M, Gotoh Y, Tachibana T, Dell K, Hattori S, Yoneda Y, Nishida E (1995) Induction of neurite outgrowth by MAP kinase in PC12 cells. Oncogene 11:239-244.

Fukuyama T, Otsuka T, Shigematsu H, Uchida N, Arima F, Ohno Y, Iwasaki H, Fukuda T, Niho Y (2000) Proliferative involvement of ENX-1, a putative human polycomb group gene, in haematopoietic cells. Br J Haematol 108:842-847.

Furuta Y, Ilic D, Kanazawa S, Takeda N, Yamamoto T, Aizawa S (1995) Mesodermal defect in late

phase of gastrulation by a targeted mutation of focal adhesion kinase, FAK. Oncogene 11:1989-1995.

Garrigue-Antar L, Barker C, Kadler KE (2001) Identification of amino acid residues in bone morphogenetic protein (BMP)-1 important for procollagen C-proteinase activity. J Biol Chem 29:29.

Garrington TP, Johnson GL (1999) Organization and regulation of mitogen-activated protein kinase signaling pathways. Curr Opin Cell Biol 11:211-218.

GeneScreen GPa Transfer and Detection Protocols. In: Hybridisation Transfer Memebranes. Boston: NEN Life Science Products, Inc.

Gervais FG, Thornberry NA, Ruffolo SC, Nicholson DW, Roy S (1998) Caspases cleave focal adhesion kinase during apoptosis to generate a FRNK-like polypeptide. J Biol Chem 273:17102-17108.

Getchell TV, Doty, R.L., Bartoshuk, L.M. and Snow Jr, J.B. (1991) Smell and Taste in Health and Disease. New York.: Raven Press.

Glantschnig H, Rodan GA, Reszka AA (2002) Mapping of MST1 kinase sites of phosphorylation. Activation and autophosphorylation. J Biol Chem 277:42987-42996.

Goldstein BJ, Schwob JE (1996) Analysis of the globose basal cell compartment in rat olfactory epithelium using GBC-1, a new monoclonal antibody against globose basal cells. J Neurosci 16:4005-4016.

Goldstein BJ, Wolozin BL, Schwob JE (1997) FGF2 suppresses neuronogenesis of a cell line derived from rat olfactory epithelium. J Neurobiol 33:411-428.

Gordon MK, Mumm JS, Davis RA, Holcomb JD, Calof AL (1995) Dynamics of MASH1 expression in vitro and in vivo suggest a non-stem cell site of MASH1 action in the olfactory receptor neuron lineage. Mol Cell Neurosci 6:363-379.

Graham SM, Oldham SM, Martin CB, Drugan JK, Zohn IE, Campbell S, Der CJ (1999) TC21 and Ras share indistinguishable transforming and differentiating activities. Oncogene 18:2107-2116.

Grant SG, Karl KA, Kiebler MA, Kandel ER (1995) Focal adhesion kinase in the brain: novel subcellular localization and specific regulation by Fyn tyrosine kinase in mutant mice. Genes Dev 9:1909-1921.

Graves JD, Draves KE, Gotoh Y, Krebs EG, Clark EA (2001) Both Phosphorylation and Caspase-Mediated Cleavage Contribute to Regulation of the Ste-20-like Protein Kinase Mst1 During CD95/Fas-Induced Apoptosis. J Biol Chem 13:13.

Graves JD, Gotoh Y, Draves KE, Ambrose D, Han DK, Wright M, Chernoff J, Clark EA, Krebs EG (1998) Caspase-mediated activation and induction of apoptosis by the mammalian Ste20-like kinase Mst1. Embo J 17:2224-2234.

Graziadei PPCaMG, G.A. (1978) Continuous Nerve Cell Renewal in the Olfactory System. In: Handbook of Sensory Physiology, Development of Sensory Systems (M. J, ed), pp 55-83. Berlin: Springer.

Green CD, Simons JF, Taillon BE, Lewin DA (2001) Open systems: panoramic views of gene expression. J Immunol Methods 250:67-79.

Greene LA, Tischler AS (1976) Establishment of a noradrenergic clonal line of rat adrenal pheochromocytoma cells which respond to nerve growth factor. Proc Natl Acad Sci U S A 73:2424-2428.

Grewal SS, York RD, Stork PJ (1999) Extracellular-signal-regulated kinase signalling in neurons. Curr Opin Neurobiol 9:544-553.

Guan JL (1997) Role of focal adhesion kinase in integrin signaling. Int J Biochem Cell Biol 29:1085-1096.

Guan JL, Trevithick JE, Hynes RO (1991) Fibronectin/integrin interaction induces tyrosine phosphorylation of a 120-kDa protein. Cell Regul 2:951-964.

Guillemot F, Lo LC, Johnson JE, Auerbach A, Anderson DJ, Joyner AL (1993) Mammalian achaete-scute homolog 1 is required for the early development of olfactory and autonomic neurons. Cell 75:463-476.

Hagemann C, Rapp UR (1999) Isotype-specific functions of Raf kinases. Exp Cell Res 253:34-46.

Hagemann D, Troppmair J, Rapp UR (1999) Cot protooncoprotein activates the dual specificity kinases MEK-1 and SEK-1 and induces differentiation of PC12 cells. Oncogene 18:1391-1400.

Hanks SK, Calalb MB, Harper MC, Patel SK (1992) Focal adhesion protein-tyrosine kinase phosphorylated in response to cell attachment to fibronectin. Proc Natl Acad Sci U S A 89:8487-8491.

Harbour JW, Dean DC (2000) Rb function in cell-cycle regulation and apoptosis. Nat Cell Biol 2:E65-67.

Hemler ME, Masumoto, A., Chan, B.M.C., Kassner,P., & Teixido, J. (1993) Cellular Adhesion Molecules. New York: Plenum Press.

Hens MD, DeSimone DW (1995) Molecular analysis and developmental expression of the focal adhesion kinase pp125FAK in Xenopus laevis. Dev Biol 170:274-288.

Herskowitz I (1995) MAP kinase pathways in yeast: for mating and more. Cell 80:187-197.

Hinds JW, Hinds PL, McNelly NA (1984) An autoradiographic study of the mouse olfactory epithelium: evidence for long-lived receptors. Anat Rec 210:375-383.

Hobert O, Jallal B, Ullrich A (1996) Interaction of Vav with ENX-1, a putative transcriptional regulator of homeobox gene expression. Mol Cell Biol 16:3066-3073.

Holbrook EH, Szumowski KE, Schwob JE (1995) An immunochemical, ultrastructural, and developmental characterization of the horizontal basal cells of rat olfactory epithelium. J Comp Neurol 363:129-146.

Holcomb JD, Mumm JS, Calof AL (1995) Apoptosis in the neuronal lineage of the mouse olfactory epithelium: regulation in vivo and in vitro. Dev Biol 172:307-323.

Howard MK, Burke LC, Mailhos C, Pizzey A, Gilbert CS, Lawson WD, Collins MK, Thomas NS, Latchman DS (1993) Cell cycle arrest of proliferating neuronal cells by serum deprivation can result in either apoptosis or differentiation. J Neurochem 60:1783-1791.

Huang S, Ingber DE (1999) The structural and mechanical complexity of cell-growth control. Nat Cell Biol 1:E131-138.

Hubank M, Schatz DG (1994) Identifying differences in mRNA expression by representational difference analysis of cDNA. Nucleic Acids Res 22:5640-5648.

Ilic D, Damsky CH, Yamamoto T (1997) Focal adhesion kinase: at the crossroads of signal transduction. J Cell Sci 110:401-407.

Ilic D, Furuta Y, Kanazawa S, Takeda N, Sobue K, Nakatsuji N, Nomura S, Fujimoto J, Okada M, Yamamoto T (1995) Reduced cell motility and enhanced focal adhesion contact formation in cells from FAK-deficient mice. Nature 377:539-544.

Ip YT, Davis RJ (1998) Signal transduction by the c-Jun N-terminal kinase (JNK)--from inflammation to development. Curr Opin Cell Biol 10:205-219.

Irigoyen JP, Nagamine Y (1999) Cytoskeletal reorganization leads to induction of the urokinase-type plasminogen activator gene by activating FAK and Src and subsequently the Ras/Erk signaling pathway. Biochem Biophys Res Commun 262:666-670.

Iwasaki S, Hattori A, Sato M, Tsujimoto M, Kohno M (1996) Characterization of the bone morphogenetic protein-2 as a neurotrophic factor. Induction of neuronal differentiation of PC12 cells in the absence of mitogen-activated protein kinase activation. J Biol Chem 271:17360-17365.

Iwasaki S, Iguchi M, Watanabe K, Hoshino R, Tsujimoto M, Kohno M (1999) Specific activation of the p38 mitogen-activated protein kinase signaling pathway and induction of neurite outgrowth in PC12 cells by bone morphogenetic protein-2. J Biol Chem 274:26503-26510.

Jackson RJ, Standart N (1990) Do the poly(A) tail and 3' untranslated region control mRNA translation? Cell 62:15-24.

Johnsen JI, Aurelio ON, Kwaja Z, Jorgensen GE, Pellegata NS, Plattner R, Stanbridge EJ, Cajot JF (2000) p53-mediated negative regulation of stathmin/Op18 expression is associated with G(2)/M cell-cycle arrest. Int J Cancer 88:685-691.

Jones P, Murray RM (1991) The genetics of schizophrenia is the genetics of neurodevelopment. Br J Psychiatry 158:615-623.

Jordan JD, Landau EM, Iyengar R (2000) Signaling networks: the origins of cellular multitasking [In Process Citation]. Cell 103:193-200.

Jumaa H, Guenet JL, Nielsen PJ (1997) Regulated expression and RNA processing of transcripts from the Srp20 splicing factor gene during the cell cycle. Mol Cell Biol 17:3116-3124.

Kakeya H, Onose R, Osada H (1998) Caspase-mediated activation of a 36-kDa myelin basic protein kinase during anticancer drug-induced apoptosis. Cancer Res 58:4888-4894.

Kakeya H, Onose R, Osada H (1999) Activation of a 36-kD MBP kinase, an active proteolytic fragment of MST/Krs proteins, during anticancer drug-induced apoptosis. Ann N Y Acad Sci 886:273-275.

Kaufman RJ (2000) Overview of vector design for mammalian gene expression. Mol Biotechnol 16:151-160.

Kienzle N, Young D, Zehntner S, Bushell G, Sculley TB (1996) DNaseI treatment is a prerequisite for the amplification of cDNA from episomal-based genes. Biotechniques 20:612-616.

Kito K, Ito T, Sakaki Y (1997) Fluorescent differential display analysis of gene expression in differentiating neuroblastoma cells. Gene 184:73-81.

Klesse LJ, Meyers KA, Marshall CJ, Parada LF (1999) Nerve growth factor induces survival and differentiation through two distinct signaling cascades in PC12 cells. Oncogene 18:2055-2068.

Kojima T (2000) Molecular biology of ryudocan, an endothelial heparan sulfate proteoglycan. Semin Thromb Hemost 26:67-73.

Kolch W (2000) Meaningful relationships: the regulation of the Ras/Raf/MEK/ERK pathway by protein interactions. Biochem J 351 Pt 2:289-305.

Kolkova K, Novitskaya V, Pedersen N, Berezin V, Bock E (2000) Neural cell adhesion molecule-stimulated neurite outgrowth depends on activation of protein kinase C and the Ras-mitogen-activated protein kinase pathway. J Neurosci 20:2238-2246.

Konicek BW, Xia X, Rajavashisth T, Harrington MA (1998) Regulation of mouse colony-stimulating factor-1 gene promoter activity by AP1 and cellular nucleic acid-binding protein. DNA Cell Biol 17:799-809.

Kornberg LJ, Earp HS, Turner CE, Prockop C, Juliano RL (1991) Signal transduction by integrins: increased protein tyrosine phosphorylation caused by clustering of beta 1 integrins. Proc Natl Acad Sci U S A 88:8392-8396.

Kortesmaa J, Yurchenco P, Tryggvason K (2000) Recombinant laminin-8 (alpha(4)beta(1)gamma(1)). Production, purification,and interactions with integrins. J Biol Chem 275:14853-14859.

Kuo WL, Chung KC, Rosner MR (1997) Differentiation of central nervous system neuronal cells by fibroblast-derived growth factor requires at least two signaling pathways: roles for Ras and Src. Mol Cell Biol 17:4633-4643.

Kyriakis JM, Avruch J (2001) Mammalian mitogen-activated protein kinase signal transduction pathways activated by stress and inflammation. Physiol Rev 81:807-869.

Labourier E, Rio DC (2001) Purification of Drosophila snRNPs and characterization of two populations of functional U1 particles. Rna 7:457-470.

Laemmli UK (1970) Cleavage of structural proteins during the assembly of the head of bacteriophage T4. Nature 227:680-685.

LaMantia AS, Colbert MC, Linney E (1993) Retinoic acid induction and regional differentiation prefigure olfactory pathway formation in the mammalian forebrain. Neuron 10:1035-1048.

Lavoie JN, Rivard N, L'Allemain G, Pouyssegur J (1996) A temporal and biochemical link between growth factor-activated MAP kinases, cyclin D1 induction and cell cycle entry. Prog Cell Cycle Res 2:49-58.

Leberer E, Thomas DY, Whiteway M (1997) Pheromone signalling and polarized morphogenesis in yeast. Curr Opin Genet Dev 7:59-66.

Leberer E, Dignard D, Harcus D, Thomas DY, Whiteway M (1992) The protein kinase homologue Ste20p is required to link the yeast pheromone response G-protein beta gamma subunits to downstream signalling components. Embo J 11:4815-4824.

Lee BN, Elion EA (1999) The MAPKKK Ste11 regulates vegetative growth through a kinase cascade of shared signaling components. Proc Natl Acad Sci U S A 96:12679-12684.

Lee KK, Ohyama T, Yajima N, Tsubuki S, Yonehara S (2001) MST, a physiological caspase substrate, highly sensitizes apoptosis both upstream and downstream of caspase activation. J Biol Chem 7:7.

Lee KK, Murakawa M, Nishida E, Tsubuki S, Kawashima S, Sakamaki K, Yonehara S (1998a) Proteolytic activation of MST/Krs, STE20-related protein kinase, by caspase during apoptosis. Oncogene 16:3029-3037.

Lee SW, Tomasetto C, Sager R (1991) Positive selection of candidate tumor-suppressor genes by subtractive hybridization. Proc Natl Acad Sci U S A 88:2825-2829.

Lees E (1995) Cyclin dependent kinase regulation. Curr Opin Cell Biol 7:773-780.

Leeuw T, Wu C, Schrag JD, Whiteway M, Thomas DY, Leberer E (1998) Interaction of a G-protein beta-subunit with a conserved sequence in Ste20/PAK family protein kinases. Nature 391:191-195.

Lehrach H, Diamond D, Wozney JM, Boedtker H (1977) RNA molecular weight determinations by gel electrophoresis under denaturing conditions, a critical reexamination. Biochemistry 16:4743-4751.

Lendahl U, McKay RD (1990) The use of cell lines in neurobiology. Trends Neurosci 13:132-137.

Leppa S, Saffrich R, Ansorge W, Bohmann D (1998) Differential regulation of c-Jun by ERK and JNK during PC12 cell differentiation. Embo J 17:4404-4413.

Leppa S, Eriksson M, Saffrich R, Ansorge W, Bohmann D (2001) Complex functions of AP-1 transcription factors in differentiation and survival of PC12 cells. Mol Cell Biol 21:4369-4378.

Li R, Thode S, Zhou J, Richard N, Pardinas J, Rao MS, Sah DW (2000) Motoneuron differentiation of immortalized human spinal cord cell lines. J Neurosci Res 59:342-352.

Li S, Kim M, Hu YL, Jalali S, Schlaepfer DD, Hunter T, Chien S, Shyy JY (1997) Fluid shear stress activation of focal adhesion kinase. Linking to mitogen-activated protein kinases. J Biol Chem 272:30455-30462.

Lian JP, Toker A, Badwey JA (2001) Phosphorylation of the activation loop of gamma p21-activated kinase (gamma-Pak) and related kinases (MSTs) in normal and stressed neutrophils. J Immunol 166:6349-6357.

Liang P, Pardee AB (1992) Differential display of eukaryotic messenger RNA by means of the polymerase chain reaction [see comments]. Science 257:967-971.

Liang P, Pardee AB (1995) Recent advances in differential display. Curr Opin Immunol 7:274-280.

Liang P, Zhu W, Zhang X, Guo Z, O'Connell RP, Averboukh L, Wang F, Pardee AB (1994) Differential display using one-base anchored oligo-dT primers. Nucleic Acids Res 22:5763-5764.

Lin JL, Chen HC, Fang HI, Robinson D, Kung HJ, Shih HM (2001) MST4, a new Ste20-related kinase that mediates cell growth and transformation via modulating ERK pathway. Oncogene 20:6559-6569.

Liou J, Kiefer F, Dang A, Hashimoto A, Cobb MH, Kurosaki T, Weiss A (2000) HPK1 is activated by lymphocyte antigen receptors and negatively regulates AP-1. Immunity 12:399-408.

Livesey FJ, Hunt SP (1998) Differential display cloning of genes induced in regenerating neurons. Methods 16:386-395.

Lockhart DJ, Dong H, Byrne MC, Follettie MT, Gallo MV, Chee MS, Mittmann M, Wang C, Kobayashi M, Horton H, Brown EL (1996) Expression monitoring by hybridization to high-density oligonucleotide arrays. Nat Biotechnol 14:1675-1680.

Lodish H, Baltimore, D., Berk, A., Zipursky, S.L., Matsudaira, P., and J. Darnell, ed (1995) Molecular Cell Biology, Third Edition. New York: Scientific American Books.

Lopez E, Figueroa S, Oset-Gasque MJ, Gonzalez MP (2003) Apoptosis and necrosis: two distinct events induced by cadmium in cortical neurons in culture. Br J Pharmacol 138:901-911.

Lycke K, Larsen F DYNAL*ogue*. In: Dynal Research and Development. Norway: Dynal Biotech AS.

MacDonald KP, Mackay-Sim A, Bushell GR, Bartlett PF (1996) Olfactory neuronal cell lines generated by retroviral insertion of the n-myc oncogene display different developmental phenotypes. J Neurosci Res 45:237-247.

Mackay-Sim A, Kittel P (1991) Cell dynamics in the adult mouse olfactory epithelium: a quantitative autoradiographic study. J Neurosci 11:979-984.

Mackay-Sim A, Chuah MI (2000) Neurotrophic factors in the primary olfactory pathway [In Process Citation]. Prog Neurobiol 62:527-559.

Madden TL, Tatusov RL, Zhang J (1996) Applications of network BLAST server. Methods Enzymol 266:131-141.

Mannironi C, Bonner WM, Hatch CL (1989) H2A.X. a histone isoprotein with a conserved C-terminal sequence, is encoded by a novel mRNA with both DNA replication type and polyA 3' processing signals. Nucleic Acids Res 17:9113-9126.

Manser E, Leung T, Salihuddin H, Zhao ZS, Lim L (1994) A brain serine/threonine protein kinase activated by Cdc42 and Rac1. Nature 367:40-46.

Margolis RL, Chuang DM, Post RM (1994) Programmed cell death: implications for neuropsychiatric disorders. Biol Psychiatry 35:946-956.

Mathews CK, Van Holde KE (1990) Biochemistry. Redwood City: The Benjamin/Cummings Publishing Company.

Matz MV, Lukyanov SA (1998) Different strategies of differential display: areas of application. Nucleic Acids Res 26:5537-5543.

Maul RS, Chang DD (1999) EPLIN, epithelial protein lost in neoplasm. Oncogene 18:7838-7841.

McCarthy C (1998) Chromas 1.5. In, 1.5 Edition. Mt Gravatt: Technelysium PTY LTD.

McCarthy JB, Skubitz, A.P.N., Furcht, L.T., Wayner, E.A., & Iida, J. (1993) Co-ordinate Role for Proteoglycans and Integrins in Cell Adhesion. In: Cell Adhesion Molecules, pp p127-140. New York: Plenum Press.

McClelland M, Chada K, Welsh J, Ralph D (1993) Arbitrary primed PCR fingerprinting of RNA applied to mapping differentially expressed genes. Exs 67:103-115.

Mikheev AM, Mikheev SA, Zhang Y, Aebersold R, Zarbl H (2000) CArG binding factor A (CBF-A) is involved in transcriptional regulation of the rat Ha-ras promoter. Nucleic Acids Res 28:3762-3770.

Miyamoto S, Akiyama SK, Yamada KM (1995) Synergistic roles for receptor occupancy and aggregation in integrin transmembrane function. Science 267:883-885.

Mochizuki N, Yamashita S, Kurokawa K, Ohba Y, Nagai T, Miyawaki A, Matsuda M (2001) Spatio-temporal images of growth-factor-induced activation of Ras and Rap1. Nature 411:1065-1068.

Moodie SA, Paris MJ, Kolch W, Wolfman A (1994) Association of MEK1 with p21ras.GMPPNP is dependent on B-Raf. Mol Cell Biol 14:7153-7162.

Morrison DK, Cutler RE (1997) The complexity of Raf-1 regulation. Curr Opin Cell Biol 9:174-179.

Moulton DG (1974) Dynamics of cell populations in the olfactory epithelium. Ann N Y Acad Sci 237:52-61.

Murrell W, Bushell GR, Livesey J, McGrath J, MacDonald KP, Bates PR, Mackay-Sim A (1996) Neurogenesis in adult human. Neuroreport 7:1189-1194.

Musacchio A, Gibson T, Rice P, Thompson J, Saraste M (1993) The PH domain: a common piece in the structural patchwork of signalling proteins. Trends Biochem Sci 18:343-348.

Nagase H, Woessner JF, Jr. (1999) Matrix metalloproteinases. J Biol Chem 274:21491-21494.

Nakamura Y, Yoshioka K, Shirakawa H, Yoshida M (2001) Hmg box a in hmg2 protein functions as a mediator of dna structural alteration together with box b. J Biochem (Tokyo) 129:643-651.

Newman MP, Feron F, Mackay-Sim A (2000) Growth factor regulation of neurogenesis in adult olfactory epithelium. Neuroscience 99:343-350.

Nishinaka N, Hongo S, Zhou CJ, Shioda S, Takahashi R, Yamauchi Y, Ohashi T, Ohki T, Nakada N, Takeda F, Takeda M (2000) Identification of the novel developmentally regulated gene, Bdm2, which is highly expressed in fetal rat brain. Brain Res Dev Brain Res 120:57-64.

Nobes CD, Hall A (1995) Rho, rac, and cdc42 GTPases regulate the assembly of multimolecular focal complexes associated with actin stress fibers, lamellipodia, and filopodia. Cell 81:53-62.

Nolan K, Lacoste J, Parsons JT (1999) Regulated expression of focal adhesion kinase-related nonkinase, the autonomously expressed C-terminal domain of focal adhesion kinase. Mol Cell Biol 19:6120-6129.

Ohnuma S, Philpott A, Harris WA (2001) Cell cycle and cell fate in the nervous system. Curr Opin Neurobiol 11:66-73.

O'Regan A, Berman JS (2000) Osteopontin: a key cytokine in cell-mediated and granulomatous inflammation. Int J Exp Pathol 81:373-390.

O'Rourke SM, Herskowitz I (1998) The Hog1 MAPK prevents cross talk between the HOG and pheromone response MAPK pathways in Saccharomyces cerevisiae. Genes Dev 12:2874-2886.

Pang L, Sawada T, Decker SJ, Saltiel AR (1995) Inhibition of MAP kinase kinase blocks the differentiation of PC-12 cells induced by nerve growth factor. J Biol Chem 270:13585-13588.

Pawson T, Scott JD (1997) Signaling through scaffold, anchoring, and adaptor proteins. Science 278:2075-2080.

Pearson G, Robinson F, Beers Gibson T, Xu BE, Karandikar M, Berman K, Cobb MH (2001) Mitogen-activated protein (MAP) kinase pathways: regulation and physiological functions. Endocr Rev 22:153-183.

Perris R, Kuo HJ, Glanville RW, Bronner-Fraser M (1993) Collagen type VI in neural crest development: distribution in situ and interaction with cells in vitro. Dev Dyn 198:135-149.

Perron JC, Bixby JL (1999) Distinct neurite outgrowth signaling pathways converge on ERK activation. Mol Cell Neurosci 13:362-378.

Pleasure SJ, Page C, Lee VM (1992) Pure, postmitotic, polarized human neurons derived from NTera 2 cells provide a system for expressing exogenous proteins in terminally differentiated neurons. J Neurosci 12:1802-1815.

Poindessous-Jazat V, Augery-Bourget Y, Robert-Lezenes J (2002) C-Jun modulates apoptosis but not terminal cell differentiation in murine erythroleukemia cells. Leukemia 16:233-243.

Pombo CM, Bonventre JV, Molnar A, Kyriakis J, Force T (1996) Activation of a human Ste20-like

kinase by oxidant stress defines a novel stress response pathway. Embo J 15:4537-4546.

Promega (1998) Technical Manual. In: pGEM®–T and pGEM®-T Easy Vector Systems, p 30. Madison: Promega.

Pruyne D, Bretscher A (2000a) Polarization of cell growth in yeast. I. Establishment and maintenance of polarity states. J Cell Sci 113:365-375.

Pruyne D, Bretscher A (2000b) Polarization of cell growth in yeast. J Cell Sci 113:571-585.

Qi Y, Wang JKT, McMillian M, Chikaraishi DM (1997) Characterization of a CNS cell line, CAD, in which morphological differentiation is initiated by serum deprivation. J Neurosci 17:1217-1225.

QIAGEN PL (1999) Oligotex™ Handbook. In: Purification of poly A^+ RNA from total RNA, directly from cultured cells or tissues and of polyadenylated in vitro transcripts, 1st Edition, p 86: QIAGEN.

Qian Z, Lin C, Espinosa R, LeBeau M, Rosner MR (2001) Cloning and characterization of MST4, a novel Ste20-like kinase. J Biol Chem 276:22439-22445.

Qiu J, Li X, Frank G, Shen B (2000) Cell cycle-dependent and DNA damage-inducible nuclear localization of FEN-1 nuclease is consistent with its dual functions in DNA replication and repair. J Biol Chem 25:25.

Ramage P, Cheneval D, Chvei M, Graff P, Hemmig R, Heng R, Kocher HP, Mackenzie A, Memmert K, Revesz L, et al. (1995) Expression, refolding, and autocatalytic proteolytic processing of the interleukin-1 beta-converting enzyme precursor. J Biol Chem 270:9378-9383.

Ramer SW, Davis RW (1993) A dominant truncation allele identifies a gene, STE20, that encodes a putative protein kinase necessary for mating in Saccharomyces cerevisiae. Proc Natl Acad Sci U S A 90:452-456.

Rassart E, Bedirian A, Do Carmo S, Guinard O, Sirois J, Terrisse L, Milne R (2000) Apolipoprotein D. Biochim Biophys Acta 1482:185-198.

Reiske HR, Zhao J, Han DC, Cooper LA, Guan JL (2000) Analysis of FAK-associated signaling pathways in the regulation of cell cycle progression. FEBS Lett 486:275-280.

Richardson A, Parsons T (1996) A mechanism for regulation of the adhesion-associated proteintyrosine kinase pp125FAK [published erratum appears in Nature 1996 Jun 27;381(6585):810]. Nature 380:538-540.

Roghi C, Allan VJ (1999) Dynamic association of cytoplasmic dynein heavy chain 1a with the Golgi apparatus and intermediate compartment. J Cell Sci 112:4673-4685.

Roovers K, Assoian RK (2000) Integrating the MAP kinase signal into the G1 phase cell cycle machinery [In Process Citation]. Bioessays 22:818-826.

Roskams AJ, Cai X, Ronnett GV (1998) Expression of neuron-specific beta-III tubulin during olfactory neurogenesis in the embryonic and adult rat. Neuroscience 83:191-200.

Rozen S, Skaletsky HJ (1998) Primer3. In: http://www-genome.wi.mit.edu/genome_software/other/primer3.html.

Rudel T, Bokoch GM (1997) Membrane and morphological changes in apoptotic cells regulated by caspase-mediated activation of PAK2. Science 276:1571-1574.

Ryder EF, Snyder EY, Cepko CL (1990) Establishment and characterization of multipotent neural cell

lines using retrovirus vector-mediated oncogene transfer. J Neurobiol 21:356-375.

Sambrook J, Fritsch EF, Maniatis T (1989) Molecular Cloning: A Laboratory Manual. In, 2nd Edition. New York: Cold Spring Harbour Press.

Sano M, Kitajima S (1998) Activation of mitogen-activated protein kinases is not required for the extension of neurites from PC12D cells triggered by nerve growth factor. Brain Res 785:299-308.

Sarras MP (1996) BMP-1 and the astacin family of metalloproteinases: a potential link between the extracellular matrix, growth factors and pattern formation. Bioessays 18:439-442.

Sasaki K, Tamura S, Tachibana H, Sugita M, Gao Y, Furuyama J, Kakishita E, Sakai T, Tamaoki T, Hashimoto-Tamaoki T (2000) Expression and role of p27(kip1) in neuronal differentiation of embryonal carcinoma cells. Brain Res Mol Brain Res 77:209-221.

Schadt EE, Li C, Su C, Wong WH (2000) Analyzing high-density oligonucleotide gene expression array data. J Cell Biochem 80:192-202.

Schaller MD, Borgman CA, Parsons JT (1993) Autonomous expression of a noncatalytic domain of the focal adhesion-associated protein tyrosine kinase pp125FAK. Mol Cell Biol 13:785-791.

Schaller MD, Borgman CA, Cobb BS, Vines RR, Reynolds AB, Parsons JT (1992) pp125FAK a structurally distinctive protein-tyrosine kinase associated with focal adhesions. Proc Natl Acad Sci U S A 89:5192-5196.

Schena M, Shalon D, Davis RW, Brown PO (1995) Quantitative monitoring of gene expression patterns with a complementary DNA microarray. Science 270:467-470.

Schena M, Shalon D, Heller R, Chai A, Brown PO, Davis RW (1996) Parallel human genome analysis: microarray-based expression monitoring of 1000 genes. Proc Natl Acad Sci U S A 93:10614-10619.

Schinkmann K, Blenis J (1997) Cloning and characterization of a human STE20-like protein kinase with unusual cofactor requirements. J Biol Chem 272:28695-28703.

Schlaepfer DD, Jones KC, Hunter T (1998) Multiple Grb2-mediated integrin-stimulated signaling pathways to ERK2/mitogen-activated protein kinase: summation of both c-Src- and focal adhesion kinase-initiated tyrosine phosphorylation events. Mol Cell Biol 18:2571-2585.

Schoenwaelder SM, Burridge K (1999) Bidirectional signaling between the cytoskeleton and integrins. Curr Opin Cell Biol 11:274-286.

Schubert D, Heinemann S, Carlisle W, Tarikas H, Kimes B, Patrick J, Steinbach JH, Culp W, Brandt BL (1974) Clonal cell lines from the rat central nervous system. Nature 249:224-227.

Seger R, Krebs EG (1995) The MAPK signaling cascade. Faseb J 9:726-735.

Seidel B, Keilhoff G, Reinheckel T, Wolf G (1998) Differentially expressed genes in hippocampal cell cultures in response to an excitotoxic insult by quinolinic acid. Brain Res Mol Brain Res 60:296-300.

Sells MA, Chernoff J (1997) Emerging from the Pak: the p21-activated protein kinase family. Trends in Cell Biology 7:162-167.

Sells MA, Boyd JT, Chernoff J (1999b) p21-activated kinase 1 (Pak1) regulates cell motility in mammalian fibroblasts. J Cell Biol 145:837-849.

Sequenase (1993) Version 2.0 DNA Sequencing Kit. In: Step-By-Step Protocols For DNA Sequencing

With Sequenase® Version 2.0 T7 DNA Polymerase, 7th Edition, p 27. Ohio: United States Biochemical Corporation.

Serpente N, Birling MC, Price J (1996) The regulation of the expression, phosphorylation, and protein associations of pp125FAK during rat brain development. Mol Cell Neurosci 7:391-403.

Sewing A, Wiseman B, Lloyd AC, Land H (1997) High-intensity Raf signal causes cell cycle arrest mediated by p21Cip1. Mol Cell Biol 17:5588-5597.

Sherr CJ (1994) G1 phase progression: cycling on cue [see comments]. Cell 79:551-555.

Sjaastad MD, Angres B, Lewis RS, Nelson WJ (1994) Feedback regulation of cell-substratum adhesion by integrin-mediated intracellular Ca2+ signaling. Proc Natl Acad Sci U S A 91:8214-8218.

Small EM, Vokes SA, Garriock RJ, Li D, Krieg PA (2000) Developmental expression of the Xenopus Nkx2-1 and Nkx2-4 genes. Mech Dev 96:259-262.

Sonoda Y, Matsumoto Y, Funakoshi M, Yamamoto D, Hanks SK, Kasahara T (2000) Anti-apoptotic role of focal adhesion kinase (FAK). Induction of inhibitor-of-apoptosis proteins and apoptosis suppression by the overexpression of FAK in a human leukemic cell line, HL-60. J Biol Chem 275:16309-16315.

St John TP, Davis RW (1979) Isolation of galactose-inducible DNA sequences from Saccharomyces cerevisiae by differential plaque filter hybridization. Cell 16:443-452.

Stratagene (1998) Epicurian Coli® Solopack™ Gold Competent/Supercompetent Cells. In: Instruction Manual, p 10. California: Stratgene.

Streuli C (1999) Extracellular matrix remodelling and cellular differentiation. Curr Opin Cell Biol 11:634-640.

Su YC, Treisman JE, Skolnik EY (1998) The Drosophila Ste20-related kinase misshapen is required for embryonic dorsal closure and acts through a JNK MAPK module on an evolutionarily conserved signaling pathway. Genes Dev 12:2371-2380.

Su YC, Maurel-Zaffran C, Treisman JE, Skolnik EY (2000) The Ste20 kinase misshapen regulates both photoreceptor axon targeting and dorsal closure, acting downstream of distinct signals. Mol Cell Biol 20:4736-4744.

Sun HQ, Yamamoto M, Mejillano M, Yin HL (1999) Gelsolin, a multifunctional actin regulatory protein. J Biol Chem 274:33179-33182.

Sun S, Ravid K (1999) Role of a serine/threonine kinase, Mst1, in megakaryocyte differentiation. J Cell Biochem 76:44-60.

Suri C, Fung BP, Tischler AS, Chikaraishi DM (1993) Catecholaminergic cell lines from the brain and adrenal glands of tyrosine hydroxylase-SV40 T antigen transgenic mice. J Neurosci 13:1280-1291.

Suter DM, Pollerberg GE, Buchstaller A, Giger RJ, Dreyer WJ, Sonderegger P (1995) Binding between the neural cell adhesion molecules axonin-1 and Nr-CAM/Bravo is involved in neuron-glia interaction. J Cell Biol 131:1067-1081.

Takagaki Y, MacDonald CC, Shenk T, Manley JL (1992) The human 64-kDa polyadenylylation factor contains a ribonucleoprotein-type RNA binding domain and unusual auxiliary motifs. Proc Natl Acad Sci U S A 89:1403-1407.

Tang J, Abovich N, Fleming ML, Seraphin B, Rosbash M (1997) Identification and characterization of a yeast homolog of U1 snRNP-specific protein C. Embo J 16:4082-4091.

Taylor LK, Wang HC, Erikson RL (1996) Newly identified stress-responsive protein kinases, Krs-1 and Krs-2. Proc Natl Acad Sci U S A 93:10099-10104.

Telenius H, Carter NP, Bebb CE, Nordenskjold M, Ponder BA, Tunnacliffe A (1992) Degenerate oligonucleotide-primed PCR: general amplification of target DNA by a single degenerate primer. Genomics 13:718-725.

Tibbles LA, Woodgett JR (1999) The stress-activated protein kinase pathways. Cell Mol Life Sci 55:1230-1254.

Tomaselli KJ, Hall DE, Flier LA, Gehlsen KR, Turner DC, Carbonetto S, Reichardt LF (1990) A neuronal cell line (PC12) expresses two beta 1-class integrins-alpha 1 beta 1 and alpha 3 beta 1-that recognize different neurite outgrowth-promoting domains in laminin. Neuron 5:651-662.

Traverse S, Cohen P (1994) Identification of a latent MAP kinase kinase kinase in PC12 cells as B-raf. FEBS Lett 350:13-18.

Tsuneishi S, Sano K, Nakamura H (1993) Serum depletion increases the neurofilament protein mRNA levels in a neuroblastoma cell line, GOTO. Brain Res Mol Brain Res 17:119-128.

Tsuzuki S, Kojima T, Katsumi A, Yamazaki T, Sugiura I, Saito H (1997) Molecular cloning, genomic organization, promoter activity, and tissue-specific expression of the mouse ryudocan gene. J Biochem (Tokyo) 122:17-24.

Ura S, Masuyama N, Graves JD, Gotoh Y (2001a) MST1-JNK promotes apoptosis via caspase-dependent and independent pathways. Genes Cells 6:519-530.

Ura S, Masuyama N, Graves JD, Gotoh Y (2001b) Caspase cleavage of MST1 promotes nuclear translocation and chromatin condensation. Proc Natl Acad Sci U S A 98:10148-10153.

Vleminckx K, Kemler R (1999) Cadherins and tissue formation: integrating adhesion and signaling. Bioessays 21:211-220.

Walter BN, Huang Z, Jakobi R, Tuazon PT, Alnemri ES, Litwack G, Traugh JA (1998) Cleavage and activation of p21-activated protein kinase gamma-PAK by CPP32 (caspase 3). Effects of autophosphorylation on activity. J Biol Chem 273:28733-28739.

Wan JS, Sharp SJ, Poirier GM, Wagaman PC, Chambers J, Pyati J, Hom YL, Galindo JE, Huvar A, Peterson PA, Jackson MR, Erlander MG (1996) Cloning differentially expressed mRNAs. Nat Biotechnol 14:1685-1691.

Wang HC, Erikson RL (1992) Activation of protein serine/threonine kinases p42, p63, and p87 in Rous sarcoma virus-transformed cells: signal transduction/transformation-dependent MBP kinases. Mol Biol Cell 3:1329-1337.

Wang HC, Fecteau KA (2000) Detection of a novel quiescence-dependent protein kinase. J Biol Chem 275:25850-25857.

Wary KK, Mariotti A, Zurzolo C, Giancotti FG (1998) A requirement for caveolin-1 and associated kinase Fyn in integrin signaling and anchorage-dependent cell growth. Cell 94:625-634.

Watabe M, Kakeya H, Osada H (1999) Requirement of protein kinase (Krs/MST) activation for MT-21-induced apoptosis. Oncogene 18:5211-5220.

Watabe M, Machida K, Osada H (2000a) MT-21 is a synthetic apoptosis inducer that directly induces cytochrome c release from mitochondria. Cancer Res 60:5214-5222.

Watabe M, Kakeya H, Onose R, Osada H (2000b) Activation of MST/Krs and c-Jun N-terminal

kinases by different signaling pathways during cytotrienin A-induced apoptosis [In Process Citation]. J Biol Chem 275:8766-8771.

Weber M (1999) Mitogen-Activated Protein Kinase Cascades....Pathways to Transcription. In: Upstate News and Views, p 1.

Weil M, Raff MC, Braga VM (1999) Caspase activation in the terminal differentiation of human epidermal keratinocytes. Curr Biol 9:361-364.

Widmann C, Gibson S, Johnson GL (1998) Caspase-dependent cleavage of signaling proteins during apoptosis. A turn-off mechanism for anti-apoptotic signals. J Biol Chem 273:7141-7147.

Wilfinger WW, Mackey K, Chomczynski P (1997) Effect of pH and ionic strength on the spectrophotometric assessment of nucleic acid purity. Biotechniques 22:474-476, 478-481.

Woods A, Couchman JR (1994) Syndecan 4 heparan sulfate proteoglycan is a selectively enriched and widespread focal adhesion component. Mol Biol Cell 5:183-192.

Woods D, Parry D, Cherwinski H, Bosch E, Lees E, McMahon M (1997) Raf-induced proliferation or cell cycle arrest is determined by the level of Raf activity with arrest mediated by p21Cip1. Mol Cell Biol 17:5598-5611.

Wurfel J, Rosel M, Seiter S, Claas C, Herlevsen M, Weth R, Zoller M (1999) Metastasis-association of the rat ortholog of the human epithelial glycoprotein antigen EGP314. Oncogene 18:2323-2334.

Xiong W, Pestell R, Rosner MR (1997) Role of cyclins in neuronal differentiation of immortalized hippocampal cells. Mol Cell Biol 17:6585-6597.

Xu F, Zhao ZJ (2001) Cell density regulates tyrosine phosphorylation and localization of focal adhesion kinase. Exp Cell Res 262:49-58.

Xu S, Khoo S, Dang A, Witt S, Do V, Zhen E, Schaefer EM, Cobb MH (1997) Differential regulation of mitogen-activated protein/ERK kinase (MEK)1 and MEK2 and activation by a Ras-independent mechanism. Mol Endocrinol 11:1618-1625.

Yamamori B, Kuroda S, Shimizu K, Fukui K, Ohtsuka T, Takai Y (1995) Purification of a Ras-dependent mitogen-activated protein kinase kinase kinase from bovine brain cytosol and its identification as a complex of B-Raf and 14-3-3 proteins. J Biol Chem 270:11723-11726.

Yung Y, Yao Z, Hanoch T, Seger R (2000) ERK1b, a 46-kDa ERK isoform that is differentially regulated by MEK. J Biol Chem 275:15799-15808.

Yung Y, Yao Z, Aebersold DM, Hanoch T, Seger R (2001) Altered regulation of ERK1b by MEK1 and PTP-SL and modified Elk1 phosphorylation by ERK1b are caused by abrogation of the regulatory C-terminal sequence of ERKs. J Biol Chem 276:35280-35289.

Zachary I (1997) Focal adhesion kinase. Int J Biochem Cell Biol 29:929-934.

Zehntner SP (1998b) Gene Expression in Developing Olfactory Neurones. In: Faculty of Science, p 167. Brisbane: Griffith University.

Zehntner SP, Mackay-Sim A, Bushell GR (1998a) Differentiation in an olfactory cell line. Analysis via differential display. Ann N Y Acad Sci 855:235-239.

Zermati Y, Garrido C, Amsellem S, Fishelson S, Bouscary D, Valensi F, Varet B, Solary E, Hermine O (2001) Caspase Activation Is Required for Terminal Erythroid Differentiation. J Exp Med 193:247-254.

Zeuner A, Eramo A, Peschle C, De Maria R (1999) Caspase activation without death. Cell Death Differ 6:1075-1080.

Zhao S, Ooi SL, Pardee AB (1995) New primer strategy improves precision of differential display. Biotechniques 18:842-846, 848, 850.

Zmuda JF, Rivas RJ (1998) The Golgi apparatus and the centrosome are localized to the sites of newly emerging axons in cerebellar granule neurons in vitro. Cell Motil Cytoskeleton 41:18-38.

APPENDICES

Appendix I: Reagents And Buffer Recipes

Section 2.3.2.1 Total RNA Extraction

Solution D (in MQ H_2O)

4 M	Guanidinium Thiocyanate (Sigma)
25 mM	Sodium Citrate, pH 7.0 (Sigma)
0.5%	Sarcosyl (Sigma)
	Add 0.1 M 2-mercaptoethanol (BioRad) prior to use

TE Buffer

10 mM	Tris-HCl, pH 8.0 (ICN Biochemicals)
1 mM	EDTA (Sigma)

Section 2.3.2.3 RNA Integrity: RNA Formaldehyde Gel Electrophoresis

RNA Sample Loading Buffer

50%	deionised Formamide, pH<8.0 (Sigma)
1X	MOPS buffer
0.66 M (6%)	deionised 37% Formaldehyde, pH >4 (Sigma)
5%	Glycerol (ICN Biochemicals)
0.5%	Bromophenol blue (Sigma)

Formamide, Deionized

Add 50 mLs of Formamide to 5 gms mixed-bed resin (eg. anion/cation exchanger -Amberlite). Stir gently for ~30 mins until pH is below 8.0. Filter solution through Whatman 3MM filter paper. For best results prepare fresh daily. Deionized formamide may also be aliquoted and stored @-20˚C.

Formaldehyde, Deionized

Is prepared as per that done for formamide but the pH should be greater than 4.0.

10 X MOPS Buffer

0.4 M	Morpholinopropanesulfonic acid (ICN Biochemicals)
0.1 M	Sodium acetate-$3H_2O$ (BDH Biochemicals)
10 mM	EDTA-Na_2-$2H_2O$
	Adjust pH to 7.2 with NaOH

Section 2.3.2.4 Isolation of mRNA

Oligotex Suspension (Qiagen)

10% (w/v) suspension (= 1 mg/10 μL) Oligotex particles in:	
10 mM	Tris.Cl, pH 7.5
500 mM	NaCl
1 mM	EDTA
0.1%	SDS
0.1%	NaN_3 (sodium azide)

Buffer OBB (Qiagen)

20 mM	Tris.Cl, pH 7.5
1 M	NaCl
2 mM	EDTA
0.2%	SDS

Wash Buffer OW2 (Qiagen)

10 mM	Tris.Cl, pH 7.5
150 mM	NaCl
1 mM	EDTA

Elution Buffer (Qiagen)

5 mM	Tris.Cl, pH 7.5

Section 2.3.2.8 cDNA Integrity

GAPDH forward primer 5'-ACAGTCCATGCCATCACTGCC-3' (Sigma GenoSys)
GAPDH reverse primer 5'-GCCTGCTTCACCACCTTCTTG-3' (Sigma GenoSys)

Section 2.3.2.9 PCR Product Analysis

6X DNA Gel Loading Buffer

0.25%	Bromophenol Blue (Sigma)
30%	Glycerol (AJAX Chemicals)
10mg/mL	RNase A (Boehringer Mannheim)

5X TBE

225mM	Tris Borate
5mM	EDTA

Section 2.3.2.10 Differential Display (DD) PCR

Degenerate Anchored Oligo DD-C [T_{11}-CC/T_{11}-AC/ T_{11}-GC]
Arbitrary Oligo (W2) 5'-TGGATTGGTC-3'

Section 2.3.2.12 Sequencing Gel

Formamide Loading Buffer

95%	deinoized Formamide
20 mM	EDTA
0.09%	Bromophenol blue (Sigma)
0.09%	Xylene cyanol FF (Sigma)
	store @ 4˚C

6% Denaturing Polyacrylamide Sequencing Gel Mix

6%	Acrylamide (BioRad)
0.3%	Bis-acylamide (BioRad)
7 M	Urea (Pharmacia)
1X	TBE
0.1%	Ammonium Persulphate (APS, BioRad)
0.035%	N,N,N',N'-tetra-methethylenediamine (TEMED, BioRad)

30% Acrylamide (Store in dark bottle @ R/T)

Acrylamide 29g (BioRad)
N,`N`-methylenebisacrylamide 1g (BioRad)
H_2O to 100mL
Heat solution to 37˚C to dissolve and filter sterilise.

10% Ammonium persulphate (Store @ 4˚C)

APS 1g
H_2O to 10 mL.

Section 2.3.4 PCR Product Cloning

SOC Medium (100 mL)

2.0 gm	Bacto-tryptone (Gibco)
0.5 gm	Bacto-yeast extract (Gibco)
1 mL	1 M NaCl
0.25 mL	1 M KCl
1 mL	2 M Mg^{2+} stock, filter sterilised
1 mL	2 M glucose, filter sterilised (Sigma)

Add Bacto-tryptone, Bacto-yeast extract, NaCl and KCl to 97 mL of MQ H_2O, stir to dissolve, autoclave and cool to room temperature. Add 2 M Mg^{2+} and 2 M glucose to a final concentration of 20 mM, bring volume up to 100 mL and filter sterilise through a 0.2 µm filter. Final pH should be 7.0.

LB plates with Ampicillin (AMP)

Add 40gm LB agar (Gibco) to 1 litre of water. Autoclave. Allow the medium to cool to approximately 60˚Çbefore adding AMP (100 µg/mL; Sigma) to a final concentration of 100 µg/mL. Pour 25-30 mL of medium into 90 mm petri dishes. Let stand until the agar sets, store at 4˚C.

IPTG (0.1 M)

1.2 g IPTG (Sigma) in 50 mL MQ H_2O, filter sterilise and store at 4˚C.

X-Gal (2 mL)

100 mg X-gal (Sigma) in 2 mL N,N'-dimethyl-formamide. Cover with aluminium foil and store at -20˚C.

LB AMP/IPTG/X-gal plates

Prepare LB AMP plates as above and spread 100 µLof 100 mM IPTG and 20 µLof 50 mg/mL X-gal over the surface of the plate and allow to absorb for 15-30 min at room temperature before use.

Section 2.3.4.5.1 Plasmid Isolation - STET Preparation

STET Solution

8%	Sucrose
0.5%	Triton X-100 (Sigma)
20 mM	EDTA pH 8.0
50 mM	Tris.HCl pH 8.0

Section 2.3.5 Expression Analysis Of Differential Display Fragments

20X SSPE

3 M	NaCl
0.2 M	NaH_2PO4-H_2O
0.02 M	$EDTA-Na_2$
	Add dsH_2O to 800 mLs adjust pH to 7.4 with NaOH
	Add dsH_2O to make 1 L

100X Denhardts Solution

1 gm	Polyvinylpyrrolidone (MW 40,000) (Sigma)
1 gm	Bovine Serum Albumin (Sigma)
1 gm	Ficoll 400 (Sigma)
	Add dsH_2O to make 50 mLs and filter sterilise. Store @ 4°C

20X SSC

3M	NaCl
0.3M	Sodium Citrate Dihydrate (BDH Biochemicals)
	Dissolve in dsH_2O to 1 L

Section 3.3.1 Mouse Olfactory Epithelium cDNA Library Screening

XL1-Blue
(endA1, gyrA96, hsdR17, lac-, recA1, relA1, supE44, thi-1, [F' lacl^{q}Z M15, proAB, Tn10]

E.Coli BM25.8
(supE44, thi (lac-proAB) [F' traD36, proAB$^+$, lacl^{q}Z M15] imm434 (kan^R)P1 (cam^R) hsdR (r_{k12} – m_{k12}-)

XL10-Gold
(Tet^R (mcrA)183, (mcrCB-hsdSMR-mrr)173, endA1, supE44, thi-1, recA1, gyrA96, relA1, lac Hte [F' proAB, lacl^{q}Z M15, Tn10 (Tet^R) Amy Cam^R]

Section 3.3.2 Full-length MST Kinase Isolation From cDNA

M13 (-40 universal) Primer 5'-GTTTTCCCAGTCACGAC-3' (Sigma GenoSys)

SMART III Oligonucleotide
5'-AAGCAGTGGTATCAACGCAGAGTGGCCATTATGGCCGGG-3'

CDS III/3' PCR Primer 5'-ATTCTAGAGGCCGAGGCGGCCGACATG-d$(T)_{30}N_{-1}$N-3'

5'-PCR Primer 5'-AAGCAGTGGTATCAACGCAGAGT-3'

Section 3.3.3 Full-length Amplification Using Rat MST2 Kinase Primers

rMST2F Primer 5'-GCTCTAGAATTCCATTCGGTCCCTCTTTC-3'
(Sigma GenoSys)

rMST2R primer 5'-CCTTGTGTCCTTAACTTCCTTCCTAGGGCCCCCT-3'
(Sigma GenoSys)

Section 3.3.4 Mouse MST2 Kinase Putative Sequence And Primer Design

mMST2F Primer 5'-ATGGAGACCGTGCAGCTGAGGAAC-3' (Sigma GenoSys)

mMST2R Primer 5'-GGCTGGGCTGGTGTTGTCAGAAGT-3' (Sigma GenoSys)

Section 4.3.2 Protein Analysis

Protein Extraction Buffer
(Equal parts of Gel Loading Buffer and Suspension Buffer)
Gel Loading Buffer

0.1 M	NaCl
10 mM	Tris.HCl, pH 7.6
1 mM	EDTA, pH 8.0
574 µM	PMSF (Sigma)
1X	Complete Stock (Boehringer Mannheim)
10 nM	Okadaic Acid (Sigma)
1 mM	Sodium Orthovanadate (Sigma)

Suspension Buffer

0.1 M	Tris.HCl, pH 6.8
50 mM	DTT (Sigma)
20%(v/v)	Glycerol

10X SDS-PAGE Stacking Buffer

310 mM	Tris.HCl, pH6.8
0.25%(v/v)	SDS

5X SDS-PAGE Separating Buffer

1.86 M	Tris.HCl, pH8.8
0.5%(v/v)	SDS

4% SDS-PAGE Stacking Gel

4%(v/v)	Acrylamide Stock Solution
1X	SDS-PAGE Stacking Buffer
0.03%(v/v)	APS
0.1%(v/v)	TEMED

10% SDS-PAGE Separating Gel

10%(v/v)	Acrylamide Stock Solution
1X	SDS-PAGE Stacking Buffer
0.03%(v/v)	APS
0.1%(v/v)	TEMED

5X SDS-PAGE Running Buffer

0.124 M	Tris base (15g)
0.96 M	Glycine (72g)
0.5% (v/v)	SDS

Transfer Buffer

39 mM	Glycine
48 mM	Tris.HCl, pH 8.3
0.04%(v/v)	SDS
20% (v/v)	Methanol

Coomassie Destaining Solution

30% (v/v)	Methanol (AJAX Chemicals)
10% (v/v)	Acetic acid (AJAX Chemicals)

Coomassie Staining Solution

0.125%	Coomassie Brilliant Blue (Sigma)
30% (v/v)	Methanol
10% (v/v)	Acetic acid

10X TBS

0.2 M	Tris base
1.5 M	NaCl

Section 5.4.1 Mutant Primer Design

MST1K59R Primer 5'-GAGACTGGCCAGATTGTTGCAATCAGGCAAG-3'
(Sigma GenoSys)

MST1D326N Primer 5'-CTCGAACCATCGTGCCGGAATTCATTT-3'
(Sigma GenoSys)

Appendix II: Affymetrix array data clustered into functional categories

UPREGULATED GENES			DOWNREGULATED GENES		
Fold change	**GenBank accession no.**	**Gene Name or product**	**Fold change**	**GenBank accession no.**	**Gene Name or product**
			Signalling molecules		
6.6	AA727845	EST, vp33f01.r1 (99% homol. with Fas-binding protein, Daxx)	-6.6	AA104254	mo50c04.r1 (96% homol. with Rat serine threonine kinase Pim3)
5.7	M21019	R-ras	-3.7	Msa.3454.0	Homologous to Ser/thr protein phosphatase PP1-alpha 2 subunit (PP-1A)
~5.6 / 3.7	AF001863	FYN binding protein	-3.6	Z49085	Mouse developmental kinase 2 (MDK2)
5.3	D19392	EST, MUSGS00761 (87% homol. with mouse Fas-binding protein, Daxx)			
5.3	X63039	RSP-1 mRNA for p33 protein			
~3.7	D30731	Neurofibromatosis type-1-GTPase activating-protein type IV			
3.4	X12761	mouse mRNA for protein homologous to human c-JUN			
3.3	Msa.6768.0	Rho-related GTP-binding protein (RHOG)			
			Cell cycle control		
~5.9	X69026	PCTAIRE-3	-6.2	AA426917	vf20h04.s1 (96% homol. with Cyclin B1)
~3.5	I76150	CDK4 & CDK6 inhibitor protein (p16ink4a)	-4.7	Msa.1702.0	Retinoblastoma-binding protein (mRbAp46)
~3.0	U36799	Retinoblastoma-related protein (Rb2/p130)	-4.6	Z26580	Cyclin A
			-4.4	L11316	Oncogene (ect2)
			-4.1	D26089	cdc21
			-4	AA289122	vb32f05.r1 (94% homol. with human cdc28 protein kinase 2, CKS2)
			-3.9	X64713	Cyclin B1
			-3.9	Msa.16907.0	Homologous to 26S protease regulatory subunit 4 (MTS2 protein/p15INK4b)
			-3.7	AA272465	vb81f10.r1 (90% homol. with Rat cdc25A)
			-3.6	X82786	Ki-67
			-3.4	AA475191	vg97h10.r1 (99% homol. with cdc28 protein kinase 1, CKS1)
			-3.1	D26091	cdc47
			-3.1	AF004105	BM28 homolog
			-3	D26090	cdc46
			-3	U58633	p34 cdc2 kinase

UPREGULATED GENES			DOWNREGULATED GENES		
Fold change	**GenBank accession no.**	**Gene Name or product**	**Fold change**	**GenBank accession no.**	**Gene Name or product**
		Molecules involved in cell death control			
~3.9	U59463	ICH-3	-5	Msa.1413.0	Bcl-2 binding protein (BAG-1)
		Growth factors and growth factor/other receptors			
~5.7	M85078	Granulocyte-macrophage colony stimulating factor receptor low affinity subunit	-4.4	U42385	Fibroblast growth factor inducible gene 16 (FIN16)
5	U70622	Lysophosphatidic acid receptor (vzg-1)	-3.4	U42384	Fibroblast growth factor inducible gene 15 (FIN15)
4.6	M59377	Tumor necrosis factor II receptor (TNFR-2)			
~3.7	U05683	Receptor-type tyrosine kinase (rse)			
3.5	M21952	Macrophage colony-stimulating factor			
~3.4	Msa.397.0	Nicotinic acetylcholine receptor beta subunit (nAChRE)			
3.1	X63535	ufo			
		Secretory proteins/neurotransmitters/chemokines, chemoattractants/axon guidance			
~41.4	J04596	Platelet-derived growth factor-inducible KC protein			
29.8	M19681	Platelet-derived growth factor inducible JE protein			
~23.3	U27267	LPS-induced C-X-C chemokine LIX precursor			
~12.5	Z12297	Intercine			
~7.3	U92565	Fractalkine			
~7.0	X85990	Semaphorin A			
~6.1	Msa.30310.0	Cathepsin L precursor (Major excreted protein - MEP)			
3.7	I01695	Calmodulin-dependent phospho diesterase (PDE1B1)			
3.5	D30798	unc-18			
3.4	X06086	Major excreted protein (MEP)			
3.1	Msa.1979.0	Ulip			
3	X70296	Protease, Nexin 1			
		Nuclear proteins (transcription factors, DNA/RNA processing enzymes and binding proteins)			
~16.0	L28117	NF-kappa-B (p105)	~ -15	K02927	Ribonucleotide reductase subunit M1
~12.2	AA611262	EST, vo51b09.r1 (97% homol. with N-myc downstream regulated 2)	-9.3	Z46757	High mobility group 2 (HMG2) protein
~11.1	D76432	Transcriptional repressor deltaEF1	-5.5	Msa.22528.0	Homologous to Cleavage stimulation factor, P33240
~9.8	X61800	C/EBP delta	-5.3	Msa.16618.0	Homologous to Pre-mRNA splicing factor SRP20 (X16 protein), P23152
6.3/3.3	Msa.1690.0	I-kappa B alpha chain	-3.5	Msa.28141.0	Homologous to Carg-binding factor A (CBF-A), Q99020

UPREGULATED GENES			DOWNREGULATED GENES		
Fold change	**GenBank accession no.**	**Gene Name or product**	**Fold change**	**GenBank accession no.**	**Gene Name or product**
		Nuclear proteins (transcription factors, DNA/RNA processing enzymes and binding proteins)			
~4.9	AA237297	EST, mw96f09.r1 (89% homol. with Rat Hnrpab)	-4.9	Msa.27327.0	Homologous to possible global transcription activator, P 41877
4.6	M83380	Transcription factor relB	-4.8	X58069	Histone (H2A.X)
~4.3	Msa.11622.0	Nuclear factor NF-kappa-B P100 subunit (contains P52 subunit)	-4.4	M37736	Replication-dependent histone (H2A.1)
4	AA270796	EST, va70c01.r1 (99% homol. with transcription factor like protein, ODA-10)	-4.4	Z11870	Cellular nucleic acid binding pro tein (CNBP)
4	Msa.17890.0	Elongation factor 2 (EF-2)	-4.3	Msa.2743.0	U1 snRNP-specific protein C
3.8	U09816	GM2 activator protein (Gm2a)	~ -4	D17384	DNA polymerase alpha catalytic subunit p180
3.6	X67209	npdcf-1 protein	-4	Msa.194.0	Large ribosomal subunit protein
3.5	U70475	p45 NF-E2 related factor 2 (NRF2)	-4	AF012709	Centromere binding protein A (CENP-A)
			-3.9	AA269806	va63d03.r1 (98% homol. with histone H2A.X, BC005468)
			-3.9	Msa.1905.0	Deleted in splithand/split foot homolog (Dss1)
			-3.6	L26320	Flap endonuclease-1 (FEN-1)
			-3.5	X68193	Nucleoside diphosphate kinase B
			-3.3	Msa.2413.0	Ribosomal protein L36
			-3.3	Msa.788.0	Helix-loop-helix DNA binding protein regulator
			-3.1	D13544	Primase small subunit
			-3.1	U52951	Putative transcriptional regulator mEnx-1
			-3	Msa.28808.0	Homologous to 60S Ribosomal protein L6/TAXREB107, Q02878
			-3	Msa.12983.0	Homologous to Elongation factor 1-delta (EF-1-delta), P29692
		Protein processing, protein/vesicle transport, chaperones and protein folding molecules			
~9.4	R75432	EST, MDB0601 (91% homol. with Rat synaptotagmin binding zygin I)	-6	D55720	Nuclear pore-targeting complex (PTAC)
5.3	Msa.43186.0	Rab11b	-5.6	Z22593	Homologous to Fibrillarin, P22087
4.8	C77861	EST, C77861 (95% homol. with major vault protein, Mvp)	-5.4	X56045	Hypothetical protein A
~4.4	Msa.1092.0	Peroxisome membrane protein (PMP70)	-3.7	Msa.3842.0	Fibrillarin (34 kDa Nucleolar scleroderma antigen)
~4.4	X72966	Rab3A	-3.5	Msa.29092.0	Homologous to GTP-binding nuclear protein RAN (TC4), P28746
~3.6	Msa.31440.0	Mitochondrial Lon protease homolog precursor	-5.2	Msa.37326.0	Homologous to Mitochondrial stress-70 precursor protein (mthsp-70/GRP75)
3.4	U90435	Flotillin	-4.9	Y15522	Nuclear movement protein (MNUDC)
3.3	AF004591	Copper transport protein Atox1 (ATOX1)	-4.7	X53584	HSP60

UPREGULATED GENES			DOWNREGULATED GENES		
Fold change	GenBank accession no.	Gene Name or product	Fold change	GenBank accession no.	Gene Name or product
		Protein processing, protein/vesicle transport, chaperones and protein folding molecules			
~3.2	Msa.3106.0	BALB/c GDP-dissociation inhibitor (GDI-1)	~ -4.1 / -3	AA545124	vj92b08.s1 (94% homol. Rat chromosome region maintenance 1 protein CRM1)
3.1	X16319	54K subunit of signal recognition particle	-3.7	C78047	C78047 (97% homol. RAN guanine nucleotide release factor MOG1)
			-3.7	Z31399	Ccth mRNA for CCTH (chaperonin-containing TCP-1) eta subunit
			-3.6	U81030	Treacle (TCOF-1)
			-3.1	Z31555	Ccte mRNA for CCT (chaperonin-containing TCP-1) epsilon subunit
			-3.1	Msa.1669.0	GDP dissociation inhibitor beta
			-3	U64450	Nucleophosmin/nucleoplasmin-3 (Npm3)
		Metabolic associated molecules and enzymes, transporters, ion channels			
21.0	Msa.1531.0	Apolipoprotein D (apoD)	-9.8	M13362	Thymidylate synthase
7.3	U23184	Carboxypeptidase E (Cpe)	-6.3	Msa.1580.0	S-adenosyl homocysteine hydrolase (ahcy)
5.4	AA275198	EST, vc05c10.r1 (88% homol. with Hampster HMG-CoA)	-5.6	AA259483	va38e04.r1 (97% homol. with thymidylate kinase, Tmk)
4.6	X73230	Arylsulphatase A	-4.9	Msa.11648.0	Homologous to Inorganic pyrophosphatase, P37980
~4.5	M84145	Fumarylacetoacetate hydrolase (Fah)	-4.2	Msa.26582.0	Homologous to Nucleoside diphosphate kinase A (NDK A), Q05982
~4.2	I02333	Bilirubin/phenol family UDP glucuronosynltransferase (ugtBr)	-4.1	Msa.26264.0	Homologous to Adenine nucleotide translocase-2 (Ant2), P05141
~3.9	Msa.756.0	HMG-CoA reductase	-3.8	X61172	Alpha-mannosidase II
3.9	AA137436	EST, mq81e04.r1 (95% homol. with stearoyl-CoA desaturase exon 6)	-3.8	Msa.358.0	Lactate dehydrogenase A4 isoenzyme (LDH -A)
~3.8	Y00964	Beta-hexosamidase	-3.2	Msa.2642.0	Adenine nucleotide translocase-1 (Ant1)
3.8	D29016	Squalene synthase	-5.2	C81593	C81593 (97% homol. with ribonucleotide reductase M2, Rrm2)
3.5	M74495	Adenylosuccinate synthetase	-4.5	AA511301	vj22b05.r1 (99% homol. with monocarboxylate transporter 1, mMCT1)
3.3	Msa.6220.0	Glycogen phosphorylase, brain form	-3	U04827	Brain fatty acid-binding protein (B-FABP)
3.3	Msa.477.0	Carbohydrate binding protein 35			
3.2	U62295	Cytochrome P450 monooxygenase (CYP2J6)			
3.1	L10244	Spermidine/spermine N1-acetyltransferase (SSAT)			
3	Z11911	Glucose-6-phosphate dehydrogenase			
3	J04632	Glutathione S-transferase class mu (GST1-1)			
~3	Msa.14012.0	Vacuolar ATP synthase catalytic subunit A, ubiquitous isoform			

UPREGULATED GENES			DOWNREGULATED GENES		
Fold change	**GenBank accession no.**	**Gene Name or product**	**Fold change**	**GenBank accession no.**	**Gene Name or product**
		Cytoskeletal components, and accessory proteins involved in migration			
~8.8 / ~6.9	J04953	Gelsolin	-3.2	M35153	Lamin B
~6.2	M72414	Microtubule associated protein 4 (MAP4)	-3	Msa.16998.0	Homologous to Stathmin, P13668
6.1	AA590859	EST, vn60f03.r1 (95% homol. with ß-actin)			
5.6	J04181	A-X actin			
~5.1	Msa.5789.0	Dynein heavy chain, cytosolic			
~4.6	Msa.11746.0	Tubulin beta-1 chain (class-I)			
4.8	AA709861	EST, vt35a01.r1 (93% homol. with cytoskeletal ß-actin)			
3.2	AA606536	EST, vo46g05.r1 (99% homol. with Eplin)			
		Extracellular matrix proteins and molecules involved in adhesion and cell-cell interactions			
~8.7	D78572	Membrane Glycoprotein	-5	M32490	Cyr61
~7.6	U69176	Laminin alpha 4 chain			
6.3	X65582	Alpha-2 collagen VI			
5.8	U64827	Extracellular matrix associated protein (Sc1)			
5.5	U69262	Matrilin-2 precursor			
4.8	X66405	Collagen alpha1 (VI)-collagen			
~4.7	D89571	Ryudocan core protein			
4.5	X51834	Osteopontin			
4.4	Msa.21961.0	Nidogen precursor (Entactin)			
4.3	Msa.8112.0	Platelet-endothelial tetraspan antigen 3 (PETA-3)			
~4.2	M76124	EGP314 precursor			
3.7	Msa.206.0	BALB/c alpha 1 type XVIII collagen (COL18A1)			
~3.6	Msa.476.0	Bone morphogenetic protein 1 (BMP-1)			
		Other			
25.4/16.5	Msa.2536.0	WDNM1			
14.5	X67644	Gly96	-6.1	AA592163	vo19f04.r1 (98% homol. with protein regulator of cytokinesis 1, BC005475)
9.8	D14883	C33/R2/IA4	-6.1	C77497	C77497 (95% homol. with mitotic centromere-associated kinesin, BC006841)
~9.6	M11284	MHC class I Qa-Tla	-3.1	Msa.12159.0	Homologous to Serine/threonine-protein kinase IPL1, P38991
~7.3	K02782	Complement component C3 alpha & beta subunits			

UPREGULATED GENES			DOWNREGULATED GENES		
Fold change	GenBank accession no.	Gene Name or product	Fold change	GenBank accession no.	Gene Name or product
		Other			
6.6	U52073	TDD5			
6.4	W54374	EST, md05h08.r1 (100% homol. with MAGE- like protein, MAGE1-D)			
5.8	AA614971	EST, vo32e09.r1 (100% homol. with MAIL)			
5.3	AA177300	EST, mt22e12.r1 (99% homol. with 7 pass transmembrane protein)			
5.3	C77421	EST, C77421 (97% homol. with virus like retrotransposon, BVL-1)			
~4.0	Msa.20085.0	NEDD-4 related protein (KIAA0093)			
3.9	X04120	Intracisternal A-particle (IAP-IL3 genome deleted type 1 element			
3.8	Msa.1037.0	Opa repeat			
3.5	Msa.22134.0	Extensin precursor (cell wall hyd)			
~3.4	C80730	EST, C80730 (89% homol. with CD9 antigen)			
3.2	U17297	Integral membrane phosphoprotein band 7.2b (Epb72)			
3.2	Msa.6321.0	Myoblast cell surface antigen 24.1D5			
3.1	Msa.918.0	Lymphocyte differentiation antigen Ly-6C.2			
~3	AA217379	EST, mu92e10.r1 (81% Rat natural resistence-associated macrophage protein 2)			
		Expressed Sequence Tags (ESTs)			
~7.8	W82380	EST, mf03h01.r1 (90% homol. with 10 day pancreas cDNA)	-9.6	AA002925	mg40e06.r1 (100% homol. with RIKEN 10 day embryo cDNA, AK011289)
~7.6	C79775	EST, C79775 (93% homol. with 13 day embryo liver cDNA)	-7.4	AA537407	vj98c05.r1 (99% homol. with RIKEN 10 day embryo cDNA, AK012002)
~5.8	AA596237	EST, vo30h09.r1 (no significant homology)	-6.2	AA268341	va39a10.r1 (99% homol. with RIKEN 18 day embryo cDNA, AK003722)
4.9	W81884	EST, me94b04.r1 (98% homol. with clone BC004823)	-5.9	AA079910	mm33e10.r1 (100% homol. with RIKEN small intestine cDNA, AK008568)
4.8	AA018019	EST, mh45d06.r1 (100% homol. with adult male kidney cDNA)	-4.8	C76791	C76791 (98% homol. with RIKEN 8 day embryo cDNA, AK017609)
4.3	W45944	EST, mc77d12.r1(98% homol. with adult stomach cDNA - AK008866)	-4.7	AA673431	vp46h06.r1 (98% homol. with RIKEN 18 day embryo cDNA, AK004134)
4.2	AA711625	EST, vu31g07.r1(99% homol. with 18 day embryo cDNA - AK003665)	-4.6	C78101	C78101 (98% homol. with RIKEN 18 day embryo cDNA, AK004134)
4.2	C77409	EST, C77409 (96% homol. with 10/11 day enbryo cDNA - AK012755)	-4.2	AA266783	mz66h06.r1 (100% homol. with nucleolar protein, ANKT)
4	AA109907	EST, mp10c11.r1 (100% homol. with 11 day preg. female ovary cDNA -AK019885)	-4	AA267955	va04a10.r1 (100% homol. with clone clone MGC:8311)
4	C75983	EST, C75983 (96% homol. with chromosome 18 clone - AC020971)	-4	AA409194	EST03707 (97% homol. with RIKEN 10 days embryo cDNA, AK011791)
~3.7	C81439	EST, C81439 (no significant homology)	-4	C78306	C78306 (97% homol. with phosphoribosyl pyrophosphate synthetase 1, Prps1)
~3.6	W81812	EST, me93e02.r1 (no significant homology)	-3.9	AA475660	vh22f04.r1 (99% homol. with RIKEN adult male liver cDNA, AK004996)
3.6	AA387033	EST, vc81e03.r1 (99% homol. with adult male kidney cDNA - AK002546)	-3.9	AA614954	vo32c10.r1 (100% homol. with ubiquitin C-terminal hydrolase UCH-L5)
~3.5	W62701	EST, md82d07.r1 (no significant homology)	-3.8	AA241064	mv23a11.r1 (99% homol. with clone BC005507)

UPREGULATED GENES			DOWNREGULATED GENES		
Fold change	**GenBank accession no.**	**Gene Name or product**	**Fold change**	**GenBank accession no.**	**Gene Name or product**
		Expressed Sequence Tags (ESTs)			
~3.4	Z31269	EST, MMTEST707 (98% homol. with 10 day embryo cDNA)	-3.8	C79700	C79700 (95% homol. with Rat nuclear ubiquitous casein kinase 2 (Nucks)
3.3	AA273938	EST, vb99f02.r1 (98% homol. with cDNA - BC004020)	-3.7	AA182195	mt77d02.r1 (no significant homology)
3.2	AA472476	EST, vh07a10.r1 (99% homol. with 13 day embryo head cDNA - AK014042)	-3.5	AA013993	mh07a01.r1 (87% homol. with Rat prol yl endopeptidase, Prep)
3.1	AA529056	EST, vi32a01.r1 (98% homol. with RIKEN adult male cDNA - AK002765)	-3.5	AA189300	mt89g03.r1 (no significant homology)
3.1	AA688564	EST, vu17b12.r1 (99% homol. with RIKEN cDNA - BC003930)	-3.5	AA543365	vj81c07.r1 (99% homol. with RIKEN cDNA, BC003481)
3	AA274076	EST, vb96a12.r1 (no significant homology)	-3.3	AA175127	ms79d04.r1 (100% homol. with clone BC003842 similar to CGI-07 protein)
			-3.3	AA529747	vi42f11.r1 (94% homol. with RIKEN adult male small intestine cDNA, AK008255)
			-3.2	W48388	mc88c08.r1 (96% homol. with nucleolar protein family A, Nola1)
			-3.2	AA153942	mr15b03.r1 (99% homol. translocase of inner mitochondrial membrane, Timm8a)
			-3.2	AA177891	mt05b08.r1 (87% homol. with human clone BC003648)
			-3.2	AA230393	mw04e10.r1 (99% homol. with RIKEN adult male cerebellum cDNA, AK005280)
			-3.2	AA607833	vm39h10.r1 (99% homol. with RIKEN 10 days embryo cDNA, AK011744)
			-3.1	AA590060	vn57d03.r1 (99% homol. with RIKEN adult male stomach cDNA, AK008785)
			-3	AA254740	mz75d05.r1 (99% homol. with RIKEN 10/11 days embryo cDNA, AK012875)
			-3	AA407078	EST02083 (98% homol. with RIKEN 18 days embryo cDNA, AK003393)
			~ -4	AA432946	ve91b01.r1 (99% homol. with nucleolar RNA helicase II/Gu, Ddx21)
			~ -4.4	AA245578	my52c06.r1 (99% homol. with RIKEN 10 days embryo cDNA, AK011218)

Appendix III: MST1/2 mRNA Alignment

Primer sequences are highlighted in green
Other sites of interest are in bold and underlined

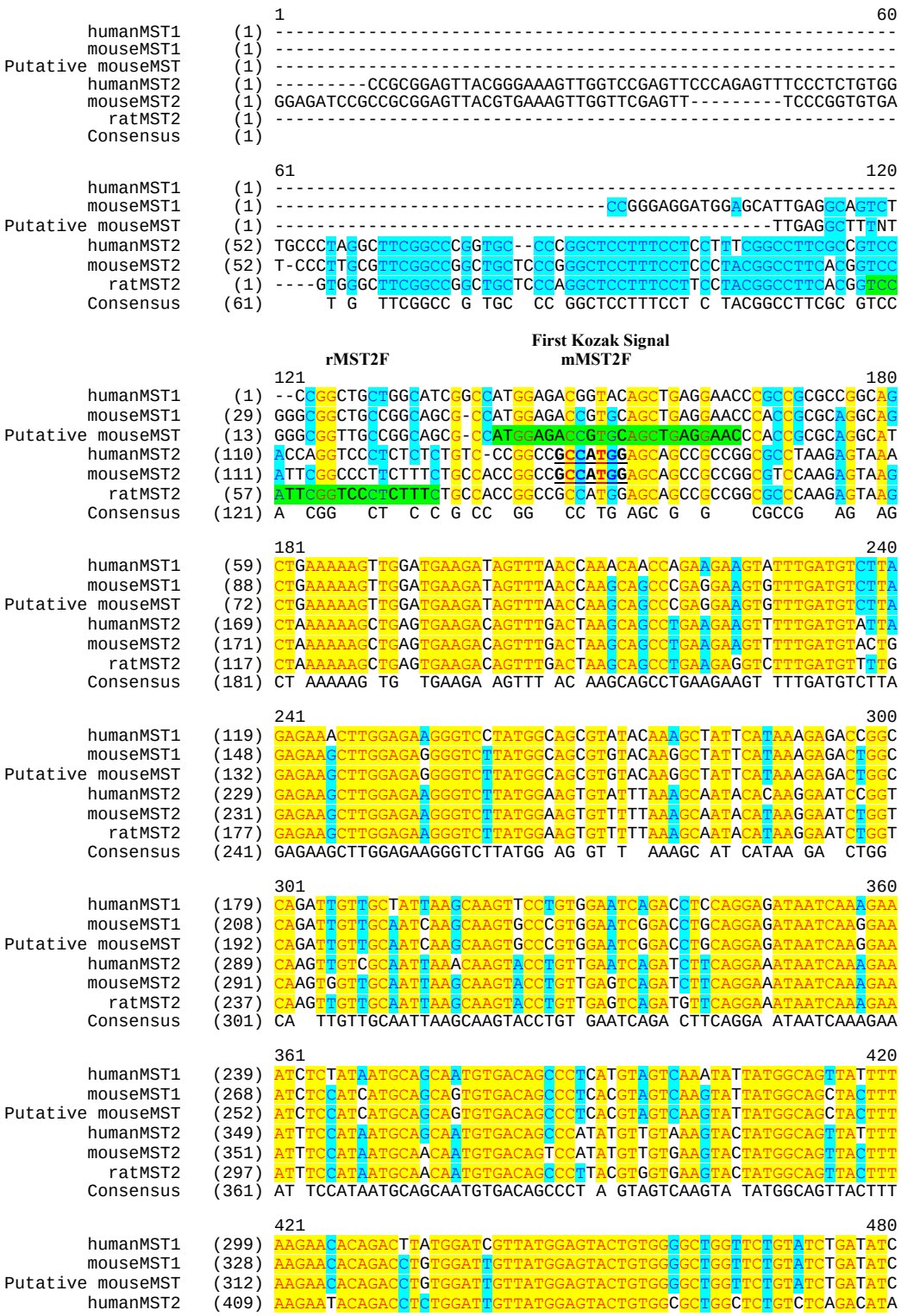

```
       mouseMST2   (411) AAGAACACAGACCTCTGGATTGTTATGGAGTACTGTGGAGCGGGTCCGTTTCAGACATA
         ratMST2   (357) AAGAACACAGACCTCTGGATTGTTATGGAGTACTGTGGGGCCGGTCCGTTTCAGACATA
       Consensus   (421) AAGAACACAGACCTCTGGATTGTTATGGAGTACTGTGGGGCTGGTTCTGTATC GA AT

                         481                                                       540
       humanMST1   (359) ATTCGATTACGAAATAAAACGTTAACAGAAGATGAAATAGCTACAATATTACAATCAACT
       mouseMST1   (388) ATTCGGCTACGGAACAAGACGTTAACAGAAGATGAAATAGCTACNATATTACAATCAACT
Putative mouseMST  (372) ATTCGGCTACGGAACAAGACGTTAACAGAAGATGAAATAGCTACAATATTACAATCAACT
       humanMST2   (469) ATTAGATTACGAAACAAGACATTAATAGAAGATGAAATTGCAACCATTCTTAAATCTACA
       mouseMST2   (471) ATTAGATTGCGAAACAAGACATTAACAGAAGATGAAATTGCAACTATTCTAAAATCCACA
         ratMST2   (417) ATTAGATTACGAAACAAGACATTAACGGAAGATGAAATTGCAACTATTCTAAAATCCACG
       Consensus   (481) ATT GATTACGAAACAAGAC TTAACAGAAGATGAAAT GC AC AT  TA AATCAACT

                         541                                                       600
       humanMST1   (419) CTTAAGGGACTTGAATACCTTCATTTTATGAGAAAAATACACCGAGATATCAAGGCAGGA
       mouseMST1   (448) CTTAAGGGACTAGAATACCTTCATTTTATGAGAAAAATACACCGAGATATCAAGGCGGGA
Putative mouseMST  (432) CTTAAGGGACTAGAATACCTTCATTTTATGAGAAAAATACACCGAGATATCAAGGCGGGA
       humanMST2   (529) TTGAAAGGACTAGAATATTTGCACTTTATGAGAAAAATACACAGAGATATAAAAGCTGGA
       mouseMST2   (531) TTGAAAGGATTAGAATATTTGCATTTTATGAGGAAAATACACAGAGATATAAAAGCCGGG
         ratMST2   (477) TTGAAAGGATTAGAATATTTGCATTTTATGAGGAAAATACACAGAGATATAAAAGCTGGG
       Consensus   (541)  T AA GGACTAGAATA  T CATTTTATGAGAAAAATACAC GAGATAT AA GC GGA

                         601                                                       660
       humanMST1   (479) AATATTTTGCTAAATACAGAAGGACATGCAAAACTTGCAGATTTTGGGGTAGCAGGTCAA
       mouseMST1   (508) AATATTTTGCTAAACACAGAAGGCCATGCAAAGCTTGCAGACTTTGGAGTCGCAGGTCAA
Putative mouseMST  (492) AATATTTTGCTAAACACAGAAGGCCATGCAAAGCTTGCAGACTTTGGAGTCGCAGGTCAA
       humanMST2   (589) AATATTCTCCTCAATACAGAAGGACATGCAAAATTGGCAGATTTTGGAGTGGCTGGTCAG
       mouseMST2   (591) AATATTCTCCTCAATACAGAAGGACATGCAAAGCTTGCAGATTTTGGAGTGGCTGGCCAG
         ratMST2   (537) AATATTCTCCTCAATACAGAAGGACATGCAAAGCTTGCAGATTTTGGAGTGGCTGGCCAG
       Consensus   (601) AATATT T CT AATACAGAAGGACATGCAAAGCTTGCAGATTTTGGAGTGGC GGTCA

                                                                        1mMST2F
                         661                                                       720
       humanMST1   (539) CTTACAGATACCATGGCCAAGCGGAATACAGTGATAGGAACACCATTTTGGATGGCTCCA
       mouseMST1   (568) CTTACAGATACCATGGCAAAGAGGAATACAGTAATAGGGACCCCGTTTTGGATGGCTCCT
Putative mouseMST  (552) CTTACAGATACCATGGCAAAGAGGAATACAGTAATAGGGACCCCGTTTTGGATGGCTCCT
       humanMST2   (649) TTAACAGATACAATGGCAAAACGCAATACTGTAATAGGAACTCCATTTTGGATGGCTCCT
       mouseMST2   (651) TTAACAGATACAATGGCAAAACGCAACACTGTAATAGGAACCCCATTTTGGATGGCTCCT
         ratMST2   (597) TTAACAGACACGATGGCAAAACGCAATACTGTAATAGGAACCCCGTTTTGGATGGCTCCC
       Consensus   (661)  T ACAGATACCATGGCAAA CG AATAC GTAATAGGAACCCC TTTTGGATGGCTCCT

                         721                                                       780
       humanMST1   (599) GAAGTGATTCAGGAAATTGGATACAACTGTGTAGCAGACATCTGGTCCCTGGGAATAACT
       mouseMST1   (628) GAAGTTATTCAGGAAATTGGGTACAACTGTGTGGCAGACATCTGGTCTCTGGGAATAACT
Putative mouseMST  (612) GAAGTTATTCAGGAAATTGGGTACAACTGTGTGGCAGACATCTGGTCTCTGGGAATAACT
       humanMST2   (709) GAGGTGATTCAAGAAATAGGCTATAACTGTGTGGCCGACATCTGGTCCCTTGGCATTACT
       mouseMST2   (711) GAGGTAATTCAAGAAATAGGTTACAACTGTGTGGCTGACATCTGGTCCCTTGGCATTACT
         ratMST2   (657) GAGGTAATTCAAGAAATAGGTTACAACTGTGTGGCTGACATCTGGTCCCTTGGCATTACG
       Consensus   (721) GA GT ATTCA GAAAT GG TACAACTGTGTGGCAGACATCTGGTCCCT GG AT ACT

                         781                                                       840
       humanMST1   (659) GCCATAGAAATGGCTGAAGGAAAGCGCCCTATGCTGATATCCATCCAATGAGGGCAATC
       mouseMST1   (688) GCCATAGAAATGGCTGAAGGAAAGCCCCCATATGCTGATATCCATCCAATGAGGGCAATA
Putative mouseMST  (672) GCCATAGAAATGGCTGAAGGAAAGCCCCCATATGCTGATATCCATCCAATGAGGGCAATA
       humanMST2   (769) TCTATAGAAATGGCTGAAGGAAAACCTCCTTATGCTGATATACATCCAATGAGGGCTATT
       mouseMST2   (771) TCTATAGAAATGGCAGAAGGAAAACCTCCTTATGCTGATATACATCCGATGAGGGCTATT
         ratMST2   (717) TCTATAGAAATGGCAGAAGGAAAACCTCCTTATGCTGATATACATCCAATGAGGGCTATT
       Consensus   (781)  C ATAGAAATGGCTGAAGGAAA CC CCTTATGCTGATAT CATCCAATGAGGGC ATT

                         841                                                       900
       humanMST1   (719) TTCATGATTCCTACAAATCCTCCTCCCACATTCCGAAAACCAGAGCTATGGTCAGATAAC
       mouseMST1   (748) TTCATGATTCCTACAAACCCTCCTCCCACATTCCGTAAGCCAGAGCTGTGGTCAGACAAC
Putative mouseMST  (732) TTCATGATTCCTACAAACCCTCCTCCCACATTCCGTAAGCCAGAGCTGTGGTCAGACAAC
       humanMST2   (829) TTTATGATTCCCACAAATCCACCACCAACATTCAGAAAGCCAGAACTTTGGTCCGATGAT
       mouseMST2   (831) TTTATGATCCCTACAAACCCACCACCAACATTCAGGAAACCTGAACTTTGGTCTGATGAC
         ratMST2   (777) TTTATGATTCCTACAAACCCACCACCAACATTCAGGAAACCTGAGCTCTGGTCTGACGAC
       Consensus   (841) TT ATGATTCCTACAAACCC CC CC ACATTC G AA CCAGAGCT TGGTCAGA  AC

                         901                                                       960
       humanMST1   (779) TTTACAGATTTTGTGAAACAGTGTCTTGTAAAGAGCCCTGAGCAGAGGGCCACAGCCACT
       mouseMST1   (808) TTCATGGATTTTGTGAAGCAGTGTCTGGTAAAAAGCCCGGAGCAGAGAGCCACAGCCACT
Putative mouseMST  (792) TTCATGGATTTTGTGAAGCAGTGTCTGGTAAAAAGCCCGGAGCAGAGAGCCACAGCCACT
       humanMST2   (889) TTCACCGATTTTGTTAAAAAGTGTTTGGTGAAGAATCCTGAGCAGAGAGCTACTGCAACA
       mouseMST2   (891) TTCACCGATTTTGTGAAGAAGTGCTTGGTGAAGAGTCCTGAGCAGAGAGCCACTGCGACA
         ratMST2   (837) TTCACGGATTTTGTGAAGAAGTGCTTGGTGAAGAGTCCTGAGCAGAGGGCCACTGCCACC
       Consensus   (901) TTCACGGATTTTGTGAAG AGTGT TGGT AAGAG CCTGAGCAGAGAGCCAC GCCACT

                         961                                                      1020
       humanMST1   (839) CAGCTCCTGCAGCACCCATTTGTCAGGAGTGCCAAAGGAGTGTCAATACTGCGAGACTTA
       mouseMST1   (868) CAGCTCCTACAGCACCCGTTTGTTAAGAGTGCCAAAGGAGTGTCAATATTGCGAGACTTA
```

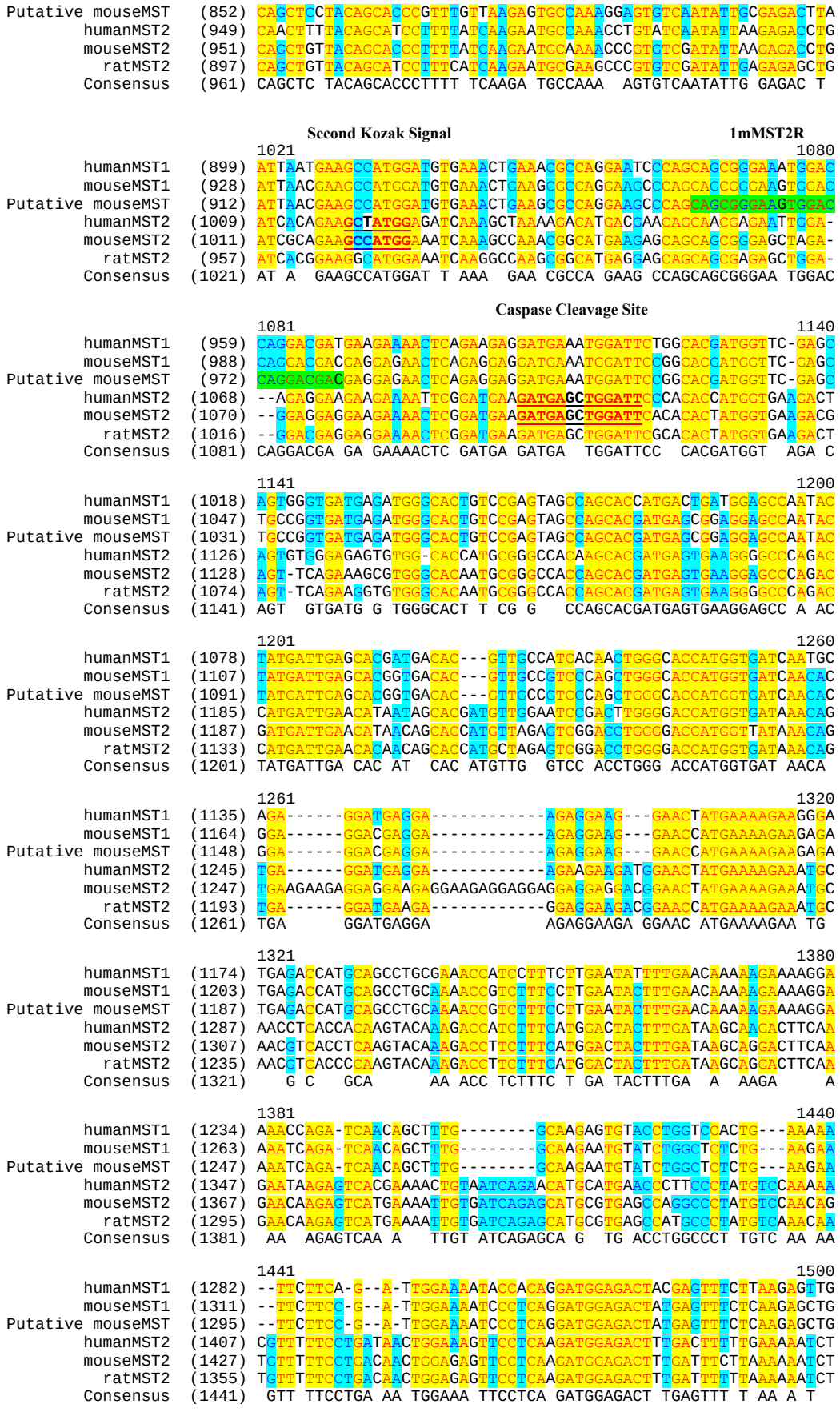
Second Kozak Signal
1mMST2R
Caspase Cleavage Site

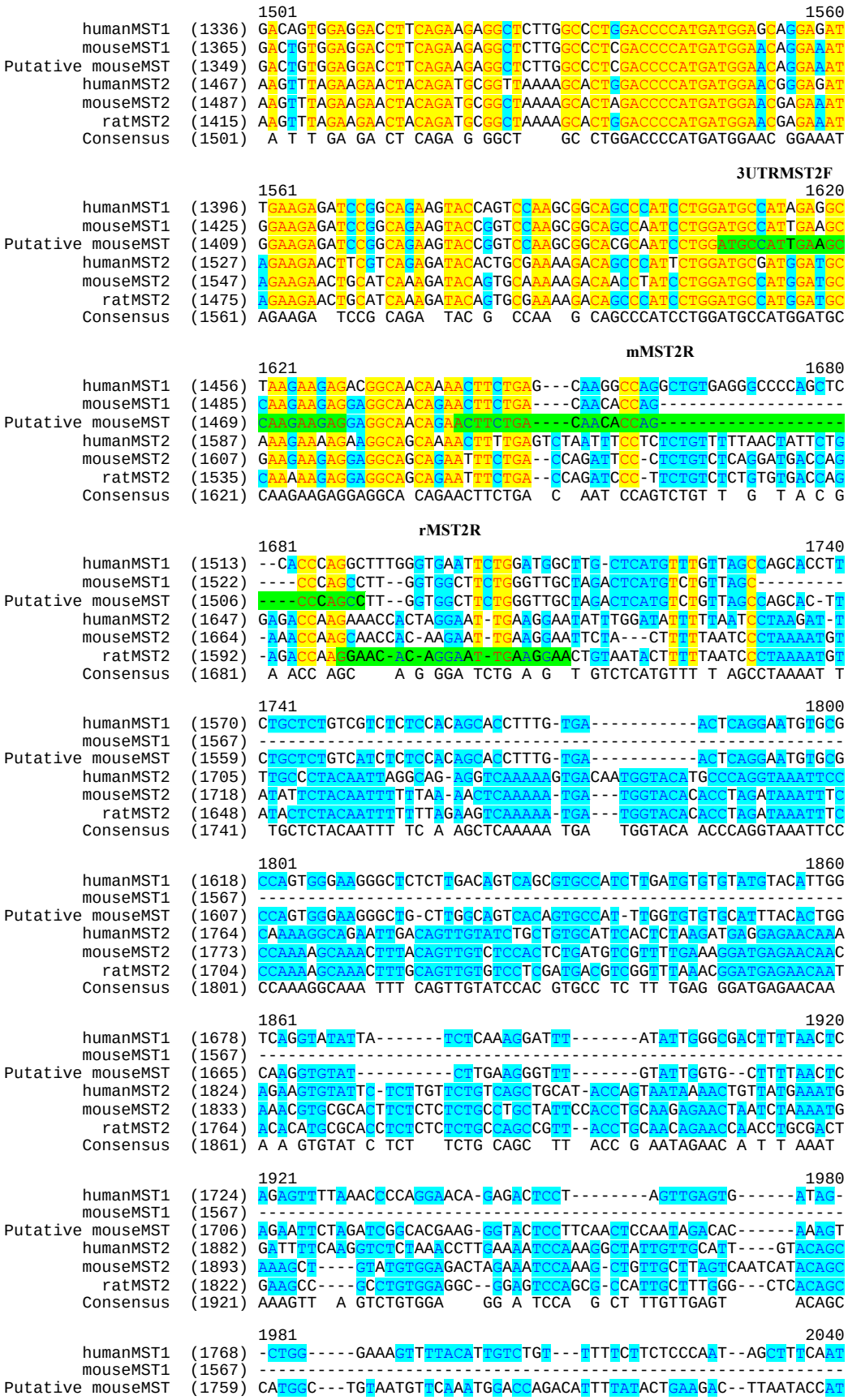
3UTRMST2F
mMST2R
rMST2R

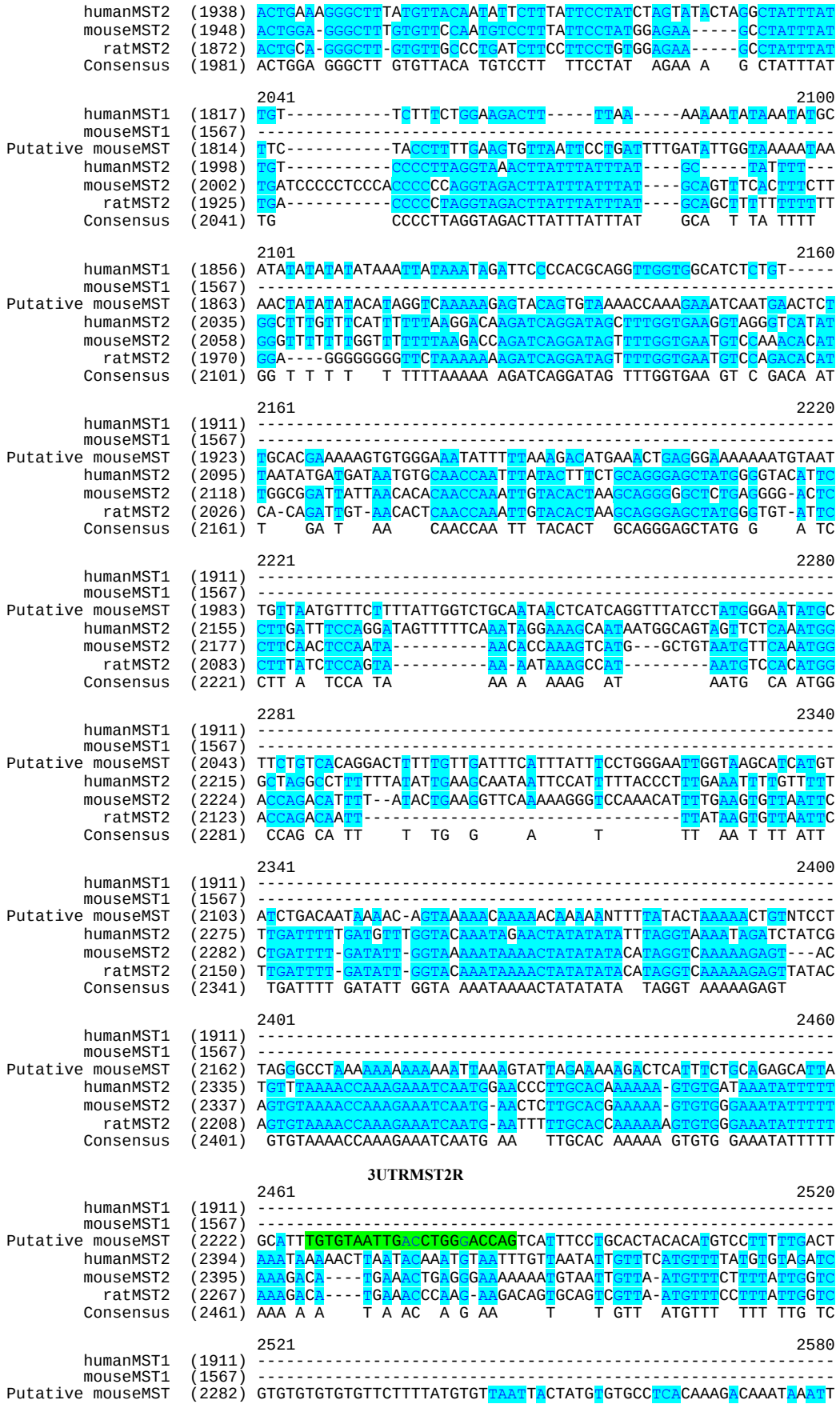
3UTRMST2R

```
        humanMST2  (2454) TAATAGCTGAACTGATTCAAACTGTAATAAGCTCATCAATTTCATTTCTATGAAAATGTG
        mouseMST2  (2450) C----------------------GCAATAA-CTCATCAGGTTTATC-CTATGGGAATATG
          ratMST2  (2321) T----------------------GTAGTAA-CT--TCAAGTTCATT-CTATGGGAC-ATG
        Consensus  (2521)                        GTAATAA CT  TCA  TTCAT  CTATG  AA ATG

                           2581                                                  2640
        humanMST1  (1911) ------------------------------------------------------------
        mouseMST1  (1567) ------------------------------------------------------------
Putative mouseMST  (2342) GCATTGTGCCACCC-------------------------------------------
        humanMST2  (2514) CTCTGTTGTCACAGGATGTTTCTGTTGATTTTATTCATTTCCTGGGAATTGGTAAACATC
        mouseMST2  (2486) CTTC--TGTCACAGGACTTTTT-GTTGATTTCATTTATTTCCTGGGAATTGGTAAGCATC
          ratMST2  (2354) CTTC--TGTCACAGGGCTTTT--GTTGACTTCATTCTACTCCTGGGAATTGGTAAGCATC
        Consensus  (2581) CT    TGTCACAGG   TTT  GTTGA TT ATT    TCCTGGGAATTGGTAA CATC

                           2641                                                  2700
        humanMST1  (1911) ------------------------------------------------------------
        mouseMST1  (1567) ------------------------------------------------------------
Putative mouseMST  (2356) ------------------------------------------------------------
        humanMST2  (2574) ATGTTCCTGATGATAACCCAGTAGCAAAAACA---------TTTGTACTGAGTGGTACAA
        mouseMST2  (2543) ATGTATCTGCCAATAAACCAGTAAAAACAAAAAACAAAAACTTTTATACTAAAAAC-TGTA
          ratMST2  (2410) ATGTATCTGACAATAAAGCAGTAATATG-------------TTTATACTAAAACTGTGTG
        Consensus  (2641) ATGT  CTG   ATAA  CAGTA  A               TTT TACT A

                           2701                                                  2760
        humanMST1  (1911) ------------------------------------------------------------
        mouseMST1  (1567) ------------------------------------------------------------
Putative mouseMST  (2356) ------------------------------------------------------------
        humanMST2  (2625) GCCTTGGGGACTGAAAAAAAAAAAGATTAAAACCATTAAAAGAAACTCATTTTTACGC
        mouseMST2  (2602) TCCTTAGGGTTAAAAAAAAAAAA----------AAAAAAAAAA--------------
          ratMST2  (2457) TCCTTAGGGCCTAAAAATGAAAGC----------ATTAGAAAAAGGCTCCTTTCTGAGA
        Consensus  (2701)  CCTT GGG    AAAAA  AAA            A  A AAA A

                           2761                                                  2820
        humanMST1  (1911) ------------------------------------------------------------
        mouseMST1  (1567) ------------------------------------------------------------
Putative mouseMST  (2356) ------------------------------------------------------------
        humanMST2  (2685) TG-AATGAACATTTATATGATTGCATTGGGACCAGTCATTTCCTAAGCTACATATGGCCA
        mouseMST2  (2638) ------------------------------------------------------------
          ratMST2  (2507) AGCAATTAGCATTTGTGTAATTGACCTGGGACCAGTCATTTCCTGCACTACACAGGGCCA
        Consensus  (2761)

                           2821                                                  2880
        humanMST1  (1911) ------------------------------------------------------------
        mouseMST1  (1567) ------------------------------------------------------------
Putative mouseMST  (2356) ------------------------------------------------------------
        humanMST2  (2744) TCTTGACAGTGTTTTTTCTTTTGTGTGTTTAATTATTATGTGTAAATCATAAAGACAAAT
        mouseMST2  (2638) ------------------------------------------------------------
          ratMST2  (2567) TTTTGATATCGTGTTCTTTTATGTGT---TAATTACTATGTGTGCAG------------
        Consensus  (2821)

                           2881        2897
        humanMST1  (1911) -----------------
        mouseMST1  (1567) -----------------
Putative mouseMST  (2356) -----------------
        humanMST2  (2804) AAATTTCACTGTGCCAC
        mouseMST2  (2638) -----------------
          ratMST2  (2611) -----------------
        Consensus  (2881)
```

Appendix IV: MST1/2 Amino Acid Alignment

```
                                                                                                                60
mouse MST1    (1) METVQLRNPPRRQ--LKKLDEDSLTKQPEEVFDVLEKLGEGSYGSVYKAIHKETGQIVAI
mouse MST2    (1) -----MEQPPASKSKLKKLSEDSLTKQPEEVFDVLEKLGEGSYGSVFKAIHKESGQVVAI

 Consensus    (1)      L NPP     LKKL EDSLTKQPEEVFDVLEKLGEGSYGSVFKAIHKESGQIVAI
```

K59R Point Mutation

```
                  *                                                                                             120
mouse MST1   (59) KQVPVESDLQEIIKEISIMQQCDSPHVVKYYGSYFKNTDLWIVMEYCGAGSVSDIIRLRN
mouse MST2   (56) KQVPVESDLQEIIKEISIMQQCDSPYVVKYYGSYFKNTDLWIVMEYCGAGSVSDIIRLRN

 Consensus   (61) KQVPVESDLQEIIKEISIMQQCDSPHVVKYYGSYFKNTDLWIVMEYCGAGSVSDIIRLRN

                                                                                                               180
mouse MST1  (119) KTLTEDEIATILQSTLKGLEYLHFMRKIHRDIKAGNILLNTEGHAKLADFGVAGQLTDTM
mouse MST2  (116) KTLTEDEIATILKSTLKGLEYLHFMRKIHRDIKAGNILLNTEGHAKLADFGVAGQLTDTM

 Consensus  (121) KTLTEDEIATIL STLKGLEYLHFMRKIHRDIKAGNILLNTEGHAKLADFGVAGQLTDTM

                                                                                                               240
mouse MST1  (179) AKRNTVIGTPFWMAPEVIQEIGYNCVADIWSLGITAIEMAEGKPPYADIHPMRAIFMIPT
mouse MST2  (176) AKRNTVIGTPFWMAPEVIQEIGYNCVADIWSLGITSIEMAEGKPPYADIHPMRAIFMIPT

 Consensus  (181) AKRNTVIGTPFWMAPEVIQEIGYNCVADIWSLGITAIEMAEGKPPYADIHPMRAIFMIPT

                                                                                                               300
mouse MST1  (239) NPPPTFRKPELWSDNFMDFVKQCLVKSPEQRATATQLLQHPFVKSAKGVSILRDLINEAM
mouse MST2  (236) NPPPTFRKPELWSDDFTDFVKKCLVKSPEQRATATQLLQHPFIKNAKPVSILRDLIAEAM

 Consensus  (241) NPPPTFRKPELWSD F DFVK CLVKSPEQRATATQLLQHPFIK AK VSILRDLI EAM
```

D326N Point Mutation

```
                                                  *                                                           360
mouse MST1  (299) DVKLKRQEAQQREVDQDDEENSEEDEMDSGTMVRAAGDEMGTVRVASTMSGGANTMIEHG
mouse MST2  (296) EIKAKRHEEQQRELEEEEE-NSDEDELDSHTMVKTSSESVGTMRATSTMSEGAQTMIEHN

Consensus  (301)  DIK KR E QQRELD DDE NSDEDELDS TMVK A D MGTMR  STMS GANTMIEH
```

Caspase Cleavage Site

```
                                                                                                               420
mouse MST1  (359) -DTLPSQLGTMVINTEDEEEE-------GTMKRRDETMQPAKPSFLEYFEQKEKEN---Q
mouse MST2  (355) STMLESDLGTMVINSEEEEEEEEEEEEDGTMKRNATSPQVQRPSFMDYFDKQDFKNKSHE

 Consensus  (361)    LPSQLGTMVINSEDEEEE       GTMKR   S Q  KPSFLDYFD  D  N
```

Nuclear Expost Signal (NES)1

```
                                                                                                               480
mouse MST1  (408) INSFGKNVSGSLKN---SSDWKIPQDGDYEFLKSWTVEDLQKRLLALDPMMEQEMEEIRQ
mouse MST2  (415) NCDQSMREPGPMSNSVFPDNWRVPQDGDFDFLKNLSLEELQMRLKALDPMMERETEELHQ

 Consensus  (421)          G L N      WKIPQDGDFDFLK  SVEDLQKRLLALDPMME EIEEI Q
```

Nuclear Export Signal (NES)2

```
                                      503
mouse MST1  (465) KYRSKRQPILDAIEAKKRRQQNF
mouse MST2  (475) RYSAKRQPILDAMDAKKRRQQNF

 Consensus  (481) KY AKRQPILDAIEAKKRRQQNF
```

Bipartite Nuclear Localisation Motif